

**An Experimental Study of the Oil Evolution in Critical Piston Ring Pack Regions
and the Effects of Piston and Ring Designs in an Internal Combustion Engine
Utilizing Two-Dimensional Laser Induced Fluorescence and the Impact on
Maritime Economics**

by

Adam Vokac

B.S., Marine Engineering Systems, United States Merchant Marine Academy, 2000

Submitted to the Department of Mechanical Engineering and the Department of Ocean
Engineering in Partial Fulfillment of the Requirements for the Degrees of

MASTER OF SCIENCE IN MECHANICAL ENGINEERING
and
MASTER OF SCIENCE IN OCEAN ENGINEERING MANAGEMENT

at the
MASSACHUSETTS INSTITUTE OF TECHNOLOGY
June 2004

© 2004 Massachusetts Institute of Technology, All Rights Reserved

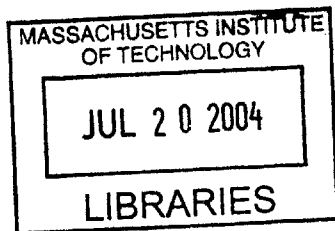
Author.....
Department of Mechanical Engineering and Ocean Engineering
May 7th, 2004

Certified by.....
Tian Tian
Lecturer, Department of Mechanical Engineering
Thesis Supervisor

Certified by.....
Henry Marcus
Professor, Department of Ocean Engineering
Thesis Supervisor

Accepted by.....
Ain A. Sonin
Chairman, Committee on Graduate Studies
Department of Mechanical Engineering

Accepted by.....
Michael S. Triantafyllou
Chairman, Committee on Graduate Studies
Department of Ocean Engineering



BARKER

**An Experimental Study of the Oil Evolution in Critical Piston Ring Pack Regions
and the Effects of Piston and Ring Designs in an Internal Combustion Engine
Utilizing Two-Dimensional Laser Induced Fluorescence and the Impact on
Maritime Economics**

by

Adam Vokac

Submitted to the Departments of Mechanical Engineering and
Ocean Engineering on May 7th, 2004 in Partial Fulfillment of the
Requirements for the Degrees of Master of Science in Mechanical
Engineering and Master of Science in Ocean Engineering Management

ABSTRACT

Faced with increasing concern for lubricating oil consumption and engine friction, it is critical to understand the oil transport mechanisms in the power cylinder system. Lubricating oil travels through distinct regions along the piston ring pack before being consumed in the combustion chamber, with the oil distribution and dominant driving forces varying substantially for each of these regions. This experimental work focuses on specific regions in the piston ring pack. A detailed 2D LIF (Two Dimensional Laser Induced Fluorescence) study has been performed on the oil distribution and flow patterns throughout the entire cycle of a single cylinder spark ignition engine. The impact of speed and load were experimentally observed with the LIF generated real time high-resolution images, as were changes in piston and ring design.

The results reveal the third land, located between the second compression ring and the oil control ring, oil flow patterns and timing are consistent and predictable at each operating point. Speed and load variation alter the basic flow pattern and oil balance through a corresponding change in inertia and gas dragging effect respectively, with ring design variation instigating specific and repeatable phenomenon onto the consistent oil flow pattern. Second land, the region between the top two compression rings, geometric changes were found to have a significant impact on inertia driven oil transport; however, their effects on oil consumption were not as clear. As the majority of lubricating oil consumed in the engine crosses the third land at some point, an understanding of the timing and magnitude of the oil transport processes will allow means to be specifically developed to reduce the net oil flow across the third land towards the combustion chamber. This work forms a foundation for developing oil control strategies for the third land and for identifying how and when oil reaches the upper piston ring pack regions that directly contribute to oil consumption.

The ability to control, or impact, oil transport on the piston ring pack will have an impact on all engine classes, including engines in the maritime community. This experiment study is directly comparable to small marine engines, and can be used to help reduce maritime exhaust emissions related to lubrication consumption; additionally, this approach would be much more rugged and cost effective than other current technological improvements being investigated. Were a similar 2D LIF experiment to be performed on large slow speed diesel engines, the annual savings per vessel, assuming only a 10% reduction in lube oil consumption was achieved, could amount to \$30,000 as cylinder lube oil is one of the most expensive operating costs for large slow speed diesel engines.

Thesis Supervisors: Tian Tian and Henry Marcus

Titles: Lecturer, Department of Mechanical Engineering; and Professor, Department of Ocean Engineering

ACKNOWLEDGEMENTS

This work has been sponsored by the Consortium on Lubrication in Internal Combustion Engines at MIT. The current consortium members are Dana CORP., Renault SA, PSA Peugeot Citroën, Volvo AB, and Mahle Gmbh. I would like to express special thanks to Benoist Thirouard for his endless support and input on the continuation and advancement of his Doctoral project at MIT. I would also like to thank the PSA Research Department for providing the prototype single-cylinder research engine used in this work, and for their continued support in part procurement. Mahle Gmbh and Dana CORP are also thanked for their assistance in designing and producing pistons and rings for this work, particularly R.F. Fiedler from Mahle Gmbh and Rémi Rabuté, Patrick Guchet, and Randy Lundsford from Dana CORP. I would also like to thank Bengt Olsson and Fredrick Stromstedt for their camaraderie in Goteburg.

Tian Tian has been of tremendous assistance with his expertise and guidance of this research endeavor, as well as a friend. I would like to thank Henry Marcus for his guidance in Maritime Business, and will never forget his thoughts about “other peoples’ money”.

I would also like to thank those in the lab who have made my stay at MIT a unique and eventful time, in particular: Liang Liu, Mohammad Rasulli, and Colonel Li. Without you guys, I may never have known when new email arrived.

I wish all of you the best, and sincerely hope our paths may cross again.

Adam Vokac

TABLE OF CONTENTS

Abstract	2
Acknowledgments	3
Table of Contents	4
CHAPTER 1: INTRODUCTION	7
1.1 Background	7
1.2 Lubrication Environment	9
1.3 Previous Work	10
1.4 Experimental Objectives and Approach	11
CHAPTER 2: EXPERIMENT CONFIGURATION	14
2.1 Experimental Strategy	14
2.2 Experimental Setup	15
Engine Characteristics	16
Optical Access	17
Coolant System	18
Lubrication System	20
2.3 Data Acquisition	21
Fluorescence Overview	21
Laser Induced Fluorescence (LIF) Calibration	23
Imaging System	26
Blowby Measurement	33
2.4 Experimental Variations	39
Operating Conditions	39
Data Location	41
Ring and Piston Design	43
2.5 Data Analysis	48

CHAPTER 3: BASIC OIL TRANSPORT MECHANISMS	50
3.1 Piston Land Transport	52
Inertia Driven Oil Transport on the Piston Lands	52
Gas Flow Driven Oil Transport on the Piston Lands	61
3.2 Ring Scraping	70
Poor Ring Scraping	73
3.3 Oil Transport Through the Ring Grooves	73
Inertia Driven Flow	75
Ring Pumping/Squeezing	76
Blowby Gas Dragging	79
Piston Secondary Motion	80
3.4 Ring Gap Driven Transport	82
Gas Driven Ring Gap Oil Transport	82
Inertia Driven Ring Gap Oil Transport	86
Timescale Effects of Ring Gap Transport	87
CHAPTER 4: REGIONAL ANALYSIS	88
4.1 Piston Skirt (Region Zero)	90
Cavitation	90
Oil Return to Crankcase	92
4.2 Third Land (Region One)	94
General Evolution of the Third Land	94
Second Ring Gap Effects	114
Speed and Load Effects on the General Evolution	114
Influence of Ring Type on Evolution	118
U-Flex Oil Control Ring	120
Twin Land Oil Control Ring	122
Three-Piece Oil Control Ring	132
Net Oil Transport to the Second Land	134
Impact of Third Land Experimental Study	135
4.3 Second Land (Region Two)	136
Second Land V-Cut	137
Second Land Hook	140
Net Oil Transport to the Crown Land	141
4.4 Crown Land (Region Three)	142
Top Ring Groove	143
Oil Evaporation	143

CHAPTER 5: THE ROLE OF LIF TECHNOLOGY IN MARITIME ECONOMICS & EXHAUST EMISSIONS	145
5.1 The Maritime Industry and the Environment	146
Marine Transportation System	146
Waterborne Transportation in Comparison to Other Modes	149
Marine Engines	157
Pollutants	160
5.2 Regulations	164
EU Directive 1999/32	165
EPA U.S. Clean Air Act	165
MARPOL Annex VI	169
Regulation Overview	170
5.3 Exhaust Emission Reduction Techniques	171
Primary and Secondary Measures	172
NO _x Reduction Techniques	173
Reduction Techniques for Other Pollutants	176
Reduction Technique Costs	178
5.4 Lubricating Oil	179
Medium and High Speed Marine Engines	179
Slow Speed Marine Engines	180
Anti-Polishing Ring	184
Application of LIF to Marine Engines	185
5.5 LIF Implications to the Maritime Industry	187
CHAPTER 6: CONCLUSIONS	188

CHAPTER 1: INTRODUCTION

1.1 Background

Lubricating oil consumption is a prominent concern for all internal combustion engine manufacturers concerned with controlling associated exhaust emissions and reducing service cost. Enough lubricating oil must be provided to the upper ring pack region to prevent dry running and limit friction and wear, but any excess oil will hasten oil degradation or become consumed and contribute to unnecessary oil consumption. This oil consumption leads to harmful hydrocarbon and soot emissions as well as poisoning of the exhaust after-treatment equipment [1,2,3,4]; many lubricant additives that are consumed with the lube oil, particularly ones containing sulfur, reduce the efficiency of devices such as the catalytic converter [5,6]. More recently, particulate filters have begun to be severely degraded by the ash content of the oil. Lubricating oil consumption may be the most prominent application of this experimental study, due to ever increasing government regulations, but engine friction and oil degradation are significant concerns. Ring friction on the cylinder liner, related to the ring sealing ability and thus oil consumption, is estimated to account for 10 to 20% of total friction power loss in an engine [7,8]. Oil degradation results from high temperature oxidation and combustion soot contamination [1,9], limiting the lubricant lifetime and directly affecting the oil change interval and as a result, affecting customer satisfaction.

The complex and intricate oil transport processes within the power cylinder system prevent a comprehensive understanding of the path oil takes from the crankcase to the combustion chamber [10,11,12]. This lack of understanding creates difficulty for engineers designing ring pack systems; often they must rely heavily on trial and error means to test the effects of small design changes on oil consumption, and other performance indicators. The detailed examination of oil transport mechanisms and patterns in this experimental study will decrease reliance on trial and error measures, reducing lead times and costs for new ring pack designs, as well as provide experimental data to assist analytical models predicting oil transport and consumption. The

information contained in this paper is valid for any power cylinder system, though the primary focus of this study is for oil transport on the piston ring pack of a spark ignition automotive engine.

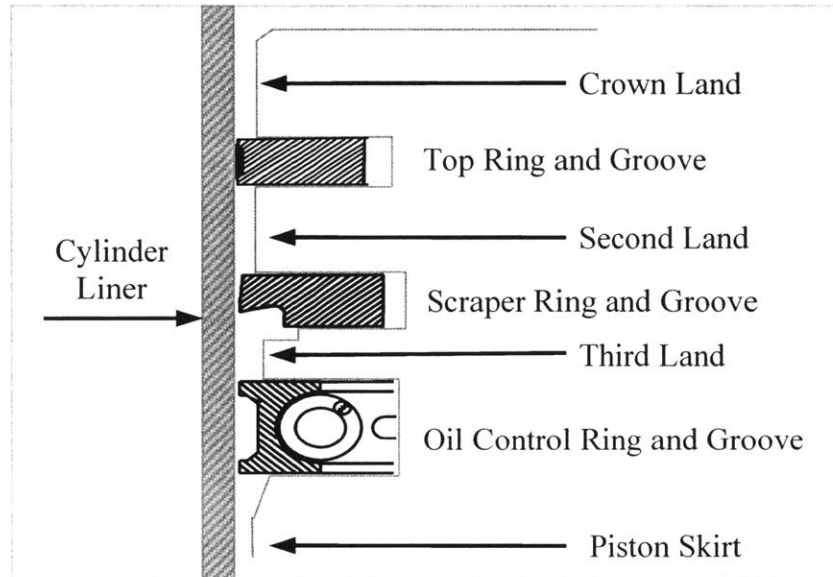


Figure 1.1 – The piston/ring/liner system

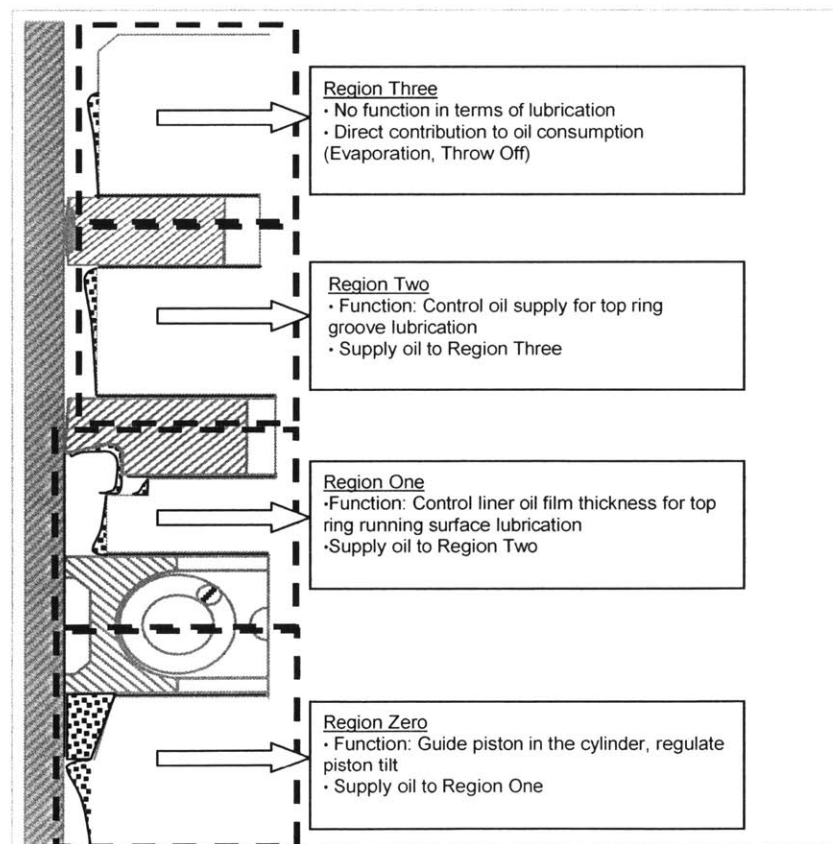


Figure 1.2 – Declaration of Regions within the piston ring pack

1.2 Lubrication Environment

The piston/ring/liner system is intricate and dynamic (see Figure 1.1). The primary function of the piston rings is to seal combustion gases within the cylinder while allowing the piston to move axially. The rings also create a path for heat to dissipate from the piston crown through the cylinder liner to the coolant. As the rings are continually sliding against the cylinder liner, and against the piston ring grooves themselves, sufficient lubrication must be present in the contact regions; the most critical region is the top ring running surface and groove as its direct link to the combustion chamber incurs the greatest pressures and temperatures in the ring pack system. The design of the ring pack system is clearly a compromise between friction, wear, and oil consumption. An oversupply of oil will certainly minimize friction and wear, but to the detriment of oil consumption. Conversely, an oil starvation situation will have low oil consumption, but high friction losses and component wear or failure. Therefore, the optimum balance lies somewhere in between. As the engine only supplies oil to the piston skirt and lower cylinder liner, it is the ring pack system that moves and distributes the oil to where it is needed. Understanding the oil transport mechanisms and patterns within the ring pack will allow them to be improved and optimized to perform the most good with the least amount of oil, thereby limiting friction and wear while lowering oil consumption.

One of the difficulties in finding this optimum solution is the number of sub-regions and flow paths; for instance, oil can flow from one land to the next through the ring groove, the ring gap, or the ring/liner interface. Further complicating the situation is the constantly changing geometry of the sub-regions. The rings are very dynamic in their grooves, moving both axially and circumferentially, as well as having various degrees of twist and waviness [12]. Beyond the complex and dynamic geometry are the many driving forces that transport oil: Pressure gradients, shear stress from gas flow, inertia forces, and mechanical transport such as ring/liner and ring/groove relative motion [13]. The pressure gradients and resulting gas flows vary greatly in magnitude and even in direction depending on engine load. Increasing a typical spark ignition automobile from idle to full load raises the absolute intake pressure from about 150 mbar to 1 bar, and it

raises the peak cylinder pressure during combustion from several bars to near 60 bars. The associated gas flows vary accordingly; at low loads the net gas flow can be toward the combustion chamber, contrasting to several liters per minute per cylinder of flow towards the crankcase at higher engine loads. Increasing the engine speed from 1,000 to 6,000 rpm increases the average inertia force induced by the piston alternating motion from about 300 to 10,000 m/s^2 , with peak inertia forces over 2,000 times the force of gravity. With this range of forces, oil transport on the piston ring pack becomes complex and dynamic as the engine operating condition is changed. The variation of these forces in orders of magnitude creates a situation where small changes in geometry of the rings, grooves, relative angles, piston lands, running surfaces, and thermal deformations have significant impact on oil transport and oil consumption, further complicating the design and optimization process. These underlying complexities require a fundamental understanding of the oil transport processes and related oil flow patterns, which can be observed experimentally with 2D LIF techniques.

1.3 Previous Work

LIF techniques have been measuring oil film thickness in the power cylinder system since at least the early 1990's, though initially quite limited in scope [14,15]. Early work used LIF in point measurements, thereby identifying the thickness of the oil film at exactly one point on the liner and piston. It was beneficial for learning the general oil film thickness; however, the oil flow, timing, and patterns were elusive as oil thickness in the region surrounding the point measurement was unknown [10,16,17]. The point LIF measurement system has been continually improved, but the inability to examine the adjacent areas to the point measurement has focused the point LIF technology towards measuring the oil thickness of the ring/liner interface [18,19]. This technology performs well for specific applications, including liner film thickness measurements during engine warm-up [20]; however, to understand oil transport on the piston ring pack the point LIF system is not adequate. For this reason, Inagaki et al. (1995) [21] developed a 2D oil distribution measuring system, utilizing a flash lamp. Even with the limitation of a narrow viewing window, the configuration clearly demonstrated the necessity of a 2D

picture to analyze oil distribution on the piston ring pack. Thirouard [13,22,23] improved on the idea by developing a 2D multiple-dye Laser Induced Fluorescence system to conduct the real time observation of oil flow patterns throughout an engine cycle. It is his exact engine and diagnostic system design that is utilized in this experimental study. The setup allows real time observation of the piston ring pack throughout an engine cycle for the entire range of operating conditions typically encountered in an automobile.

1.4 Experimental Objectives and Approach

LIF studies on oil transport by Thirouard [13,22,23] have identified the major driving forces and basic transport mechanisms for lubricating oil within the piston ring pack. His study of spark ignition (SI) and diesel engines divided the piston ring pack into specific regions (see Figure 1.2) and expressed the key elements of oil transport as: Piston alternating motion (inertia), ring and groove interaction, and blowby and reverse blowby gas dragging. While Thirouard's LIF work focused on the basic transport mechanisms and the driving forces on the entire ring pack, this study and experimental work focuses more on the oil balance throughout an engine cycle; in particular, on geometric changes to the second land and a concentrated analysis of the third land, describing the consistent evolution of the oil throughout an entire engine cycle. The geometric changes to the second land were designed to inhibit the negative effect of inertia forces, and proved to be successful at that task; however, the increased volume that resulted from the new features strengthened the negative effects of ring gap driven transport.

The concentrated analysis of critical ring pack regions focused primarily on Region One, or the third land as described in Figure 1.1 and 1.2. All experimental findings show that the greatest concentration of oil is consistently present in Region One, with much of it crossing the third land multiple times each engine cycle. Going beyond a simple description of the driving forces and transport events, this study follows the evolution of the oil throughout an entire engine cycle, describing the stable and consistent pattern that develops cycle after cycle within this Region. An oil balance was found at each operating point, where a consistent amount of oil is present on the third land, as discerned

from the repeatable timing and magnitude of the oil transport processes. Testing various piston and ring designs further substantiated the findings of the third land experimental study. The comprehensive analysis of the consistent oil evolution and balance in this Region will allow an effective oil control strategy to be developed on the third land to reduce net oil transport to the upper ring pack and the combustion chamber.

The oil distribution within the piston ring pack and the oil transport mechanisms across the ring pack regions were visualized using the 2D LIF technique. To correlate the observed oil displacements with the driving forces, one would have to know the inertia force, ring dynamics, and gas flows between the various regions of the piston ring pack, and at every crank angle. The inertia force is simply a factor of piston speed, but ring dynamics and gas flow calculations are much more complex. This real time data was enhanced through use of an elaborate piston and ring dynamic simulation code, RINGPACK-OC developed by T. Tian [12,24,25,26], which also details pressure distribution and gas flows between the ring pack regions. Cylinder pressure traces, piston expansion, and liner expansion were the main input parameters. Without a comprehensive FEA (Finite Element Analysis) effort to evaluate piston and liner deformations, it is believed a reasonable approximation of bore expansion can be found by matching the simulation's output of blowby with the actual blowby measurement at each operating point. The RINGPACK-OC code was essential for transitioning from simple viewing of the complex LIF output, to explaining the oil transport mechanisms and their origins. Knowledge of the physical forces acting within the piston ring pack allowed identification of causal relationships for the complex oil transport mechanisms viewed with the 2D LIF technique. Additionally, the effects of speed and load, as well as transient conditions, were investigated thoroughly. Their impact on the basic transport mechanisms, the second land geometrical changes, and the Region One study are all discussed in this work.

The next chapter further details the experimental setup and process. Chapter 3 overviews the basic oil transport mechanisms of the piston ring pack. The detailed study of the oil evolution throughout an entire engine cycle, including various piston and ring design

induced phenomenon, is discussed in Chapter 4. The maritime economics of 2D LIF research, in relation to both the cost effectiveness of exhaust emission reduction and to the cost savings of reduced lube oil consumption, are expressed in Chapter 5.

CHAPTER 2: EXPERIMENT CONFIGURATION

2.1 Experimental Strategy

The complexity of the ring pack geometry, and the resulting multitude of potential flow paths, requires 2-dimensional observation to understand and characterize the oil distribution on the piston ring pack. To achieve this, an optical access in the cylinder liner with an appropriate visualization technique is necessary. Laser Induced Fluorescence (LIF) is the visualization technique utilized in this experimental work; it was chosen because it can provide quantitative and qualitative images of a correctly doped media, in this case, lubricating oil. The fluorescence intensity is a function of the volume of media that is excited, and the recorded signal relays quantitative measurements of the relative volume. The intensity/volume relation also clearly relays a qualitative picture of the oil distribution on the piston ring pack. To fully characterize the oil transport processes and evolution, the oil distribution needs to be qualitatively and quantitatively linked to the amplitude and direction of the calculated driving forces, such as inertia, gas flow, and ring dynamics.

A high energy source is required to excite the fluorescence quickly, as typical automobile engines run at speeds in excess of 5,000 rpm. Utilization of a laser achieves exposure time of a few nanoseconds; for example, an exposure time of less than 1 μ s is required to obtain sharp images of the piston at 5,000 rpm [13]. Other important timescales to consider are the speed of the factors driving oil transport: A few crank angle degrees for the motion of the rings in their groove compared with one complete engine cycle for the flow of blowby gases through the entire piston ring pack. Moreover, some oil transport processes start and are completed in less than half of a piston stroke, while other transport processes occur over several engine cycles, or even several minutes. To study the evolution of the oil distribution and oil balance in the ring pack regions, experiments

were conducted for long durations and at every possible crank angle, so as to achieve a complete and thorough understanding.

2.2 Experimental Setup

The experiment centers around a single cylinder PSA spark ignition research engine, capable of operating at speeds of up to 6,000 rpm. This particular PSA engine was chosen as it offered unique characteristics for optical access. It allowed a large viewing window, about 100 mm x 12 mm, which could be placed on the thrust or anti-thrust side of the cylinder liner and view almost the entire piston stroke. The data in this experimental study was taken from the anti-thrust side.

The engine is specifically designed for research endeavors, however, it includes many parts from a 2-liter production engine such as the cylinder head, connecting rod, piston and piston rings. For better cooling control of the optical window, the cylinder liner and cylinder head have separate coolant flow paths. Many engines with modified cylinder liners cannot be operated at high loads, high speeds, or for long periods of time due to lack of effective cooling. This prevents testing of some of the most critical and severe conditions for oil consumption, as well as preventing accurate piston and liner geometry from the thermal deformation of a steady temperature distribution. Gas flows and ring motions are quite sensitive to piston geometry, thereby affecting the oil transport mechanisms. For these reasons, the cylinder liner optical access was designed to be as large as possible without restricting engine operation.

Sapphire was chosen as the window material for its superior mechanical properties. The thermal conductivity of the sapphire window is critical for minimizing liner deformation. Additionally, sapphire and cast iron have similar coefficients of thermal expansion; the thermal expansion of the window must be close to that of the liner so they expand together and maintain a gas tight seal. The viewing area is quite extensive and allows inspection of the oil transport mechanisms at virtually any point in the piston stroke.

The cooling, lubrication, and crankcase ventilation systems were carefully designed for the experimental engine to closely match a typical production engine. The oil inlet pressure, and both the lubrication and coolant temperatures, were strictly regulated.

Engine Characteristics

The PSA single cylinder spark ignition engine was specifically designed for research purposes, but includes many parts from a 2.0 liter production 4-cylinder Peugeot engine, including the cylinder head, connecting rod, piston, and rings. The cylinder head was modified to operate with only a single piston and liner. The effects of a multi-cylinder engine, and its associated bore distortion, will certainly impact oil consumption; however, the oil transport patterns and mechanisms of the piston ring pack of a production engine will not deviate substantially from the results discussed in this single cylinder work. The cylinder liner cooling jacket has been isolated from the cylinder head cooling jacket to allow more freedom in the design of the cylinder liner and optical access. An AVL pressure transducer is equipped in the cylinder head to record combustion chamber pressure throughout the engine cycle. Balancing shafts were required and equipped to allow the single cylinder engine to operate at speeds of up to 6,000 rpm. The general characteristics of the PSA single cylinder engine used in this experimental study are shown in Table 2.1.

Engine	PSA Research Single Cylinder
Type	Spark Ignition - 4 Valves
Bore	86.6 mm
Stroke	88.0 mm
Displacement	0.511 liter
Max Specific Power*	37.3 kW / liter at 5400 rpm
Max Specific Torque*	80.0 Nm / liter at 4200 rpm
Lubricant	SAE – 10W30

Table 2.1 – Characteristics of experimental engine (* specific torque and power values are for the 4-cylinder engine, from which the single cylinder engine is derived)

Optical Access

The window in the cylinder liner was designed with two main goals: To be as large as possible, and to have the ability to operate at all engine operating conditions. Most engines with a large optical access cannot operate at high loads or high speeds for more than 30 seconds from lack of effective cooling [13]. Some of the most critical conditions for lube oil consumption are high speed/high load and high speed/low load. The inability to run the engine for long durations prevents taking data at stable operating points. As ring motion and gas flows are sensitive to the exact geometry of the piston and liner, thermal deformations will have an effect on oil distribution and transport mechanisms. The engine needs to be able to operate long enough to achieve a steady temperature distribution, to truly mimic the oil transport in a passenger car.

Designed in collaboration with the PSA Research Department, the cylinder liner accommodates the largest possible window, while optimizing cooling efficiency and minimizing liner deformation. A slot was machined into the liner and a sapphire window glued into place. The sapphire window is about 100 x 20 mm (see Figure 2.1). To limit mechanical or thermal deformation around the optical access, a large steel clamp was placed to support the back of the window and seal the machined slot (see Figure 2.2). The thermal conductivity of the window material is critical, as the optical access is so large. For this reason, sapphire was chosen over the more common synthetic fused silica. Sapphire had some additional advantages over synthetic fused silica: Superior mechanical properties to resist combustion chamber pressure and a very similar thermal expansion coefficient to the cast iron liner to ensure the window and liner expand uniformly and maintain a tight seal. The window/liner seal was maintained with a high temperature, high thermal conductivity epoxy glue (ECCOBOND 276). Once the window was glued into place, the cylinder bore was carefully honed to within all tolerances (18 μm); the roughness measurements of the liner and window were between an Ra of 0.30 and 0.48 μm . The sapphire window is polished on the outside, but honed on the inside. The honed surface is not optically clear, but as the refraction index of oil is very close to that of sapphire (1.55 compared to 1.77), the roughness cavities fill up with

oil during normal engine operation, become transparent, and allow clear observations of the oil distribution.

The final viewing area is quite extensive and allows inspection of the oil evolution and transport mechanisms at virtually any point in the piston stroke. The viewing area is 98.5 x 18 mm and extends from bottom dead center (BDC) of the oil control ring to top dead center (TDC) of the second compression ring.

Coolant System

As discussed in the Optical Access Section above, the cylinder liner cooling jacket was designed to optimize the cooling efficiency of the window area (see Figure 2.2). Fresh coolant flows into the steel clamp, and then into the liner jacket through six holes located symmetrically around the window. This assists homogenous cooling of the entire sapphire window. The coolant then flows around the liner and exits the jacket on the opposite side of the window.

To minimize temperature flux within the cylinder liner, the coolant temperature difference between the inlet and outlet of the cooling jacket was curtailed by equipping the system with a high flow rate pump. The pump sustains a 50 liter/minute flow rate with 2 bar backpressure, and is 4 times what is normally used for single cylinder engines of this size. The coolant inlet temperature for the system was regulated at 50°C for all tests.

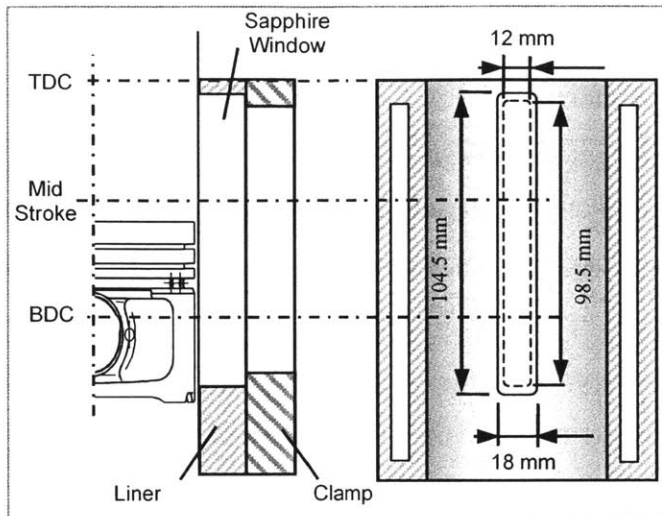


Figure 2.1 – Dimensions and position of the sapphire window installed in the cylinder liner

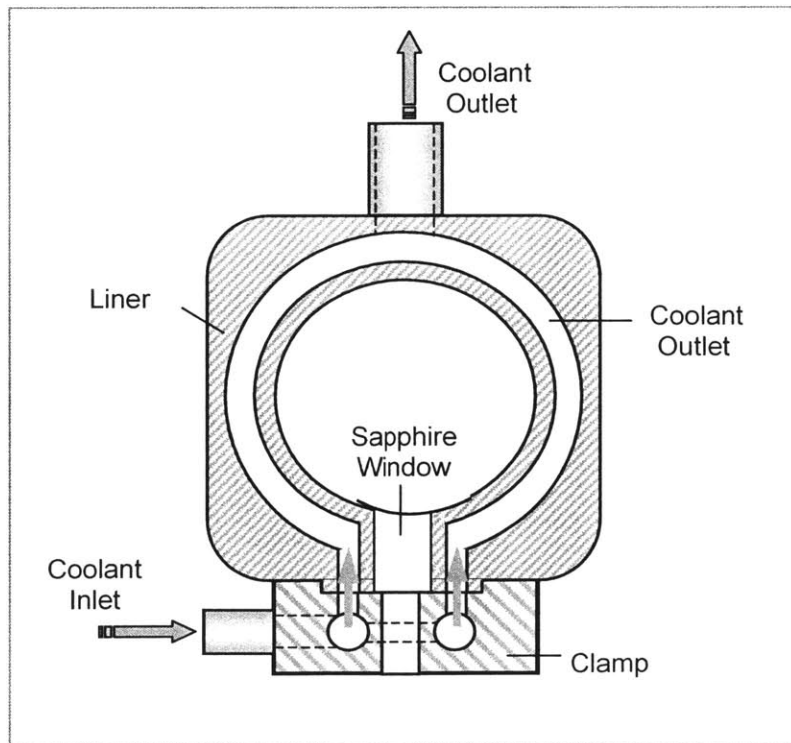


Figure 2.2 – Cylinder liner, clamp, window, and coolant flow arrangement

Lubrication System

The lubrication system for this single cylinder PSA engine was designed to behave similar to a production engine. As the focus of this experimental study is oil transport, it is necessary to replicate the lubrication conditions of a typical passenger car as closely as possible. Lubricating oil is delivered to the single cylinder engine at a chosen temperature and pressure. As the engine operates with a dry sump, the lubricant is stored in an external tank that includes a heat exchanger and electric heater. One pump takes suction on this tank and directs the oil into the engine, with the pressure regulated by a standard relief valve and recirculation line. Another pump, a variable speed type, takes suction on the crankcase and delivers the oil back to the external tank. This scavenging pump is variable speed to limit the amount of crankcase vapor circulated through the oil tank. As blowby flow rate is an important measurement to this experimental work, the crankcase and the sealed lube oil tank are piped together to avoid any pressure build up between them. Figure 2.3 is a schematic of the lubrication system.

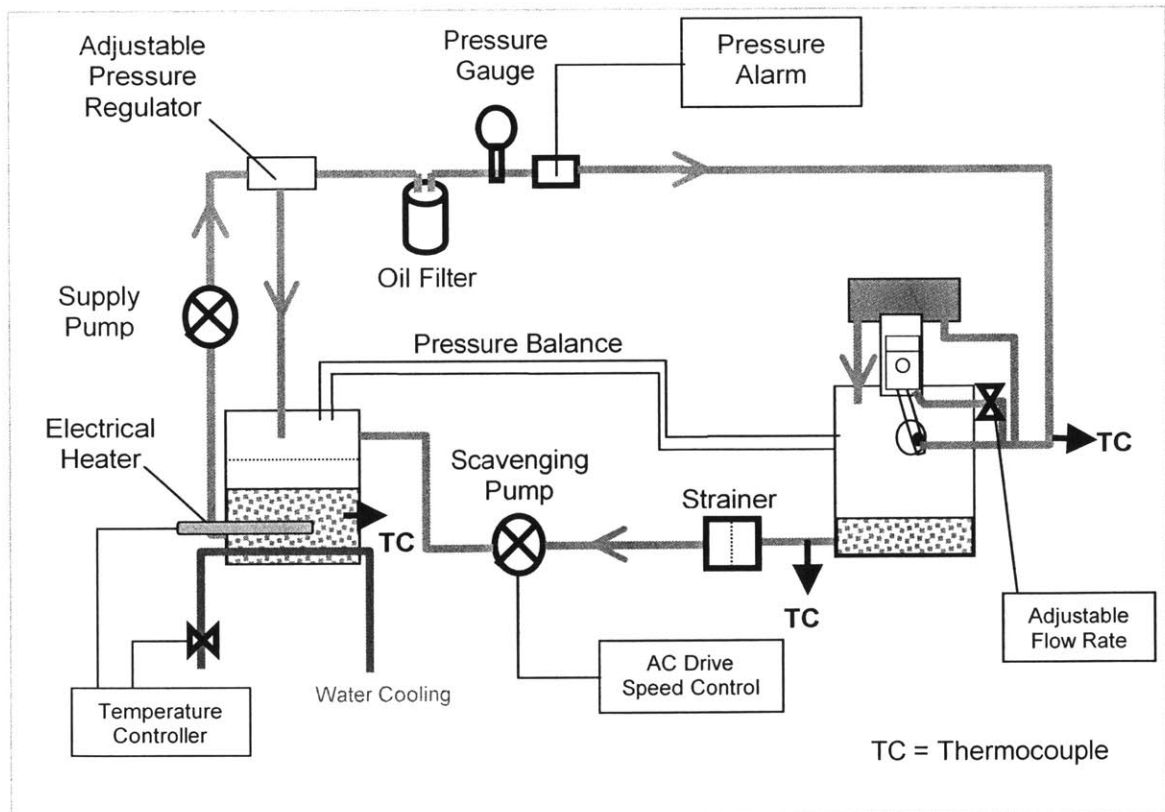


Figure 2.3 – Lubrication System

2.3 Data Acquisition

Fluorescence Overview

The fluorescence process involves three main stages that occur in certain molecules called fluorophores or fluorescent dyes [27]. The three stages are outlined below in words, and visually in an electron state diagram shown in Figure 2.4.

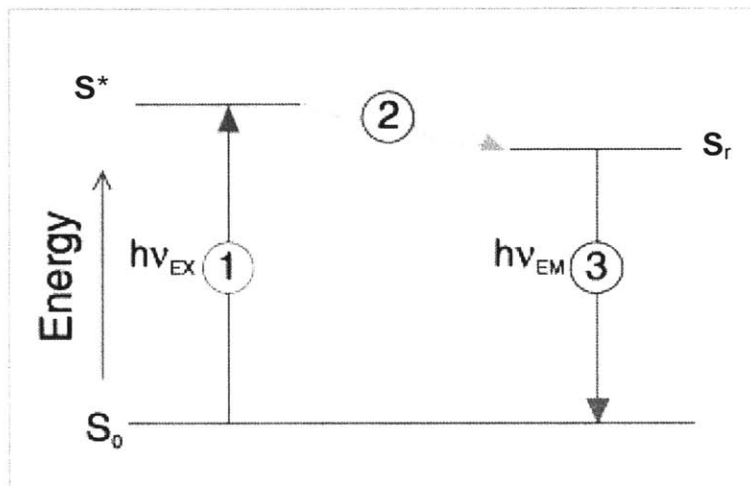


Figure 2.4 – Fluorescence process

Stage 1 is excitation. An excited electron singlet state S^* is created when the fluorescent dye absorbs a photon of energy h_{ex} (wavelength ν_{ex}), often supplied by an external source such as a laser or flash lamp. Stage 2 is the lifetime of the excited state, generally 1 to 10 nanoseconds. During this lifetime, the fluorophore undergoes conformational changes and is subject to possible interactions with the environment. Two main consequences result: First, the energy of S^* is partially dissipated, regressing to a relaxed singlet state S_r from which the fluorescence emission originates, and secondly, some of the particles will undergo collisional quenching or fluorescence energy transfer, acting to depopulate S_r without fluorescence emission. The ratio of the number of fluorescent photons emitted to the number of photons absorbed, is the fluorescence quantum yield. Stage 3 of the fluorescence process is fluorescence emission. As the fluorophore returns to its ground state S_0 , a photon of energy h_{em} (wavelength ν_{em}) is emitted. Because of the energy dissipation during Stage 2, the energy of the emitted photon is lower than the excitation photon, and therefore the wavelength of the emitted photon is longer than the excitation

one. This wavelength disparity is known as the Stokes Shift, and is fundamental to fluorescence technique as it allows the emission photons to be isolated from their excitation counterparts. After the fluorescent emission, the fluorophore is ready to be excited again; this process can occur indefinitely, unless the fluorescent dye is irreversibly destroyed, such as through photobleaching.

For polyatomic molecules in solution, as in this experimental work, the discrete electron transition represented in Figure 2.4 is replaced by broad energy spectra called the fluorescence excitation spectrum and the fluorescence emission spectrum (see Figure 2.5). For the same reasons discussed above, these spectrums are independent of each other due to the partial dissipation of excitation energy during Stage 2, the lifetime of the excited state. The specific bandwidths of these spectra become particularly important in applications of two or more fluorescing dyes.

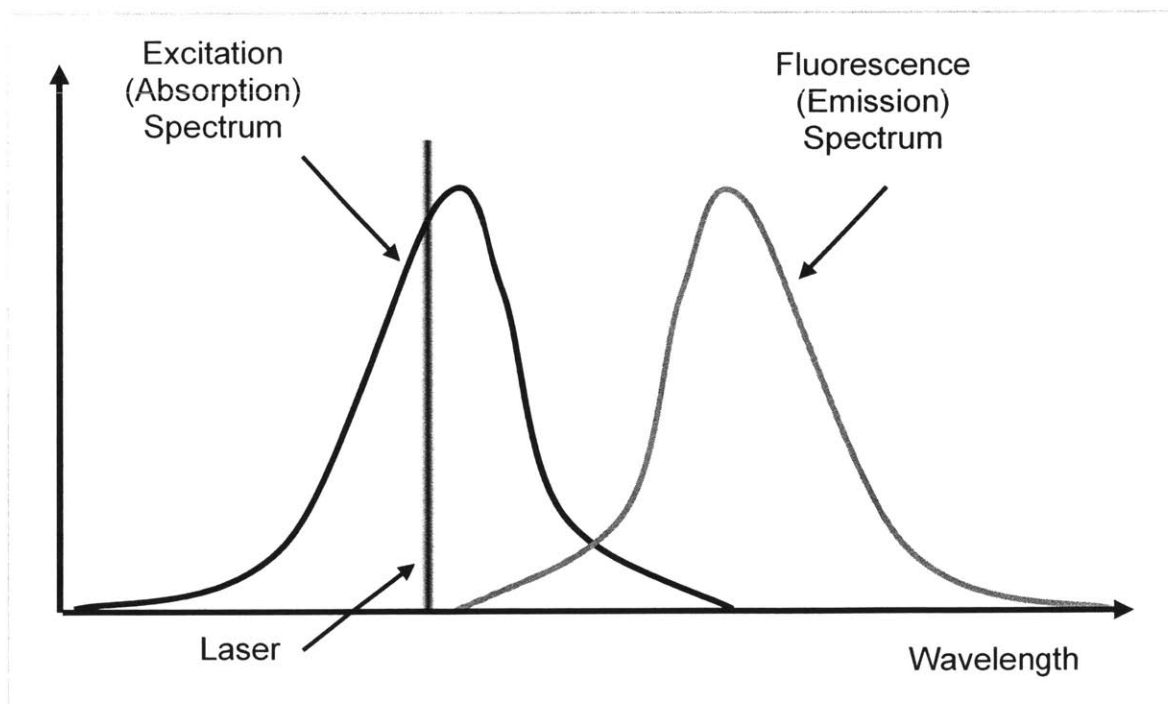


Figure 2.5 – Excitation and emission spectrum

Laser Induced Fluorescence (LIF) Calibration

The selection of the type and quantity of the fluorescence dye to mix into the lube oil must take into consideration the harsh environment of the piston cylinder system. The temperature of the fluorescence doped oil on the piston can be assumed to be equal, or close to, the piston surface temperature. There is a significant temperature gradient along the piston while firing [28], with a strong correlation to engine load, where crown temperatures can exceed 250°C while the skirt is a mere 80°C. The fluorescence efficiency of most dyes is sensitive to temperature, with some common dyes having no detectable fluorescence emission at 170°C [13], and others changing their molecular structure and permanently losing the ability to fluoresce when exposed to high temperatures. This clearly would impact the benefit of LIF images on determining true oil distribution throughout the ring pack, and thus careful selection of the oil/dye mix was necessary.

Thirouard [13] performed the work to find a combination of dyes that reduced the thermal effect on the detected fluorescence to an extent that relative oil film thickness could be obtained without the need to account for temperature variations. Different dyes have independent responses with regard to fluorescence emission strength and temperature variation. Finding a combination of dyes that behave very dissimilarly to temperature is one approach to this problem, thereby reducing the combined solution's temperature sensitivity of the detectable fluorescence emission. This effect originates from the spectral interactions that can occur when two dyes are mixed together (see Figure 2.6). To have an effective dye combination, both dyes must first have overlapping absorption spectra if a single excitation device is to be used. Secondly, the two emission spectra must be independent enough so that the fluorescence from each dye can be measured separately. Depending on the amount of Stokes Shift, there will often be an overlap between the emission spectrum of one dye and the absorption spectrum of the other. The result is a phenomenon called pumping, where the fluorescence emission from one dye is partially absorbed by the second dye. The detectable fluorescence of the first dye will be reduced, and the emission of the second dye increased, as it is now being excited by both the laser and the pumping effect of the first dye.

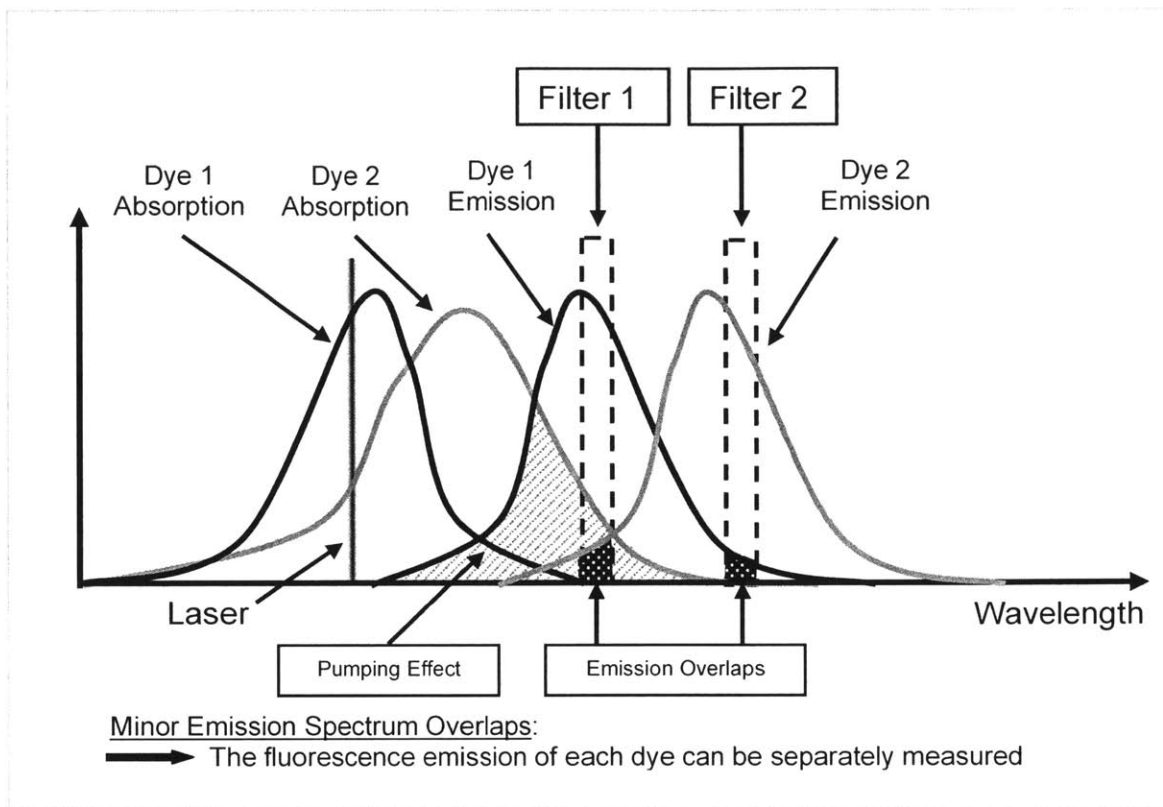


Figure 2.6 – Absorption and emission spectra for two dyes with minimal emission overlap, and substantial pumping effect

The list of potential dyes for this work was first narrowed by the desire to use the second harmonic of an Nd-Yag laser (532 nm) as an excitation source. This source was chosen as it is fairly safe, in the green spectrum (as opposed to non-visible), and easy to operate. The next step was to exclude all dyes with a melting temperature below 200°C, and those not soluble in lubricating oil. Thirouard tested the top ten choices for quantum yield efficiency, high temperature stability, and temperature sensitivity. Six dyes were found acceptable, with two combinations of them providing emission spectra far enough apart to measure the fluorescence signals independently: Pyrromethene 567 + Rhodamine 640 and Pyrromethene 650 + Rhodamine 590. As discussed above, dyes with the most different temperature response will provide the least temperature sensitive oil film thickness measurements. As Pyrro 650 and Rhod 590 were found to have a very similar behavior to temperature changes, the optimum dye combination was Pyrro 567 and Rhod 640. Once the dyes were chosen, Thirouard began working to find the optimum concentrations. To minimize the effect of temperature variation on the fluorescence

emission of the oil/dye solution, the optimum concentration of dyes was found to be: 1.0×10^{-4} mol/liter of Pyrromethene 567 and 1.0×10^{-4} mol/liter of Rhodamine 640. The effect of temperature on the relative fluorescent intensity of the solution with these dye concentrations is shown in Figure 2.7. To maintain the integrity of this oil/dye solution, the 8-liter doped oil supply is replaced every 20 hours of engine operation to mitigate any bleaching effects or carbon buildup in the oil.

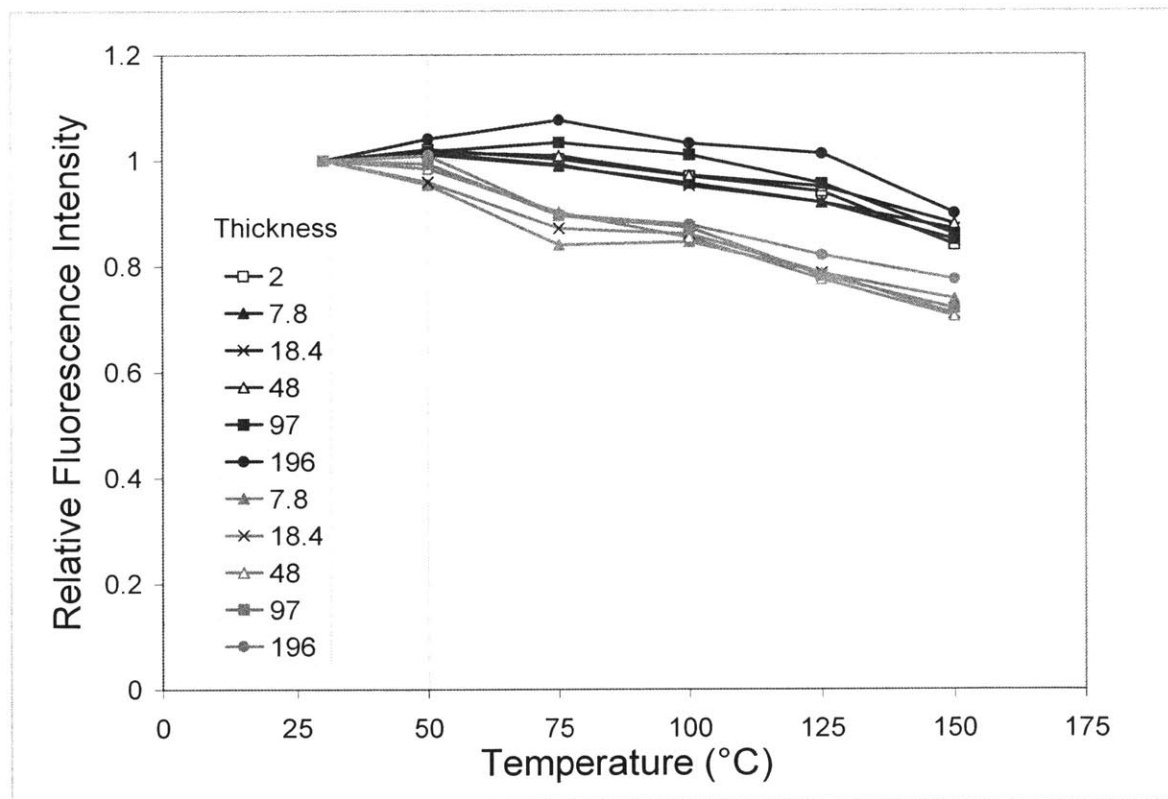


Figure 2.7 – Temperature response of Pyrromethene 567 (1.0×10^{-4} mol/liter) and Rhodamine 640 (1.0×10^{-4} mol/liter) while mixed together in SAE 10W30 lubricating oil

Imaging System

The imaging diagnostics for this experiment relies on 2D LIF technology. The engine oil, doped with a combination of fluorescing dyes, is excited by the second harmonic of an Nd-Yag pulsed laser (wavelength 532 nm). Thus resulting fluorescence signal emitted by the dye molecules is isolated from the laser light by a narrow band-pass filter and recorded by an intensified Charge Couple Device (CCD) camera. An overview of the imaging system is shown in Figure 2.8.

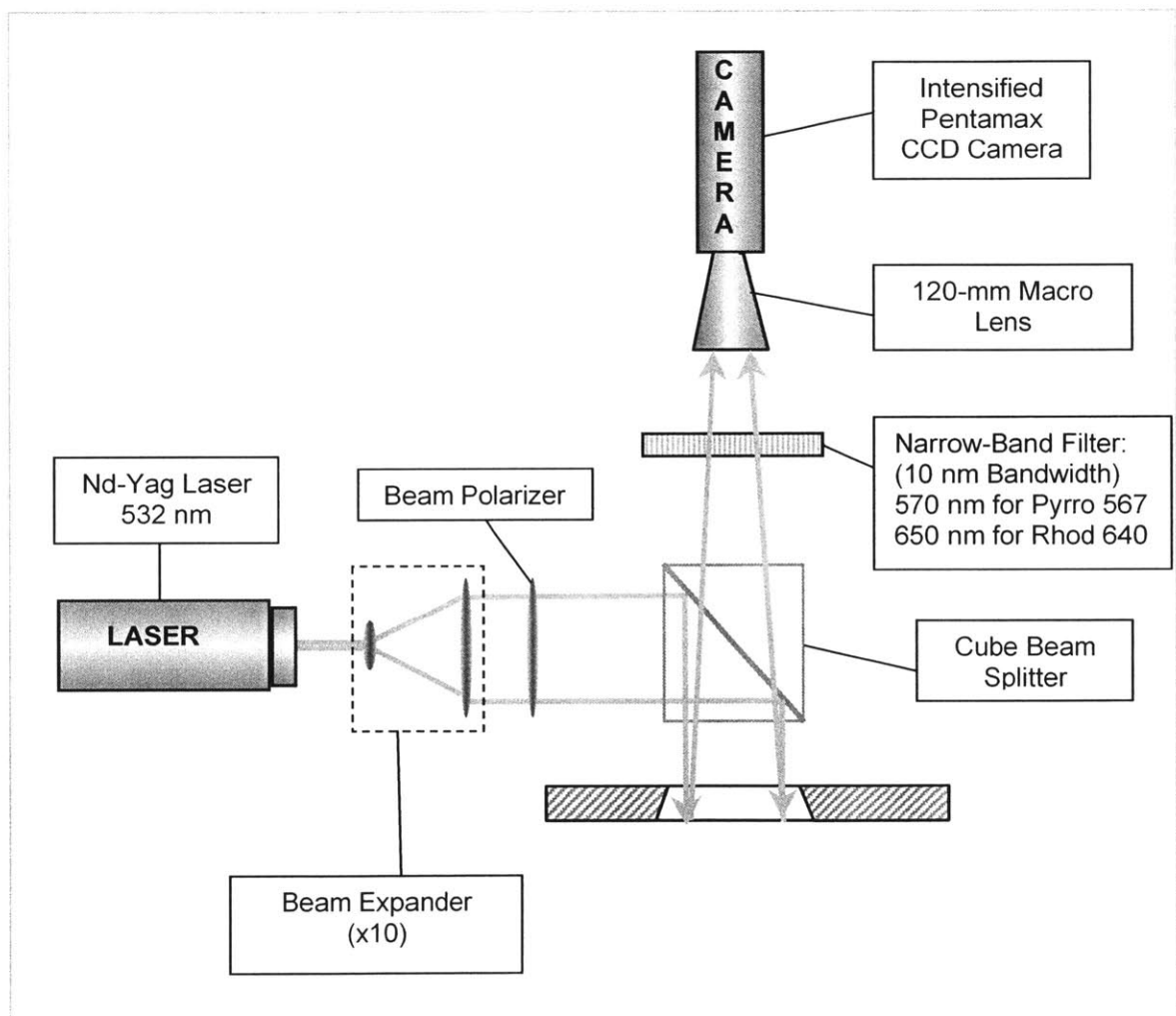


Figure 2.8 – Overview of the imaging system

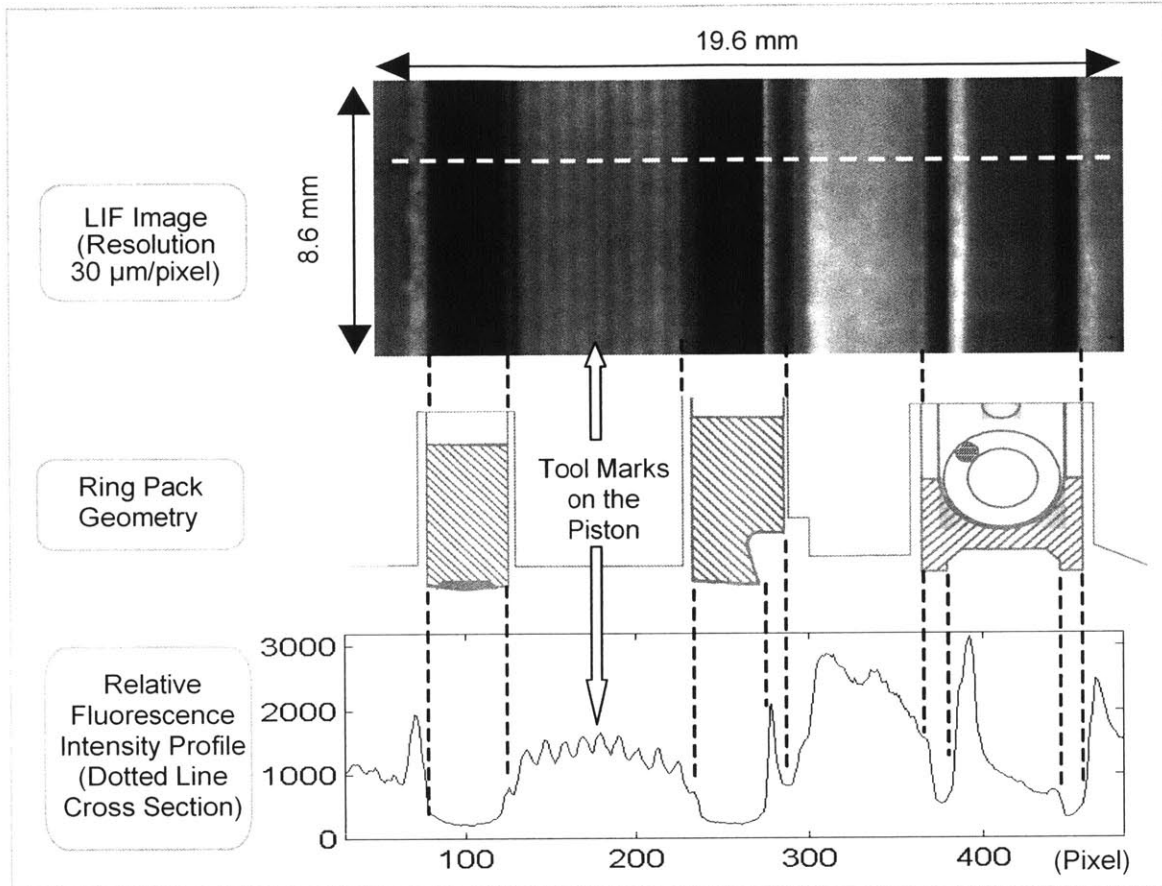


Figure 2.9 – Sample Laser Induced Fluorescence (LIF) image of the oil distribution on the piston ring pack (intake stroke, 30 CAD after TDC, 3500 rpm, medium load)

An example of the oil distribution image obtained with this 2D LIF technique is shown in Figure 2.9. This image was taken at an operating condition of 3500 rpm, with an absolute intake pressure of 500 mbar. The ring pack, which is also shown in the figure, contains a barrel faced top ring, Napier style second ring, and Twin Land oil control ring. The 2D LIF image is a measure of relative fluorescence intensity; the greater the thickness of oil, the greater the intensity recorded. A clear picture of oil patterns can then be discerned, as an accumulation of oil will appear brighter, regardless of whether the surrounding region is void of oil or covered by a thin film. Similarly, the geometric features of the piston and ring can be seen. The darkest regions are where the rings are pressed against the cylinder liner, as little oil is between the running surface of the ring and the liner. Another easily distinguishable feature is the tool marks on the piston

second land (the region between the top two compression rings); it appears as stripes, because the valleys of the cuts contain some oil and only a small film exists on the peaks.

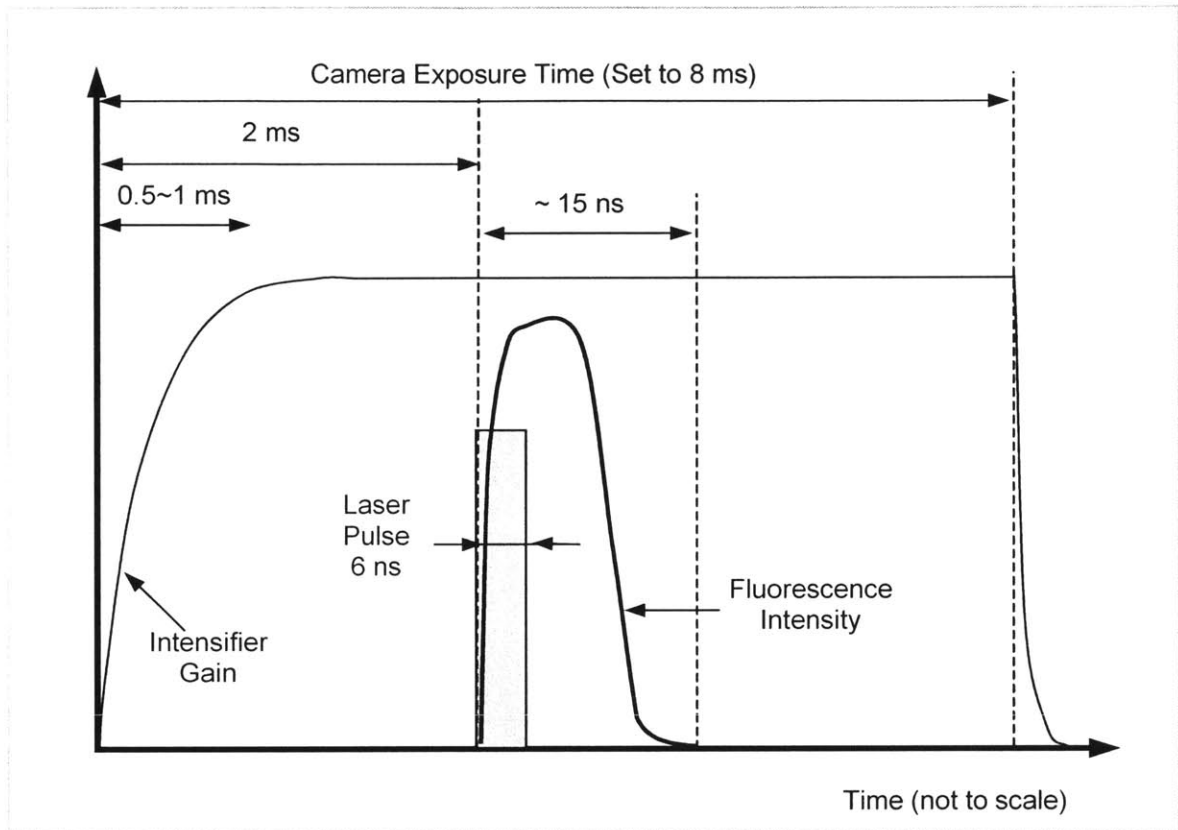


Figure 2.10 – Camera and laser timing

As stated, the excitation source for this experimental study is an Nd-Yag pulsed laser operating in the second harmonic (green spectrum). Ultraviolet lasers are more suitable for LIF experiments as they can utilize a wide range of dyes; however, this specific 532 nm wavelength laser was chosen for its availability and safety, as the laser light is in the visible spectrum. This choice of laser was a strong limitation in regards to suitable fluorescence dyes. In order to obtain sharp images at engine speeds of up to 6,000 rpm, the exposure time of the imaging system had to be less than $1 \mu\text{s}$ [13]. Pulsing the excitation source or utilizing a high-speed electronic shutter camera can both obtain the required short exposure time. The method of pulsing the laser was employed in this work, with the laser pulse lasting only 6 nanoseconds. The fluorescence process, triggered by the laser excitation, generally has a duration of 1 to 10 nanoseconds. Fluorescence emission, therefore, will last between 7 and 16 nanoseconds. Activating

and deactivating the image intensifier controlled the camera shutter. This operation was controlled by a 1,000 volt pulse generator, which had the limitation of a 1 millisecond minimum duration. Consequently, the resulting signal acquired by the CCD camera was the integration of the fluorescence emission over the possible 16 nanoseconds of the fluorescence process. The 1,000 volt pulse required to drive the intensifier had a rising time of about 1 ms. This meant full intensification was only available after 1 ms of intensifier operation, and therefore, the acquisition of the LIF images was timed so that the intensifier was activated 2 ms prior to the laser pulse. A chart of the camera and laser timing is shown in Figure 2.10.

The power output of the Nd-Yag laser was approximately 20 mJ/pulse, with a maximum repetition rate of about 20 Hz. The 20 mJ/pulse is adequate for the visualization needs in this experiment; however, it is believed a 100 mJ/pulse laser would be more suitable, as less intensifier gain and/or a smaller lens aperture would be necessary [13]. The beam profile at the output of the laser, or near field, was roughly Gaussian. As the divergence of the beam changes its profile along the beam path, the beam was found to exhibit a 'top hat' profile about two meters from the laser head, or far field. This latter profile resulted in a nearly uniform intensity distribution, and is more appropriate for detailed LIF measurements; therefore, the laser was aligned in the far field where its profile was optimal for oil film thickness evaluations. The maximum repetition rate of about 20 Hz enables data to be taken once each engine cycle at speeds of 2,500 rpm and below, and once every other cycle for speeds between 2,500 and 5,000 rpm. This recording rate was quite adequate to gain an understanding of the transport mechanisms and oil distribution along the piston ring pack.

As with most lasers, the total energy delivered each pulse was found to vary, but was maintained under +/- 3% by allowing the laser temperature to stabilize and maintaining the cavity chamber free of oxidation. Beam profile variations from the continuously changing thermal loading of the Nd-Yag rod were significantly attenuated by operating the laser in the far field. The other major conditioning to the laser was expansion. The

diameter of the beam at the laser head was 2.5 mm. To record the entire ring pack region, the beam was expanded by a factor of 10.

The expanded beam was then polarized, and directed into the cylinder by a cube beam splitter (see Figure 2.8). The cube beam splitter was necessary due to the geometrical limitations of the optical access. A cube beam splitter is preferred over a dichroic mirror because it does not produce ghost images; however, the disadvantage of a cube beam splitter is that it equally transmits and reflects all wavelengths. This results in 50% of the incoming laser light being transmitted away from the engine, and 50% of the emitted fluorescence reflected away from the camera. Therefore, 75% of the laser energy is not in the detectable signal. A cube beam splitter is quite sensitive to beam polarization, and thus the laser beam was polarized to optimize the portion of laser light reflected into the engine. This adjustment takes advantage of the fact that the portion of the transmitted and reflected light depends on the direction of polarization of the incoming light. As a result, the amount of laser energy lost was reduced to only about 50%.

An intensified CCD camera (Princeton Instrument Pentamax 512) was used to acquire the fluorescence emission as a two-dimensional image of the oil distribution. The intensification feature was necessary due to the relatively low power laser utilized in this experiment; the intensifier was generally set to about one-third its possible gain. One previous work on oil film thickness used the same excitation wavelength as this study, but with no intensification. That particular experiment required a laser 5 times as powerful and up to 100 times the fluorescence dye concentrations as in this work [29].

The CCD panel of the camera contains 1,024 X 512 pixels, and is divided into two parts. Evenly divided into sections of 512 X 512 pixels, one side is exposed for image acquisition, while the other is permanently concealed and used as a memory buffer. By transferring an image from the exposed part of the panel to the memory buffer, another image can be acquired while the previous one is being read, converted, and downloaded to a computer. The minimum time between frame acquisitions, therefore, is simply determined by the time necessary to shift the frame from one side of the CCD panel to

the other, or about 1 ms. The camera is equipped with a 120-macro lens, which produces an image resolution as high as 30 $\mu\text{m}/\text{pixel}$ onto the 512 X 512 CCD panel. To mitigate any noise resulting from thermally induced charge buildup on the CCD panel, the cooling feature of the camera was employed to maintain the CCD panel at -20°C . The CCD panel did exhibit significant blooming, however, preventing a very thin oil film thickness, which is adjacent to a very thick oil accumulation, from being measured accurately as the exact border between the regions would become slightly blurred or averaged.

The camera is also equipped with a 12-bit, 5 MHz Analog/Digital (A/D) converter. The 12-bit dynamic range was found to be more than adequate to detail the range of oil film thickness encountered in this study. When in continuous operation, the A/D converter can output up to 15 full frames per second (fps) and up to 30 half-size fps. As the engine's optical access is rectangular in shape, only a half frame is necessary to capture its entire width; therefore, the 512 X 256 pixel half frame was used, allowing the camera to output 30 frames per second (30 Hz). This maximum frame rate allows the camera to record data once every engine cycle at speeds up to 3,600 rpm.

A continuous acquisition setup was controlled with a programmable counter-board, arranging for the proper timing of the LIF image acquisition with the piston position. One image of the oil distribution was acquired every engine cycle, at a pre-selected crank angle, for speeds of 2,500 rpm and below. The maximum laser repetition rate of 20 Hz limits LIF image acquisition to every other engine cycle at speeds between 2,500 rpm and 5,000 rpm, and to every third cycle at speeds above 5,000 rpm.

The camera is equipped with both a digital and a video output. The digital output allows a chosen number of snapshots to be taken, whereas the video feature allows real time viewing of the oil distribution and evolution. The real time video output is saved by a digital video recorder, which can easily handle 10 minutes or longer of data acquisition. It operates in the continuous acquisition setup described above, where an image of the oil distribution is acquired once every engine cycle, at one specific piston position. The video rate is limited by the 30 half-size frames per second rate described above, and

independent of engine speed. This means each new video frame did not always correspond to a new oil distribution image. Each time the video signal was refreshed (30 times per second) the last frame acquired by the CCD panel was sent to the digital video recorder. As the acquisition of the LIF images is limited by the laser pulse repetition rate of about 20 Hz, the video rate (30 Hz) is always greater than the acquisition rate; therefore, every image acquired by the CCD camera was displayed on the video output. The timing of the image acquisition and video frame output is displayed in a chart for different engine speeds in Figure 2.11. A schematic diagram for the engine and data acquisition controls is shown in Figure 2.12.

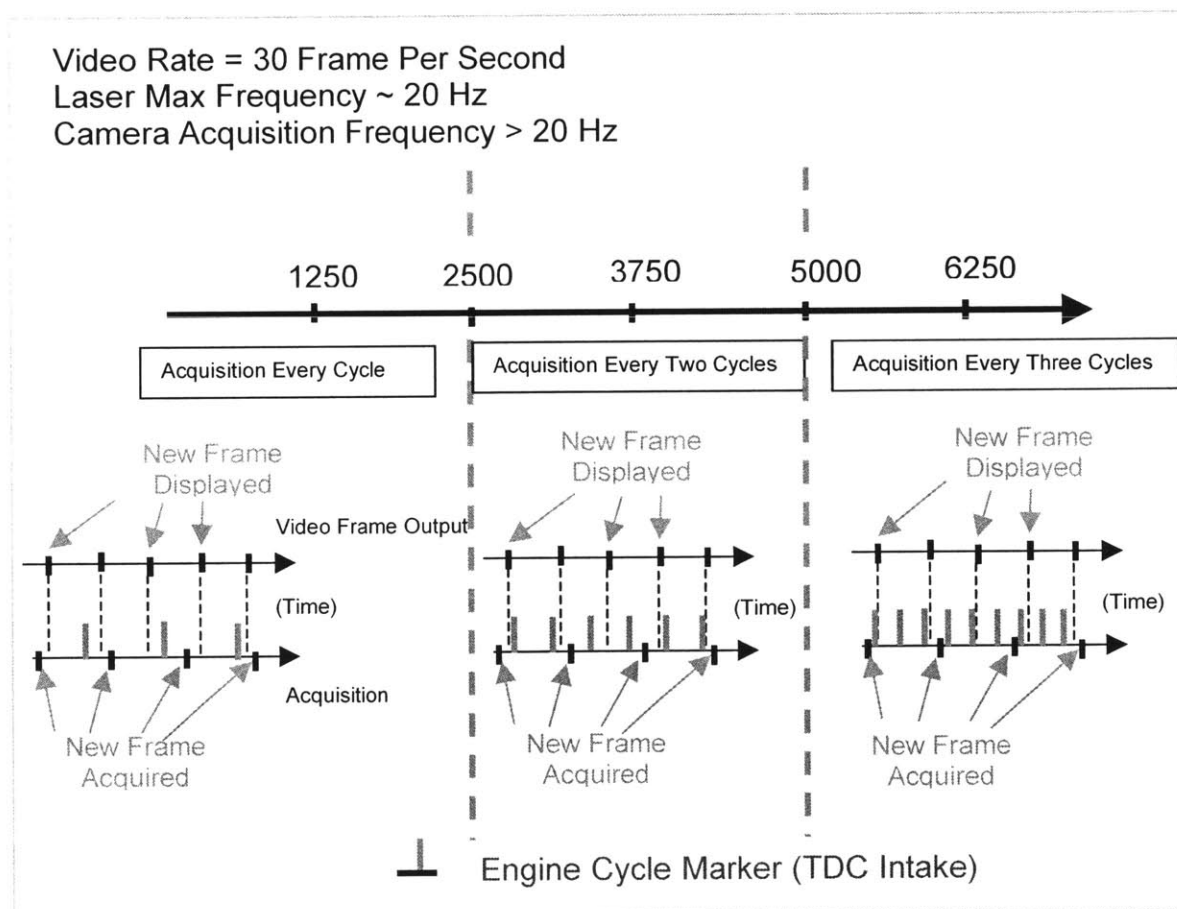


Figure 2.11 – Timing of the LIF image acquisition and video frame rate

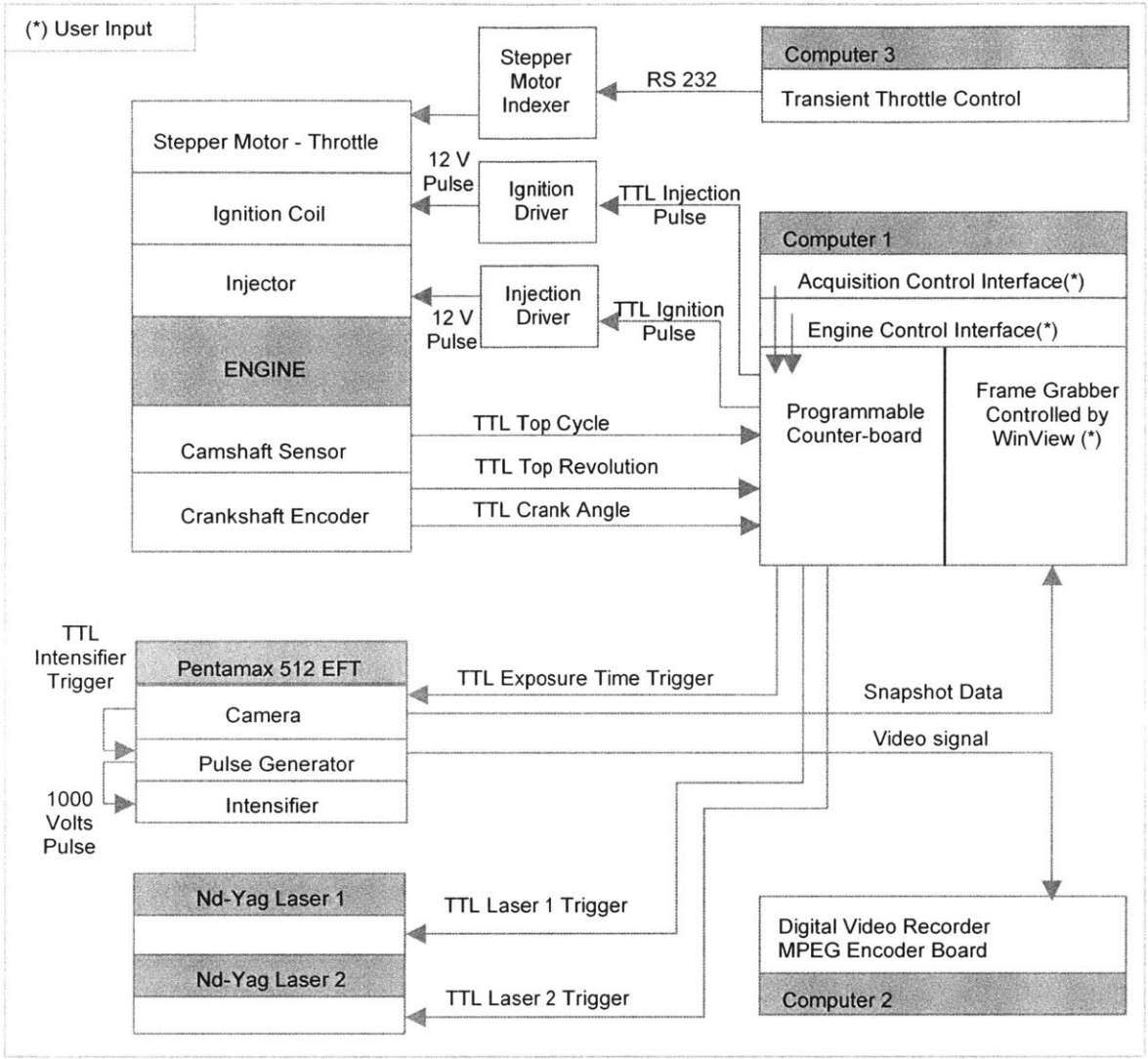


Figure 2.12 – Engine and LIF acquisition control diagram

Blowby Measurement

This experimental study requires accurate blowby measurement to correctly evaluate the recorded LIF oil distribution images. As previously discussed, blowby has a strong influence on ring dynamics and oil transport through the many sub-regions of the piston ring pack. Accurately measuring the blowby flow rate is fairly involved, particularly for a single cylinder engine.

The first challenge of blowby measurement stems from the nature of the blowby gases itself. Blowby gases commonly contain contaminants such as soot, oil droplets, and a considerable amount of water; this inhibits the use of sensitive flow measurement devices like laminar elements or rotameters. Displacement flow meters would work effectively, but only over long measuring periods. A meter such as this would lack the real time blowby information required to couple it with the real time LIF images. Two common gas flow measurement means are the vortex shading technique and the orifice pressure drop method. Either type will provide accurate blowby readings, but only between the range of a few liters per minute (lpm) to several hundred. A 0.5 liter displacement single cylinder engine, such as the one used in this work, will generally only produce a blowby flow rate between 0.2 and 15 lpm, making both the vortex shading and orifice pressure drop technique not feasible [13]. This lack of adequate equipment in the marketplace forced a customized blowby measurement device to be developed for this engine.

The second major challenge of blowby measurement is the dampening of flow pulsations, originating from cylinder pressure peaks during combustion and also from piston alternating motion. The latter source of flow pulsations, piston alternating motion, is almost negligible in multi-cylinder engines as the crankcase volume is held constant; the volume displaced by one piston is compensated by the volume swept by another one. Therefore, piston alternating motion is not a source of significant blowby pulsations in a typical automobile. In the single cylinder engine, however, the crankcase volume variation induced by the alternating piston motion can create an oscillating flow up to 4 orders of magnitude greater than the average engine blowby rate [13]. To dampen these oscillations, an attenuation device was designed to be able to focus the measurement on only the engine blowby rate. As Benoist Thirouard constructed this experimental engine and testing equipment, he designed a low-pass acoustic filter to be placed between the engine and the blowby flow meter. The pulsations caused by combustion pressure peaks are much smaller in amplitude and occur at half the frequency of the piston alternating motion oscillations, and thus are easily suppressed by the low-pass filter.

The requirements on the low-pass filter were optimized to limit the size of the components. To keep the maximum oscillation level below 0.1 liter/min, the filter had to achieve a minimum attenuation of 80 dB at 16 Hz (1,000 rpm) and 100 dB at 100 Hz (6,000 rpm). It was also essential not to disturb the gas flow through the ring pack, as this was the focus of the measurement, and so it was necessary to limit the crankcase pressure variation to 10 mbar. To achieve this, the acoustic filter was designed so that the resonance frequency associated with the crankcase pressure would be lower than the frequency corresponding to an idle engine speed, about 1,000 rpm.

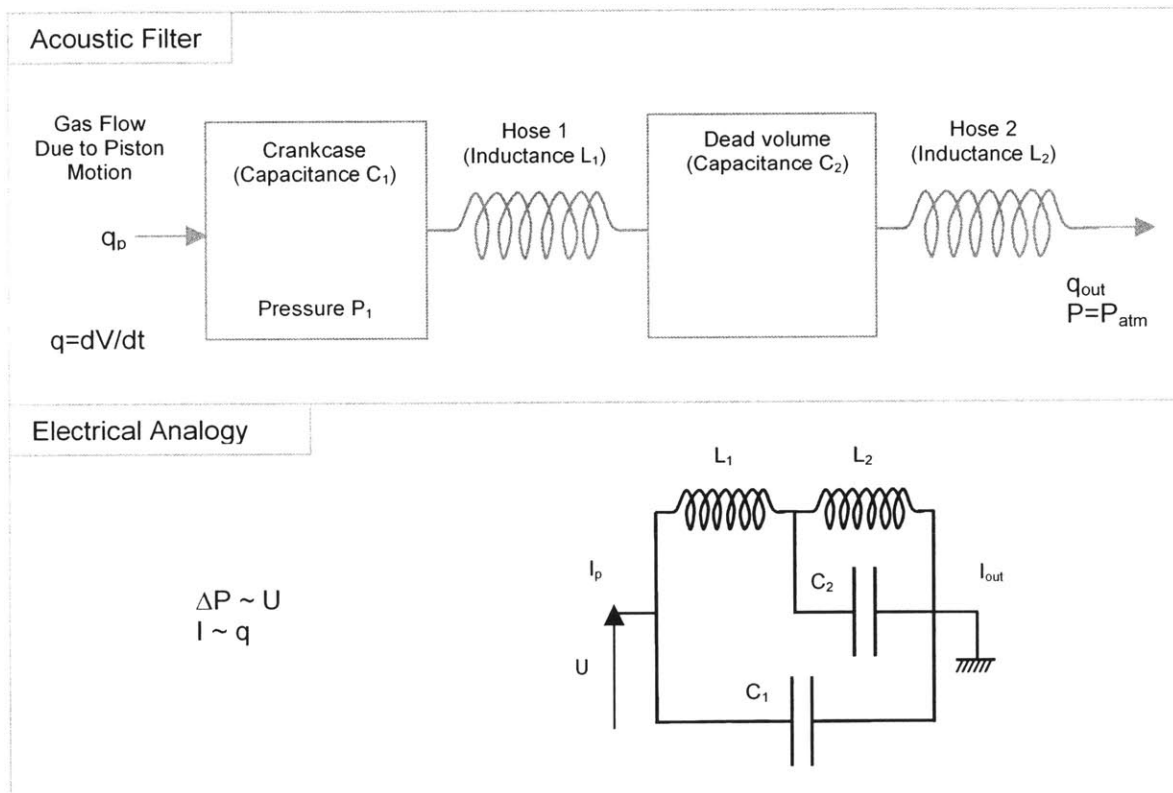


Figure 2.13 – Fourth order acoustic filter and electrical analogy

An acoustic filter is generally composed of various volume elements and hoses, which act as capacitance and inductance to the system respectively. If a simple first order filter were designed to achieve the requirements above, a 120 m³ container would be required to achieve the attenuation level; a higher order filter was the more practical solution. Thirouard decided upon a fourth order, low-pass filter composed of two volumes and two hoses, with the aim to minimize the container volumes. The crankcase volume was set as the first capacitance, with the other volume, hose lengths, and hose cross sections

optimized. The acoustic model, and corresponding electrical analogy, for this fourth order filter is shown in Figure 2.13. The final dimensions of the various components are detailed in Figure 2.14.

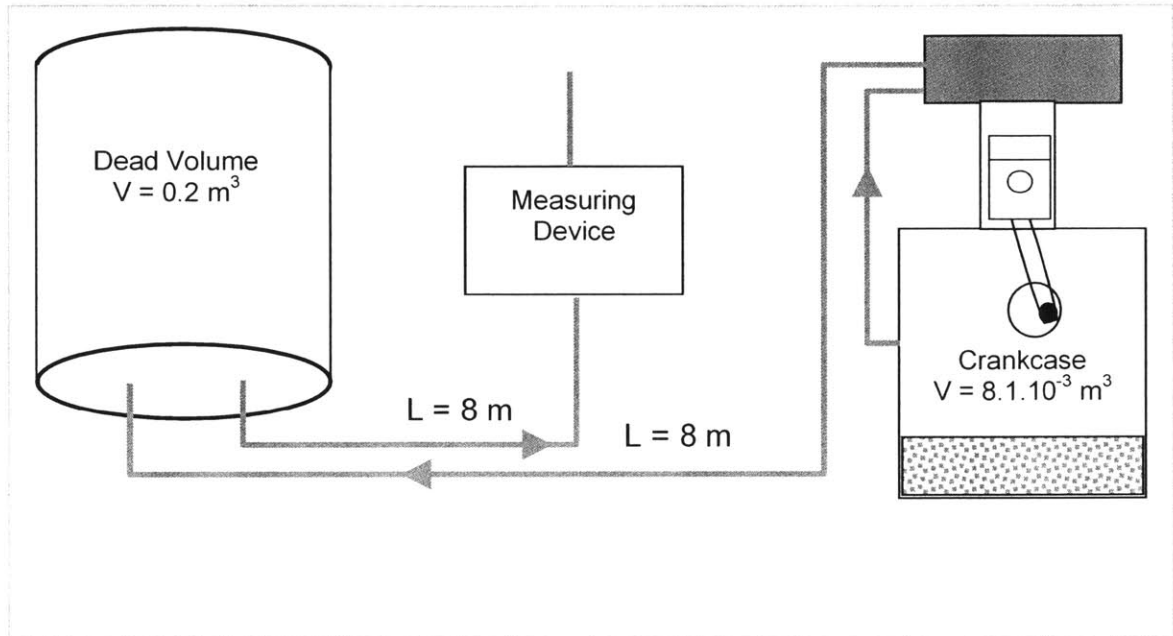


Figure 2.14 – Actual acoustic filter employed

The attenuation of the designed filter, as found by Thirouard, is shown in Figure 2.15 [13]. It can be seen that the amplitude of the filtered blowby oscillations is lower than 0.1 liter/min at any engine speed between 1,000 and 6,000 rpm. Compliance with the other major stipulation, avoidance of the engine resonant frequency with the crankcase pressure variation, is shown in Figure 2.16 [13]. The resonance frequency of the crankcase pressure, near 3 Hz (180 rpm), is well below the average idle speed for an automotive engine. These two figures show how the designed acoustic filter achieved the required attenuation without amplification of the crankcase pressure variations.

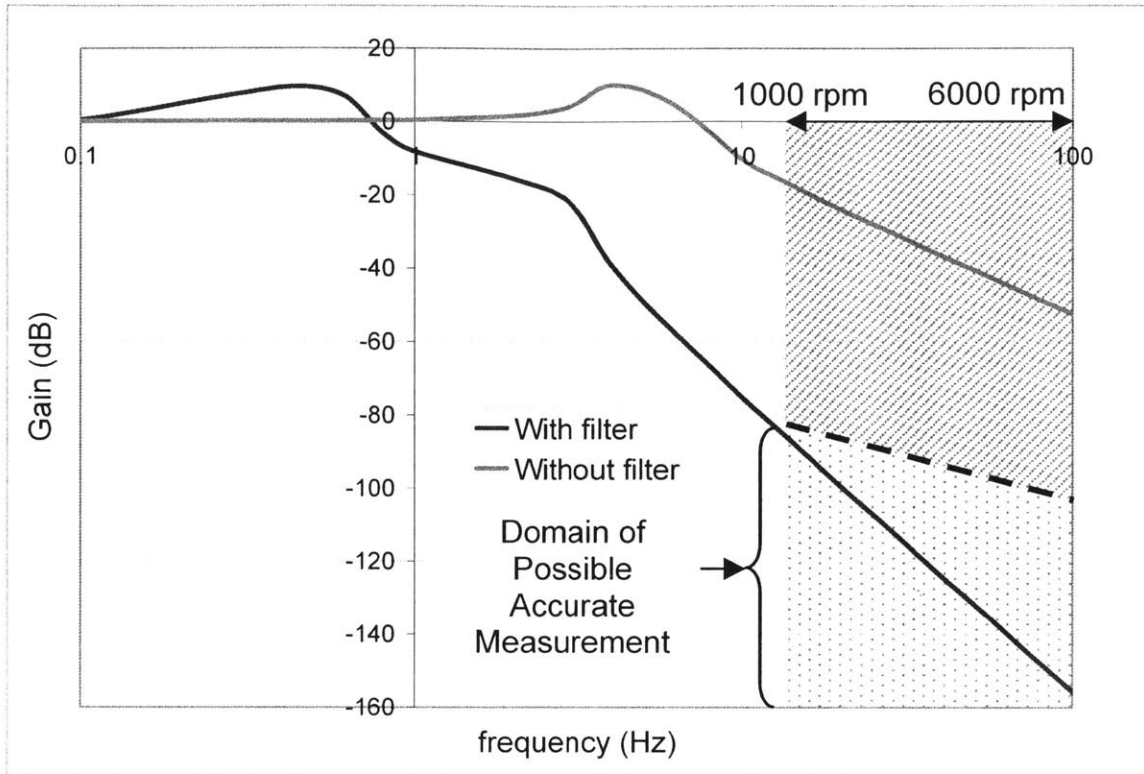


Figure 2.15 – Performance of the blowby acoustic filter in attenuating the flow oscillations from piston alternating motion [13]

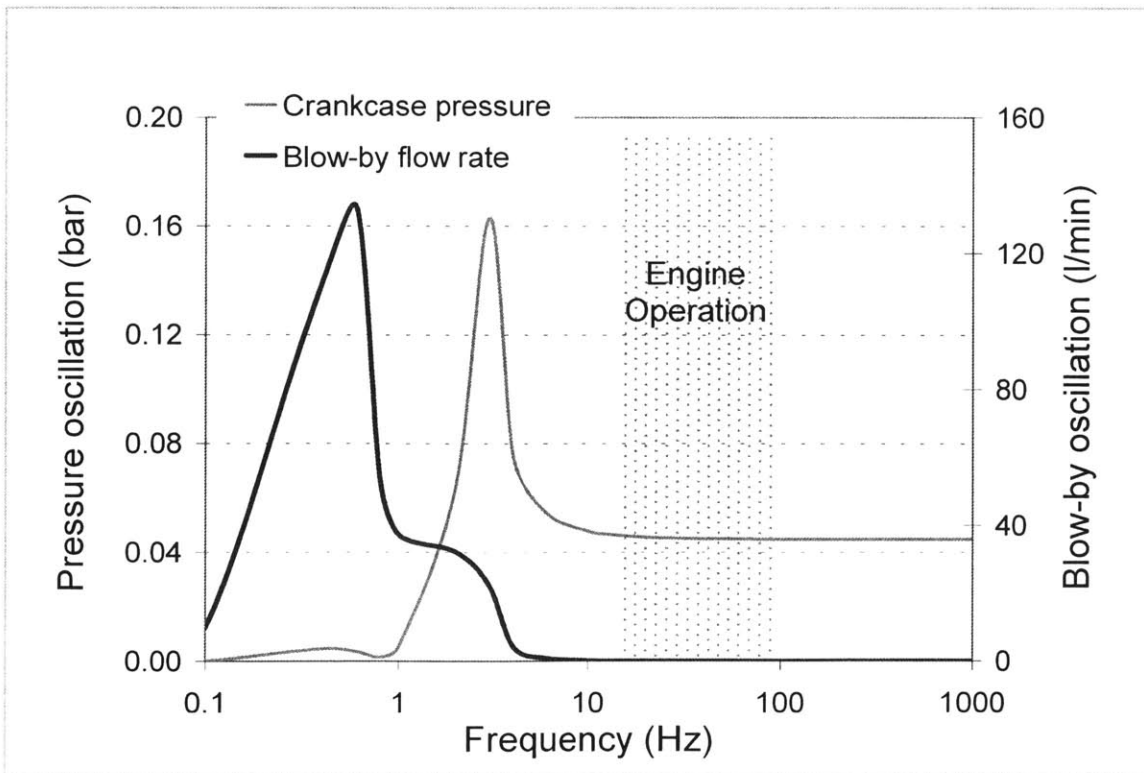


Figure 2.16 – Performance of the blowby acoustic filter in attenuating crankcase pressure oscillations [13]

The device to finally measure the blowby flow rate at the end of the acoustic filter was chosen to be a rotameter. A rotameter is a common flow measurement device where the flow rate is determined by the position of a small sphere in a vertical conic tube through which the gases are flowing. Extensive care was taken to ensure the rotameter tube would not become contaminated with oil and water entrained in the blowby gasses. A series of condensers and condensate traps was employed to avoid any complications from such debris. Furthermore, a nitrogen flushing line was installed just upstream of the rotameter, though the condition of the rotameter never degraded to warrant activation of this cleaning mechanism. A diagram of the blowby meter and contamination traps is shown in Figure 2.17.

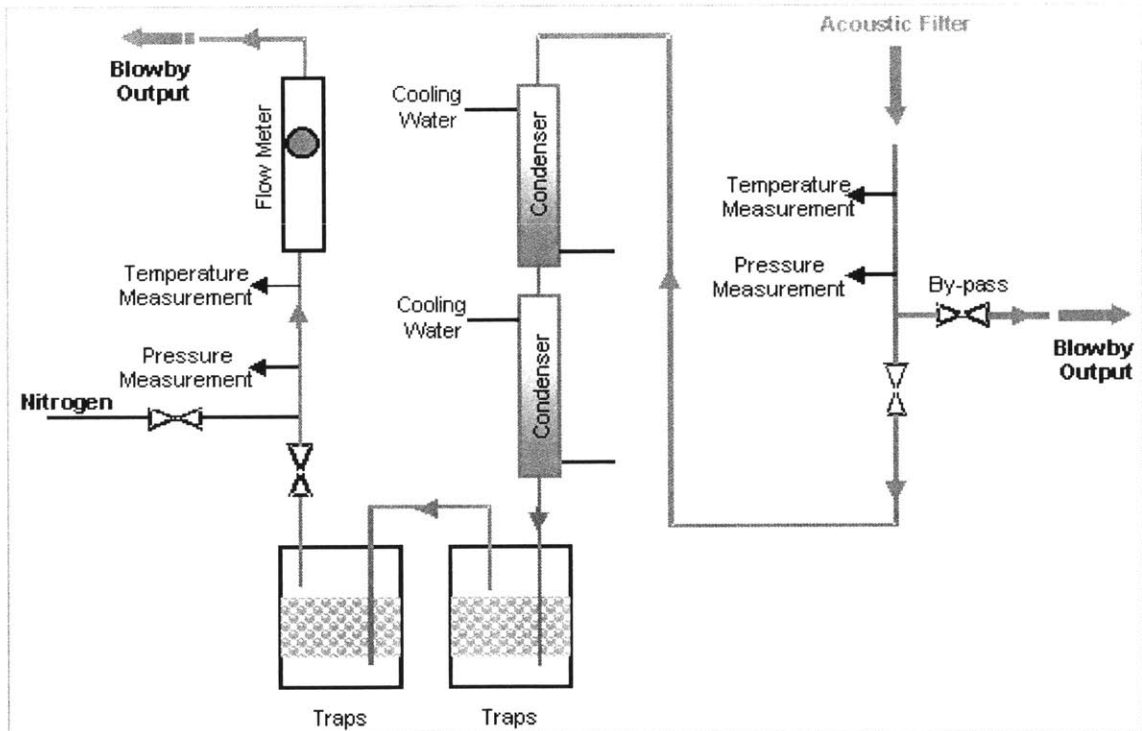


Figure 2.17 – Blowby meter and contamination traps

2.4 Experimental Variations

Operating Conditions

A main challenge in engine studies is the simple fact that an engine is not a basic on/off machine. Almost every automotive engine can operate at every speed between 1,000 and 6,000 rpm; furthermore, for each of these speeds, the engine can operate at low load, full load, or anywhere in between. And clearly, cars do not always travel at a set speed and on a consistently inclined roadway, the speed and load of the automotive engine is ever changing and adapting to the driver and roadway demands. So not only must all the possible speed and load combinations be investigated, but the transient effects of changing from one to any other must also be considered. Couple the operating point variability with the intricacy and dynamics of the rings and piston sub-regions, and this makes understanding the lubricating oil evolution on the piston ring pack a comprehensive and daunting task.

To further complicate matters, the oil patterns and ring dynamics are not always consistent, even at a stable operating point. Ring rotation is not always repeatable from one experiment to the next, often changing direction, and sometimes the ring gaps even chase each other for periods of time. Ring rotation has been experimentally seen to vary from negligible values up to a speed of 2 rpm. Ring rotation leaves certain oil patterns in the wake of the gap, especially when two or more ring gaps align, creating a variable and constantly changing oil landscape. Furthermore, a build up of oil in a ring groove can change the gas dynamics throughout the engine cycle, sometimes causing the ring to become unstable and flutter in its groove. This only occurs at certain operating points, but even then the timing is variable, sometimes occurring as often as every thirty seconds and sometimes occurring only once every ten minutes.

In an automotive engine, the specific spark timing will also induce variability in the oil transport mechanisms, even when load and speed are held constant. The advancement or retarding of spark timing (often a compromise between fuel efficiency and emissions) will change the cylinder pressure trace and blowby measurement, and thus have an effect

on oil patterns. Retarding the spark timing is often employed to accelerate warm-up of the catalytic converter, thereby increasing its efficiency upon engine start-up. The experimental engine was equipped with a motoring dynamometer, to allow virtually any speed, load, and spark combination desired.

The variability in the range of engine operating conditions creates a similar variability in the dominant forces driving lubricating oil transport on the piston ring pack. For instance, piston acceleration varies from only 400 m/s^2 at 1,000 engine rpm to $20,000 \text{ m/s}^2$ at 6,000 rpm, which is more than 2,000 times the acceleration induced by gravity. The effect gas flow has on oil transport is also strongly related to the engine operating condition. The net blowby flow rate of a spark ignition engine can vary from around zero to several liters per minute per cylinder, as the engine load is varied from low to high. The load is varied on this experimental engine by controlling the intake manifold pressure with the throttle position.

The domain of operating conditions for the PSA single cylinder engine are shown in Figure 2.18, with steady state and transient tests conducted across the entire map. As the cylinder head is from a standard 4-cylinder production engine, increased friction from the presence of the complete valve train and four balancing shafts changes the single cylinder engine's torque output level from a typical automobile. Accordingly, the line separating the positive and negative torque output on Figure 2.18 was measured from the 4-cylinder production engine from which the single cylinder engine of this experiment is derived. Negative loads are encountered in typical driving conditions when the accelerator is suddenly released while driving at a significant speed; the throttle shifts to the closed position and the engine is driven by the car's inertia, resulting in a strong vacuum in the intake manifold. Spark ignition engines, unlike their diesel engine counterparts who vary load with fuel injection and not throttle position, suffer from reverse blowby when the crankcase pressure exceeds the intake manifold pressure. A closed throttle position with high speed operation can easily drop the intake manifold pressure to as low as 200 mbar, while the crankcase pressure hovers around atmospheric. This creates an upward flow of gases from the crankcase, through the piston ring pack, towards the combustion chamber;

the flow of gases will entrain and act to drag some oil with it as it flows upward in the cylinder. The reverse blowby phenomenon can contribute significantly to oil consumption, especially if the operating point is sustained for some time [21]. Therefore, it was important to test for this high load to low load transient condition, as well as any other conceivable transient condition. A timescale chart of how the transient data was acquired for this high to low load situation is shown in Figure 2.19, but the process is identical for capturing the transient effects from any one load/speed to any other load/speed operating condition.

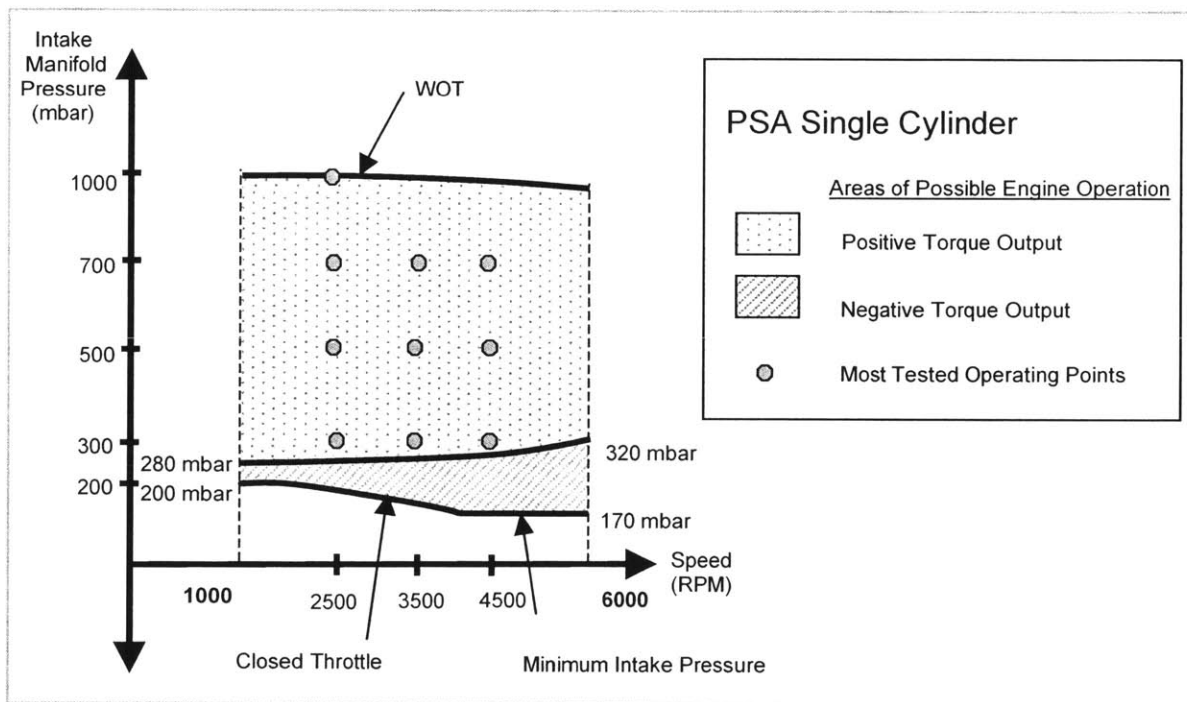


Figure 2.18 – Range of engine operating conditions

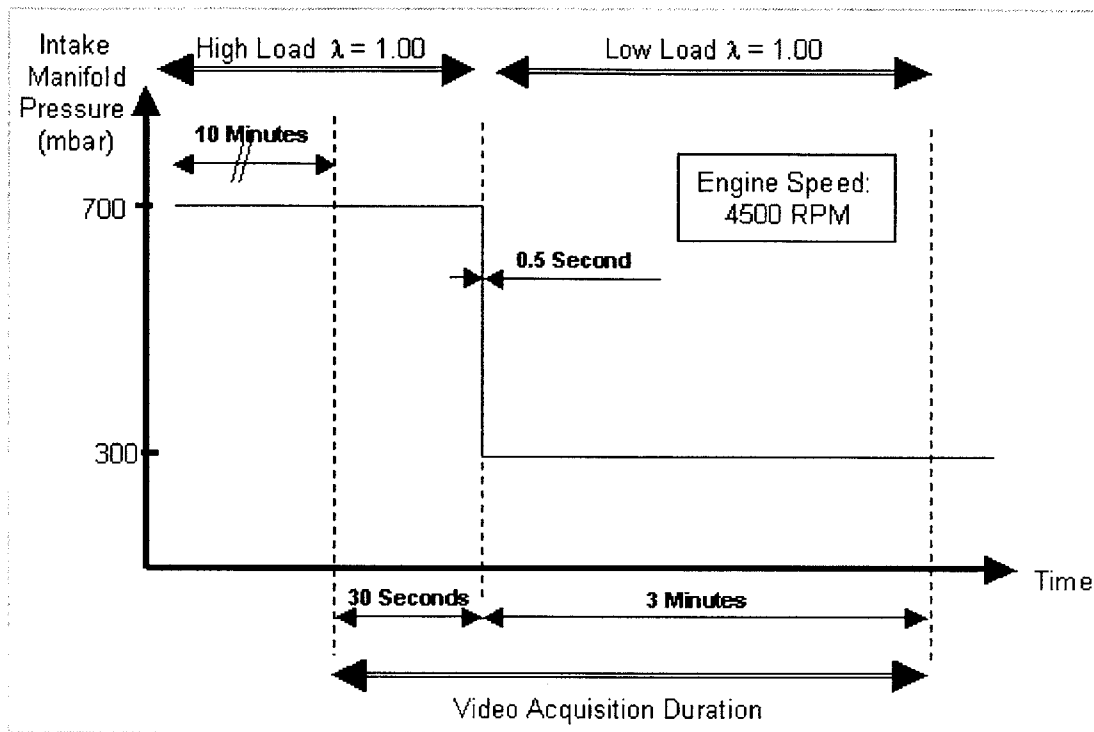


Figure 2.19 – Description of transient test procedures

Data Location

The cylinder liner of the single cylinder engine was designed so that the sapphire window could be placed on either the thrust or anti-thrust side of the engine. This allows investigation into the effects of piston secondary motion on the oil transport process, as it is known that secondary motion affects ring motion, gas flows, and oil consumption [18,25,30]. Despite this, however, the option was never utilized in this experimental work and the window was kept on the anti-thrust side for all of the tests. The ability to test more ring pack configurations, including ring and piston design effects, was chosen in lieu of intensive investigation into the effects of piston secondary motion.

Aside from all the operating point variations to test, the location of data acquisition is also very important. Some transport phenomena occur over the timescale of several engine cycles; these transport mechanisms can be recorded during any engine stroke and at any crank angle. However, many transport mechanisms occur within a single piston stroke, or even within a few crank angle degrees. To capture all of the transport mechanisms, therefore, data must be taken about every 10 crank angle degrees along all 4

piston strokes: Intake, Compression, Expansion, and Exhaust. This equates to 18 tests for each stroke, or about 58 tests for the entire engine cycle (TDC and BDC data is identical for stroke transitions). And these numbers are for just one operating point; to gain a complete picture, these 58 tests would have to be conducted for every possible load/speed combination, and even for transient conditions as well. This number of tests becomes cumbersome and time consuming. Performing full data sets on a few select load/speed operating points, and sampling the other load/speed combinations for abnormalities, can achieve a similar comprehensive output. This is due in large part to the consistency of some of the oil transport phenomenon, and knowledge of how the magnitude and timing of the driving forces react to operating point changes.

Ring and Piston Design

Each type of production engine has a ring pack that is designed specifically for it. The design of a ring pack for an engine can be seen as the best compromise between many competing elements: Bore distortion, friction, blowby, running-in, wear, piston seizure, and lube oil consumption to name just a few. The multitude of considerations helps to explain the almost limitless number of ring packs in production, as there are a plethora of variations possible: Land heights, land/liner clearance, groove heights, ring heights, groove tilt angles, piston ovality, ring tension, ring gap size, ring profile, piston profile, etc. This experimental work focused on testing the most common elements of production ring packs, as well as testing some new concepts, particularly in regard to piston profiles. The most common ring types employed in spark ignition automobile engines are displayed in Figure 2.20. The experimental study began by testing the original production engine ring pack, and then testing some of the other common elements and innovative ideas. This progression allowed observation and comparison of specific features and ring related oil transport mechanisms, and provides a better understanding of the benefits and shortcomings of various ring pack features.




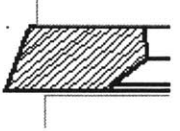
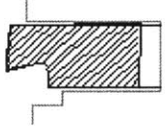
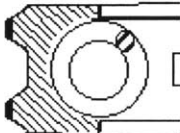
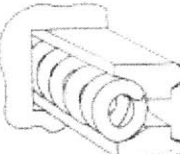

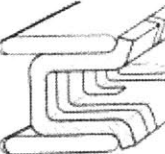
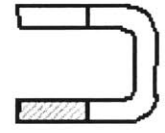
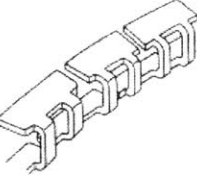
First Ring	 Rectangular Top Ring	 Positive Twist Top Ring	 Offset-Barrel-Face Top Ring
Second Ring	 Negative Twist Scraper Ring	 Napier Ring	
Oil Control Ring	  Twin-Land OCR	  Three-Piece OCR	  U-Flex OCR

Figure 2.20 – Common ring types employed in SI automobile engines

The choice of which ring types were tested in this work is directly related to the region of strongest interest. At all engine running conditions, and at every possible crank angle, the third land was found to contain a substantial amount of lube oil. This large accumulation, and its relation with ring dynamics, directly determines the net oil transport to the upper regions of the piston ring pack, and ultimately to oil consumption. Therefore, our analysis of ring pack designs focused on the two boundaries of the third land, the second compression ring and the oil control ring. The original PSA engine ring pack is shown in Figure 2.21, and the tested variations are shown in Figure 2.22.

The Napier style second ring is common in automobile engines, and is easily identifiable by its hook, which is used as a containment area to store oil. The hook is designed with the third land cutout, or chamfer, so that the geometry matches exactly; this accentuates

oil flow between the chamfer and the hook, without depositing oil into the second ring groove. The other type of second ring tested was a Negative Twist scraper ring.

Three different types of oil control rings were investigated for this work: A Twin Land oil control ring (OCR), a Three-Piece OCR, and a U-Flex OCR. The Twin Land OCR, sometimes called a two-piece OCR, has two small lands, one at the top and one at the bottom, and has a spring to help set the ring tension. A Three-Piece OCR is designed to seal both the upper and lower groove clearances through the ear angles of the expander and the two rails. The U-Flex oil control ring is a fairly unique design in the automotive industry; instead of having one large gap, as most rings do, the U-Flex OCR has approximately 50 small gaps offset from each other on the top and bottom ring lands [31]. This is highly beneficial in limiting upward oil transport through the ring gap, a large problem for the more common style of rings with only one large gap. Additionally, the many small gaps create an effective purging of the third land by distributing the downward gas flow evenly around the circumference of the piston. For further clarification, some detailed drawings of the U-Flex OCR and the Three-Piece OCR tested in this work are shown in Figures 2.23 and 2.24 respectively.

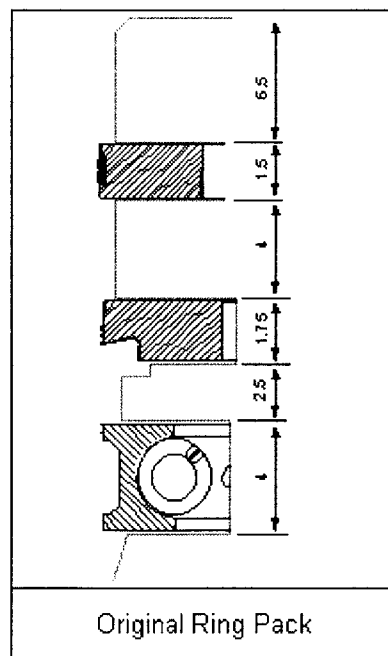


Figure 2.21 – Original PSA ring pack (measurements in millimeters)

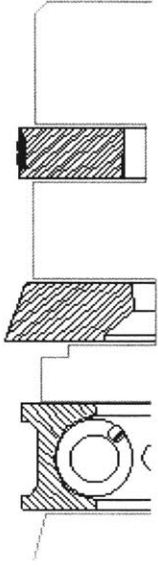
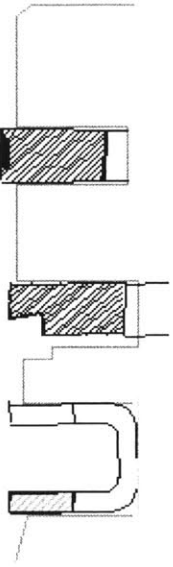
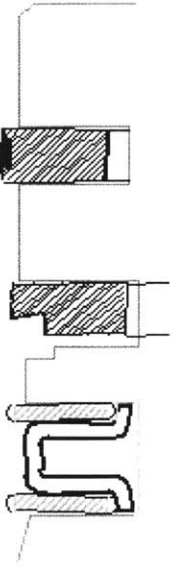
Ring Combinations Tested		
		
Negative Twist Scraper Ring	U-Flex Oil Control Ring	Three-Piece Oil Control Ring

Figure 2.22 – Tested ring pack variations

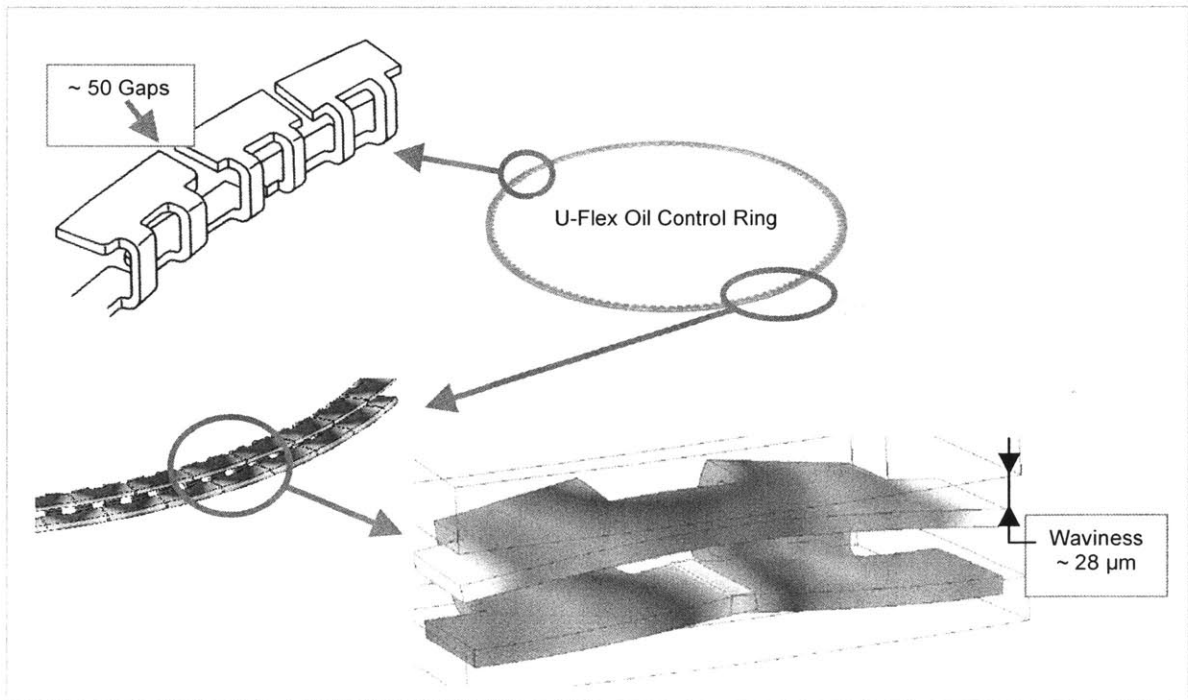


Figure 2.23 – U-Flex oil control ring details

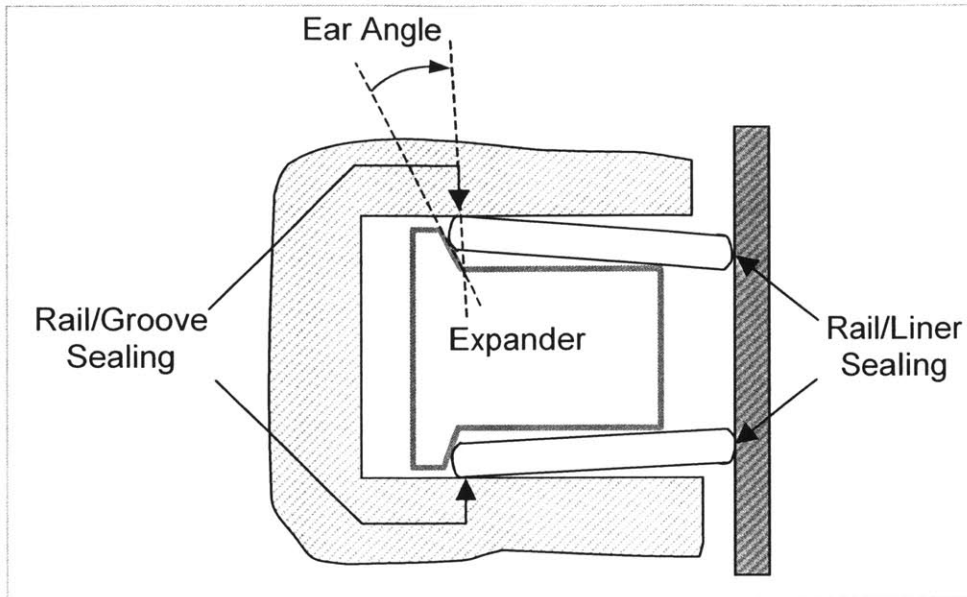


Figure 2.24 – Mechanics of a Three-Piece oil control ring

Previous 2D LIF work was performed on piston ring packs with the ring gap locations pinned [13]. The aim was to remove ring circumferential movement from affecting the oil transport processes, but the pinned rings created a uniform oil pattern at the window location and made oil transport analysis difficult. As with other possible testing directions, pinned rings were not investigated in this work so as to concentrate more on various piston and ring designs.

To inhibit the effect of inertia force on oil transport, a V-Cut and a Hook were designed and machined into the second land of two separate pistons respectively. Changing piston geometry is a powerful way to control oil transport on the piston ring pack, but it cannot be done without considering all the effects. For example, altering set piston geometry will have an effect on gas flow rates, because as the volume of space in the land/liner clearance increases, so does gas flow required to have the same pressure fluctuations as without the volume increase. The effects and the reasoning behind the V-Cut and Hook will be discussed in detail in a later section, and the schematics of these design features are illustrated as well.

Data Analysis

To correlate the observed 2D LIF oil displacement images with the driving forces encountered in the power cylinder system, one would have to know the inertia force, ring dynamics, and gas flows between the various regions of the piston ring pack, and at every crank angle. The inertia force is simply a factor of piston speed, but ring dynamics and gas flow calculations are much more complex. Tian [12,24] developed RINGPACK-OC, the main code used in this work, which calculates piston and ring dynamics as well as gas flows and pressure distributions. Cylinder pressure traces, piston expansion, and liner expansion were the main input parameters. Without a comprehensive FEA (Finite Element Analysis) effort to evaluate piston and liner deformations, it is believed a reasonable approximation of bore expansion can be found by matching the simulation's output of blowby with the actual blowby measurement at each operating point. The RINGPACK-OC code was essential for transitioning from simple viewing of the complex LIF output, to explaining the oil transport mechanisms, their origins, and predicting their response to speed/load changes.

The value of knowing the pressures, gas flows, and ring dynamics of the various ring pack regions cannot be stressed enough. To help illustrate this point, the impact of ring dynamics knowledge will be discussed further. Ring dynamics mainly affects the oil evolution by forcing lubricating oil out of the ring grooves, or by moving to allow oil to enter the ring grooves. When oil accumulates at the intersection of the piston ring and the land, and the ring moves axially in its groove, it allows space for the accumulation to spread out on the ring surface and enter the ring groove. Similarly, if oil is in the ring groove when a ring moves axially in the groove, some of that oil will be pushed to the back of the ring, deeper into the ring groove, but some of it will also be forced out of the ring groove onto the piston land. Knowledge of the location of the ring within its groove, coupled with the magnitude and direction of the inertia force acting on the oil allows understanding of the oil flow pattern and its timing. As an example, a chart of the ring axial movement within its groove is shown in Figure 2.25, for a medium speed, low load operating point. A more detailed analysis of the oil transport mechanisms, along with

some additional output of the RINGPACK-OC software, will be discussed in the next chapter.

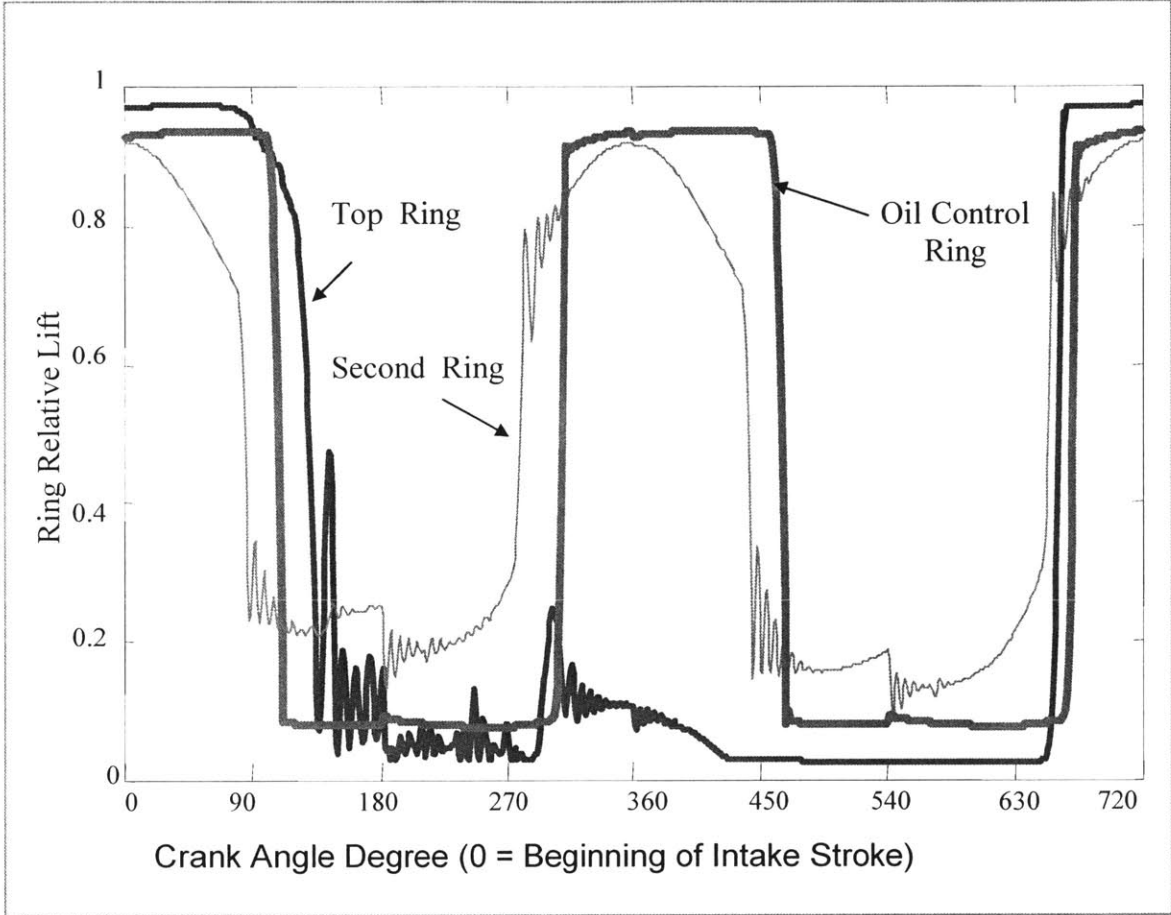


Figure 2.25 – Example of ring dynamics; the engine operating point is 3,500 rpm, low load (relative lift of 1 denotes the ring is resting against the top flank of the ring groove, a relative lift of 0 denotes it is against the bottom flank of the ring groove)

CHAPTER 3: BASIC OIL TRANSPORT MECHANISMS

LIF studies on oil transport by Thirouard [22,23] have identified the major driving forces and basic transport mechanisms for lubricating oil within the piston ring pack. His study of spark ignition (SI) and diesel engines divided the piston ring pack into three regions and expressed the key elements of oil transport as: Piston alternating motion (inertia), ring and groove interaction, and blowby and reverse blowby gas dragging. Thirouard's LIF work focused on the basic transport mechanisms and the driving forces on the entire ring pack; this study and experimental work increases the fundamental knowledge of the basic mechanisms, but more importantly, it focuses intensely on the individual regions, particularly the 3rd land, and describes the consistent evolution of the oil throughout an entire engine cycle. This comprehensive analysis of the magnitude and timing of the consistent oil evolution creates a more advanced understanding of how oil travels upward in the piston ring pack and will allow an effective oil control strategy to be developed to reduce oil consumption.

Before the oil evolution and patterns can be detailed, however, the major driving forces and oil transport mechanisms must be discussed. Knowledge of these forces and basic mechanisms greatly increases the value of the 2D LIF real time oil distribution images, as they are necessary to understanding the overall oil evolution. The major forces driving oil transport on the piston ring pack are detailed in Figure 3.1. The basic transport mechanisms of lubricating oil on the piston ring pack are described in Figure 3.2. Of principal importance to these transport mechanisms are key characteristics such as volume of oil necessary for a puddle to cross an entire land, and location of ring gaps relative to the significance of blowby driven circumferential oil transport [13]. Knowledge of the magnitude and timing of the forces is also critical to assessing the oil transport mechanisms.

Mechanical Displacement — The lubricant can be transported by a moving part; the piston moving relative to the liner or a ring moving in its groove for example.

Inertia — A strong body force (up to 2000g) originating from the alternating piston motion; this force acts on all lubricant attached to the piston or rings.

Pressure Gradient — A significant pressure difference exists between the combustion chamber and crankcase; the difference results in various pressure gradients and pressure drops across the piston ring pack.

Gas Flow — Gases will flow between and across the various regions of the piston ring pack, for example combustion gases will flow downward during the expansion stroke and crankcase gases can flow upward during the intake stroke; these gas flows induce a shear stress on the lubricant at the interface between the gas and the oil layer.

Figure 3.1 – Primary forces that drive the oil transport processes on the piston ring pack [22]

On The Piston Land — Oil is driven axially on the piston land by inertia, and to a much lesser degree by gas dragging. Engine speed heavily influences axial transport. Oil is driven circumferentially around the piston land by gas dragging. Engine load heavily influences circumferential transport.

Between the Liner and Lands — Ring scraping of the liner walls during the piston stroke is the main type of this transport. Additionally, if enough oil accumulates at the intersection of a ring and a land, the oil can 'bridge' across to the liner and attach to the cylinder wall. Similarly, if the oil has accumulated at this intersection when inertia shifts, oil can leave the ring surface as a drop, traveling in the clearance between the piston land and the liner and coming in contact with either.

Through the Ring Grooves — Oil will flow into or out of a ring groove for several reasons. Ring mechanical pumping/squeezing can suck oil in or pump oil out from a ring's movement in its groove. Inertia and gas dragging can bring oil into or out of a groove as well. And finally, the lateral motion of the piston relative to a ring can induce a shear force on the oil layer between them.

Through the Ring Gaps — A main path for gases to flow from the combustion chamber to the crankcase are through the ring gaps. This high concentration of gas flow transports a significant quantity of oil downward, much of which becomes an oil mist. Reverse blowby and upward inertia are also critical and transport a significant amount of liquid oil upward through the ring gaps.

Figure 3.2 – Basic transport mechanisms of oil on the piston ring pack

3.1 Piston Land Transport

Oil transport on and across the piston lands is the most visually compelling of all modes studied with the 2D LIF technique. The relatively large surface area of the lands, coupled with knowledge of the boundary conditions and gas flows from ring dynamics software, allows strong conclusions to be made about the origins, timing, and magnitude of the oil transport patterns on the piston lands. Two forces dominate transport on the piston lands, inertia force drives oil axially and gas flows predominantly drive oil circumferentially.

Inertia Driven Oil Transport on the Piston Lands

As inertia is a major driving force of oil throughout the piston ring pack, it is important to understand its general timing. The computation of the inertia force acting on the lubrication is rather trivial, and is merely the oil density multiplied by the piston acceleration. The force of inertia varies quite dramatically throughout one engine cycle, and is seen to have a strong correlation to oil movement, particularly to the large concentrations of oil on the third land. Figure 3.3 is a chart of piston acceleration throughout one cycle for an engine speed of 4,500 rpm. Engine speed is a critical parameter affecting the oil evolution on the piston lands, because it is directly linked to the dominating inertia force – proportional to the second order. At an engine speed of 6,000 rpm, piston acceleration reaches $20,000 \text{ m/s}^2$, which is 2,000 times the force of gravity. A force of this magnitude has strong implications for oil transport; note also how inertia changes direction each engine stroke, or 4 times per engine cycle.

To understand how inertia force acts on an oil accumulation, let's start with a large round puddle at the center of a piston land. Around mid-stroke, piston speed is at a maximum; as the piston is passing the midpoint of the intake stroke, for example, it begins to decelerate. The oil begins to feel the inertia force, and wants to keep moving downward as the piston slows. This force grows to a maximum until the piston stops upon reaches bottom dead center (BDC); the force continues to drive the oil axially downward on the piston land. The piston now begins to accelerate upward as the compression stroke begins. The oil again feels this force, and is driven downward relative to the piston.

Around mid-compression stroke, the inertia shifts again, now to the upward direction, as the piston again begins to decelerate. The oil is driven upward axially. The piston comes to a stop at top dead center (TDC), whereupon it now begins to accelerate downward for the start of the expansion stroke. This downward acceleration continues to drive the oil upward relative to the piston. Around mid-expansion stroke, the inertia again shifts as the piston decelerates. The second half the engine cycle just repeats the first half; the net force of inertia throughout an engine cycle is zero, canceling itself out. However, the nice round puddle we began with is now going to look like a tall, thin accumulation as it has been spread upward, and downward, and upward, and so on. The faster the engine's speed, the greater the inertia force, and the thinner and farther the accumulation spreads. This diagram of events can be seen in Figure 3.4. Similarly, it is the size of the accumulation that dictates how far the accumulation spreads at a set speed. The larger the volume of oil, the more it will be affected by inertia, and the farther axially it will be transported. Therefore, it must be said that a minimum volume of oil is required for an oil puddle to cross an entire piston land during one upward or downward inertia period.

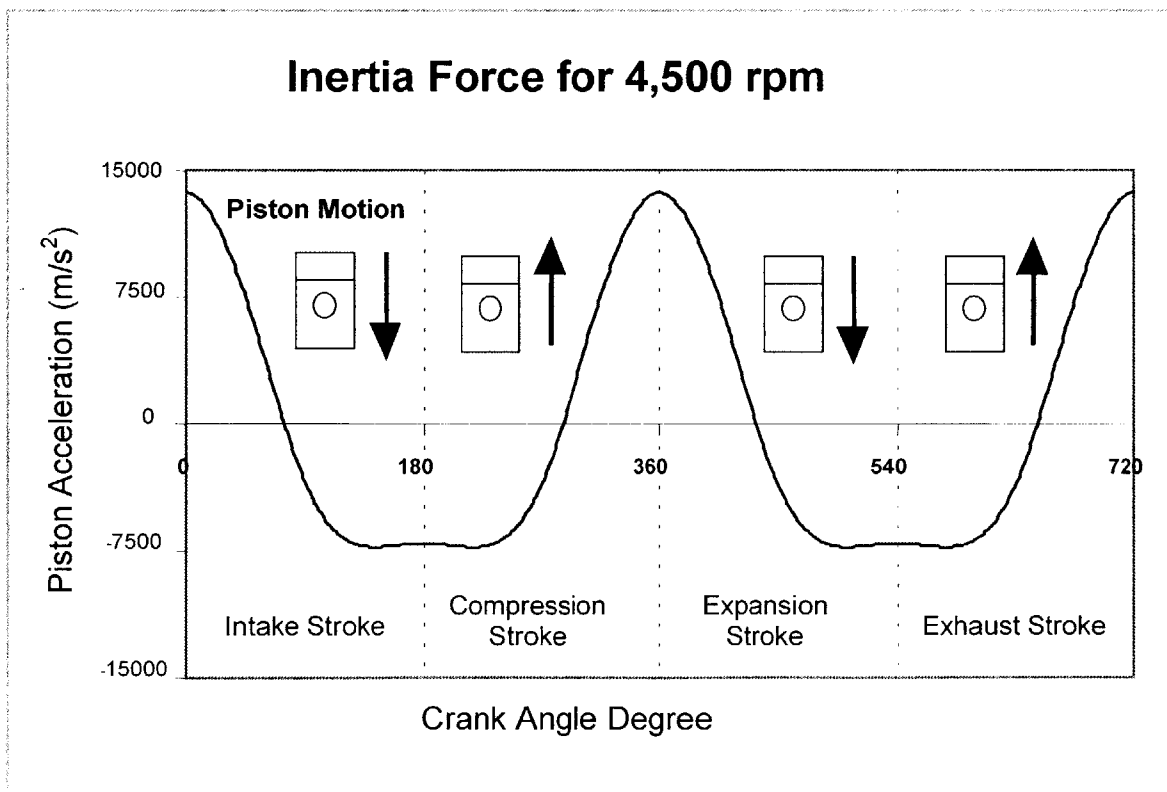


Figure 3.3 – Inertia force calculation to illustrate magnitude and timing of inertia in comparison to piston motion

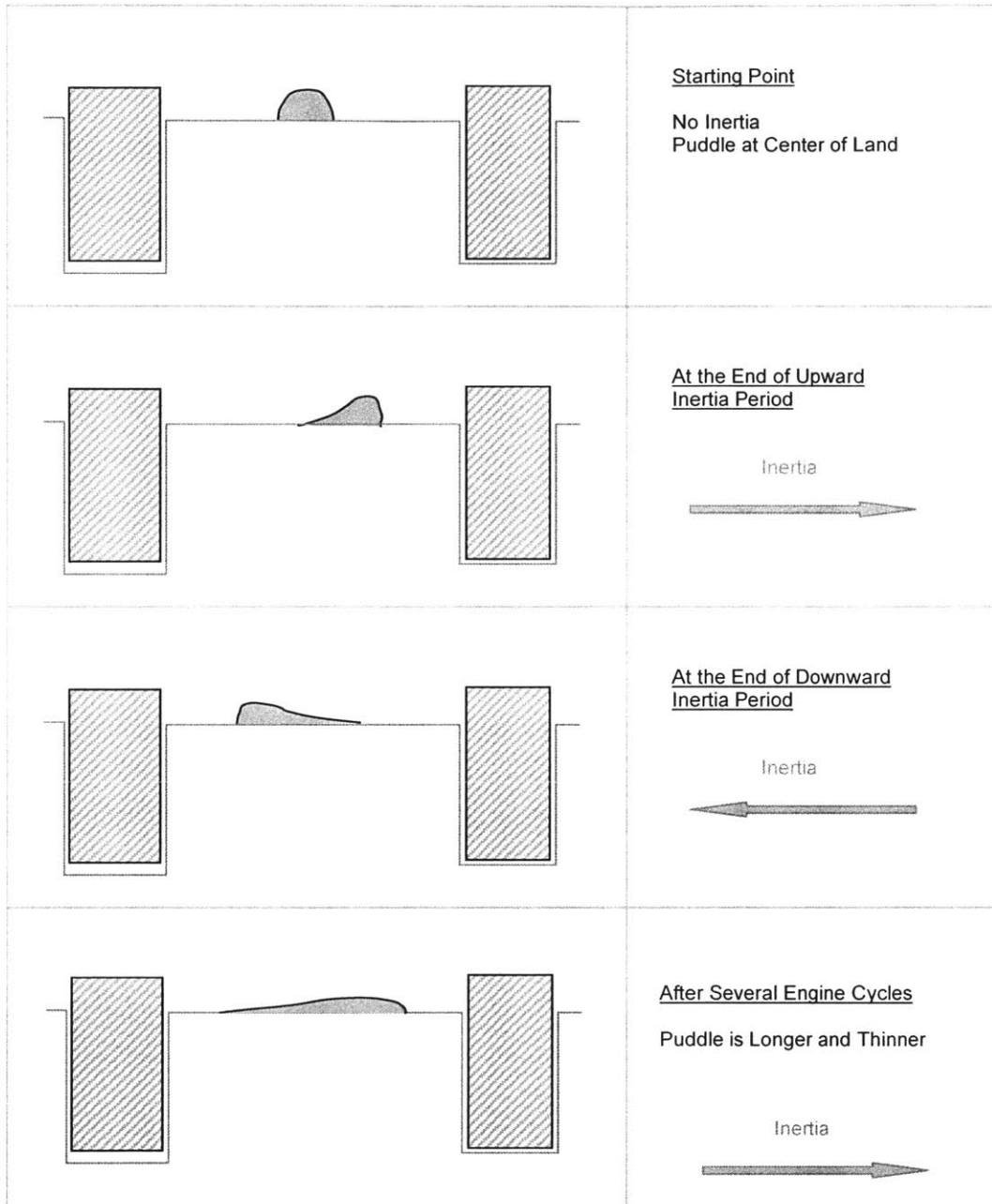


Figure 3.4 – Description of inertia driven transport on a piston land, over the course of several engine cycles

The consideration of the volume of oil present on the impact of inertia force is an important distinction, as inertia is the dominate oil transport force on only the third land, where the greatest concentration of oil is seen in every 2D LIF experimental test. Figure 3.5 contains LIF images of oil being driven across the third land by inertia. At this particular engine operating point, a large accumulation of oil is forced out of the OCR

groove and onto the third land around 50 CAD before TDC of the compression stroke. Inertia is well established in the upward direction, and quickly acts to drive the oil across the land. Each frame shown is 5 CAD apart, and it can be seen in the complete LIF data that the accumulation crosses the third land in approximately 30 crank angle degrees. The engine operating point for these frames is 3,500 rpm, with 300 mbar absolute intake pressure. The same wave phenomenon occurs in the down direction, as illustrated in Figure 3.6. The third land oil evolution, and the other regions of the piston ring pack, will be discussed in detail in the next chapter.

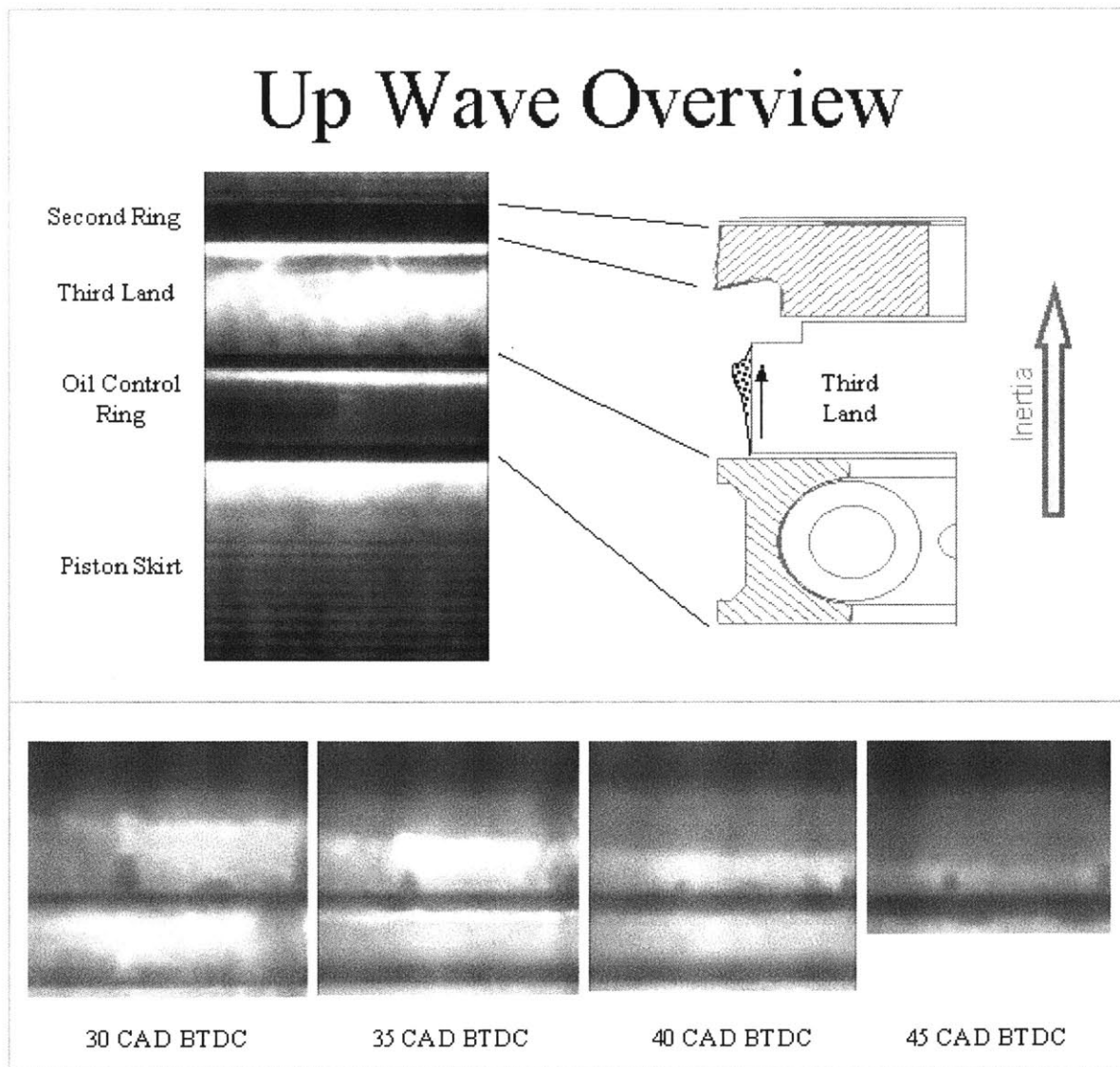


Figure 3.5 – Illustration of an up wave driven across the third land by inertia; note the fast timescale, with the complete accumulation crossing the entire land in only about 30 crank angle degrees

Down Wave Overview

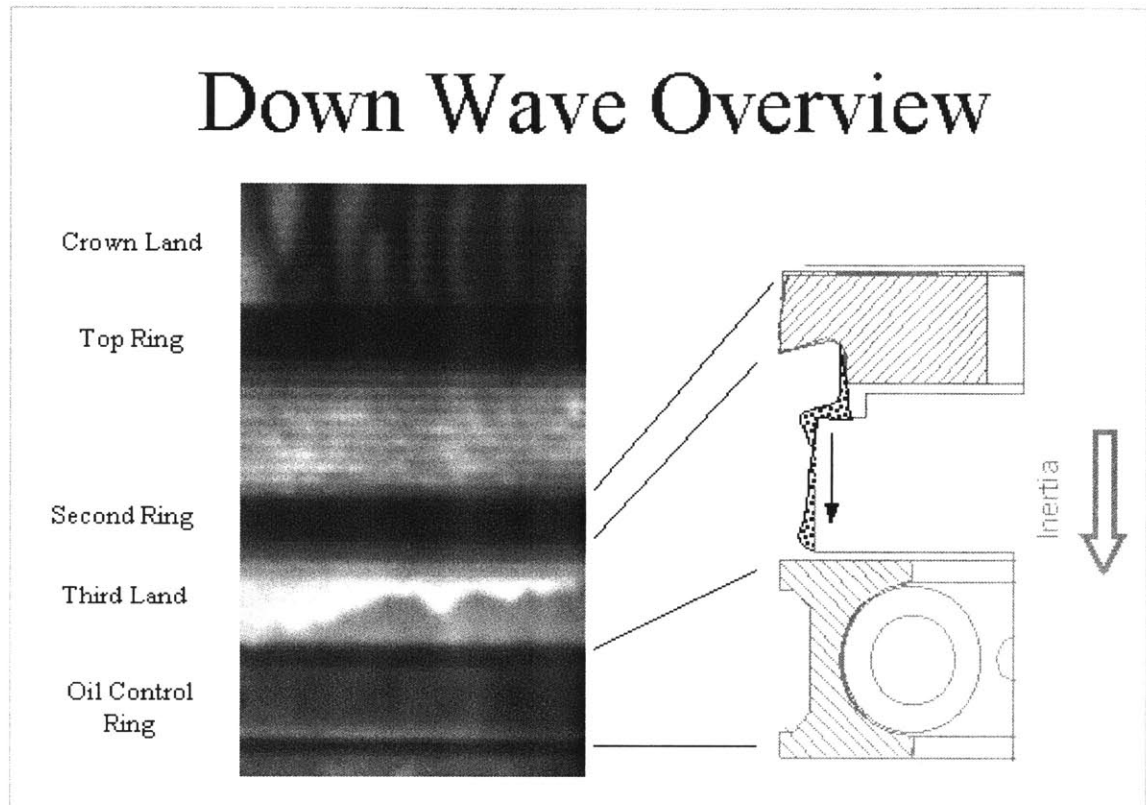


Figure 3.6 – Illustration of a down wave driven across the third land by inertia; this particular image was captured at 2,500 rpm and 300 mbar absolute intake pressure, at the beginning of the exhaust stroke

The relationship between accumulation size and inertia force can be loosely compared to a house window on a rainy day. Small accumulations of water will remain ‘stuck’ to a perfectly vertical window. The force of gravity (inertia force in the piston case) is not strong enough to push the small drops down the window. When the accumulation grows, usually by a few of these drops joining together, the water is seen streaking down the window as it more effected by gravitational force.

As in the case shown in Figures 3.5 and 3.6, if the accumulation on the piston land is large enough for inertia to drive it across the land to the intersection of the ring groove, several outcomes are possible and seen to occur in the LIF data. The possible scenarios, which depend on the relative ring position, are shown in Figure 3.7 and are described here. The discussion will focus on an upward moving oil puddle, but is equally applicable to a downward moving accumulation. If when the oil accumulation crosses

the land, the ring is still seated in its groove, the oil will begin to accumulate on the ring/land interface (a). If the accumulation is large enough it will undergo 'Ring Bridging', whereupon the accumulation on the ring/liner interface spreads out to the point it begins to contact the liner (b). Some of this oil will stick to the liner as the piston continues to move axially during the stroke. Generally, much of this additional oil on the liner will be scraped by the next ring to pass by. For both cases (a) and (b), ring axial movement usually comes soon after the oil wave has crossed the land. When the ring lifts in its groove, much of the accumulation on the ring/land interface becomes pumped into the ring groove (c). Sometimes when the oil accumulation crosses the land, the ring has already moved axially in its groove. When the oil reaches the liner/groove interface it pours, or forms droplets, and crosses to the lower side of the ring surface (d). Two types of rings are shown for this scenario; a Napier style second ring will catch this oil in its hook buffer region, whereas on a Negative Twist scraper ring, or any other rectangular ring, the oil accumulation will simply spread out on the lower side of the ring. Inertia has a strong influence on oil transport, acting to drive the lubricant across the piston land and ultimately into the ring grooves through the methods discussed above.

If an oil accumulation is not large enough to cross and vacate an entire land in one inertia period, as is often the case on the second and crown lands, then the accumulation will remain on the land with its shape determined by the speed of the engine from the process shown in Figure 3.4. As stated earlier, the greater the engine speed, the longer and thinner the puddle will become. LIF images of two engine speeds, at identical loads, are shown in Figure 3.8. The left image shows how a slow engine speed will allow a larger, thicker accumulation to remain on the lands. In contrast, the right image shows how a higher engine speed will force the same accumulations to narrow and lengthen. Though the images in Figure 3.8 were taken during separate tests, transient tests show the real time evolution of thick puddles into long thin puddles when engine speed is increased.

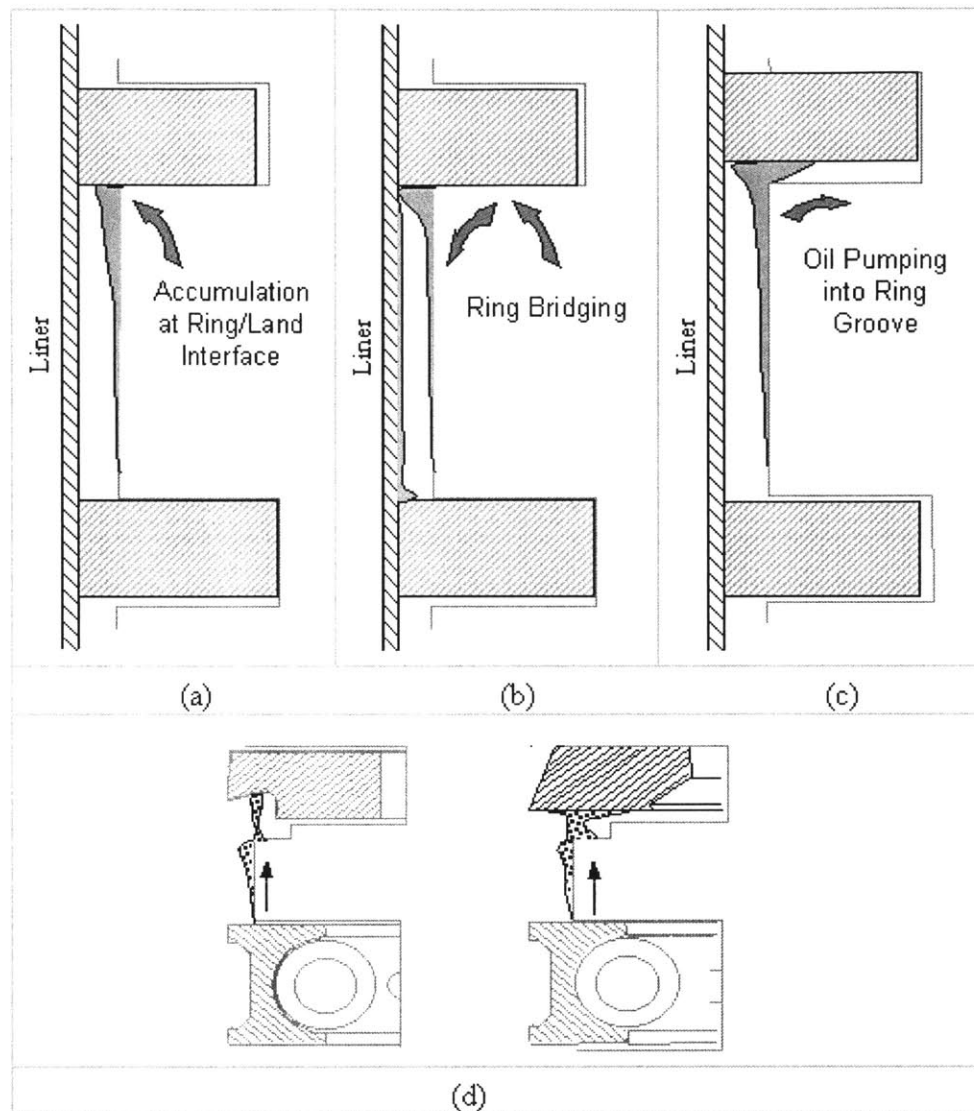


Figure 3.7 – Outcomes for an inertia driven oil accumulation crossing a piston land

As stated, if the accumulation is not large enough it won't be able to fully cross the piston land. However as time passes, more and more oil will be supplied to the land and the accumulation will grow. Eventually the puddle volume will become great enough for the inertia force to drive the puddle across the land. This net oil flux across the piston land is determined largely by the rate of oil supply, as the inertia force is stable at a set operating point. Gas flows will have an impact on net oil flux as well, but its impact on axial piston land transport is minimal and will be discussed in a later section. As the oil supply is from the crankcase, the net flux of oil transport is always towards the combustion chamber. As the oil accumulation on the land grows, Figure 3.9 shows how it moves further and further across the land, and eventually makes it to the far ring groove.

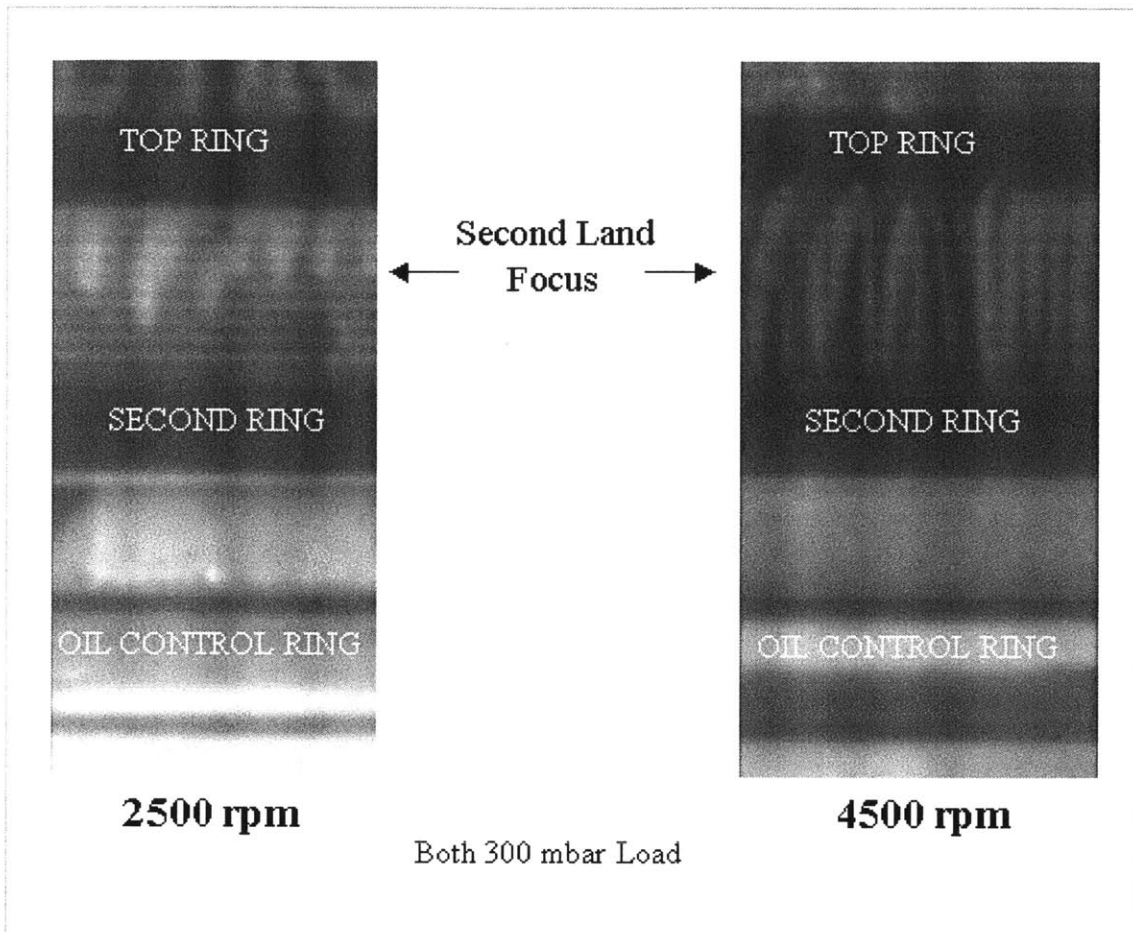


Figure 3.8 – Effect of engine speed on second land accumulations

When an oil accumulation begins at the ring/land interface and the inertia force is directed away from the ring, such as the process that instigated the transport in Figures 3.5 and 3.6, an oil wave will often form which tends to pour, or be driven, across the land. As engine speed increases, however, the high inertia force creates an additional pattern on large accumulations of oil. Some of the oil will still form a traditional puddle and move axially across the land, but some of the oil will now also form droplets. These drops will tend to leave from the ring surface, near the ring/land interface. A minimum inertia force is required for the oil to overcome surface tension and leave the ring surface as a drop, traveling towards the next ring. A higher engine speed will induce more droplets, while a lower engine speed will create less. Experiments reveal a minimum engine speed of approximately 3,000 rpm is required for significant droplet formation. The greater the amount of oil that forms into droplets results in less oil available for the

wave mechanism. The third land is the only region which has the required oil supply for this transport mechanism, and it was seen to occur for every ring type tested: Twin Land OCR, Three-Piece OCR, and U-Flex OCR in the upward direction, and Negative Twist scraper ring and the Napier scraper ring in the downward direction. Figure 3.10 shows examples of this oil droplet phenomenon. These inertia driven droplets can land on the piston land, the cylinder liner, or on the next ring's surface. In the Figure, arrows denote the droplet location on the left and right images. Note in the far right image the large arrow; this arrow points to a drop that has contacted the cylinder liner.

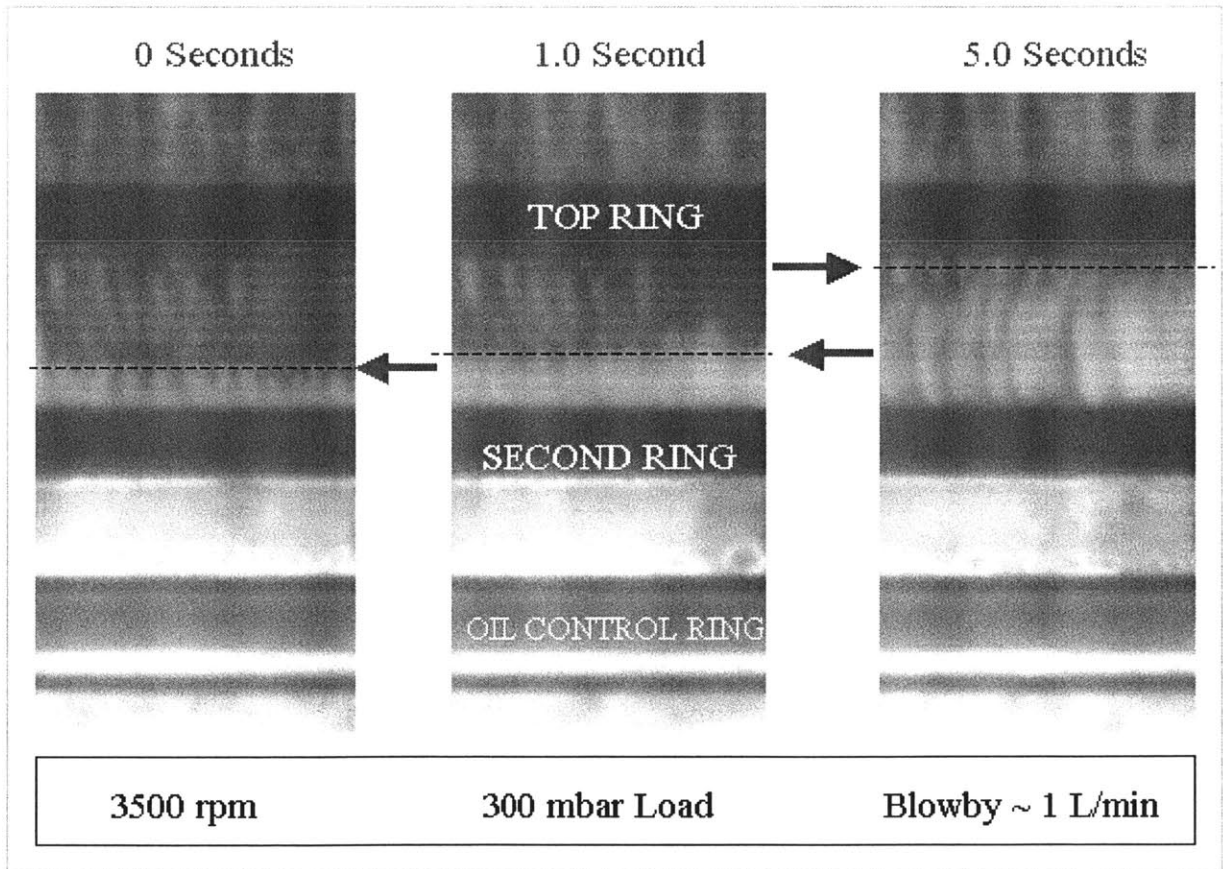


Figure 3.9 – Inertia driven transport with a growing supply of oil; as the accumulation grows, it travels further and further across the second land

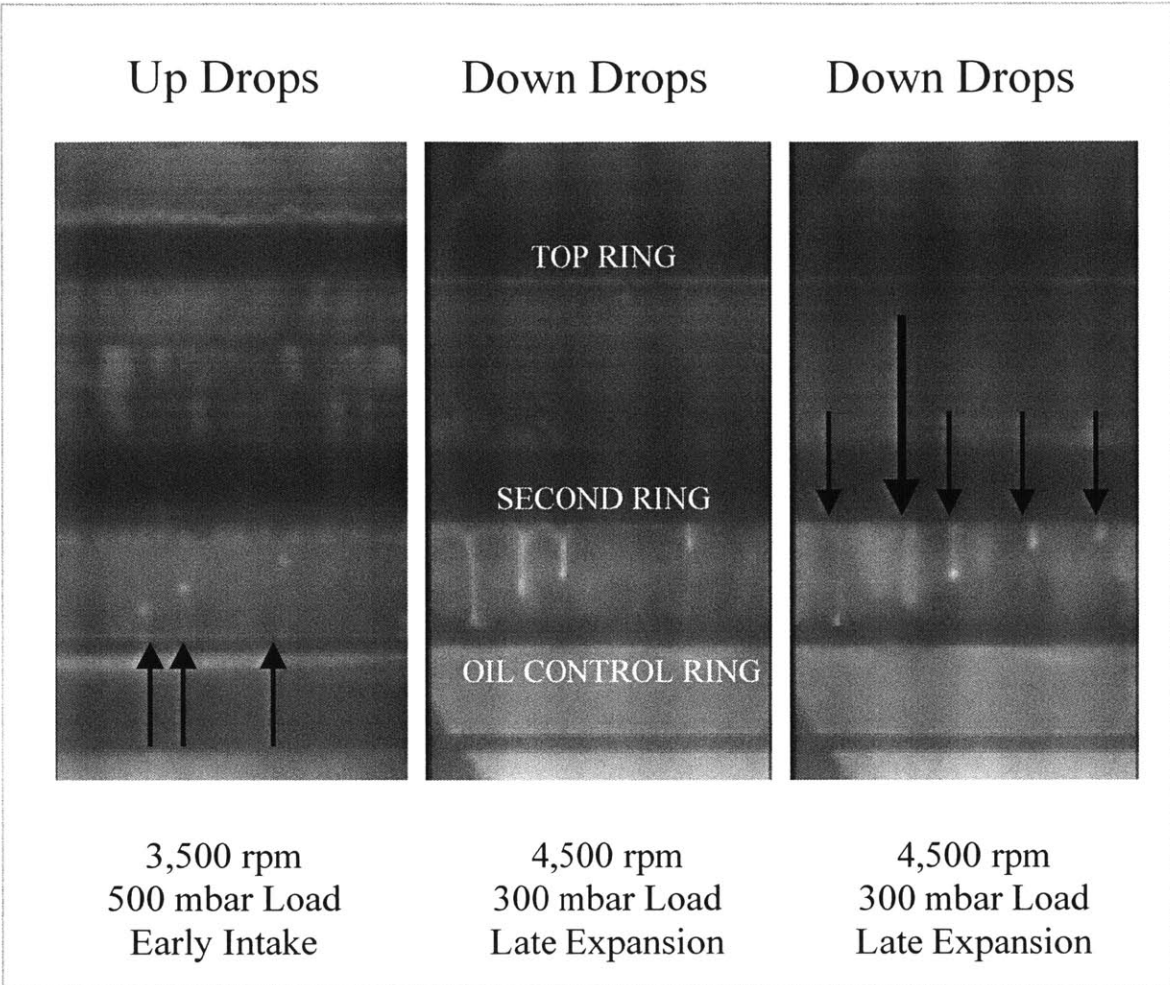


Figure 3.10 – Examples of droplet formation in the third land region; inertia driven droplets like these were seen to consistently occur at engine speeds above 3,000 rpm

Gas Flow Driven Oil Transport on the Piston Lands

Gas flow through the regions of the piston ring pack will have a tendency to drag oil with it. This phenomenon is similar to wind generating waves on a lake surface, or ripples upon a sidewalk puddle. Gas flow driven oil transport is verified with the LIF images, as oil is seen to consistently move circumferentially along the piston ring pack, and to a much lesser degree axially. As gas flows from the combustion chamber through the top ring gap, it then moves circumferentially, dragging oil with it, until the gas continues downward through the second ring gap. In essence, the experimentally observed circumferential movement of the oil is driven by the shear force on the surface layer by

the gas flow. This oil transport mechanism is strongly affected by operating conditions, such as engine load and speed, and by specific ring pack geometry, such as the relative position of the ring gaps. Moreover, this mechanism predominantly occurs on just the second land; the crown land will induce no circumferential gas flow, and inertia strongly dominates third land oil transport, making the effects of circumferential gas flow almost negligible in these two regions. An illustration of circumferential transport is shown in Figure 3.11.

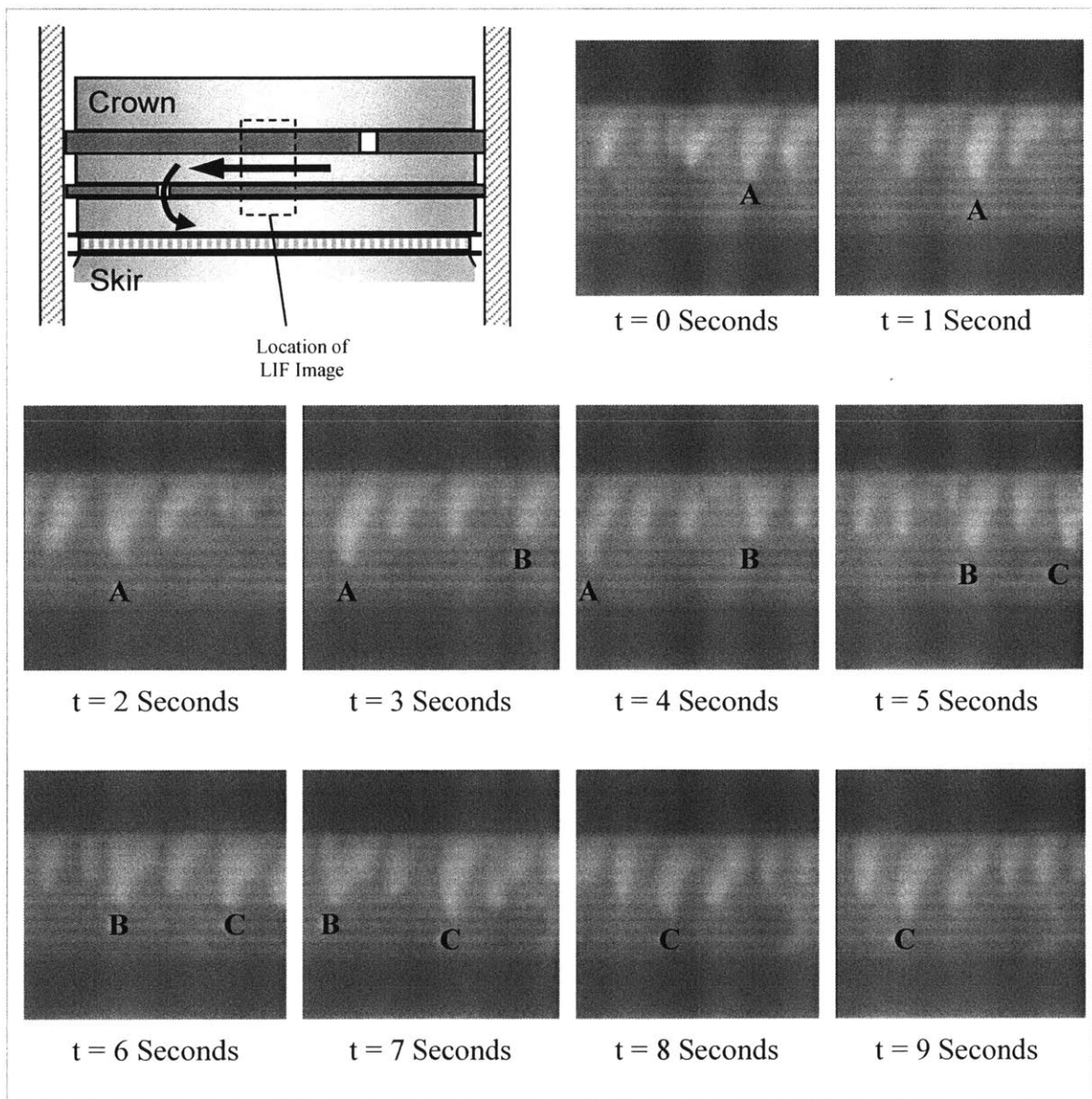


Figure 3.11 – Circumferential oil transport on the second land driven by gas flow, the letters denote a specific oil accumulation and follow its movement over the timeline; the above images were taken at 2,500 rpm and 300 mbar absolute intake pressure (the location of the ring gaps is not known exactly, but their approximate location is shown in the drawing)

The main source of gas flow is a result of combustion. Combustion results in a peak pressure within the cylinder, and gases are forced towards the lower pressure crankcase until the exhaust valve opens. The largest flow path for these gases are the ring gaps, allowing a direct path from one region of the ring pack to the next, but gas flow through the ring grooves is also significant. Other than for extremely low load operating conditions, the net flow of blowby gases throughout an engine cycle is generally in the downward direction, but the volume flow rate changes significantly depending on the individual stroke.

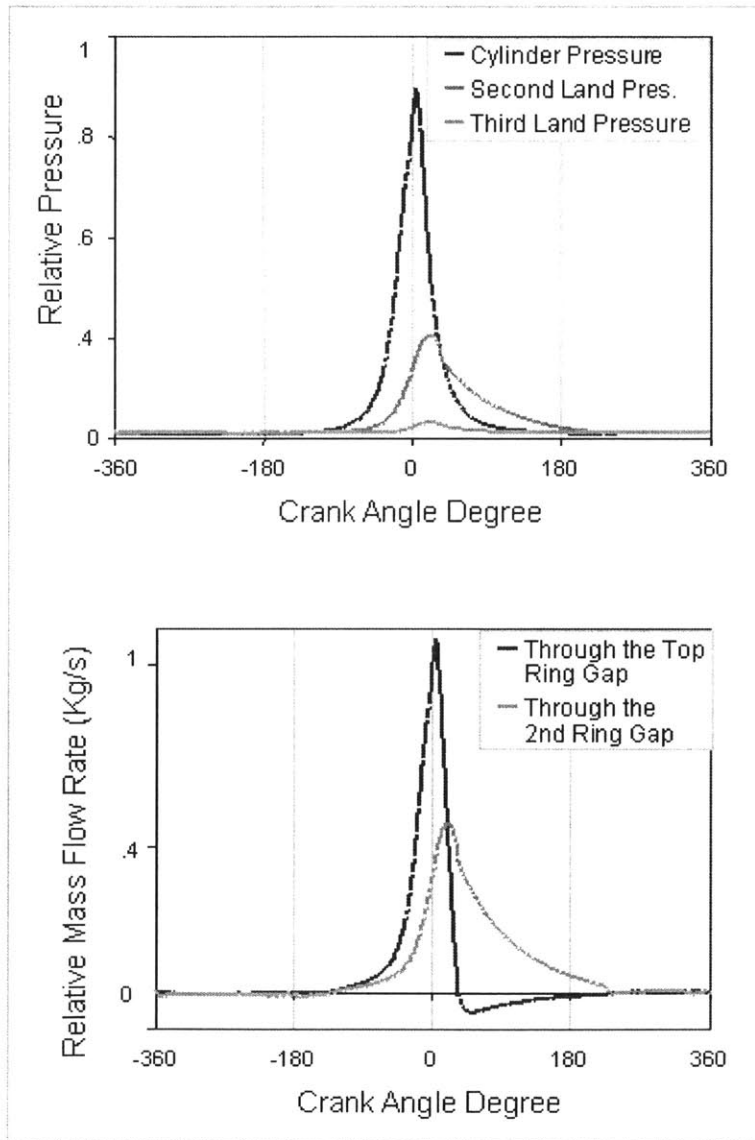


Figure 3.12 – Piston land pressure comparison and a ring gap flow comparison for a low speed, maximum load operating point (negative flow means the gas flow direction is upward)

The flow of gases through the piston ring pack regions can be computed with the simulation code RINGPACK-OC for any engine operating point. An example output of the software is shown in Figure 3.12, and described next. Two charts are shown for a low speed, full load situation: A piston land pressure comparison and a chart of gas flow through the top two ring gaps during an engine cycle. Gas flows during the compression stroke and early expansion are certainly from the crown land towards the crankcase, with much of it flowing through the ring gaps. However, during the late expansion stroke, the second land pressure becomes greater than the cylinder pressure, and the flow of gases is reversed for a short time. The exhaust stroke also creates a downward gas flow, but the intake stroke of a spark ignition engine creates a vacuum in the cylinder, which is particularly severe at low loads. In a low load scenario, the crankcase, which is about atmospheric pressure, is a supply of gasses flowing upward towards the cylinder. This reverse blowby is generally a low pressure/high volume flow, whereas the downward blowby during the expansion stroke is a high pressure/low volume flow. As stated earlier, however, the net flow of gases is generally from the crown land towards the crankcase, and thus the net effect on oil transport on the piston lands is also in the down direction. Reverse blowby is certainly a significant source of upward oil transport through the ring gap, but this will be discussed in a later section.

A prominent variable for gas driven circumferential oil transport is ring gap position. If the ring gaps are aligned, there will be virtually no circumferential gas flow around the lands, and hence no circumferential oil transport. However, the ring gaps are rarely aligned, and consistently seen to rotate independently of each other [32]. The relative distance between the gaps also changes the oil flow patterns; if two gaps are near each other, the main flow of gases will be along the short path between them. There will be little circumferential flow the long way around the circumference of the piston land, as most of the gases will 'short circuit'. Therefore, the oil accumulations between the ring gaps will be strongly effected by the gas flow, and the accumulations on the far side of the piston land will feel little to no effect. As this experimental setup had no way of measuring ring rotation, except by visual inspection of the gaps passing by the viewing window, the relative strength of the gas flows across the piston land was unknown.

The effect of gas dragging in the circumferential direction will increase with engine load. The greater the engine load, the greater the magnitude of blowby gases sweeping the piston land. For example, a low to medium load operating point will allow the thin accumulations on the second land to remain as illustrated in Figure 3.11. The blowby gases at this operating point will slowly drag them in the direction of the gas flow, from the top gap towards the second ring gap. When the load is increased, or if the ring gaps move closer together, the strength of the blowby gases increases and tends to topple these accumulations in the circumferential direction. Instead of a few slow moving thick accumulations, the puddles tend to flatten out into a large film and the circumferential flow rate increases. This evolution is shown in Figure 3.13, where the engine was running at a 2,500 rpm with an absolute intake pressure of 300 mbar, and then the load was increased quickly to 700 mbar. The first two images are before the load is changed; the transient process takes about one second for the engine to stabilize, but it takes a few seconds longer for the oil patterns on the piston land to stabilize. Note how the second land isn't consistent until about two or three seconds after the load increase is complete. As the transient state lasted less than 1 second, it can be said these effects seen on the second land are from the increase in blowby, and not the ring gap relative position. The measured blowby at the 300 mbar load is about 1 L/min, whereas it increases to about 4 L/min at 700 mbar absolute intake pressure. It is this increase in net blowby flow that topples the large, slow moving accumulations and creates fast moving, thin accumulations and a more uniform looking second land.

The blowby is known to vary significantly depending upon engine operating point. Figure 3.14 is a measured net blowby map for the ring pack shown in Figures 3.11 and 3.13. Note the timescales involved and the units; an engine speed increase will allow less time per cycle for blowby gas flow, but will have more cycles per second. Therefore, the units of blowby measurement employed in this experimental study are liters/minute (L/min), with the gas volume converted to standard pressure and temperature conditions.

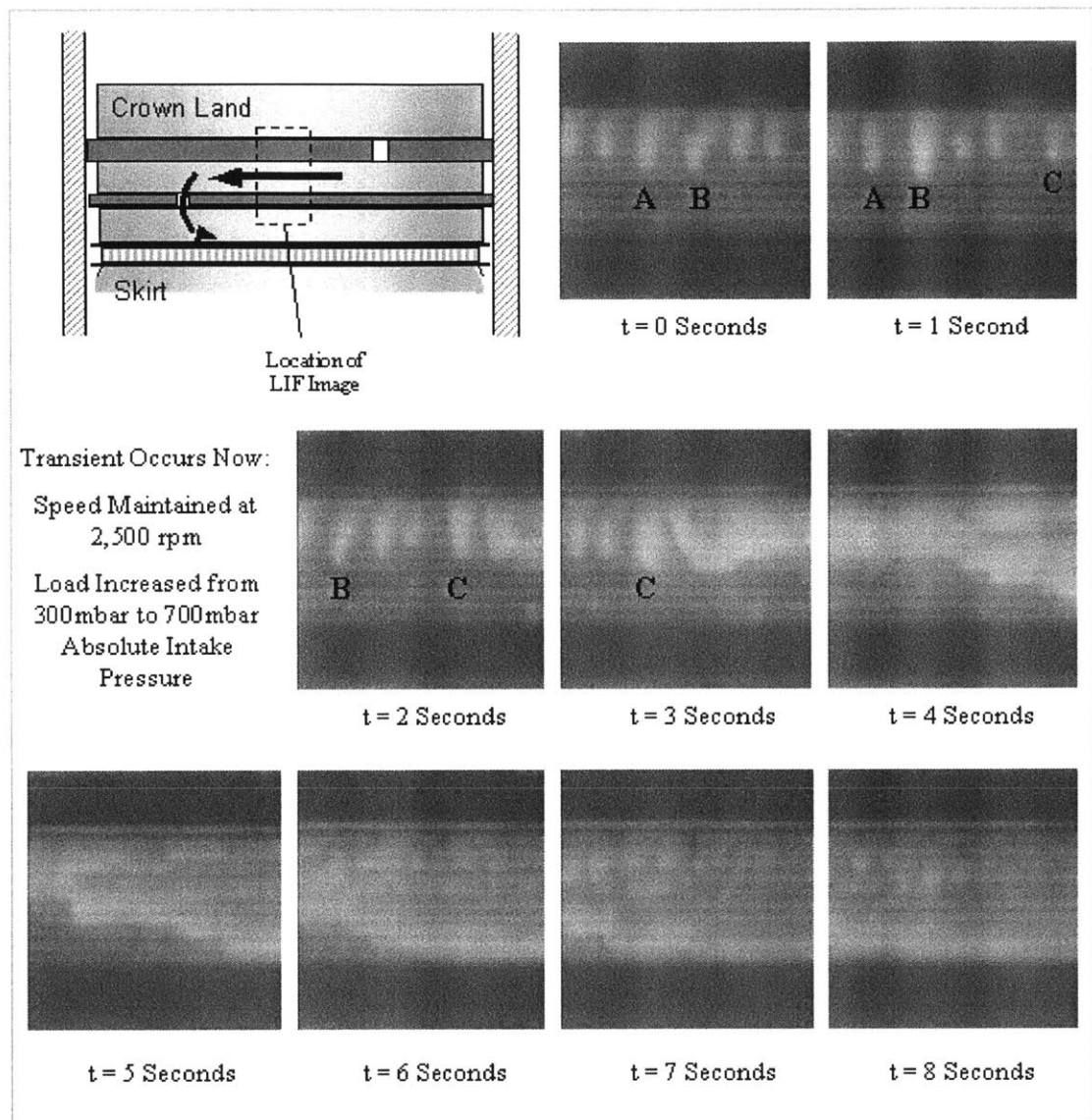


Figure 3.13 – Relationship of load, and thus blowby flow rate, on second land circumferential oil transport; the letters denote a specific oil accumulation and follow its movement over the timeline (the location of the ring gaps is not known exactly, but their approximate location is shown in the drawing)

Blowby values are generally quite consistent, however, even at a stable operating point the blowby can become unstable. A build up of oil in a ring groove can change the gas dynamics throughout the engine cycle, sometimes causing the ring to become unstable and flutter in its groove. This only occurs at certain operating points, and even then the timing is variable, sometimes occurring as often as every thirty seconds and sometimes occurring only once every ten minutes. When the ring flutters, the blowby gas flow increases dramatically, with net blowby values increasing by a factor of 5 or more. Much

of this increase in blowby will flow through the fluttering ring's groove. This large flow occurring all around the piston circumference can induce an axial dragging effect of the lubricant accumulations on the land. Axial gas dragging can occur during normal operating conditions as well, but the gas flow through the ring groove is just not great enough to have a significant effect in comparison to inertia. Axial transport induced by gas flow through the ring groove is shown in Figure 3.15. The accumulation near the top of the second land can be seen to be driven downward over the course of 0.6 seconds by a blowby burst, originating from a brief period of top ring instability. The same top ring instability is seen to also squeeze some oil out of the top ring groove and onto the crown land.

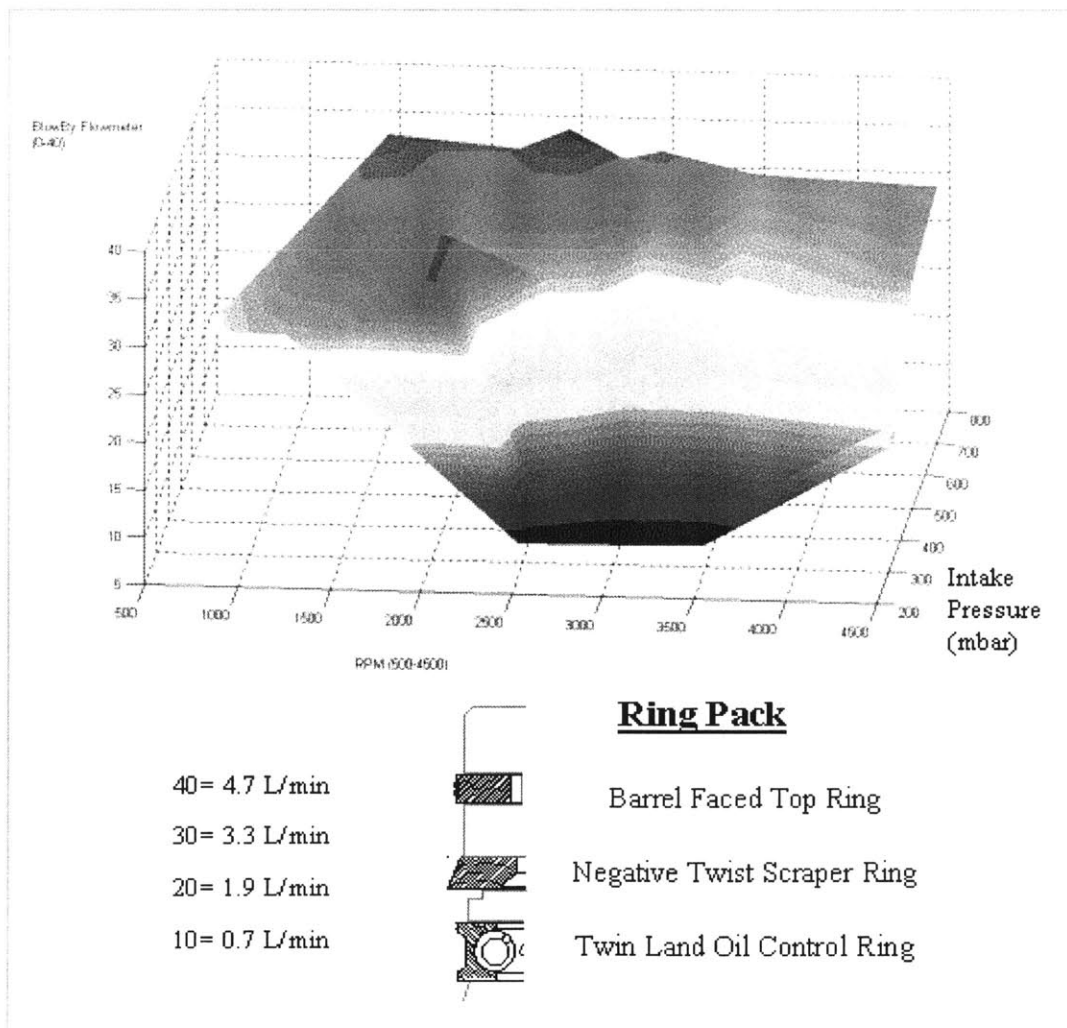


Figure 3.14 – Blowby map for the ring pack shown, influence of speed and load are illustrated

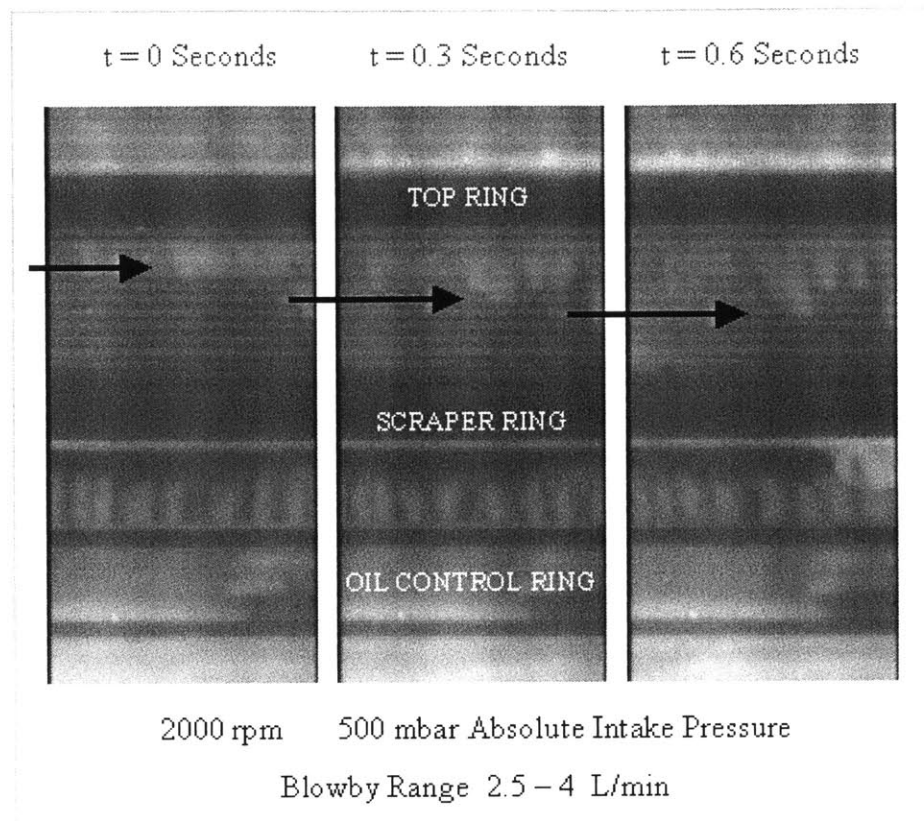


Figure 3.15 – Temporary top ring instability and the effects of axial gas dragging of oil on the second land; the blowby is seen to vary at this operating point, with a range between 2.5 and 4 liters/minute

Another source, albeit less common, for blowby gases to effect piston land transport is during a ring collapse situation. With specific ring pack geometry and land pressures, a ring can be forced inward (collapse) allowing a clearance between the ring running surface and cylinder liner. A significant amount of gas flow passes by the collapsed ring through this ring/liner clearance, and can drag oil along the piston land with it. The effect of second ring collapse can clearly be seen in the LIF image displayed in Figure 3.16, along with an illustration of the ring/liner clearance and a comparison of the gas flow rate through the ring gap versus the gas flow rate through this ring/liner clearance. The RINGPACK-OC software outputs a ring collapse situation, and same conclusion was evident in the unique oil patterns generated on the piston ring pack. The Napier ring collapse creates a ‘streaky’ pattern on the second land, as there are brief periods of high axial gas flow rates across it. The occurrence and duration of these ring collapse periods was limited to specific geometry and a few operating points, and thus this mechanism was not studied in great detail.

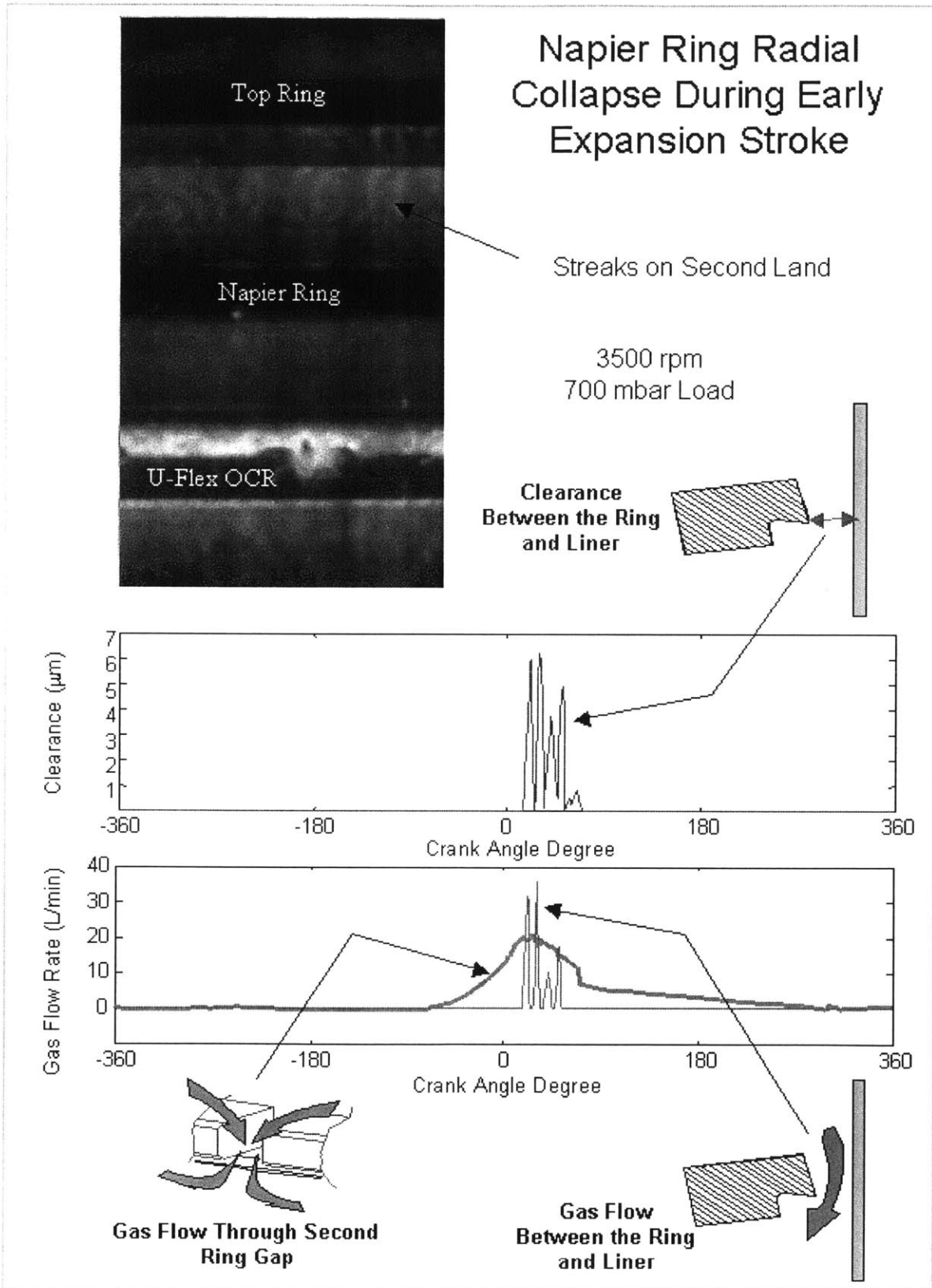


Figure 3.16 – Mechanics and LIF evidence of Napier Ring collapse

3.2 Ring Scraping

A great amount of work in the automotive field has been conducted on the ring/liner, or running surface, interface. Ring scraping is the mechanical act of a ring, which is moving axially in its cylinder liner, removing oil from the liner. This phenomenon has been described in detail and modeled by Tian [12,26,33], and will thus only be overviewed in this work. The ring/liner interface is strongly influenced by many factors, such as ring static profile, piston tilt, bore deformation, and the amount of oil left on the liner by the previous ring. Ring scraping can occur in two major lubrication conditions, both of which are illustrated in Figure 3.17: Leading edge fully flooded and loss of hydrodynamic lift.

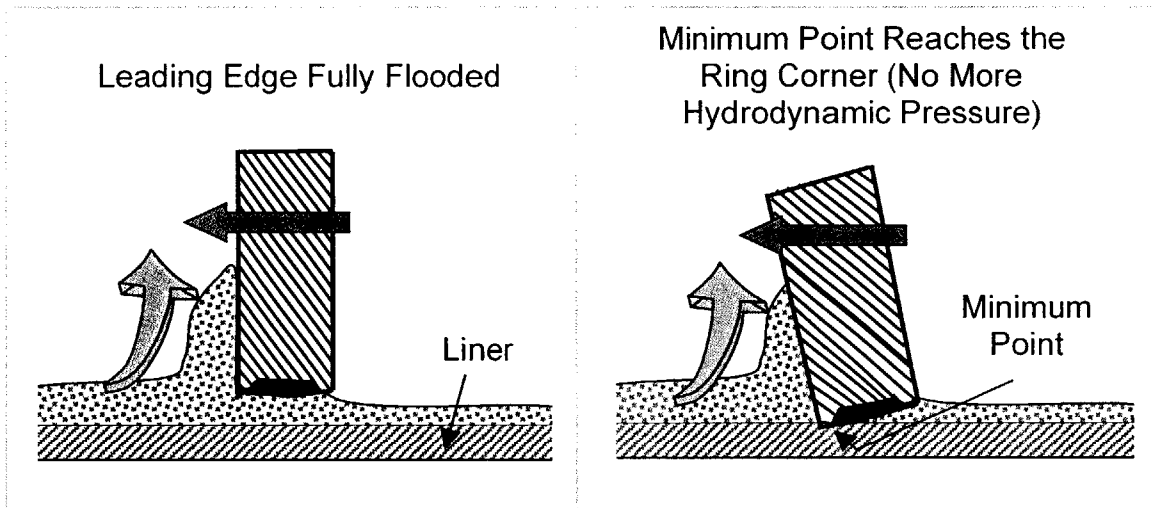


Figure 3.17 – Ring scraping conditions

The leading edge fully flooded situation generally occurs when the oil film on the liner is thick enough to prevent hydrodynamic pressure from lifting the ring leading edge above the surface of the oil layer. This condition will tend to remove oil from the liner, accumulating on the leading edge ring surface.

Loss of hydrodynamic lift occurs when the minimum point, the point of the ring running surface closest to the liner, reaches the leading corner of the piston profile. The ring

profile relative to the liner will change throughout each stroke depending on piston tilt and ring twist, and thus loss of hydrodynamic lift may only occur for a portion of a stroke, if at all. When the corner becomes the minimum point, the converging wedge that creates hydrodynamic lift disappears. Asperity contact alone now supports the ring, and the corner point will tend to scrape oil from the cylinder liner. Note that this situation is only instigated by the relative geometry and not the oil supply on the liner; excessive running wear will often induce loss of hydrodynamic lift [34].

Ring scraping will cause an accumulation to form on the leading surface of the ring. Depending on the degree of scraping, which is largely influenced by the oil supply on the liner, the accumulation can spread along the ring surface to the ring groove and piston land, representing a net transfer of oil from the liner to the piston ring pack. In practice, this phenomenon is difficult to verify with the 2D LIF technique as there are many possible sources for an accumulation to form on a ring surface, and because the quantity of oil scraped is generally small in magnitude compared to the oil transport mechanisms occurring on the piston ring pack.

One significant instance of ring scraping occurs during ‘Ring Bridging’ or droplet formation as described in the inertia portion of Section 3.1. These two phenomena act to put a large quantity of oil onto the cylinder liner, which then tends to become scraped by the next passing ring. Figure 3.18 shows a high speed scenario (~ 4,500 rpm) where both ‘Ring Bridging’ and droplet formation occurs during a downward stroke and a downward inertia period. Some oil from the second ring groove and hook pours across the third, accumulates on the OCR top surface, and crosses to the liner; additionally, some oil forms droplets falling from the second ring hook, with a few of them landing on the cylinder liner. As the piston continues to move down, the second ring scrapes this additional oil from the cylinder liner. In less than 90 crank angle degrees, this oil has left the second ring and returned through a series of transport mechanisms. As inertia is still in the downward direction, however, the scraped oil that has accumulated in the Napier Hook will again form droplets and fall towards the OCR. A more detailed description of this repeatable and cyclic process will be discussed in the third land section later.

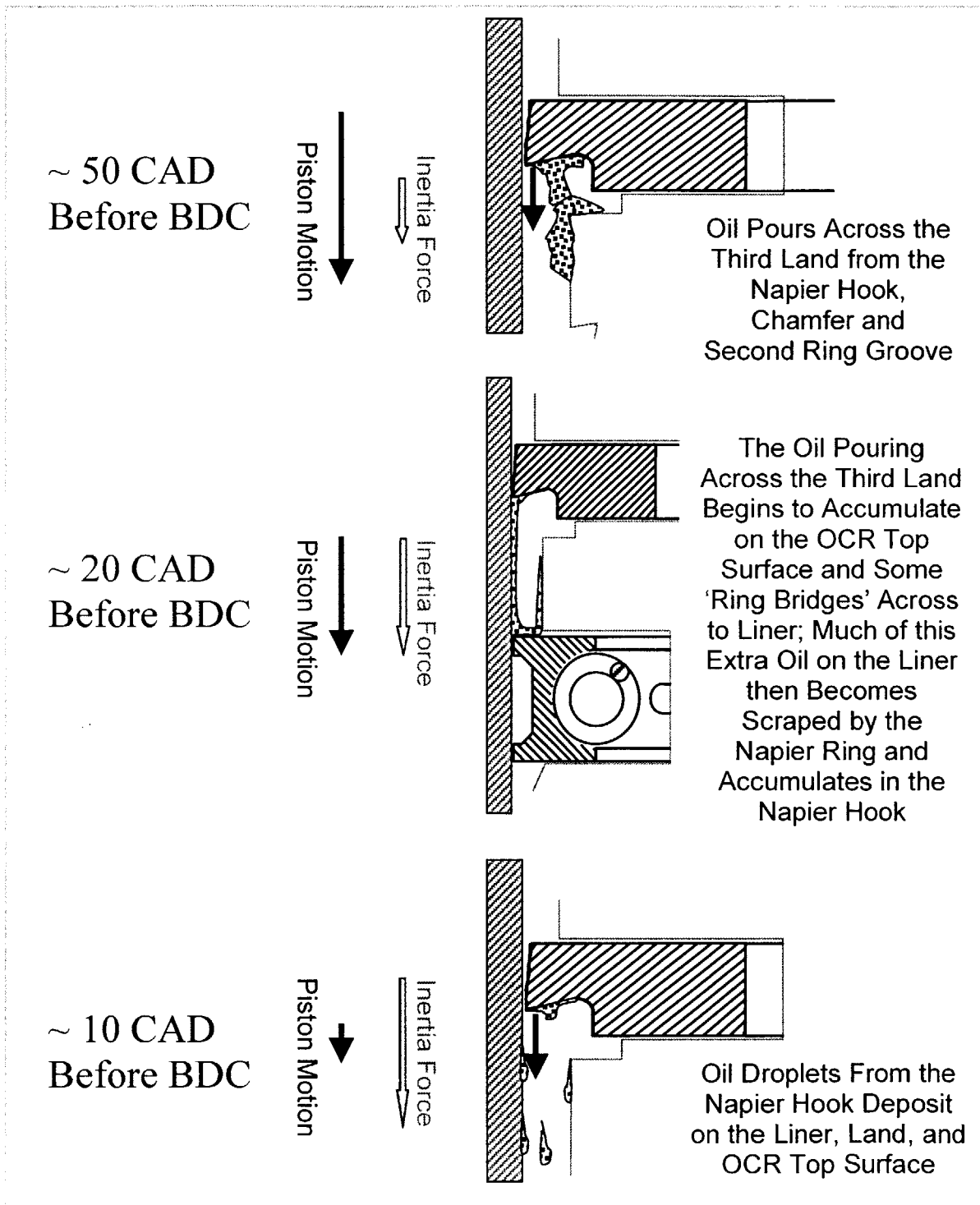


Figure 3.18 – ‘Ring Bridging’ and scraping scenario

Poor Ring Scraping

Experiments have verified the rings may drastically lose their scraping ability if the thickness of the accumulation on the liner is significant enough. Seen to occur following a heavy ‘Ring Bridging’ transport to the liner, a portion of the ring circumference allows a significantly thicker accumulation than normal to pass by it on the ring/liner interface. Sometimes this accumulation passes by a ring more than once, originating near BDC of a down stroke and remaining on the liner after the piston passes during the upstroke.

This phenomenon was seen to occur during low load situations, or when the ring gaps were aligned, causing a large accumulation on the third land with significant ‘Ring Bridging’ occurring. The excess oil on the liner that is passing by the rings was not able to be measured, but is quite easily seen on the LIF images and estimated to be at least twice the normal thickness on the liner (2 microns), and possibly as much as five times the thickness. The possibility of this unexpected event occurring only in the region of the sapphire window and due to certain mechanical properties must be considered, though it is thought to be unlikely. Although this excess oil is clearly discernable in the LIF data, it is difficult to see in general print media, and thus will not be shown in this work.

3.3 Oil Transport Through the Ring Grooves

Oil transport on the piston lands has been discussed, but for oil to move from the crankcase to the combustion chamber, it must also travel through the ring grooves or the ring gaps. In the 2D LIF images, oil was consistently seen to travel from one piston land to the next by traveling through the ring groove. Assuming an upward transport, the oil must undergo several processes for this to occur: Transport from the liner to the lower ring/groove clearance, then transport to the back of the ring groove, then transport to the upper ring/groove clearance, and finally transport out onto the piston land. This phenomenon was seen to occur to some degree for all geometries and operating conditions tested. Disregarding effects of the ring gap, the accumulation in the back of each ring groove should come to an equilibrium volume for a stable engine operating

point; this area acts as sort of a buffer region. In Figure 3.19 (same as Figure 3.09), the accumulation on the second land grows and grows, with the only possible supply coming from the second ring groove, which is in turn being supplied from the third land. In Figure 3.20, the oil control ring gap is seen to allow a tremendous amount of oil onto the third land. This ring gap phenomenon will be discussed later, but note the correlation of oil on the second land to the large accumulation of oil on the third land. Clearly this oil has traveled from the third land, through the second ring groove, and out onto the second land. Note the timescale of both of these groove flow examples is on the scale of one second.

The ring and piston relative geometry is dynamic throughout the engine cycle, creating many possible sources of oil flow into and out of the ring grooves. The main transport mechanisms for oil flow through the grooves are: Inertia driven flow, ring pumping, blowby gas dragging, and piston secondary motion.

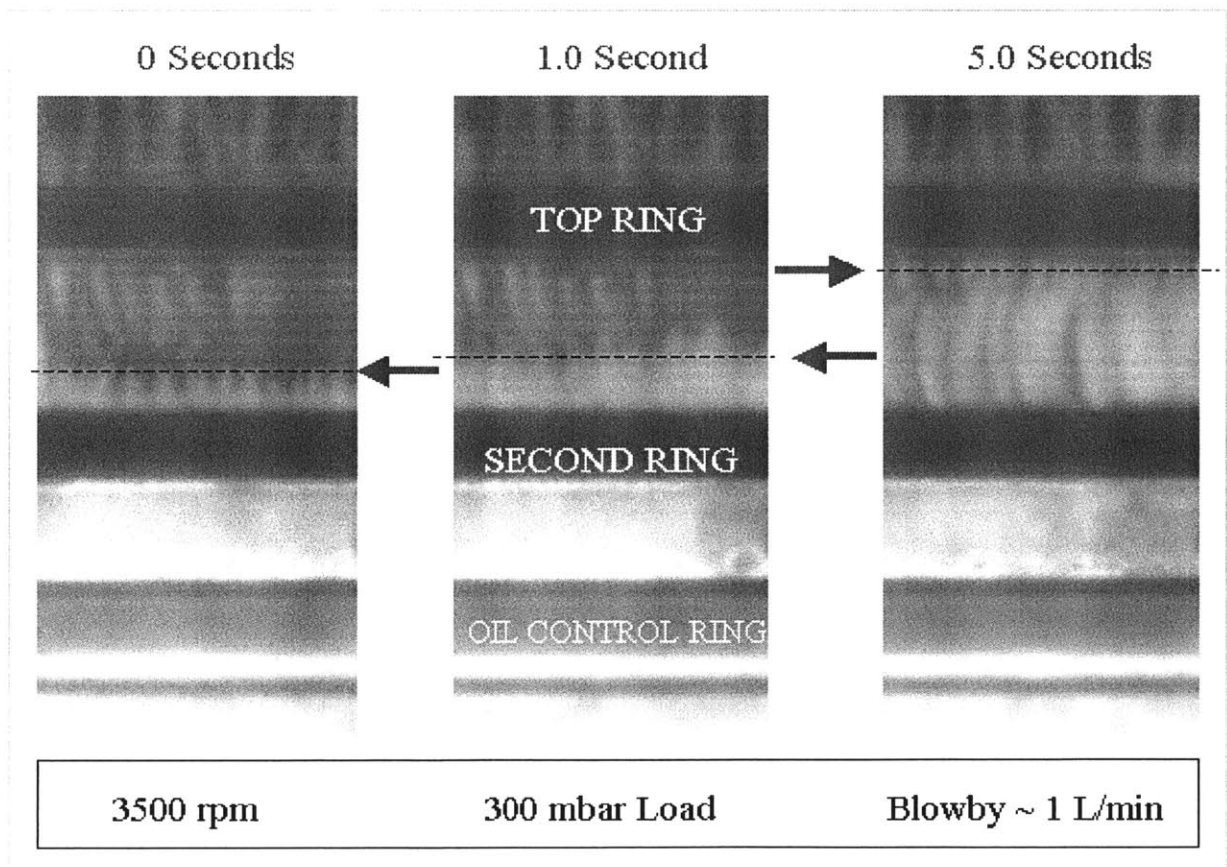


Figure 3.19 – Oil flow through the second ring groove and onto the second land

Mid-Intake Stroke 4500 rpm, 500 mbar Load

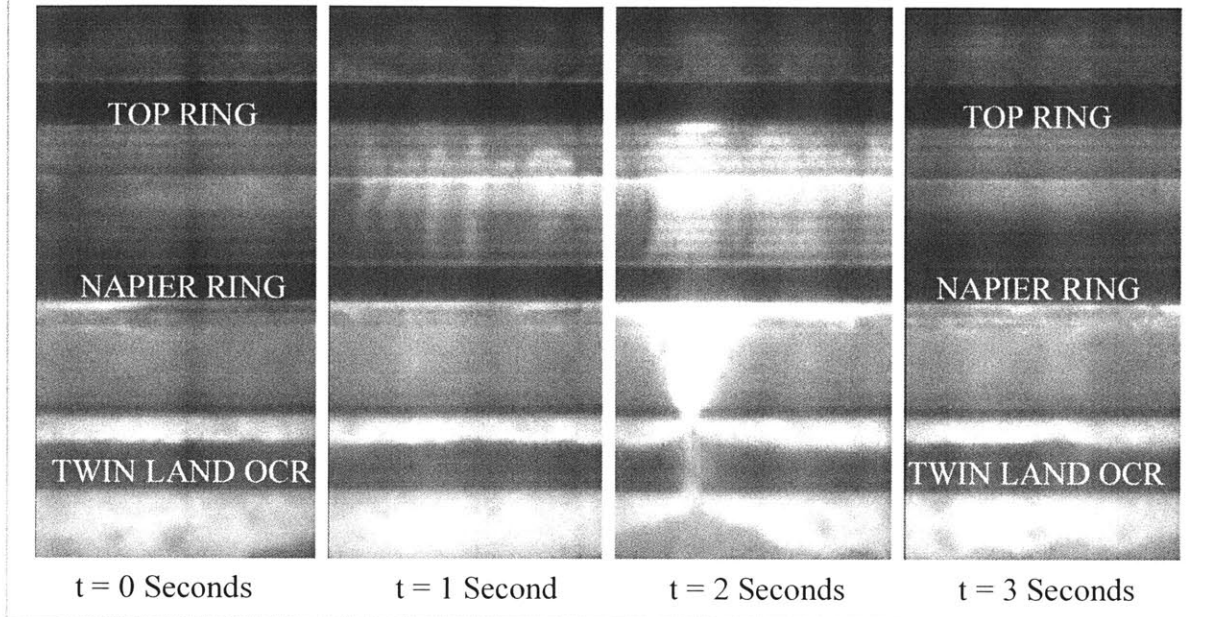


Figure 3.20 – The large oil accumulation on the third land is seen to have direct implications to the second land; the only feasible means for the oil association between them is oil flow through the second ring groove

Inertia Driven Flow

The ability of inertia to drive oil across the piston land has been discussed in great detail in Section 3.1. When an accumulation is driven across the land, it will reach the land/groove interface. If the ring is also resting on this land/groove interface, a ring pumping situation will result; however, if the ring is resting on the far groove flank, or after ring pumping has occurred, inertia will generate a pressure gradient and act to drive the accumulation into the ring groove clearance. As the pressure gradient is proportional to the thickness of the accumulation, this transport mechanism is most important on the third land and piston skirt where the most oil is consistently present. The ability of oil to be driven into the ring groove will also be enhanced at higher engine speeds, as the inertia force driving the oil will be greater. An illustration of this phenomenon is shown in Figure 3.21.

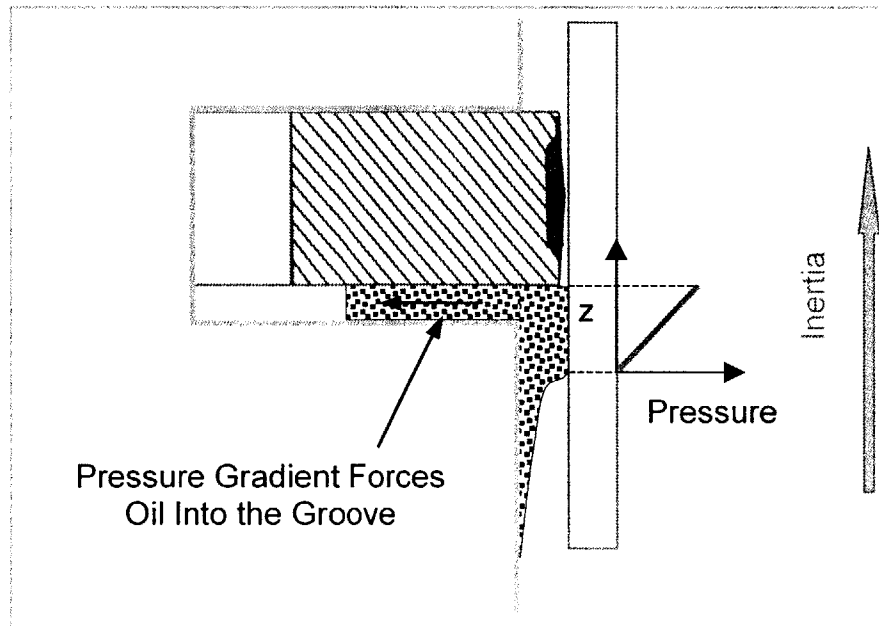


Figure 3.21 – Inertia can drive oil into the ring groove by establishing a pressure gradient

Ring Pumping/Squeezing

The ability of inertia to drive oil across the piston land has been discussed in great detail in Section 3.1. When an accumulation is driven across the land, it will reach the land/groove interface. If the ring is also resting on this land/groove interface, a ring pumping situation will result. The oil accumulation will build up at this ring/land/groove interface until inertia drives the ring to the far side of the groove. The accumulated oil will attempt to fill the open volume created by the ring's movement, becoming pumped into the ring groove. The timing of the ring's axial movement and the rate of accumulation build up are the major factors determining the amount of ring pumping. Obviously, if the ring has moved axially in its groove before the oil accumulation reaches the land/groove interface, a simple inertia driven pressure gradient, as described above, will establish. The volume created by the ring's movement in its groove is much larger than the oil supply available at the interface, limiting this transport mechanism by oil availability. Additionally, gas flows and oil from the back of the ring groove will also act to fill the volume left by the ring's movement.

The axial movement of the ring in its groove will induce the pumping effect described above, but it will also induce a ring squeezing phenomenon on the opposite groove flank. As the ring moves toward the groove flank, the oil layer residing in the ring/groove clearance will be squeezed both into and out of the groove; some of the oil is forced into the back of the ring groove, but some is also forced out of the ring groove and onto the piston land. Ring squeezing was experimentally seen to be the major mechanism of oil transport from the ring grooves to the piston lands. Ring gap driven transport, to be discussed in a later section, is the only other mechanism of comparable magnitude for oil transport out of the ring groove.

The amount of oil residing in the ring groove is clearly an important variable to the amount of ring squeezing, but the exact ring/groove geometry is also critical. Figure 3.22 shows the relationship of ring pumping and ring squeezing, while Figure 3.23 details the trade offs that ring/groove geometry have on ring squeezing.

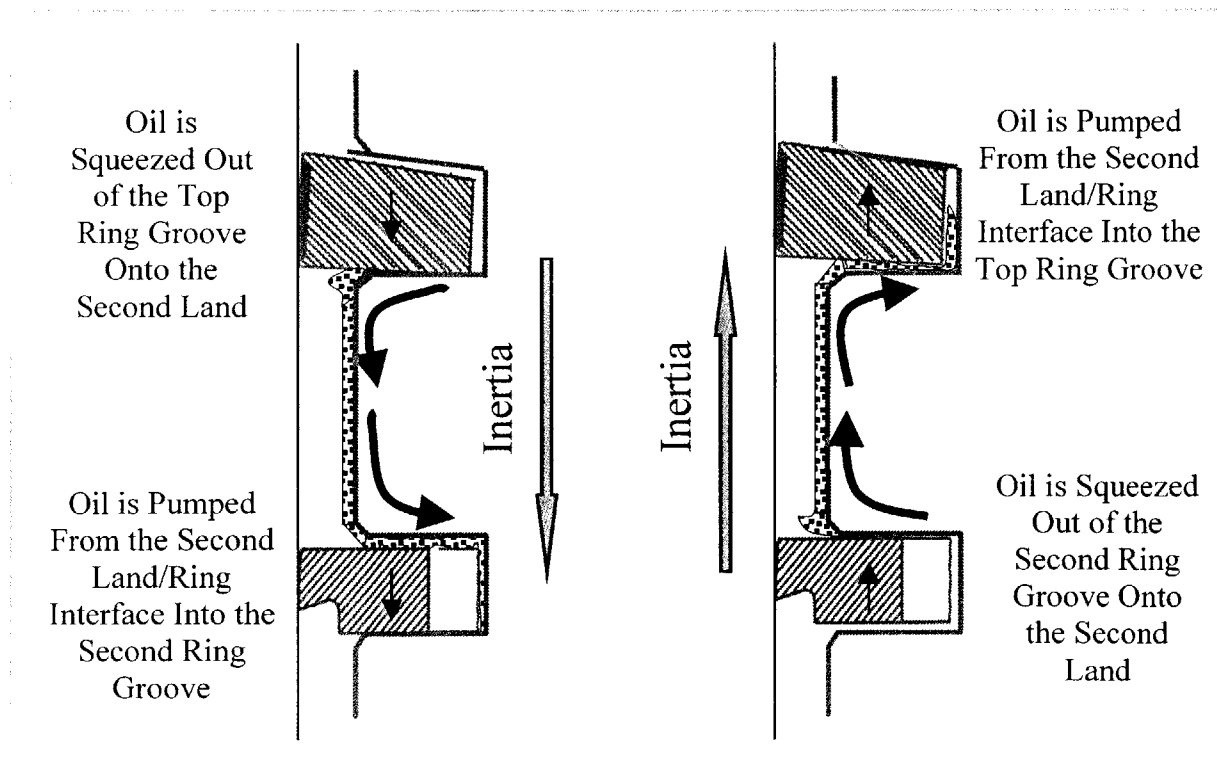


Figure 3.22 – Ring pumping and squeezing, and their relation to inertia force and ring dynamics

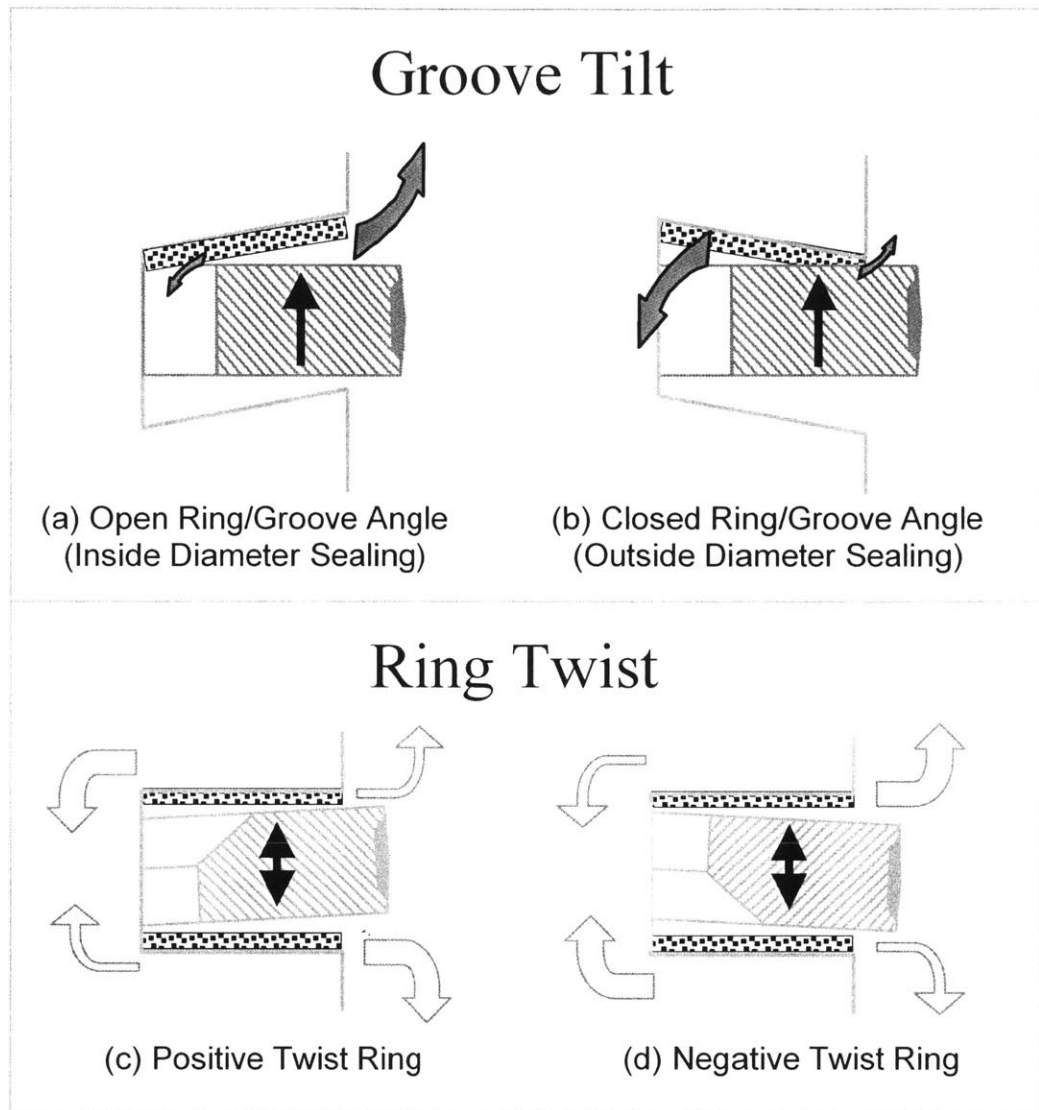


Figure 3.23 – Effect of groove tilt and ring twist on ring squeezing; the size of the arrows within each example indicate the relative magnitude of the transport direction

The geometry of the squeezing region between the ring and the groove is largely determined by the piston groove tilt and the ring twist. The relationship between these has a significant impact on how much of the oil in the ring/groove clearance is squeezed, and in what direction. Let us take a ring moving upward in its groove for example, if the groove tilt is up (inside diameter sealing, Figure 3.23a), a larger amount of oil will be forced onto the piston land than to the back of the ring groove, if the groove tilt is down (outside diameter sealing, Figure 3.23b), the majority of oil would be forced towards the back of the ring groove and only a minor amount onto the piston land. When the effect

of ring twist is investigated in a groove with no tilt (Figure 3.23c and 3.23d), a similar outcome is seen on the preferred direction of ring squeezing. The optimum design in each of these simple scenarios is clear, but the piston and ring designer must take into consideration the combination of ring twist and groove tilt, as well as a myriad of other design factors, making the final decision a compromise between the choices.

Blowby Gas Driven Flow

The effect of blowby on dragging oil from the piston lands axially into the ring grooves has been discussed in Section 3.1, and found to be mostly negligible, except in a ring flutter scenario. The effect of blowby gases on the lubricant within the ring grooves may be significant, however, as the clearances and volumes are much smaller than on the piston lands. The direct effect of the gases moving the oil out of the ring groove probably is small, but the gases certainly influence overall transport through the ring groove. Comparing two upward strokes, compression and exhaust, it was found the effect of the combustion gases during the expansion stroke acted to clean the ring/groove clearance of the oil control ring, forcing some of the oil to the back of the ring groove. The blowby gas flow during the intake stroke is much less, and even reverse in direction at times, and thus less cleaning of the OCR ring/groove clearance is conducted. During the resulting upstrokes, much more oil is forced out of the OCR groove onto the third land from squeezing during the second half of the compression stroke as compared to the second half of the exhaust stroke. The LIF comparison of the amount of oil forced out of the ring groove is shown in Figure 3.24. The specific mechanisms and a detailed explanation of this process are detailed in the third land section later.

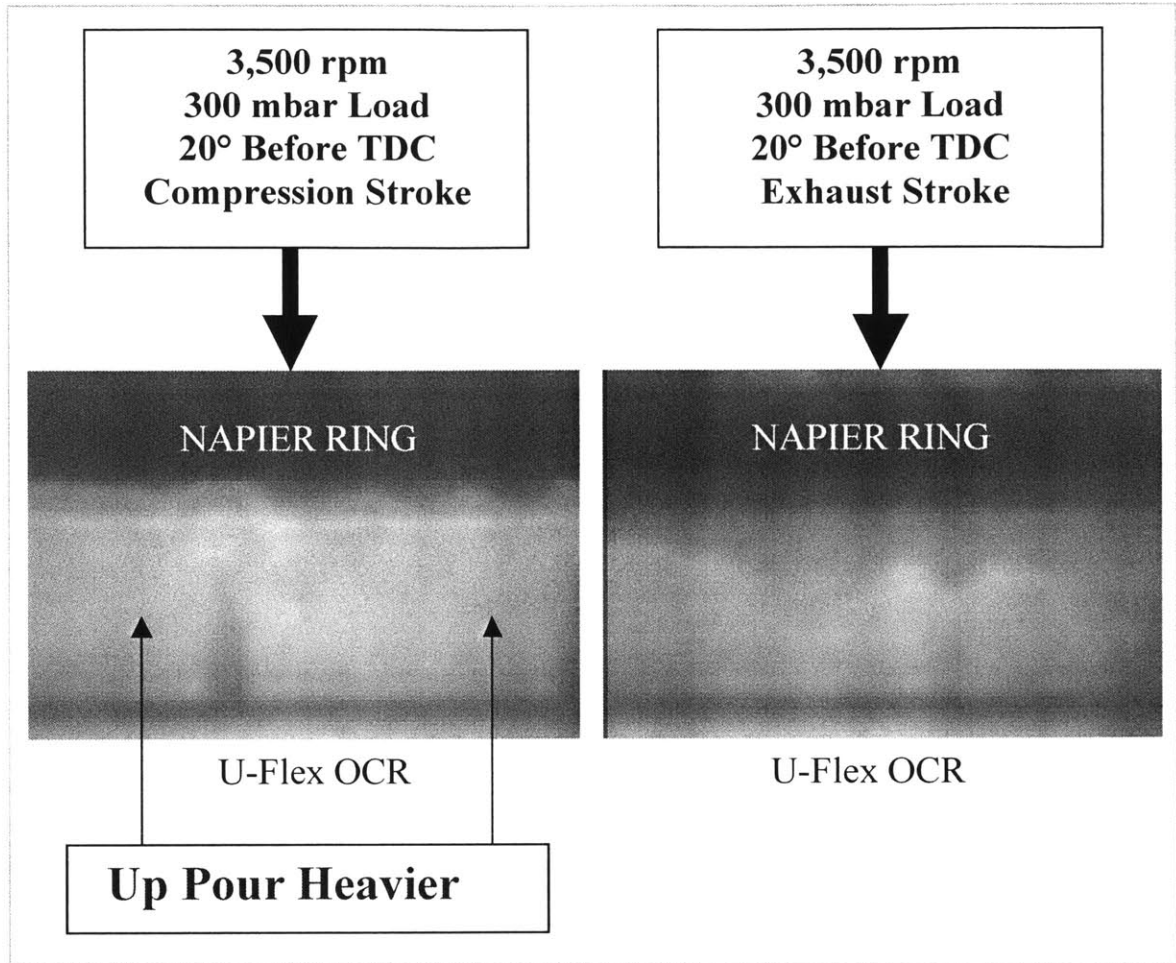


Figure 3.24 – Effect of gas flow on oil transport through the ring groove; the higher expansion gas flow rate into the OCR groove results in less transport onto and across the third land for the exhaust stroke, then the intake stroke gas flow rate allows during the compression stroke

Piston Secondary Motion

The shear force induced by lateral motion of the piston relative to the rings, caused by piston secondary motion, can cause any oil accumulated on the rings to be transported into or out of the ring/groove clearance (see Figure 3.25). Similarly the change in piston tilt from the thrust to anti-thrust side can induce some ring pumping phenomena. The change in tilt and lateral motion during the transition from intake to compression stroke, with the associated oil transport, is shown in Figure 3.26. These effects are likely to be minimal in the overall oil transport scheme, and certainly difficult to analyze further without an accurate piston secondary motion model.

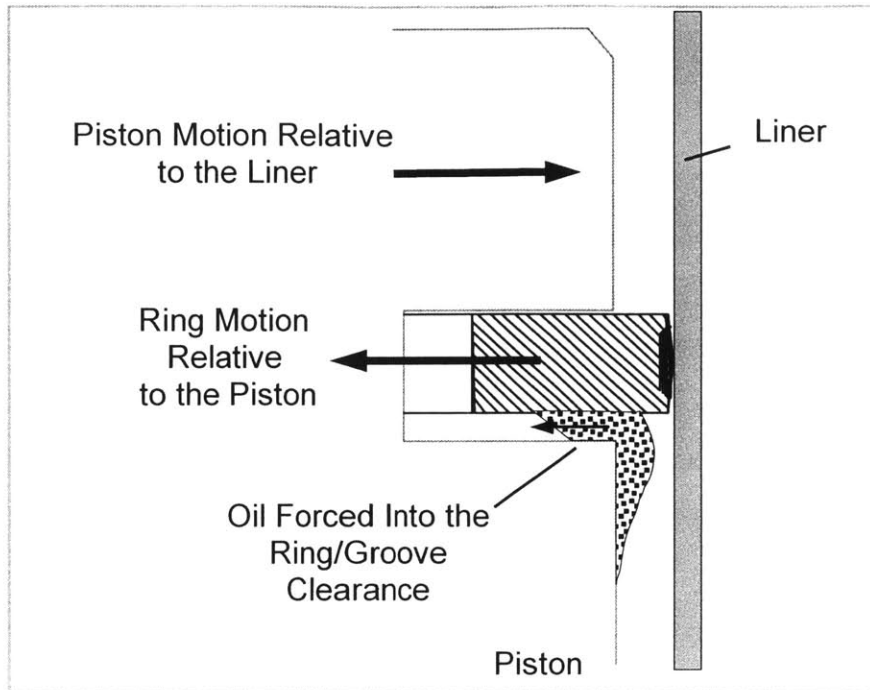


Figure 3.25 – Description of the oil transport into the ring groove resulting from the lateral motion of the piston relative to the rings

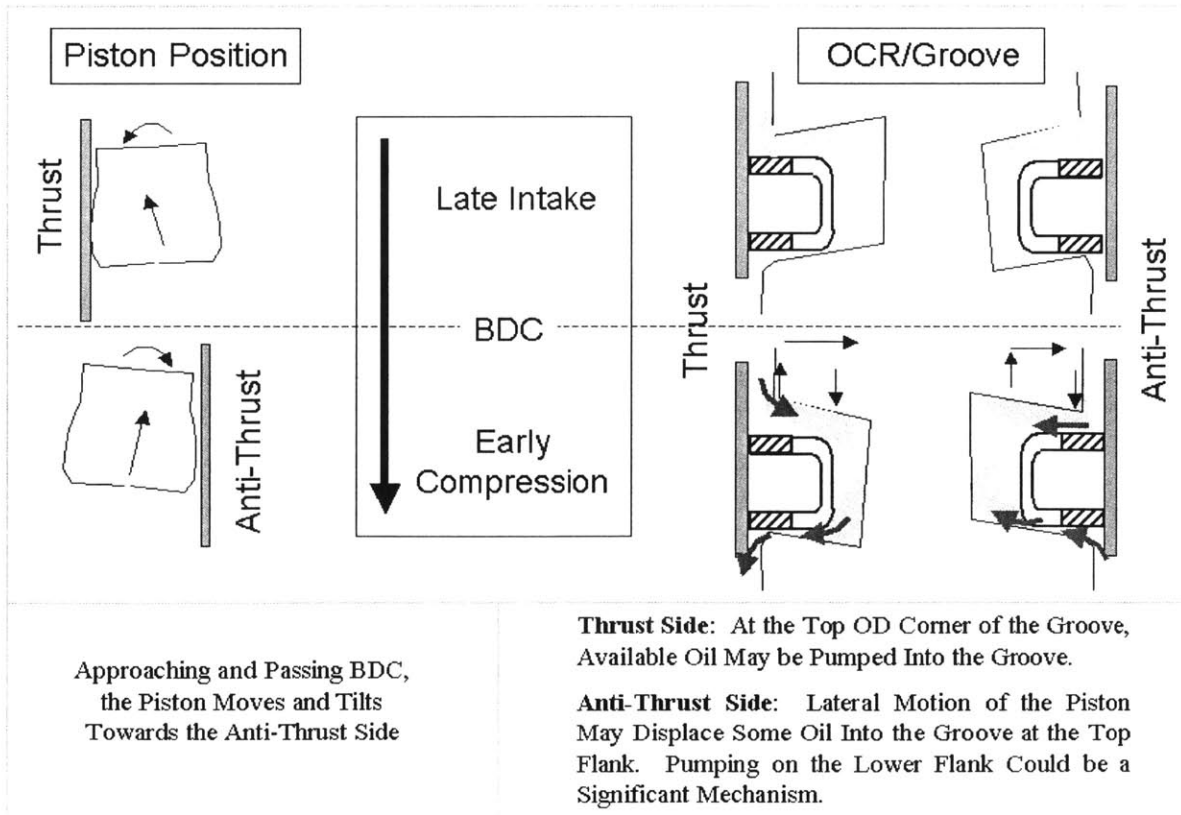


Figure 3.26 – Piston secondary motion effects on oil transport into and out of the ring groove

3.4 Ring Gap Driven Transport

The ring gaps are believed to be a major oil transport mechanism through the piston ring pack, and in particular for transporting lubricant across the second land. These ring gaps are the major path for gases to flow from the combustion chamber to the crankcase, and vice versa, acting to drag or vaporize the oil in the associated ring gap flow paths. The effects of the ring gaps were studied for each of the engine operating conditions tested, but limited by the natural ring rotation of the power cylinder system. The ring gaps could only be investigated when they were naturally passing by the viewing window, as no ring pinning was attempted. This makes a detailed study prohibitive; however, experimental ring gap data was obtained quite often and allowed a continuous study of ring gap effects throughout all the ring pack configurations tested. The ring gaps were seen to have a dramatic impact on the oil transport patterns of the piston ring pack every time they were in the viewing window. Gas driven transport through the ring gaps was seen to be the dominant oil transport mechanism for the top two rings; downward gas flow largely entrains liquid oil into the gas stream, whereas reverse blowby acts to bring liquid oil onto the land above. Inertia was the main driving force for oil through the oil control ring gap, particularly with the use of a Twin Land OCR.

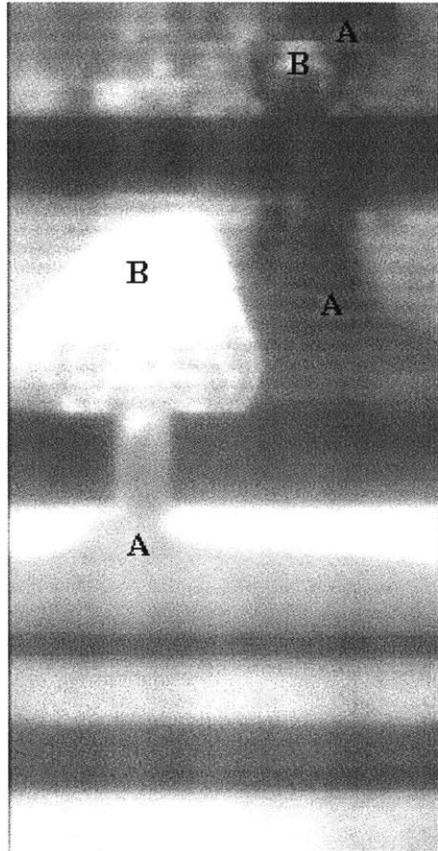
Gas Driven Ring Gap Oil Transport

The top two ring gaps, coupled with the blowby gas flow, have a major effect on the crown and second lands. Experiments reveal the main downward gas flow paths, above and below the ring gaps, are 'clean'; very little oil exists in the downward flow path regions. The lack of liquid oil in these areas suggests the gas flow breaks up the liquid layer and entrains the lubricant into the gas steam. The high velocity gas stream and oil mist cannot be detected with the equipment in this project, as the volumetric concentration of dye in the mist is low relative to the liquid layer. Figure 3.27 illustrates how the gases flow from the combustion chamber through the top ring gap, clearing out the area directly above and below it, then circumferentially around the piston land, acting to drag oil with it (depending on the ring gap relative distance), and finally through the second ring gap, clearing out the area around it. The 'clean' area was found to be larger

for the top ring gap, as opposed to the second ring gap, as the velocity of the blowby gas stream is greater.

Downward blowby is very influential in shaping the oil patterns on the piston ring pack, but the effect of reverse blowby, or upward flowing gases, also has a considerable impact and can be seen to overlap with the effect of the downward blowby. Even at low load conditions, the net flow of blowby gases is usually from the combustion chamber to the crankcase; however, there is a substantial reverse blowby flow during the intake stroke, generated from the vacuum in the combustion chamber. Even though the net gas flow may be in the downward direction, it does not necessarily mean the net oil transport through the ring gaps will also be in the downward direction. The downward flow of gases will generally be high pressure, low volume flow, whereas the upward reverse blowby will generally constitute low pressure, high volume flow. This can create a situation where there is net mass flow downward through the gap, but a net volume flow upward through the same gap. The low pressure, high volume upward flow will tend to drive large amounts of liquid oil onto the land above the gap, and is largely dependent on the amount of oil available below the gap. As the third land contains a much larger oil supply than the second land, this effect will be much more pronounced for oil transport onto and across the second land.

Figure 3.27 illustrates the dramatic effect this reverse blowby can have on the second land. The particular second ring shown in this ring gap section has a larger than normal gap width (about 1mm), so the effects are particularly enhanced. The comparison of this mechanism to the top ring gap can also be seen in the Figure. The reverse blowby effects are indicated for both ring gaps, but clearly the ‘mushroom cloud’ effect is more pronounced for the second ring gap. The effect of the downward blowby gas stream can also be distinguished; the areas directly above and below the top two ring gaps are swept clean primarily during the expansion stroke, but during the intake stroke liquid oil is driven upward through these same gaps. The effects clearly overlap, as the duration timescales of the phenomena are longer than one engine stroke.



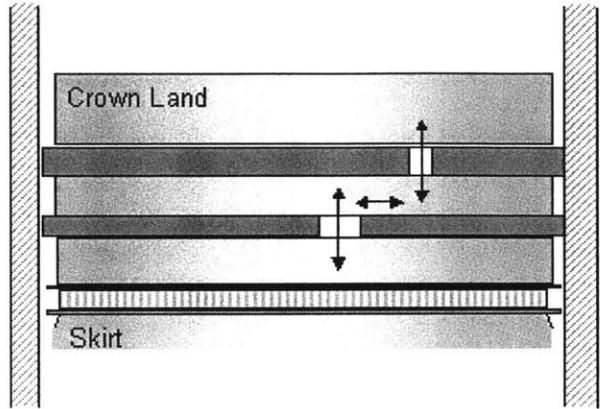
3500 rpm

300 mbar Load

Mid-Stroke Compression

A = Downward Gas Flow Effects

B = Reverse Blowby Effects



Second Land Focus

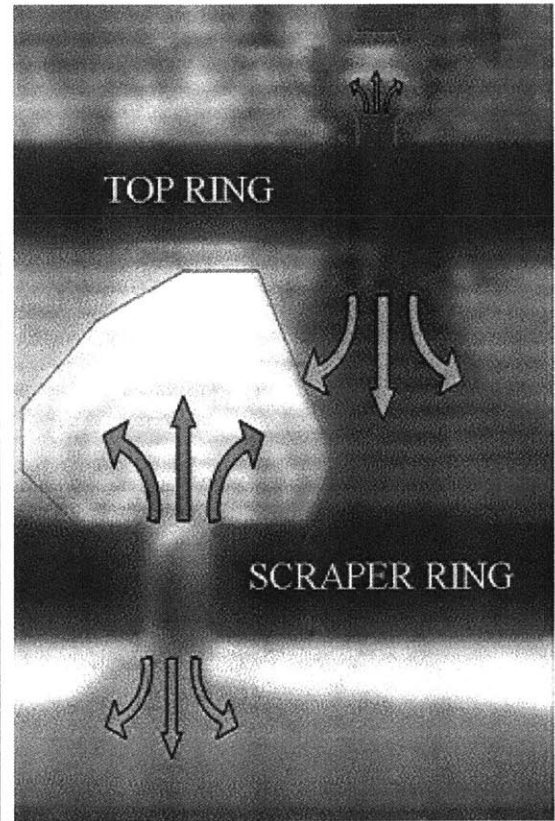


Figure 3.27 – Ring gap driven oil transport and gas flow effects

The two-directional gap flow, which occurs over the course of an engine cycle, can establish a recirculation pattern on the second land. The high pressure downward flow blows the oil away from the gap in somewhat of a cone shape; then during the intake stroke, the reverse blowby acts to drag some of that same oil back towards the gap. This creates a recirculation region or ‘Vortex Effect’ on the second land, shown in Figure 3.28. Oil on the lower part of the second land can be seen moving circumferentially away from the top ring gap, while oil near the top of the second land is seen moving circumferentially towards the second ring gap. This sort of recirculation, set up by the bi-directional gap flow, occurs only minimally on the crown land because the geometry does not promote circumferential gas flow. The recirculation phenomenon does not occur on the third either, as the large third land oil supply creates a general flow pattern which reforms each engine stroke and acts to wash out gap related effects; this third land characteristic will be discussed in more detail in the next chapter.

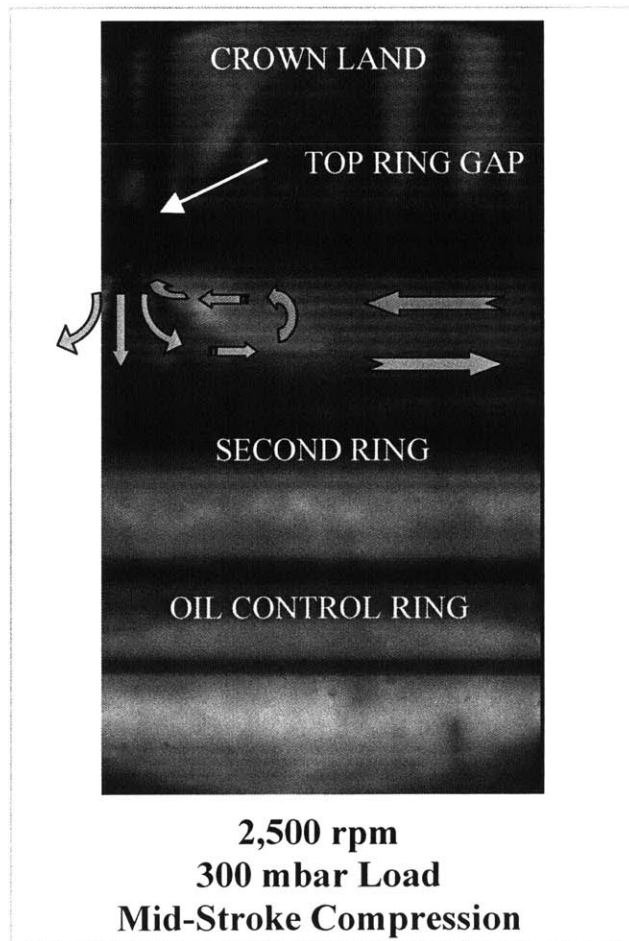


Figure 3.28 – Second land ‘Vortex Effect’

Inertia Driven Ring Gap Oil Transport

The sheer quantity of oil on the third land prevents gas flow through the oil control ring gap from becoming a major oil transport mechanism. Conversely, it makes inertia a significant transport mechanism in any oil control ring with large gaps, such as the Twin Land OCR, and the Three-Piece OCR to a lesser degree. The region below the OCR is always seen experimentally to be full of oil, and thus an upward inertia period will easily drive that oil onto the third land. The amount of oil moved by this OCR transport mechanism rivals all other ring pack modes. Figure 3.29 illustrates the magnitude of oil that can travel through an OCR gap each upward inertia period, with the rate of oil transport increasing with engine speed. This mechanism can be deterred if the quantity of blowby gases flowing downward through the OCR gap is large enough to prevent inertia from forcing oil through the gap. However, this deterring force will generally only be strong enough during the expansion stroke, and even then only for higher load and lower speed conditions. In regards to inertia driven ring gap oil transport occurring for the top two ring gaps: There isn't enough oil available and gas flow driven transport is dominant.

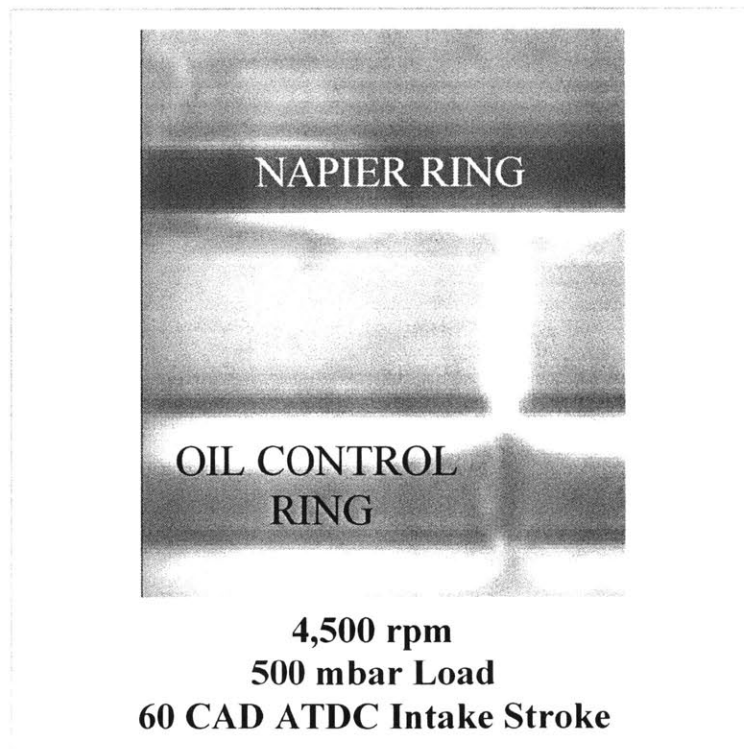


Figure 3.29 – Inertia driven oil transport through the OCR gap

Timescale Effects of Ring Gap Transport

Ring gap oil transport has been shown to be a significant mechanism of moving oil from the crankcase towards the combustion chamber. Each ring gap introduces specific phenomena onto the ring pack at its circumferential location. The net effect of ring gap transport relies heavily on two variables, engine speed and ring rotation. The faster a ring rotates, the more oil that will become spread around the circumference of the piston lands from gap driven transport. If the ring were to remain still, the negative effects of ring gap transport would become isolated to one circumferential location.

A faster engine speed will tend to dissipate the ring gap effects quicker, while a slower engine speed will leave the accumulated oil on the land long after the ring gap has rotated away. As inertia increases dramatically with engine speed, the accumulations left on the piston lands from ring gap transport are forced off the lands quicker with increased engine speed; stated another way, the piston land returns to a normal pattern quicker with increased engine speed. Figure 3.20, from earlier in the chapter, details the timescale and effects of inertia driven oil transport through the OCR gap. The OCR gap brings tremendous amounts of oil to the third land, and even the second land, as it rotates; however, the effects disappear in only a few seconds because of the high inertia force, as the oil is forced into the ring grooves.

The negative effects of ring gap transport may be mitigated by continually operating the engine at high load conditions. Unfortunately, common driving habits involve low speeds and low loads, which are the most detrimental for reverse blowby ring gap transport. This situation can occur during any driving situation, however, as all the driver needs to do is remove his foot from the accelerator for a few seconds. This transient operation to low load sets up a reverse blow by pattern and negative ring gap transport effects. Even if the low load period is brief, as soon as the driver accelerates again the oil that has accumulated on the piston lands will be forced off of the lands, with about half of it moving higher in the ring pack because of the balanced inertia force.

CHAPTER 4: REGIONAL ANALYSIS

Regional analysis of the piston ring pack is necessary to describe the overall transport process of lubricant from the crankcase to the combustion chamber. A minimum amount of oil is required on the liner and top ring groove, to limit friction and wear, but excess supply leads to oil consumption and exhaust emission problems. The basic transport mechanisms are described in Chapter 3, with each region of the piston ring pack affected differently by them; one transport mechanism may dominate in a certain region, but may be almost negligible in the neighboring region. Studying the oil evolution and balance for each ring pack region throughout an entire engine cycle provides the fundamental base to start making improvements and for computer modeling work. Knowledge of where the oil is, in what quantity, and what is driving it at each particular crank angle is necessary to devise effective means to influence and control lubricant transport. The piston ring pack is divided into three major regions, and an additional one for the piston skirt. Lubricating oil travels through these distinct regions along the piston ring pack before being consumed in the combustion chamber, with the oil distribution and dominant driving forces varying substantially for each of these regions. The oil evolution throughout an engine cycle as well as the effects of piston and ring design is discussed for each of these regions. The regions were shown in Chapter 1, but are detailed again in Figure 4.1.

The major focus of this experimental study is the third land, or Region One. This region consistently has a large supply of oil, making inertia the dominant driving force, and establishing a consistent and repeatable oil evolution cycle after cycle. The other regions are strongly affected by ring gap positions and blowby variations, making cycle to cycle analysis more difficult and less reliable; however, each region is discussed in this chapter with extensive detail into the transport evolution governing the third land. The regions of the piston ring pack are defined below. The regions in Figure 4.1 are divided at the middle of each ring groove, but in reality the regions overlap in the ring groove areas. For example, both Region One and Region Two will include the second ring and second ring groove, as the oil supply within the groove will affect oil transport to both regions.

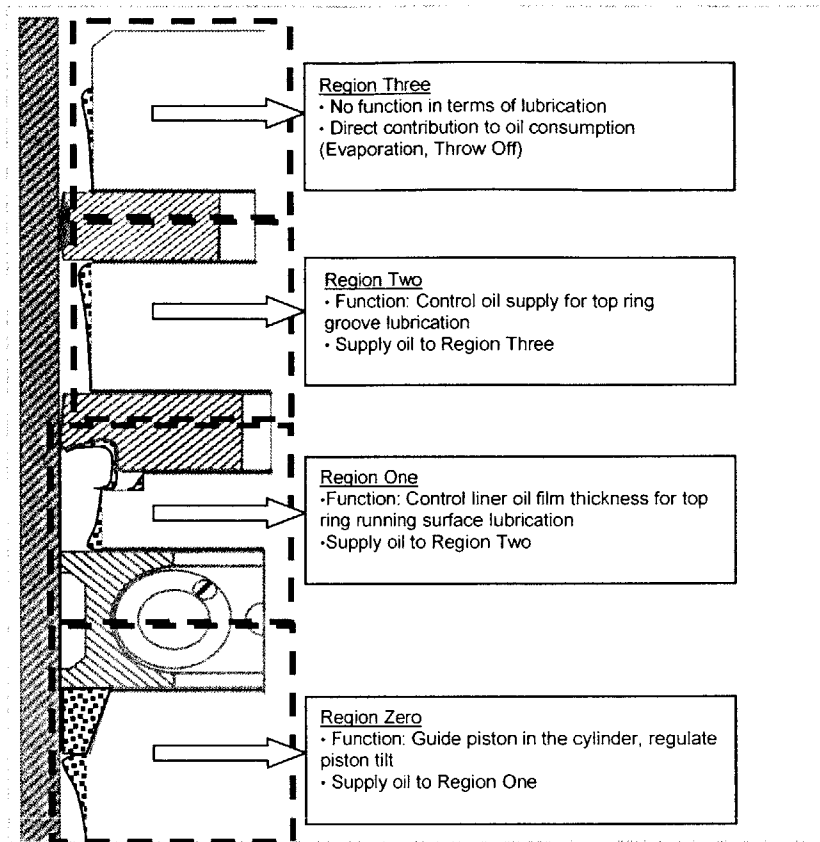


Figure 4.1 – Declaration of Regions within the piston ring pack

Region Zero includes the piston skirt and the oil control ring and groove. The piston skirt guides the piston in the liner, and is strongly affected by piston secondary motion. In every experimental test, a large supply of oil is seen to reside in the chamfer at the top of the piston skirt/start of the OCR groove. This seemingly limitless quantity of oil acts as a continual source of supply to the oil control ring groove, and thus as a supply to Region One. This oil originates from both the piston cooling jet and from the connecting rod end bearings. Additionally, the tight clearances of the skirt/liner interface establish oil cavitation patterns, which are strongly influenced by engine speed, and can easily be distinguished on the LIF images. For these reasons, the liner area adjacent to the piston skirt and OCR is included in Region Zero.

Region One begins with the oil control ring and groove, and includes the third land and the second ring and groove. It also includes the liner area adjacent to each of the

following: The third land, the second ring, and the oil control ring. A substantial amount of oil transport occurs between the piston and the liner in this region, and thus the liner portion must be included. Region One is the supply of oil for Region Two and the upper piston ring pack, and largely determines the liner oil film thickness for the top ring running surface.

Region Two encompasses the top two rings and their grooves, as well as the second land. The oil transport mechanisms in Region Two are responsible for lubricating the top ring groove, one of the harshest environments of the piston ring pack. Note the liner area adjacent to this region is not included as little land to liner transport occurs within Region Two.

Region Three includes the top ring, top ring groove, and the crown land. This region has no function in terms of lubrication; oil in this region is commonly transported across the crown land and released into the combustion chamber. Region Three experiences the most severe piston temperatures, and consequently has the greatest rates of oil vaporization. In fact, all the oil vaporization below the top ring groove can be considered negligible in comparison to the vaporization rates of Region Three.

4.1 Piston Skirt (Region Zero)

Piston skirt oil transport is elusive with cycle to cycle LIF data acquisition as the time scale of the oil transport is much faster. Additionally, the lack of consistency of the oil patterns on the piston skirt makes analysis difficult. The two main reliable features are the large quantity of oil in the chamfer just below the oil control ring groove and piston skirt cavitation.

Cavitation

Cavitation is the formation of an air or vapor pocket due to lowering pressure in a liquid [63]. It is commonly associated with propeller blades in water, but can occur in many systems. Due to the convex shape of the piston skirt, and the local pressures in the

cylinder, cavitation is seen to occur at certain locations throughout the engine cycle. Figure 4.2 details the mechanics of piston skirt cavitation. Just after the contact point of the piston skirt/liner, the pressure drops substantially as the volume is increasing rapidly. This causes the oil in the area to cavitate and form streaks or vapor pockets as seen on the LIF data.

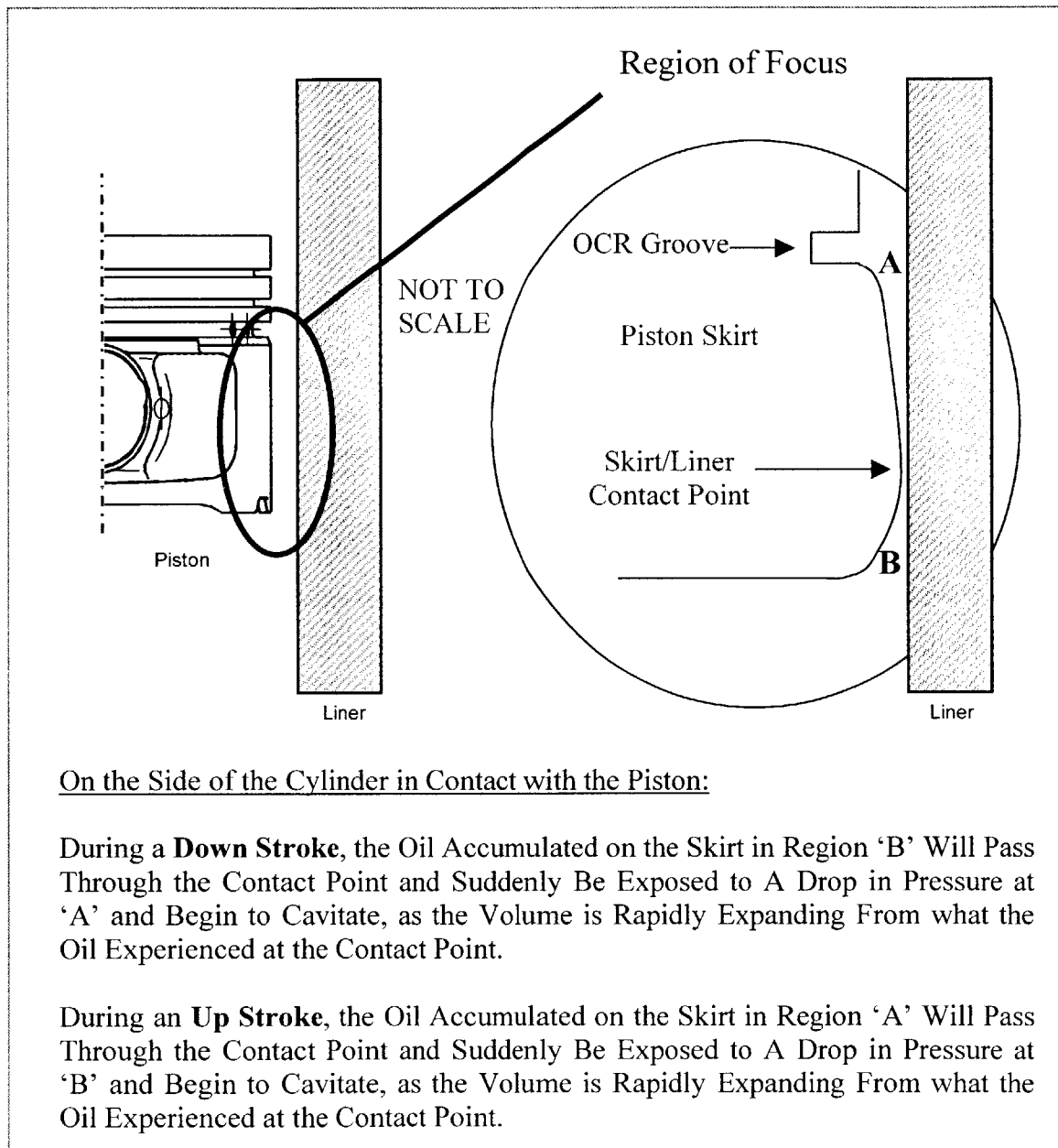


Figure 4.2 – Mechanics of piston skirt cavitation

On the side of the piston where the skirt is contacting the liner, cavitation is experimentally seen to occur on the trailing portion of the skirt, after the skirt/liner contact point; for a down stroke cavitation is seen to occur above the skirt/liner contact point, near the OCR groove, and for an upstroke cavitation is seen to occur on the bottom few centimeters of the skirt. Again, this phenomenon is only theorized to occur on the side of the piston where the skirt is running along the liner. As the experiments in this study were only conducted with the window on the anti-thrust side, cavitation was seen to occur for portions of the intake, compression, and exhaust strokes; however, cavitation was never seen during the expansion stroke, but it is believed to occur on the thrust side, where the piston skirt is contacting the liner. Examples of upward and downward cavitation are shown in Figure 4.3. LIF piston skirt images of the expansion stroke reveal no cavitation on the anti-thrust side.

Oil Return to Crankcase

Some of the oil accumulation on the piston skirt is experimentally seen to return to the crankcase. Inertia drives the oil off of the lower edge of the piston skirt, around the entire circumference. The lubricant forms droplets and returns to the crankcase supply. In the left image of Figure 4.3, droplets can be seen coming off the lower edge of the piston skirt. Note similar droplets are coming off the far edge of the piston skirt as well, but this lubricant does not appear as sharp droplets because the camera cannot focus on both the near skirt edge and the far skirt edge, which is an additional 90 mm away. It must be noted that some of the oil seen below the skirt in the LIF image could be from the crankcase oil jet.

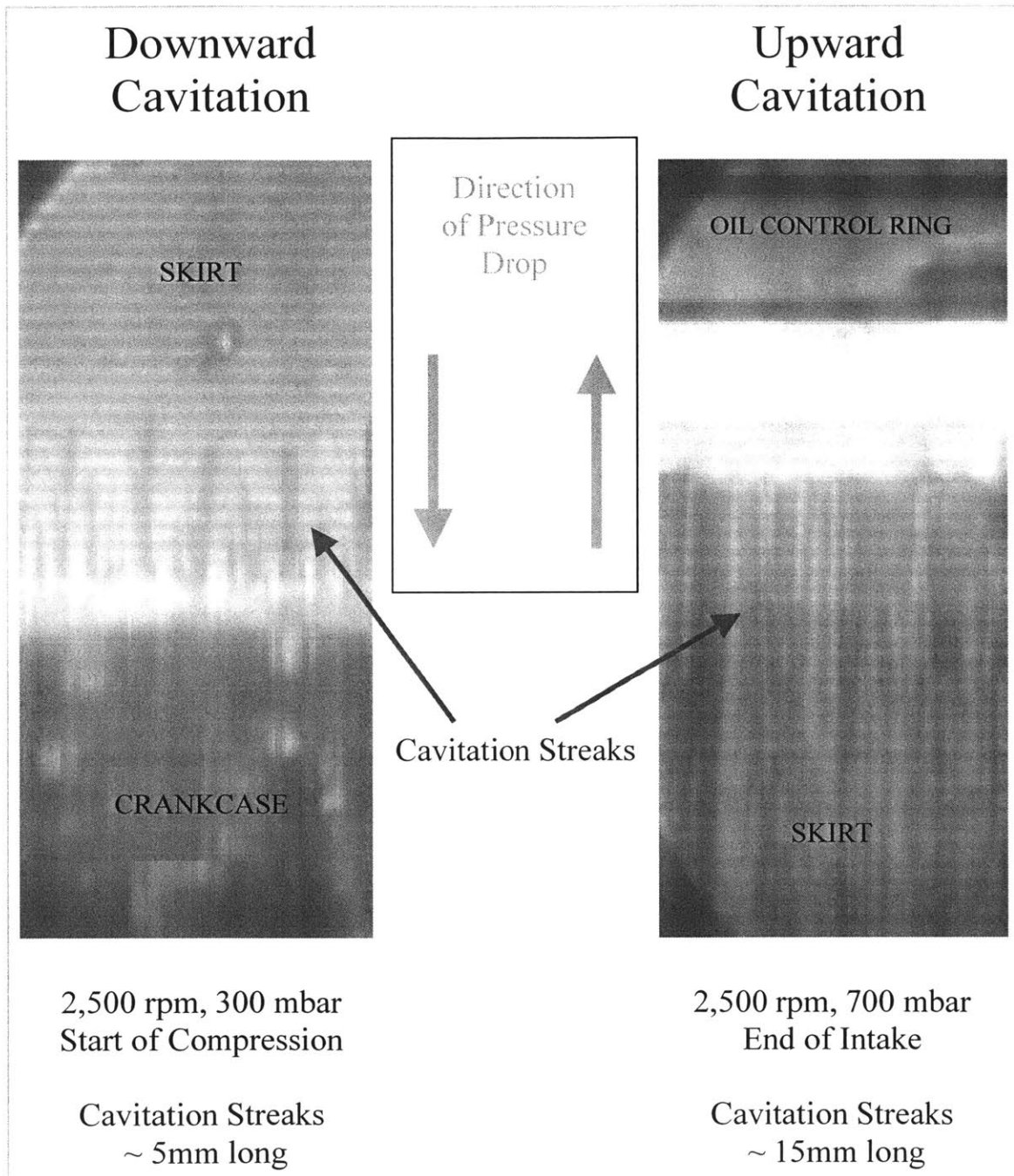


Figure 4.3 – LIF evidence of piston skirt cavitation

4.2 Third Land (Region One)

A major focus of this experimental work is on the lower region of the piston ring pack, namely the third land, which is located between the second compression ring and the oil control ring. A detailed 2D LIF study has been performed on the oil distribution and flow patterns of the third land throughout the entire cycle of a single cylinder spark ignition engine. The impact of speed and load were experimentally observed with the LIF generated real time high-resolution images, as were changes in piston and ring design.

All experimental findings show that the greatest concentration of oil is consistently present in Region One, with much of it crossing the third land multiple times each engine cycle. Furthermore, the results reveal the oil flow patterns and timing are consistent and predictable at each engine operating point. Speed and load variation alter the basic flow pattern through a corresponding change in inertia and gas dragging effect respectively, with ring design variation instigating specific and repeatable phenomenon onto the consistent oil flow pattern. As the majority of lubricating oil consumed in the engine crosses the third land at some point, an understanding of the timing and magnitude of the oil transport processes will allow means to be specifically developed to reduce the net oil flow across the third land towards the combustion chamber. This work forms a foundation for developing oil control strategies for the third land and for identifying how and when oil reaches the upper piston ring pack regions that directly contribute to oil consumption.

General Evolution of the Third Land

At all engine running conditions, and at every possible crank angle, the third land (Region One) was found to contain a substantial amount of lube oil. This large accumulation, and its relation with ring dynamics, directly determines the net oil transport to the upper regions of the piston ring pack. The significant quantity of oil in Region One is detrimental to oil consumption, but it does have one beneficial aspect as the consistency of the oil quantity creates a reliable third land pattern, repeatable from

cycle to cycle indefinitely. This attribute stems directly from the copious amount of oil, which allows two driving forces to always dominate the flow pattern. The two critical driving forces are inertia and ring dynamics – both of which are stable and consistent at most engine operating points. The relative magnitude of gas flow on the piston ring pack will affect the relative magnitude of the oil transport processes, as will be described when comparing the intake and expansion strokes, but the basic oil pattern is still governed by inertia and ring dynamics and is identical when comparing the first half of the engine cycle to the second half. Knowledge of the location, timing, and relative quantity of lubricating oil throughout Region One is essential for understanding how oil is transported to the second land and ultimately, the combustion chamber.

Before describing the third land evolution, the boundary conditions must be defined. The boundary condition at the top of Region One will be investigated first. As it is common knowledge oil consumption exists, and the presence of oil on the second land and crown land can clearly be seen in every LIF image, it can be said that some oil each cycle must leave the third land (Region One) and cross onto the second land (Region Two). Of course some oil may move downward, from Region Two to Region One, but the net transport must be in the upward direction if oil consumption is to exist. Thus, the boundary condition at the top of Region One is a net transport upward. The boundary condition at the bottom of Region One can be thought of similarly. As the third land oil supply remains constant at a steady operating point, it can be said the same net transport that leaves Region One for Region Two must be replaced by an equal net transport from the piston skirt to Region One. It should be noted, however, that the exchange rates for the lower boundary, in the upward and downward direction, are orders of magnitude greater than the exchange rates for the upper boundary. These claims are supported by the observations that there is significantly more oil in Region One than Region Two, and that the area directly below the oil control ring appears to be flooded with oil at all times during the engine cycle. It could thus be argued there is an ‘infinite supply’ of oil below the OCR, and thus net oil transport must be in the upward direction for the entire piston ring pack.

The basic oil flow patterns and transport timing of the third land will be detailed first, without regard for specific ring types. Though each ring type introduces certain phenomenon into the oil transport process, the consistent third land evolution dominates as it is driven by inertia and ring dynamics. Once the basic pattern and timing has been conveyed, specific ring types will be discussed and their impact on the general pattern shown.

As inertia and ring dynamics dictate the timing and movement of oil on the third land, it is important to understand the general timing of these driving forces. Both of these topics were covered in earlier sections, but will briefly be shown again here. Figure 4.4 is a chart of the piston acceleration, and thus inertia, throughout one engine cycle. Ring dynamics mainly affects the third land evolution by forcing oil out of the ring grooves, or by moving to allow oil to enter the ring grooves. When oil accumulates at the intersection of the piston ring and the land, and the ring moves axially in its groove, it allows space for the accumulation to spread out on the ring surface and enter the ring groove. Similarly, if oil is in the ring groove when a ring moves axially in the groove, some of that oil will be pushed to the back of the ring, deeper into the ring groove, but some of it will also be forced out of the ring groove onto the piston land. Knowledge of the location of the ring within its groove, coupled with the magnitude and direction of the inertia force acting on the oil allows understanding of the oil flow pattern and its timing. A chart of the ring axial movement for a medium speed, low load operating point, from the output of the ring dynamics software RINGPACK-OC, is shown in Figure 4.5.

To convey the third land evolution throughout an entire engine cycle, third land maps of the oil patterns observed experimentally will be shown and discussed at 30 CAD (Crank Angle Degree) intervals, beginning with the start of the intake stroke at 0 CAD or top dead center (TDC). The engine operating point chosen to relay the general pattern on the third land is 4500 rpm with an absolute intake pressure of 500 mbar. Obviously, speed and load variations will affect the timing and magnitude of these transport processes, but the general pattern will remain identical. The influence of speed and load on the third land will be discussed in detail after the general third land evolution has been outlined.

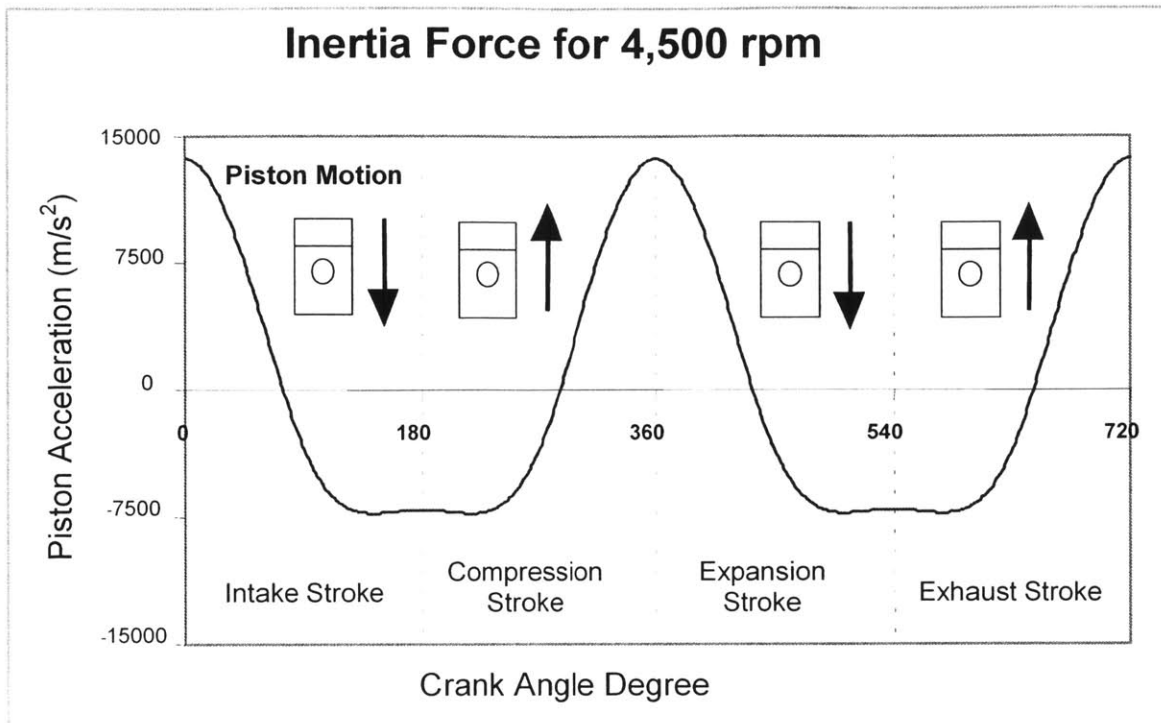


Figure 4.4 – Inertia force calculation to illustrate magnitude and timing of inertia in comparison to piston motion and ring dynamics

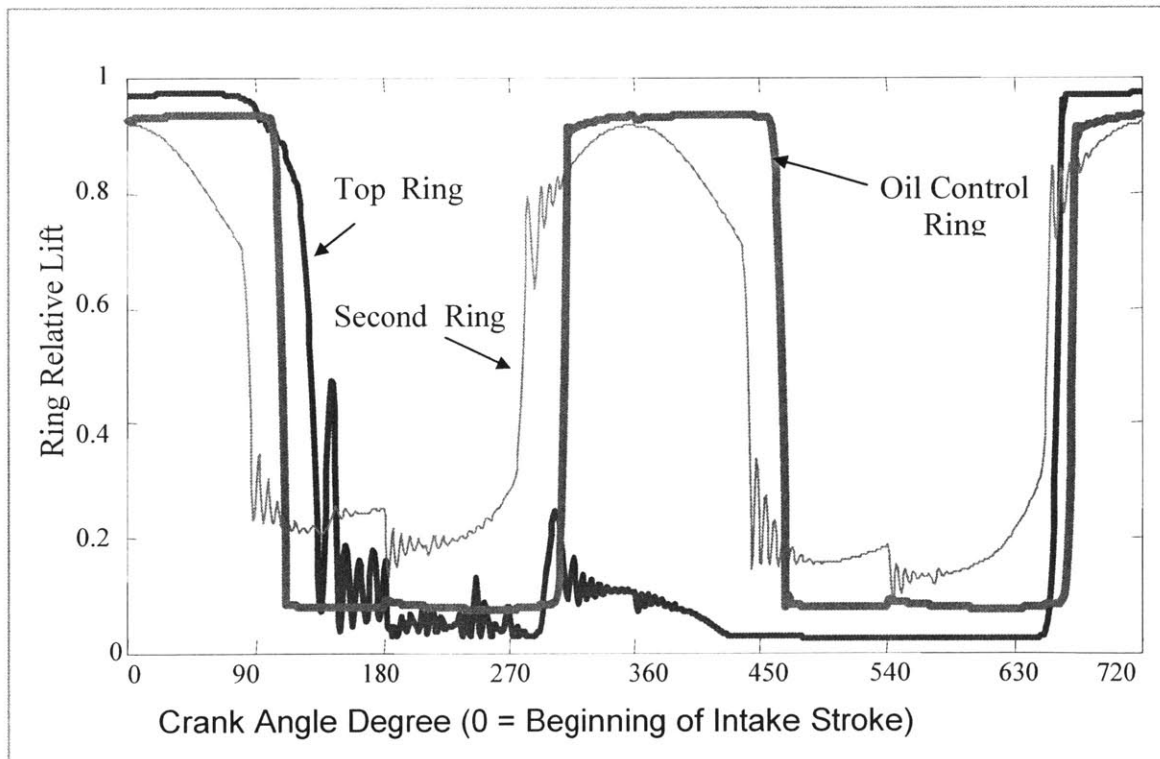


Figure 4.5 – Example of ring dynamics; the engine operating point is 3,500 rpm, low load (relative lift of 1 denotes the ring is resting against the top flank of the ring groove, a relative lift of 0 denotes it is against the bottom flank of the ring groove)

The following maps focus on Region One exclusively, with the top of the figures being the second compression ring, and the bottom of the figures bounded by the oil control ring; the rings shown here are a Napier Ring and a Twin Land oil control ring respectively. Any common production ring types would have similar effects to the rings used in these third land oil maps. The effects of various ring types do induce local phenomenon, but the general evolution remains the same. The specific effects of common ring types, which overlay on top of the general third land evolution, will be discussed in a later section. Note that the configuration shown in these maps has a third land chamfer, or cutout, which generally accompanies a Napier style second ring. This chamfer induces certain phenomenon that can easily be seen on the maps. Removing the chamfer from the ring pack would not change the general third land pattern; however, it would certainly affect oil transport into Region Two.

A sample map is shown in Figure 4.6 with a piston profile to further relay the focus of these oil schematics. The complete set of maps for the third land and their individual discussions follow the sample map. The entire circumference of the piston third land is displayed for each crank angle map, to provide you with an idea of the scale, and to illustrate the consistency of the pattern. The analysis of the entire piston circumference was made possible by an extremely stable oil control ring rotation rate (about 1 rpm) at this engine operating point. The dominance of inertia on the third land oil transport mechanisms makes the knowledge of the exact location of the top two ring gaps unnecessary. The ring gaps have intentionally been left off these general evolution maps, but will be discussed in great detail later as they introduce specific transport phenomenon on top of the general evolution outlined here.

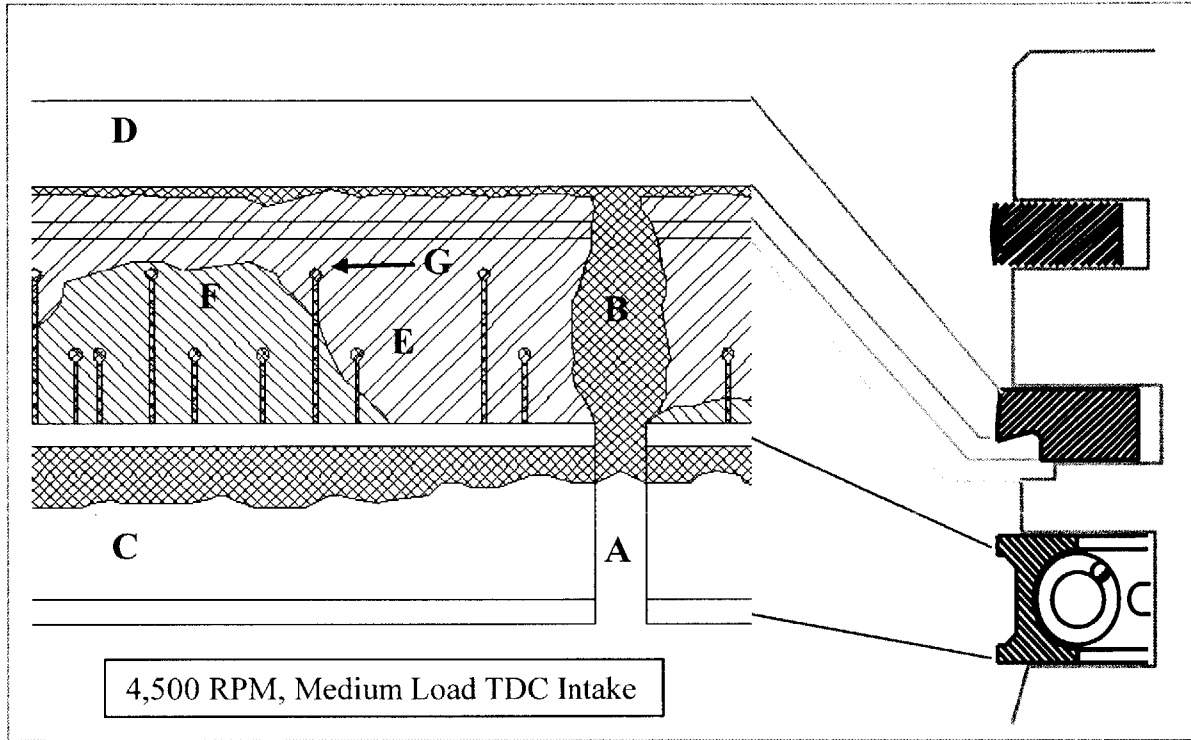


Figure 4.6 – Sample third land map with piston profile and explanation of features: A=OCR gap, B=Heavy oil flow through ring gap and into Napier hook (note dark cross hatch indicates heavy accumulation of oil), C=OCR, D=Napier Ring, E=Third land (note light cross hatch indicates thin film of oil), F=Oil wave on third land leaving OCR groove and heading towards Napier Ring, G=Oil drop leaving OCR

0 Crank Angle Degrees (Intake Stroke, TDC) – At the beginning of the intake stroke, inertia force has been acting on the oil in the upward direction for the latter half of the exhaust stroke, as the piston was decelerating. The inertia, plus the oil control ring moving from the bottom of its groove to the top, has forced lubricant out of the OCR groove and onto the third land. At TDC, this oil wave has approximately crossed half of the third land. Accompanying the third land wave is a significant number of drops originating from the OCR top surface. These drops exist in the clearance between the third land and cylinder liner, and generally stretch to the second ring, but sometimes deposit earlier onto the liner or third land. Note that not all of the oil in the third land wave or droplets is originating from the OCR groove, some has also been scraped by the OCR top land during the exhaust stroke. Additionally, inertia has also caused oil residing in the third land chamfer to form upward moving drops. These chamfer drops will land in either the Napier Hook, acting as a ‘Buffer Region’ to hold the oil until inertia forces it back downward, or the drops will land on the lower side of the Napier Ring surface with some entering the second ring groove. (See Figure 4.7)

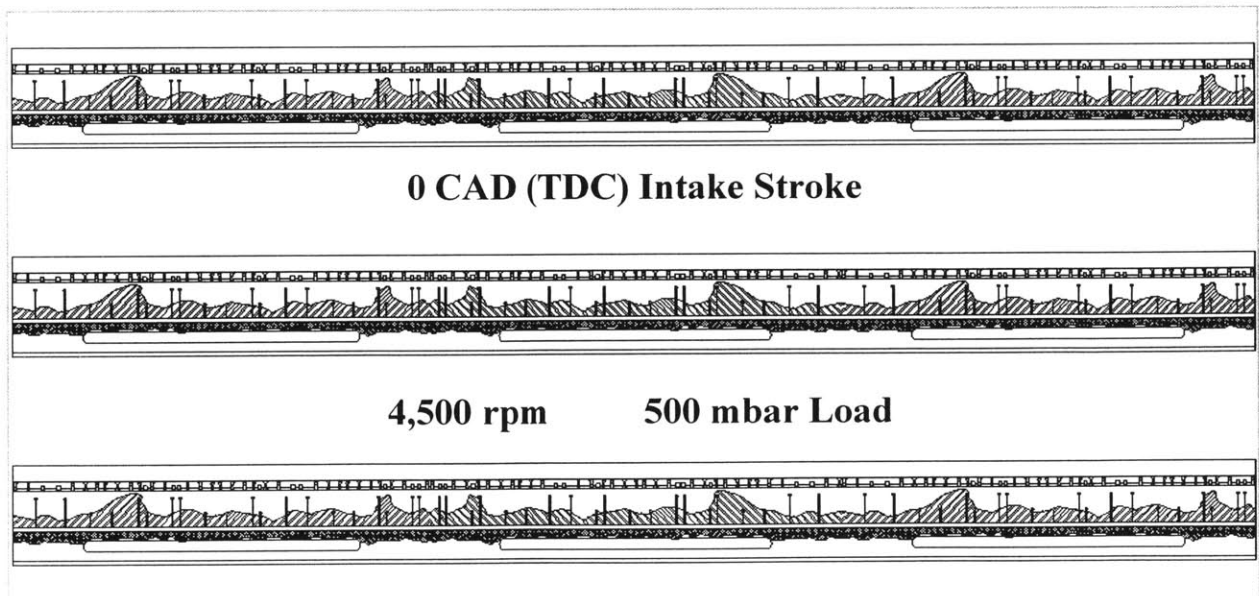


Figure 4.7 – Map of the complete circumference of the third land, for 0 CAD (TDC) of the intake stroke

30 Crank Angle Degrees (Intake Stroke) – The piston has now begun to accelerate downward, keeping inertia in the upward direction. This force has continued to drive the third land oil wave closer to the second ring. The wave has just reached the chamfer, with most of it pouring directly into the Napier Hook. There still are some upward drops emanating from the OCR, but only a few of them. (See Figure 4.8)

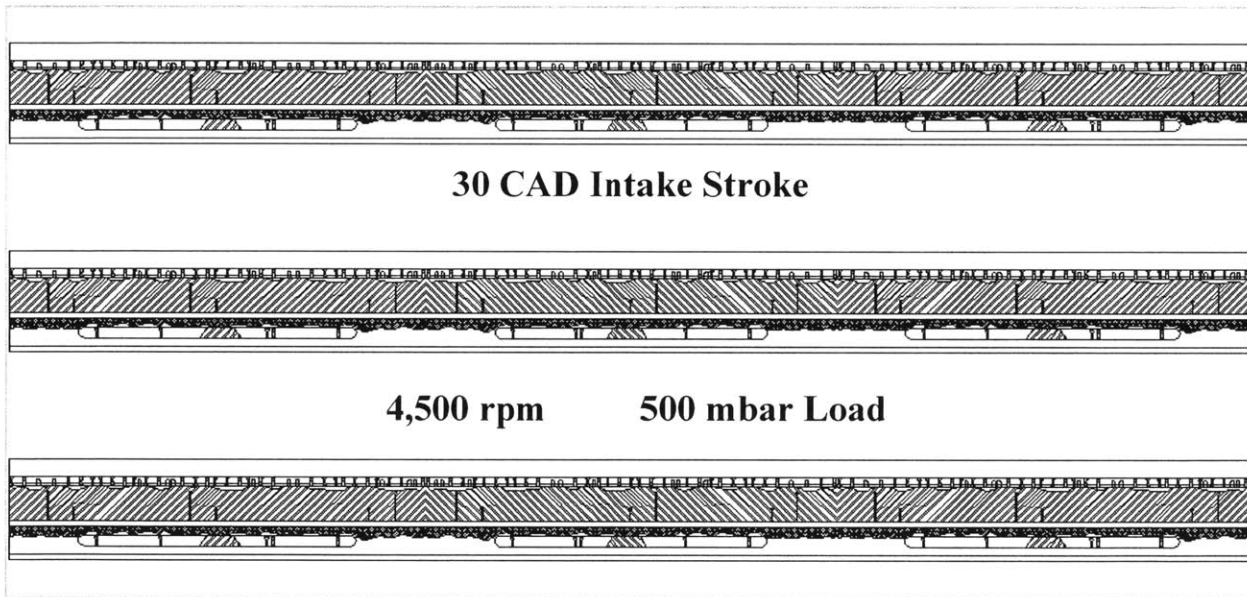


Figure 4.8 – Map of the complete circumference of the third land, for 30 CAD of the intake stroke

60 Crank Angle Degrees (Intake Stroke) – The piston is approaching its maximum speed and the upward inertia force has lessened. There remains only a thin oil film on the third land, as the majority of the oil volume has already crossed and now resides in the Napier Hook and second ring groove. Some oil can be seen crossing the chamfer region to the Napier Ring. (See Figure 4.9)

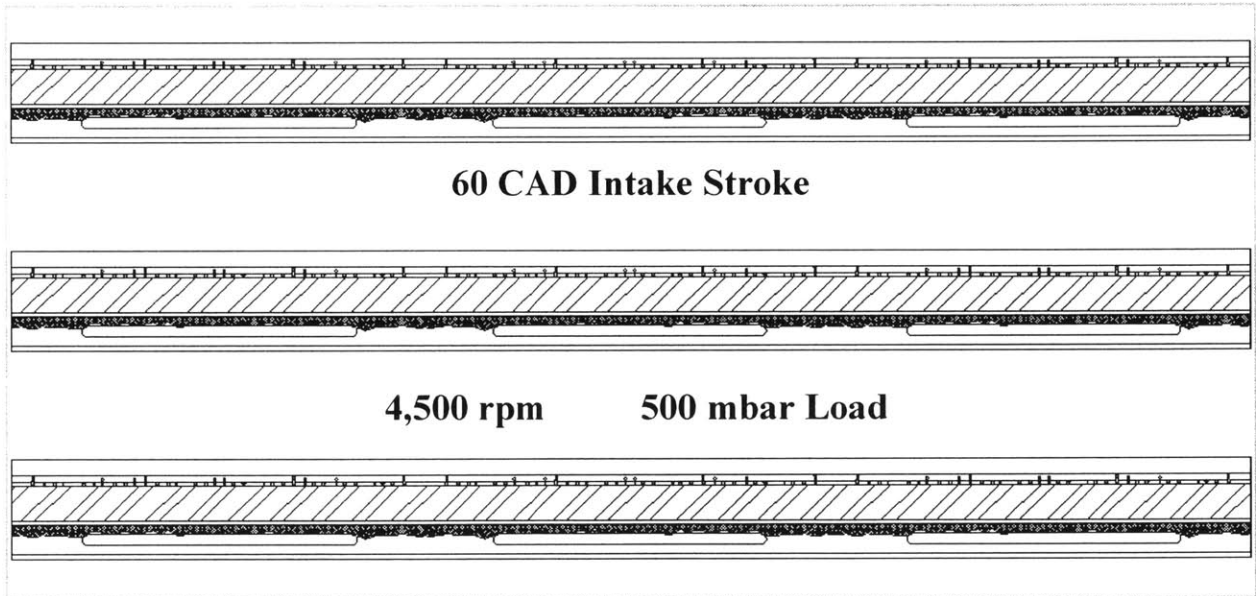


Figure 4.9 – Map of the complete circumference of the third land, for 60 CAD of the intake stroke

90 Crank Angle Degrees (Intake Stroke) – Inertia, though quite weak, has now switched directions as the piston has reached its maximum speed and begun to decelerate. Consequently, little oil is present on the third land with most of it still residing in the Napier Hook and second ring groove. (See Figure 4.10)

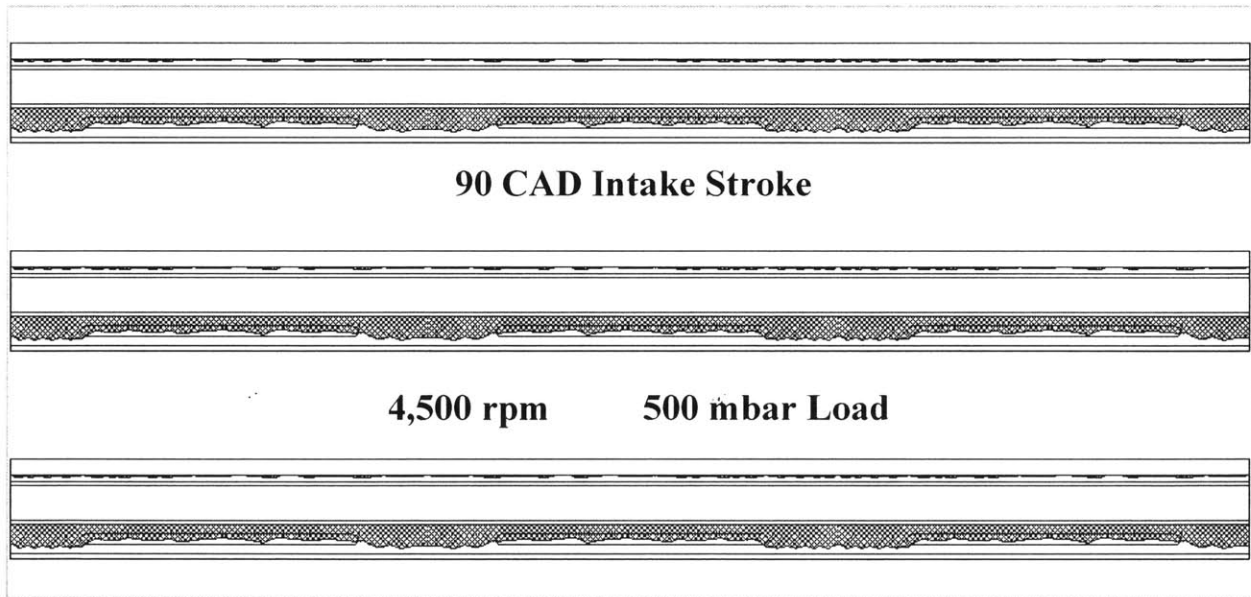


Figure 4.10 – Map of the complete circumference of the third land, for 90 CAD of the intake stroke

120 Crank Angle Degrees (Intake Stroke) – The downward inertia force has strengthened, and the Napier Ring has moved to the lower side of its ring groove. These two factors have begun to force oil out of the second ring groove and the chamfer onto the third land. Much of the oil which was stored in the Napier Hook ‘Buffer Region’ now pours out onto the third land chamfer, adding to the start of the down wave. The Napier Ring also will scrape some oil from the cylinder liner during the downward intake stroke, adding to the oil residing in the hook region. (See Figure 4.11)

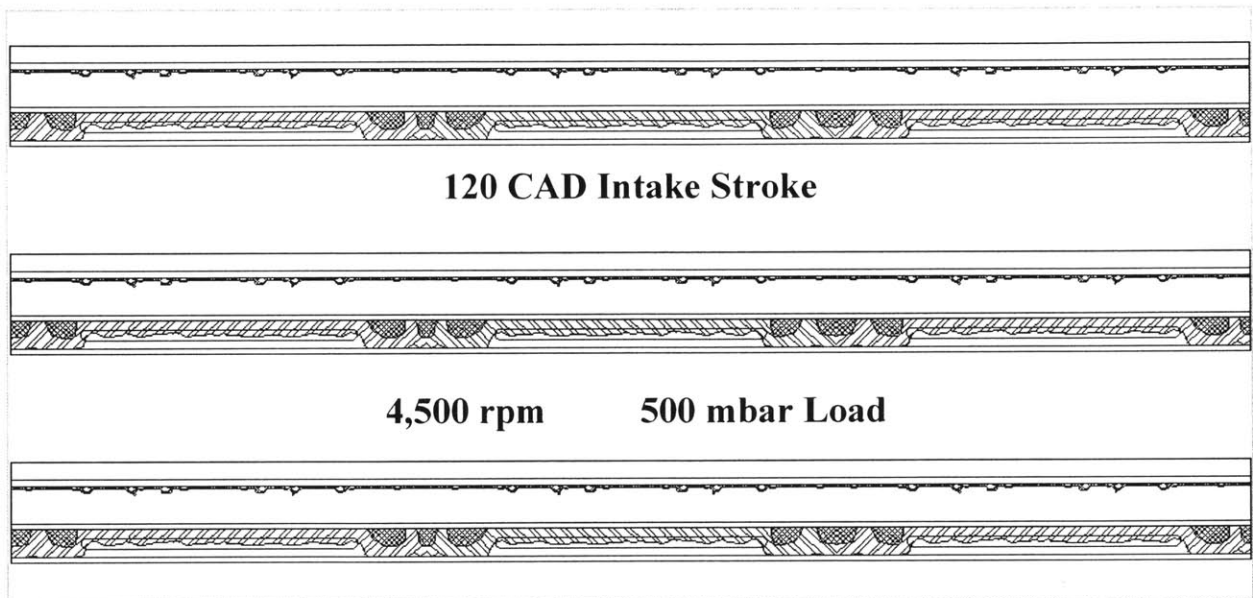


Figure 4.11 – Map of the complete circumference of the third land, for 120 CAD of the intake stroke

150 Crank Angle Degrees (Intake Stroke) – The piston is rapidly decelerating as it approaches the end of the intake stroke, creating a strong downward inertia force. This force continues to drive the oil pouring out onto the third land; the wave is about a third of the way across the land. The beginning of a few drops can be seen forming in the Napier Hook. (See Figure 4.12)

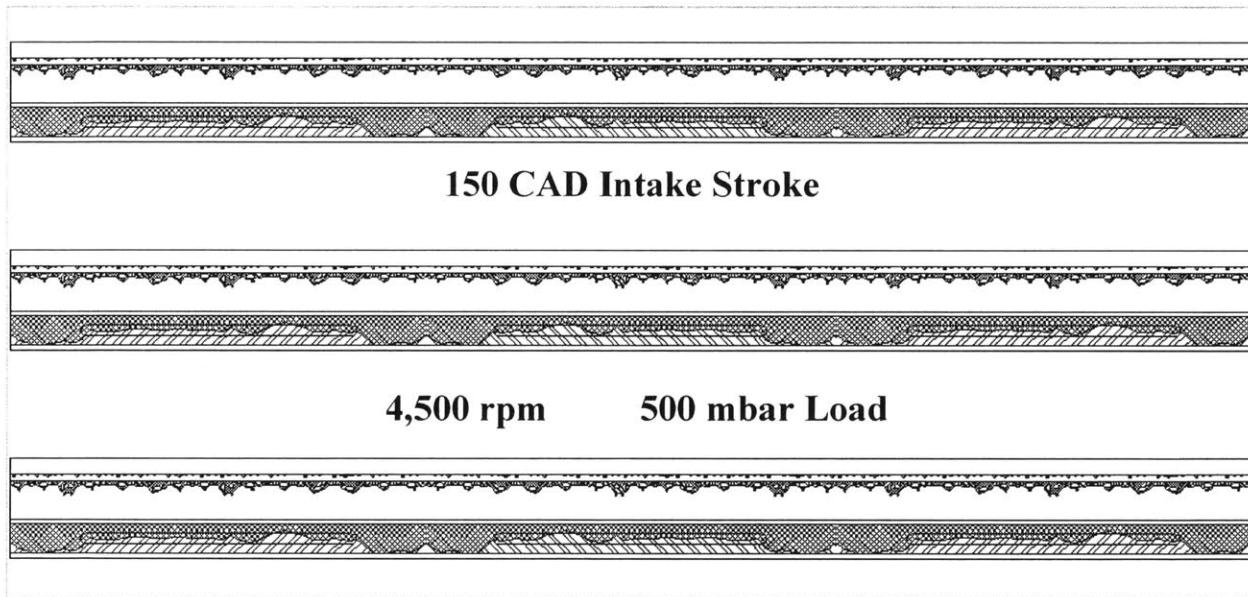


Figure 4.12 – Map of the complete circumference of the third land, for 150 CAD of the intake stroke

180 Crank Angle Degrees (Intake Stroke, BDC) – At bottom dead center, the third land was not converted to an oil map. However, by examining the 150 CAD and 210 CAD maps, it can easily be inferred what the 180 CAD map would look like. Similar to a mirror image of the TDC map, the downward oil wave is approximately half way across the third land. There is also a significant number of drops leaving the Napier Ring hook, most of which will deposit onto the OCR.

210 Crank Angle Degrees (Compression Stroke) – The compression stroke has begun as the piston accelerates upward. This keeps the inertia force in the downward direction and continues to drive the oil wave, which has nearly crossed the third land. The majority of oil that crosses the third land will enter the OCR groove. Additionally, some drops are still originating from the Napier Hook and falling towards the OCR. (See Figure 4.13)

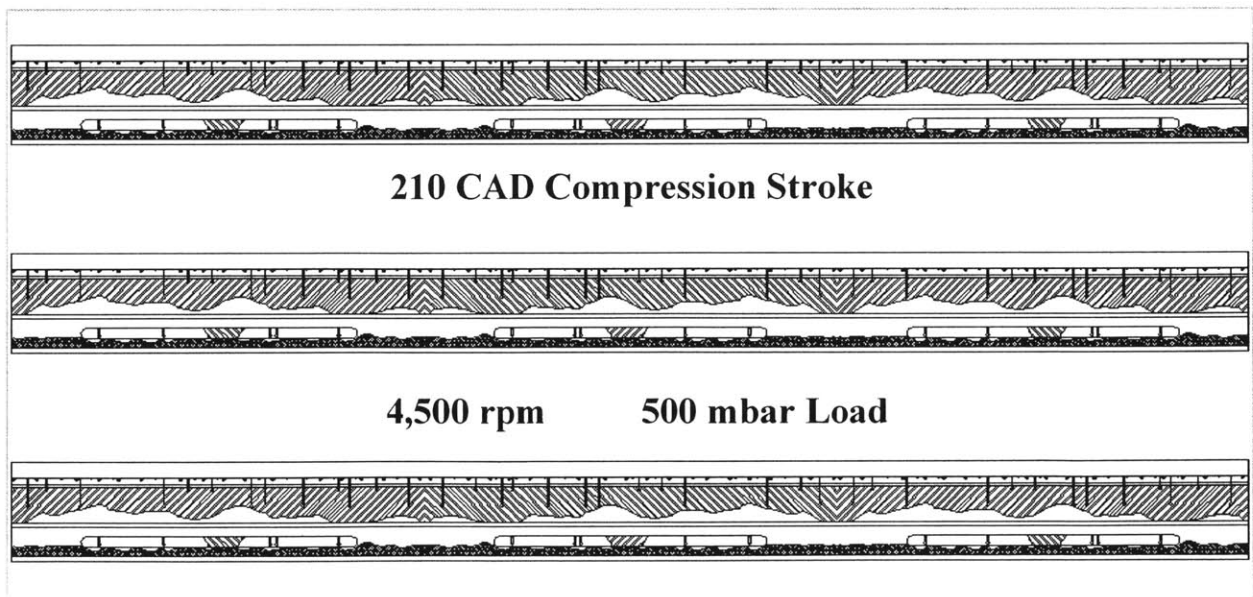


Figure 4.13 – Map of the complete circumference of the third land, for 210 CAD of the comp. stroke

240 Crank Angle Degrees (Compression Stroke) – The piston is now starting to approach its maximum speed in the upward direction, therefore, the downward inertia has begun to lessen. There is a thin film on the third land, mostly remnants of the oil wave that just crossed. There are also a few remaining drops from the Napier Hook to the oil control ring, however, the majority of oil in Region One has moved into, and now resides in, the oil control ring groove. (See Figure 4.14)

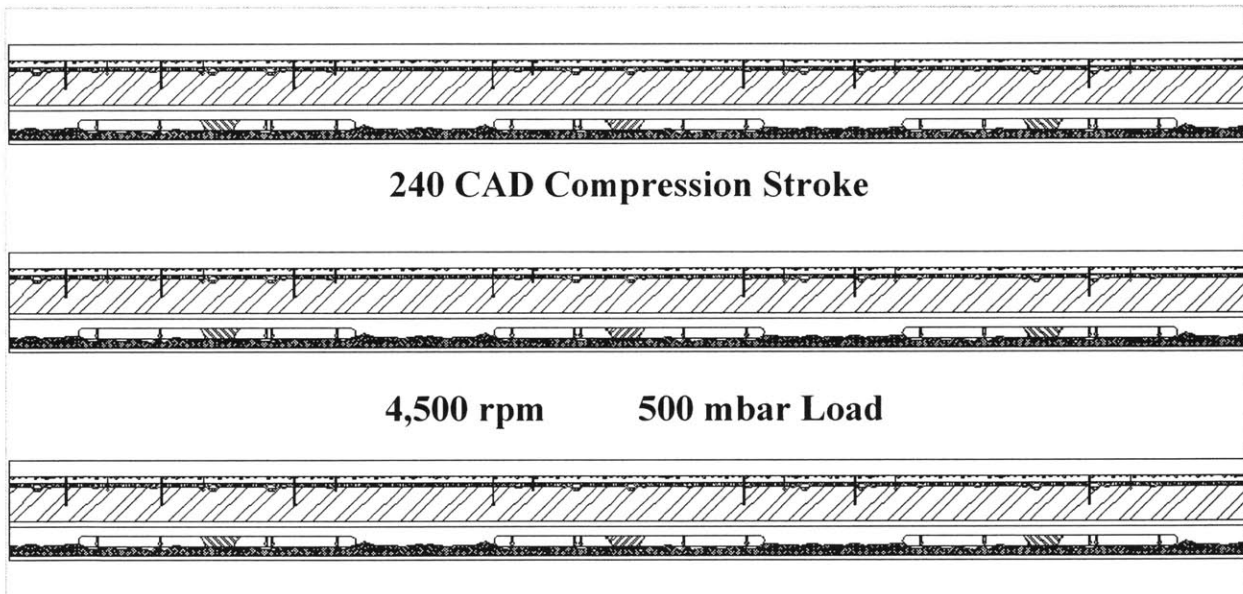


Figure 4.14 – Map of the complete circumference of the third land, for 240 CAD of the comp. stroke

270 Crank Angle Degrees (Compression Stroke) – At the midpoint of the compression stroke, the inertia force is weak. Again, a thin film remains on the third land, but no significant oil transport is taking place. (See Figure 4.15)

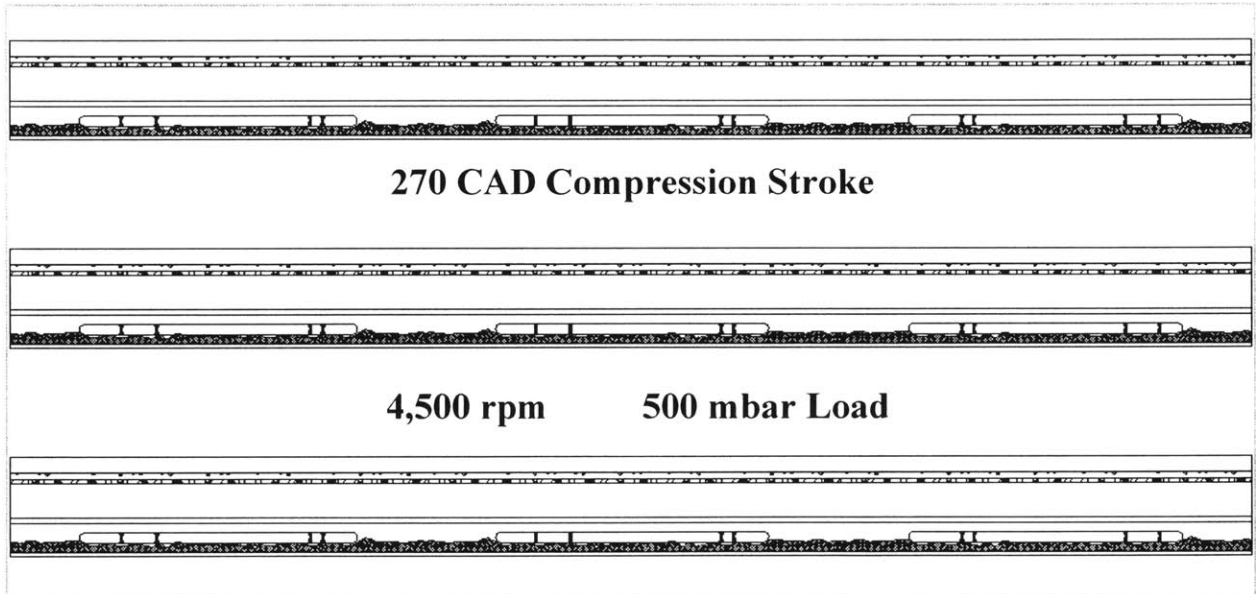


Figure 4.15 – Map of the complete circumference of the third land, for 270 CAD of the comp. stroke

300 Crank Angle Degrees (Compression Stroke) – The piston has begun to decelerate and inertia has switched to the upward direction. No significant oil transport is currently taking place, however, as the majority of the oil within Region One remains inside the OCR groove. (See Figure 4.16)

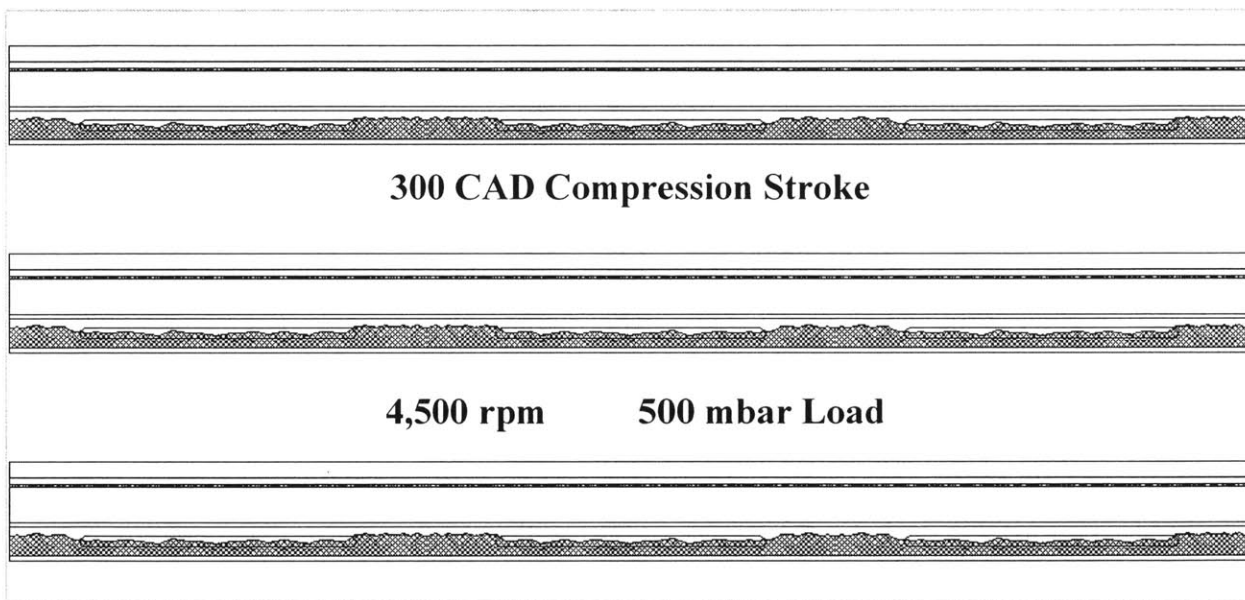


Figure 4.16 – Map of the complete circumference of the third land, for 300 CAD of the comp. stroke

330 Crank Angle Degrees (Compression Stroke) – Inertia continues to grow in the upward direction, yet the third land remains thinly covered in oil, with no significant transport occurring. During the entire compression stroke the OCR will scrape oil from the cylinder liner, which will only add to the large reservoir of oil in the OCR groove. The oil in the OCR groove will remain there until the oil control ring moves axially in its groove to the top flank. The exact timing of the OCR lift depends heavily on the engine speed. With the stated ring configuration and at an engine operating point of 4500 rpm and medium load, the OCR lift occurs just after 330 CAD. The ring lift timing is stated by the RINGPACK-OC software and confirmed by the LIF study. This action forces out a large quantity of oil from the OCR groove onto the third land in a short amount of time. This large quantity of oil will begin to move quickly across the third land, as the upward inertia force is well established at this point of the compression stroke. A large volume of oil, when driven by inertia, will move with greater velocity than a smaller volume of oil. The large accumulation forced onto the third land will eventually reach the second ring groove and directly contribute to the net oil transport to the second land. This fast moving, large quantity of oil represents the consistently best location and timing to make lube oil consumption improvements to the piston ring pack. If a means could be devised to stop, or contain, this large volume of oil from reaching the second ring groove, it would reduce the net oil transport to the upper piston ring pack. (See Figure 4.17)

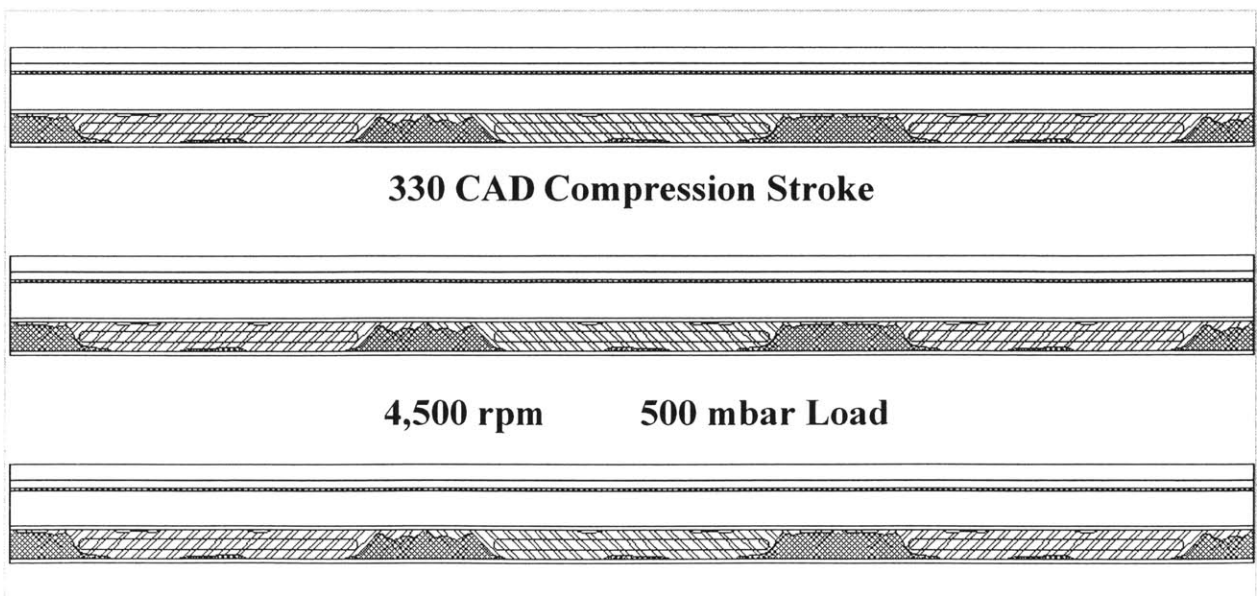


Figure 4.17 – Map of the complete circumference of the third land, for 330 CAD of the comp. stroke

360 Crank Angle Degrees (Compression Stroke, TDC) – The third land map for TDC of the compression stroke is almost identical to the map for top dead center of the intake stroke. The third land wave, induced by the OCR lift and driven by inertia, has crossed most of the third land, accompanied by some upward drops from the oil control ring to the Napier Hook (See Figure 4.18). Condensed versions of the third land maps are contained in Figure 4.19, allowing for easy comparison between them.

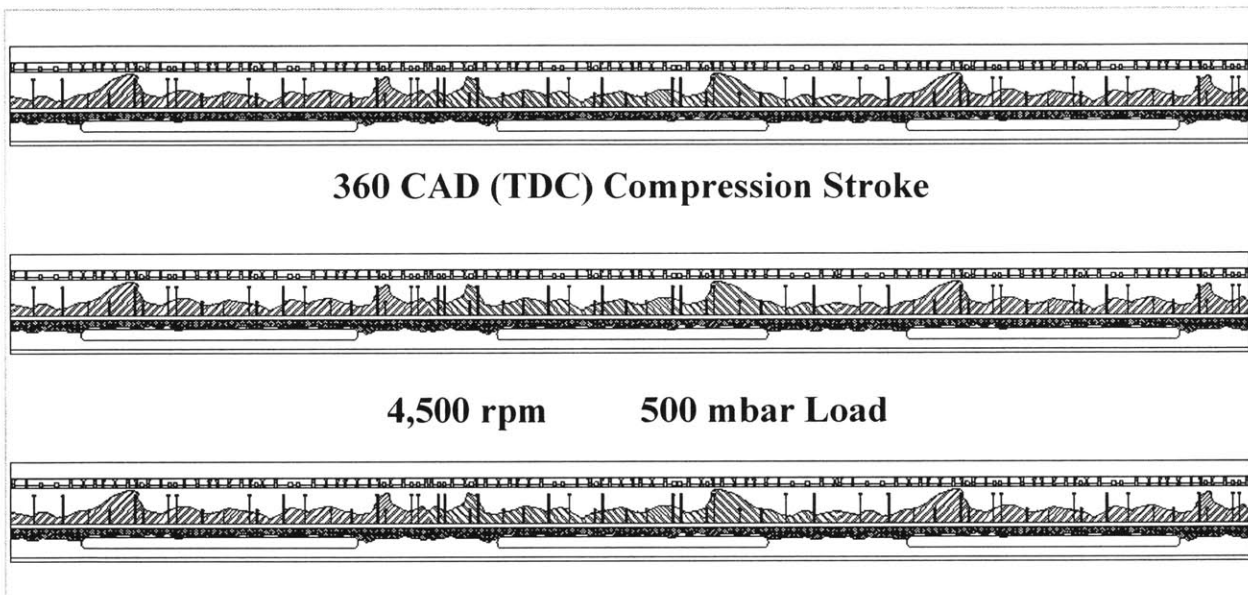


Figure 4.18 – Map of the complete circumference of the third land, for 360 CAD of the comp. stroke

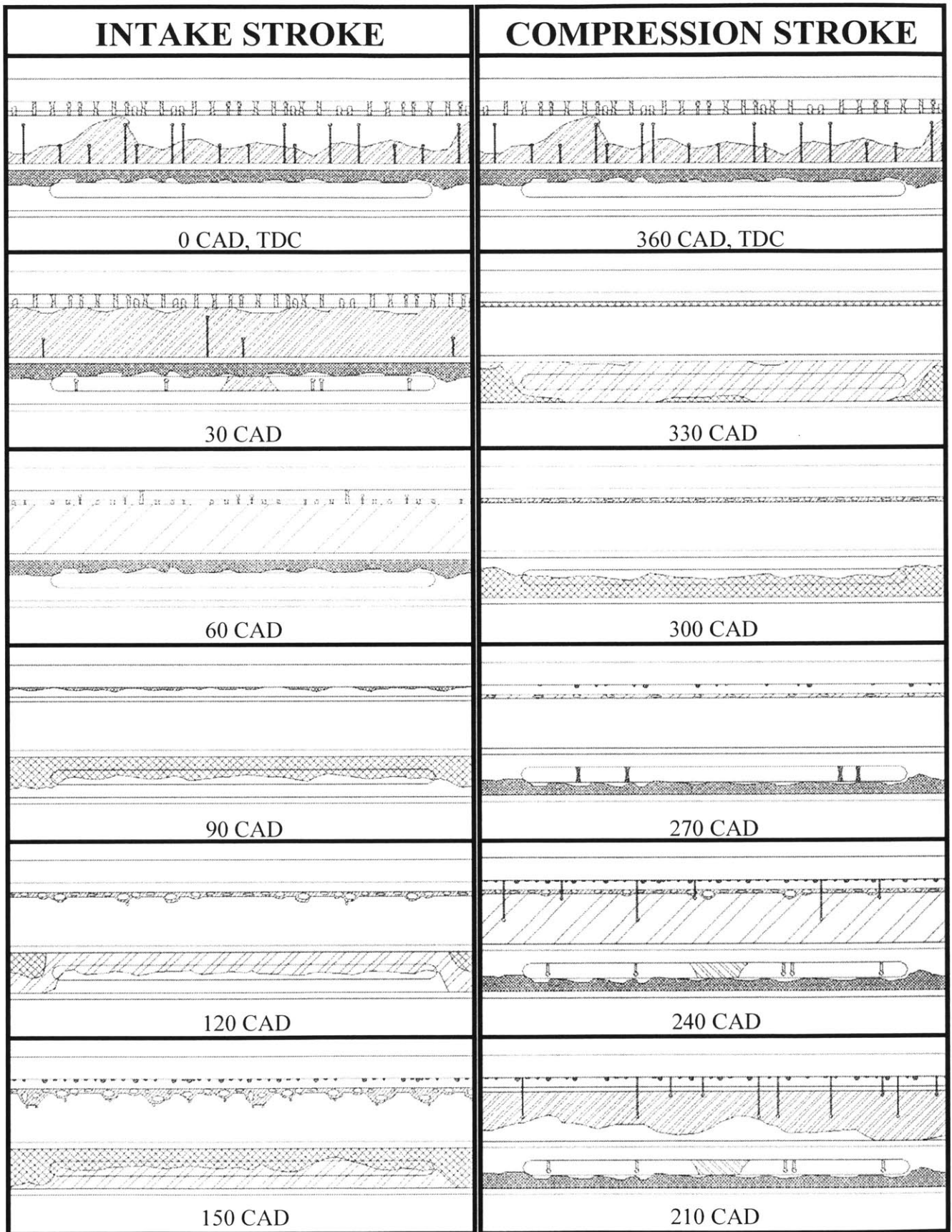


Figure 4.19 – Summary of the third land maps, condensed on one page for comparison purposes

Comparison to the Expansion and Exhaust Strokes – The continuation of this discussion into the ensuing strokes, expansion and exhaust, is unnecessary as the described transport cycle merely repeats itself. The major oil transport processes described above are driven by inertia and ring dynamics, which are nearly identical when comparing the intake and compression to the expansion and exhaust strokes. The only major exception is the oil control ring lift and ensuing oil wave described in the ‘330 CAD’ explanation above.

During the intake stroke, the low combustion chamber pressure and minimal blowby flow allows more oil from the piston skirt region to enter into the OCR groove; during low load situations this action is further aided by reverse blowby from the vacuum in the combustion chamber. During the end of the ensuing compression stroke, the oil control ring lifts and forces much of the oil in the OCR groove out onto the third land. This large quantity of oil crosses the entire third land quickly, in approximately 30 CAD. This transport mechanism exists for the end of the exhaust stroke as well, but not as dramatically. Unlike during the intake stroke, not as much oil from the piston skirt enters the OCR groove during the expansion stroke. The high combustion chamber pressure and accompanying high rate of blowby gas flow inhibit some of the oil from entering the oil control ring groove during the downward expansion stroke. Additionally, the expansion stroke blowby acts to drag some oil already present in the OCR groove downward towards the crankcase. When the OCR lifts in its groove towards the end of the ensuing exhaust stroke, less oil is present in the groove, and thus less oil is forced out onto the third land. While still significant, the resulting oil wave contains less oil, and therefore takes longer to cross the third land. In summary, it is the disparity in blowby magnitude between the intake and expansion strokes, which causes the subsequent difference between the compression and exhaust strokes. An example of this disparity is shown in Figure 4.20 (same as Figure 3.24). The images were taken at 3,500 rpm with an absolute intake pressure of 300 mbar, 20 crank angle degrees before TDC. The left image was recorded during the compression stroke; the large up wave is apparent and fully across the third land. In contrast, the right image was recorded during the exhaust stroke; a smaller magnitude wave is seen, which is only half across the third land.

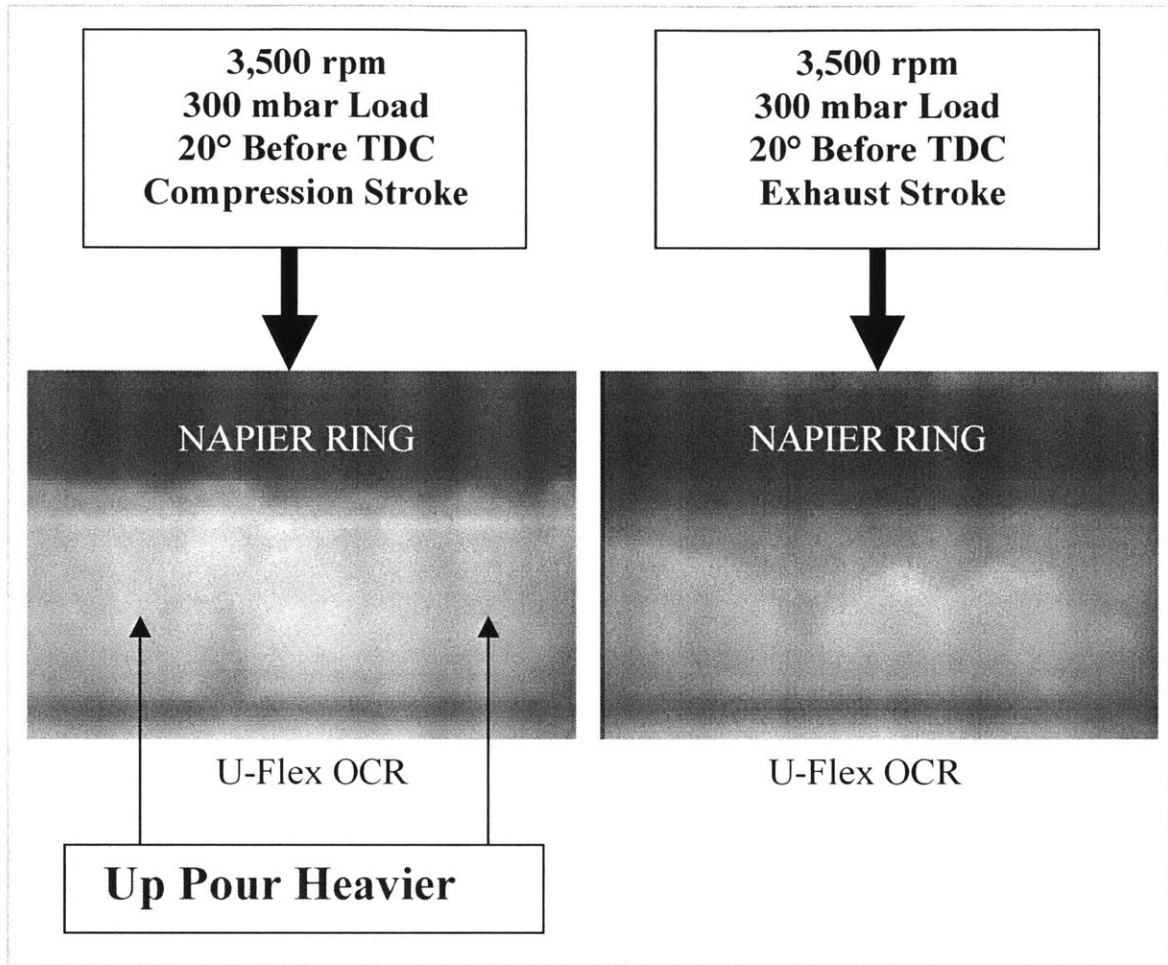


Figure 4.20 – Effect of gas flow on the up wave across the third land, which was instigated by the oil control ring lifting in its groove

This clear difference in magnitude between the compression stroke up wave and the exhaust stroke up wave will be repeated in the ensuing down waves of the expansion and intake strokes, as they are comprised of the same oil. The larger compression stroke up wave will produce a larger expansion stroke down wave, as there will be more oil available; conversely, the smaller exhaust stroke up wave will produce a smaller intake stroke down wave, as there will be less oil available.

Other than the discussed variation in magnitude of the oil wave from the OCR lift, the major transport mechanisms are quite similar between the first half of the engine cycle and the second half. Therefore, the third land maps for the latter half of the cycle will not be outlined as they are nearly identical to the maps of the first 360 crank angle degrees.

Second Ring Gap Effects

The influence of the ring gaps on oil transport has been overlooked in the discussion thus far. Though the second ring gap is a major mechanism by which oil flows towards the combustion chamber, its effects on the third land general evolution are localized. The presence of the second ring gap does create a cleaning action on the area immediate below the gap; however, the third land oil flow patterns will return to the general evolution only a few moments after the second ring gap moves circumferentially to another location. Much discussion could be made about the intricacies of oil flow through the ring gaps, but it is not the focus of this work. Unlike the top two rings, however, significant variation exists in the gap phenomenon of oil control rings and so their specific effect to the third land evolution will be discussed in a later section.

Speed and Load Effects on the General Evolution

The main transport mechanisms and general third land pattern remain the same in the face of engine speed and load changes; however, the timing and magnitude of the transport mechanisms will be affected. Increased engine speed will increase the effects of inertia, generally hastening the timing of the transport mechanisms, while increased engine load will augment blowby and pressure gradients, acting to keep oil to the back of the ring grooves and resulting in a diminished magnitude and a timing delay of the transport mechanisms.

Engine speed is the most obvious and critical parameter affecting the third land evolution, because it is directly linked to the dominating inertia force – proportional to the second order. A faster engine speed will accelerate ring dynamics during the engine cycle, namely the rings moving axially in their grooves, which will induce the general oil transport mechanisms to also occur earlier in the engine cycle. The greater inertia force has a similar effect on the lubricant itself, hastening both its appearance on the third land and its velocity across the third land. The quicker appearance of oil on the third land for high speed operation does not mean it will cross faster; the volume of oil present is still a key factor in the time it takes oil to cross the third land. Additionally, the increased lubricant speed must be weighed against the increased piston speed; although the oil may

be traveling across the third land at a greater velocity at high engines speeds, it may take more crank angle degrees in duration.

Engine speed will also effect drop formation. A minimum inertia force is required for oil to leave the ring surface as a drop and travel towards the next ring. A higher engine speed will induce more droplets, while a lower engine speed will create less. Experiments reveal a minimum engine speed of approximately 3,000 rpm is required for significant droplet formation. The greater the amount of oil that forms into droplets results in less oil available for the wave mechanism.

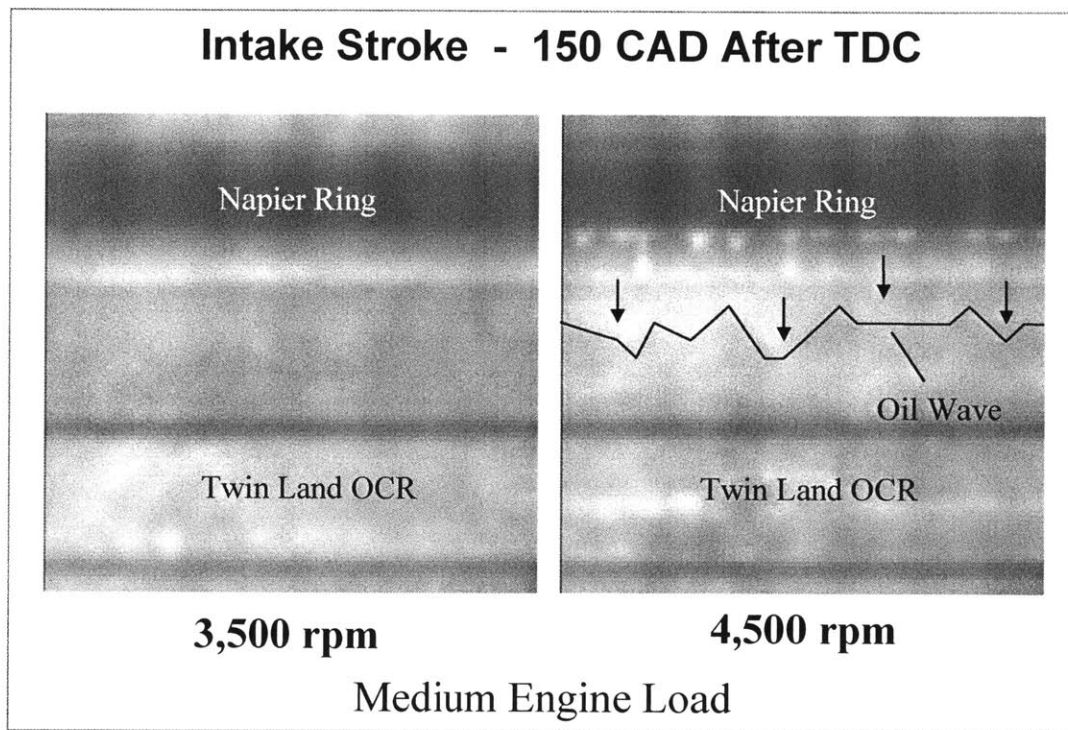


Figure 4.21 – Effect of engine speed on shaping the general third land evolution; at higher speeds the oil transport processes will begin earlier in the cycle primarily due to a larger inertia force

In Figure 4.21, 30 CAD before bottom dead center of the intake stroke is compared for two stable and repeatable mid-load situations, 3,500 rpm and 4,500 rpm, both operating at 500 mbar absolute intake pressure. In the 4,500 rpm image, lubricant can be seen beginning to pour out of the chamfer region and second ring groove. The wave is about half way across the third land, as indicated in the figure. Within the Napier Hook, oil can be seen forming drops destined to fall towards the OCR. This is a direct result of the

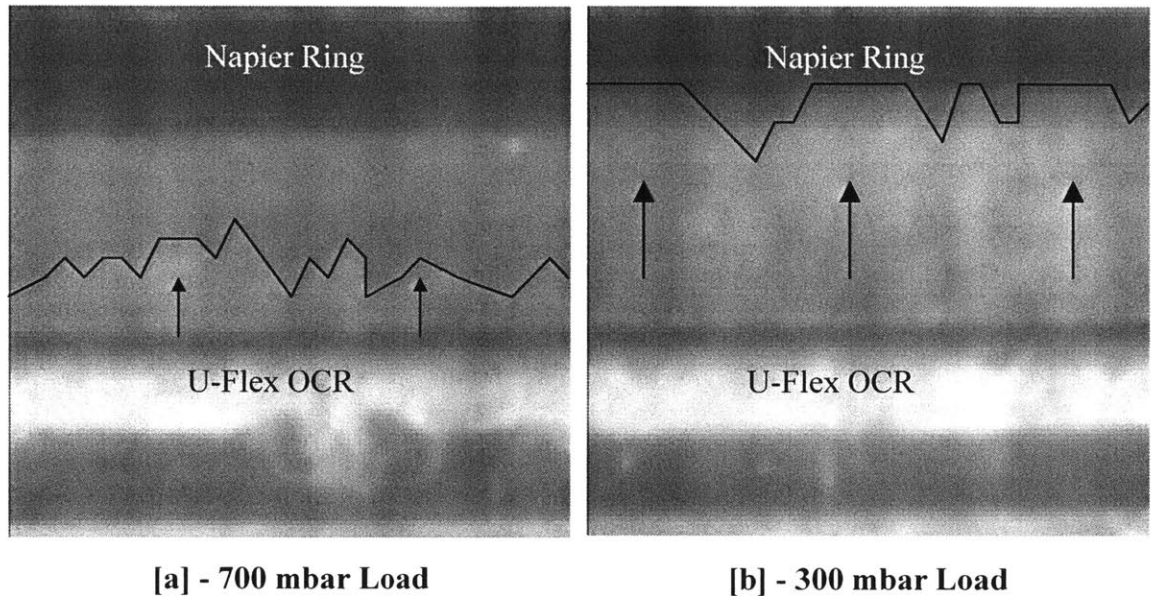
higher inertia generated by the faster engine speed; some drops, although much fewer in number, will form for the 3,500 rpm scenario as well, but not until the downward inertia force has been acting for a greater number of crank angle degrees. Along with the absence of drops in the 3,500 rpm image is the absence of the third land wave, as the oil is still residing in the chamfer and has yet to begin pouring out onto the third land. For this 3,500 rpm scenario, it takes approximately another 20 CAD for the third land oil wave to begin.

Engine load, similar to engine speed, will also have a clear impact on the timing and magnitude of the third land oil transport processes. As load increases, the volume of blowby gases flowing to the crankcase increases significantly. For this typical automobile engine, the volume of blowby gases (liters / min) more than doubles at most speeds when the load is increased from 300 – 700 mbar absolute intake pressure. The increased blowby gases, and associated pressure gradients, will act to keep oil to the back of the ring grooves as the gases move through the grooves and toward the crankcase. When the rings move axially in their grooves during a high load scenario, less oil will be forced out onto the third land. As discussed previously, this lesser volume of oil will cross the third land at a much slower rate than the larger volume of oil forced out during a low load situation. This occurrence is easily verifiable for both the upward and downward third land oil waves.

High and low load situations during the expansion stroke are compared in the images in Figure 4.22 for an engine speed of 3,500 rpm. The top images were taken 30 CAD after top dead center, while the bottom images were taken 40 CAD before bottom dead center. The low load situation (300 mbar absolute intake pressure) has an average blowby gas flow rate of 0.9 liters / min / cylinder, while the high load situation (700 mbar absolute intake pressure) has an average blowby gas flow rate of 3.3 liters / min / cylinder. This disparity helps explain the distinct difference seen in the images.

Expansion Stroke - 3,500 rpm

30 CAD After TDC



140 CAD After TDC

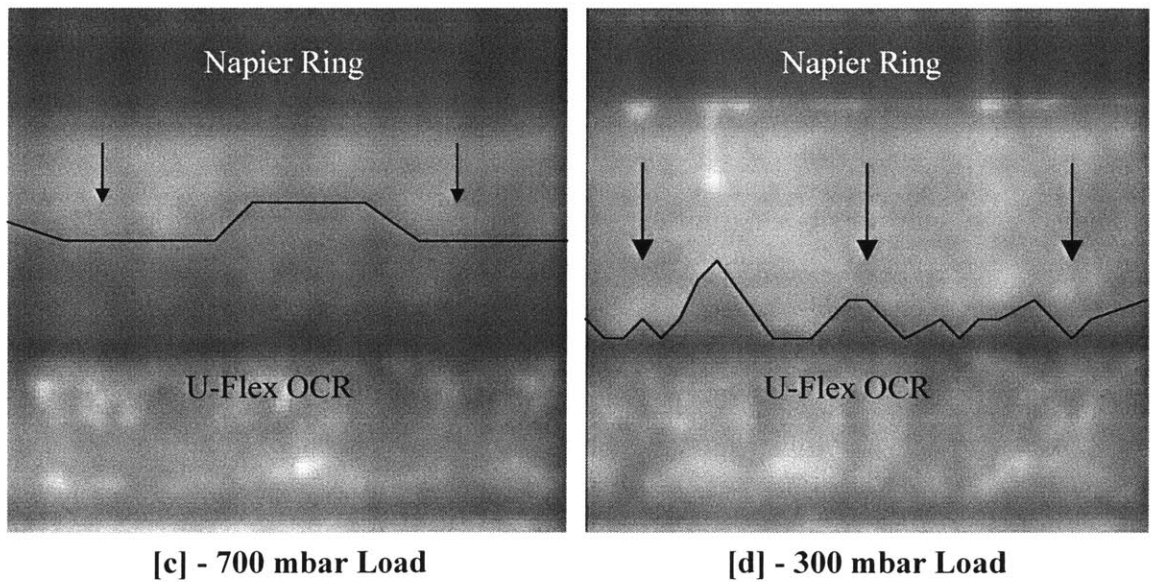


Figure 4.22 –Effect of engine load on shaping the general third land evolution; at higher loads the general oil transport processes will begin later and be smaller in magnitude

In Figure 4.22[a] for the 700 mbar scenario, inertia is in the upward direction and a thin oil wave is seen crossing the third land, near half way there. When the load is dropped to 300 mbar, it takes less than two seconds for the entire piston ring pack to adjust and stabilize to the new operating point, shown in Figure 4.22[b]. The small blowby flow rate of this low load has allowed more oil to be forced out of the oil control ring groove and onto the third land. This larger volume wave has already completely crossed the third land, in direct contrast to the smaller wave of the 700 mbar case, which is less than half across the third land at this crank angle. This is a clear example of how a larger volume of oil will travel faster than a smaller volume when acted upon by the same inertia force.

The effect of the decrease in load, and thus reduction of blowby gas flow, on a downward third land oil wave is almost identical in nature to the upward wave described above. In Figure 4.22[c], the 700 mbar scenario shows the oil wave approximately half across the third land. When the load is dropped to 300 mbar (Figure 4.22[d]), again only requiring a few seconds to stabilize, the clearly thicker third land wave is now seen to have almost fully crossed the third land. In addition to the heavier wave, oil drops can be seen leaving the Napier Hook and falling towards the OCR.

Even with speed and load variations, the general third land evolution remains constant. The timing and magnitude of the oil transport mechanisms will be slightly affected by variations in the engine operating point, but these variations are consistent and predictable, behaving as described in the examples above.

Influence of Ring Type on Evolution

A major focus for studying the third land is to examine the oil accumulation and patterns with different ring designs and operating conditions in attempt to learn how leakage to the second land is introduced. As iterated throughout this work, the choice of any common ring types for the second compression and oil control ring have minimal impact on the general third land evolution outlined in this work. Based entirely on the fact that various ring types exist, the different designs must obviously have an impact on oil

consumption. Each ring type has its own set of characteristics and transport mechanisms, which can be seen in the LIF study accompanying the general third land evolution. The general third land evolution dominates and controls the major oil flows on the third land, but certain qualities of the various ring types can have a significant impact on net oil transport across the third land towards the combustion chamber.

The main two types of scraper rings (second compression rings) in common use in automobiles are the Napier Ring and the Negative Twist scraper ring. The Napier Ring was chosen for illustration in the previous third land maps and discussed in the map explanations. In comparison, the Negative Twist scraper ring has a simple cross section, as was described in Chapter 2, and does not include a third land chamfer. The main difference between the Napier Ring and the Negative Twist ring is that the latter lacks the 'Buffer Region' made up of the Napier Hook and third land chamfer. During the first half of a down stroke, much of the oil from the third land up wave is being held in this 'Buffer Region' until inertia shifts, and the oil is forced back downward toward the OCR. The creation of this 'Buffer Region' will reduce the chance for oil to move into the second ring groove, with the goal of reducing net transport to the second land. The Negative Twist scraper ring lacks this 'Buffer Region', and thus during the first half of a down stroke most of the oil from the up wave is forced into the second ring groove. When inertia shifts downward and the Negative Twist scraper ring moves axially in its groove, it will force out much, but not all, of this oil back onto the third land and start a down pour towards the OCR. Similar to the Napier Ring, some of this oil forced out of the second ring groove, as well as some of the oil scraped from the cylinder liner during the down stroke, will form droplets leaving the Negative Twist ring and headed for the oil control ring. Both the Napier Ring and Negative Twist scraper ring will consistently produce the general third evolution described in this work, only the location of the temporary oil storage is different.

The Twin Land OCR, U-Flex OCR, and a Three-Piece OCR have been vigorously tested and consistently produce the general third evolution. As the main driving forces for the general third land evolution are inertia and ring dynamics, the geometry of the OCR

should influence oil transport, but not significantly change the basic pattern. Though the general third land evolution will remain consistent, the respective gap arrangements of the various OCR types will induce significant, but localized, effects onto the third land. The specific phenomenon for each oil control ring tested in this work will be discussed in the next sections.

U-Flex Oil Control Ring

The U-Flex oil control ring is a unique design in the automotive industry; instead of having one large gap, as many rings do, the U-Flex OCR has approximately 50 small gaps offset from each other on the top and bottom ring lands. This is highly beneficial in limiting upward oil transport through the ring gap, a large problem for the more common style of rings with only one large gap. Additionally, the many small gaps create an effective purging of the third land by distributing the downward gas flow evenly around the circumference of the piston. Any oil control ring gap will induce phenomenon onto the third land general evolution, and the U-Flex is no exception. The U-Flex strategy produces a uniform oil map around the entire third land with 50 small gaps equating to 50 small, localized, effects to the third land. This is in direct contrast to the single large gap, and accompanied significant, less localized, effect the Twin Land OCR gap has on the third land.

At sufficient engine operating speeds, approximately 3,000 rpm and above as seen experimentally, liquid oil can flow through the numerous U-Flex gaps during any down stroke. This oil is supplied from the copious amount of oil on the piston skirt region, just below the OCR. This phenomenon generally requires a minimum engine speed to generate the inertia required to overpower the surface tension force trying to keep the liquid oil in the U-Flex gap. Most of the oil that passes through the U-Flex gaps will remain on the liner, and be scraped by the second ring. In Figure 4.23, the drops from the Napier Hook are clearly aligned with the U-Flex gaps, as it is these gaps that are supplying the oil for the respective drops. The Napier Ring scrapes the ‘Gap Release’ oil from the cylinder liner during a down stroke, and inertia then forces the accumulation to drop back towards the OCR.

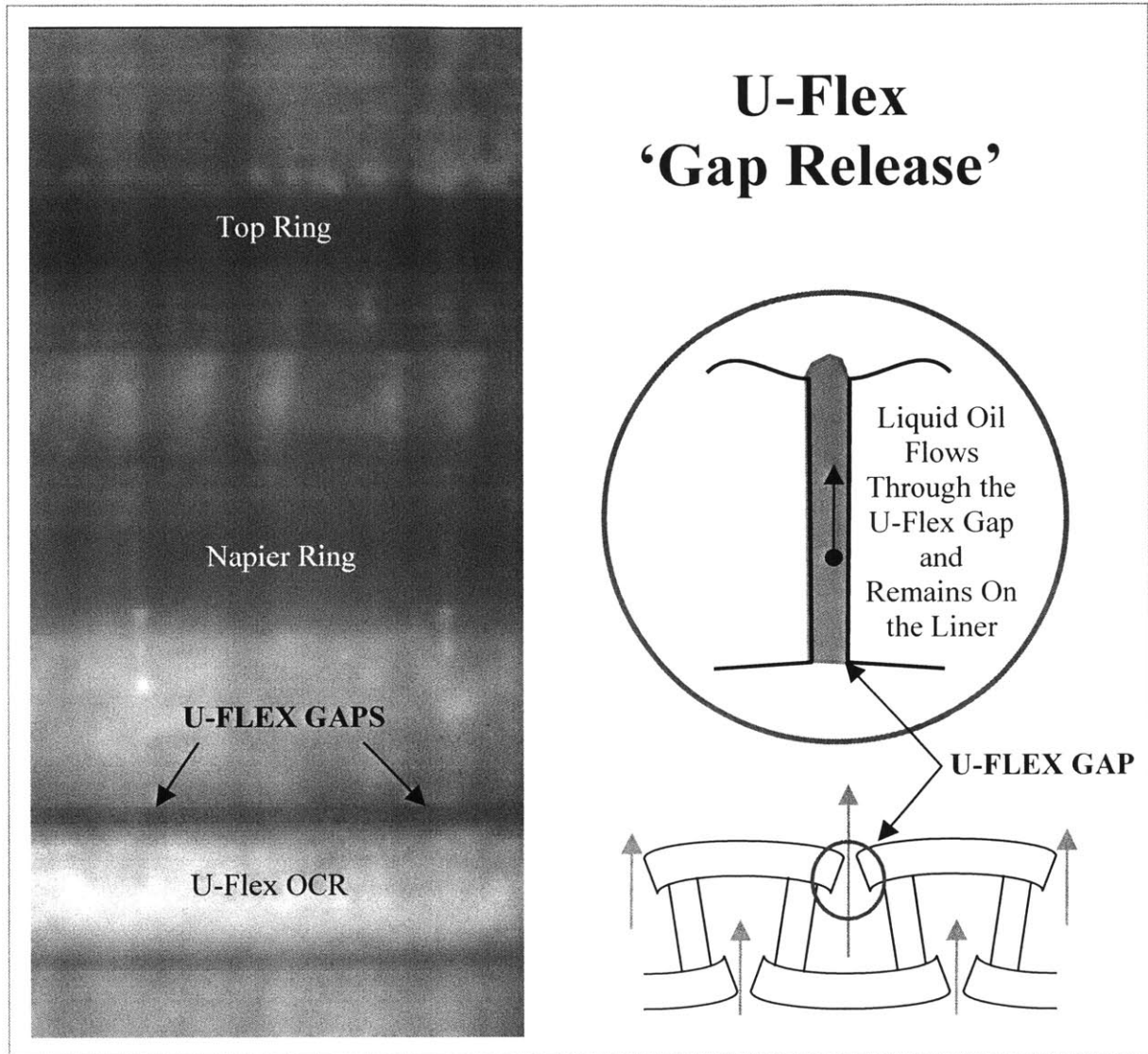


Figure 4.23 – U-Flex ‘Gap Release’ and associated accumulation and drop formation from the Napier Hook

Engine speed is the critical parameter for the ‘Gap Release’ transport discussed above, and similarly, engine load will induce a U-Flex gap related phenomenon. During the beginning and middle of the expansion stroke, the third land pressure can become great enough to blow the liquid lubricant residing in the U-Flex gaps turbulently downward (see Figure 4.24). This only happens during the first half of the expansion stroke, as the third land will increase significantly in pressure from combustion blowby gases. A minimum third land pressure is required for this phenomenon to occur, as the downward pressure force must be greater than the inertia force, which is in the upward direction for

the first half of the expansion stroke. For this reason, the ‘Gap Blowout’ phenomenon occurs for nearly all low speed operating conditions; but at higher engine running speeds, a significant load is necessary to counter the greater inertia force. For example, at 4,500 rpm experiments reveal a minimum absolute intake pressure of 500 mbar is required to induce this phenomenon.

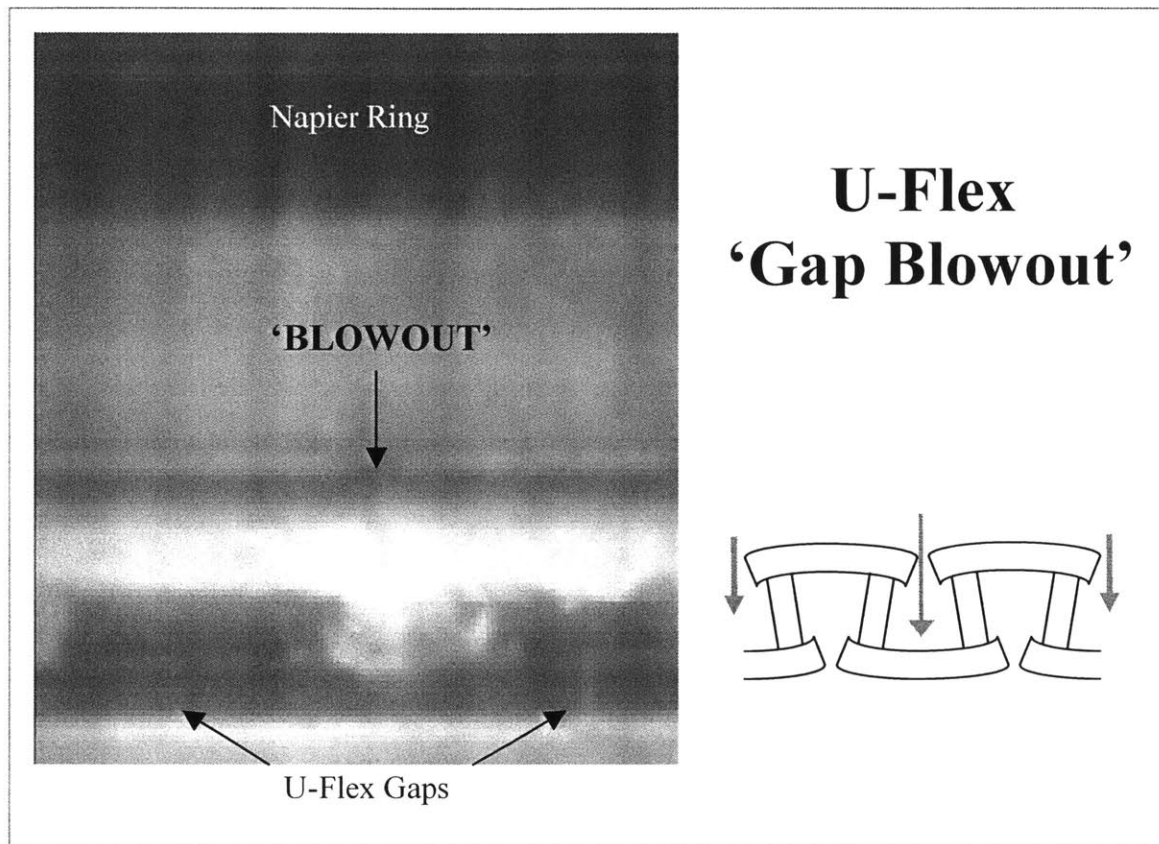


Figure 4.24 – U-Flex ‘Gap Blowout’ during the expansion stroke

Twin Land Oil Control Ring

The Twin Land OCR will generate a third land pattern that is 95% consistent. The other 5% of the third land circumference correlates directly to the location of the oil control ring gap. The single, large gap of the Twin Land OCR is a significant passage for gas flow from the combustion chamber to the crankcase, assisting the beneficial transport of oil back to the crankcase; however, the large cross section of the OCR gap also allows upward inertia to transport a substantial amount of liquid oil from the piston skirt to the

third land. Unlike the numerous, but relatively small scale transport seen through the U-Flex OCR gaps, the Twin Land OCR gap has considerable impact and is a major transport mechanism for moving oil from the piston skirt, across the third land, and onto the second land.

The effects of the gap overlay directly on top of the general third land evolution. To illustrate the magnitude of the OCR gap effect, a single map and LIF image are shown in Figure 4.25. To explain the phenomenon in the most basic sense, the portion of the third land near the OCR gap has a much greater oil volume. This oil concentration will closely follow the gap movement as the OCR rotates in its groove. It is this larger volume of oil in the OCR gap region that generates the distinction from the third land general evolution. As stated earlier, a larger quantity of oil will cross the third land quicker, making the Twin Land OCR gap a major source of oil transport across the third land, and ultimately to the second land. Inertia is still the dominant driver of this oil transport process; the general third land evolution is altered simply because inertia has a much larger supply of oil to work with in this area, and because the gap allows a direct path for oil movement from the piston skirt to the second ring groove.

Figure 4.25 shows a portion of the third land map, and LIF image, for the beginning of an intake stroke. Away from the OCR gap region, the third land behaves as described in the general evolution; compare the left side of the map (denoted with a 'Z') to the same crank angle degree in the general evolution discussion. For the majority of the third land, the upward oil wave has just about crossed the third land. For the heavy volume of oil near the OCR gap, however, the oil already crossed the third land during the end of the exhaust stroke. This quick moving oil crossed the land and filled the Napier Hook during the second half of the exhaust upstroke. In small regions on both sides of the gap, enough oil crossed during the upstroke to fill the Napier Hook completely. Once the hook is full, some of this oil can attach, or 'Ring Bridge', to the cylinder liner and be up scraped by the oil control ring during the end of the exhaust stroke. This oil accumulates on the OCR top surface and forms some drops and a second up wave on top of the initial one. Through this mechanism, indicated by an 'X' on the third land map in Figure 4.25,

the same oil can cross the third land twice during the final 90 CAD of an upstroke. Additionally, the OCR gap itself can be seen to allow a large flow of oil directly into the Napier Hook. This constant, heavy flow of liquid oil through the oil control ring gap quickly fills the Napier Hook and the accumulation begins to spread out to the left and right of the gap location. This local saturation at the second ring/groove/liner interface is a major source of oil transport from Region One to Region Two, and the most prominent shortcoming of the Twin Land OCR.

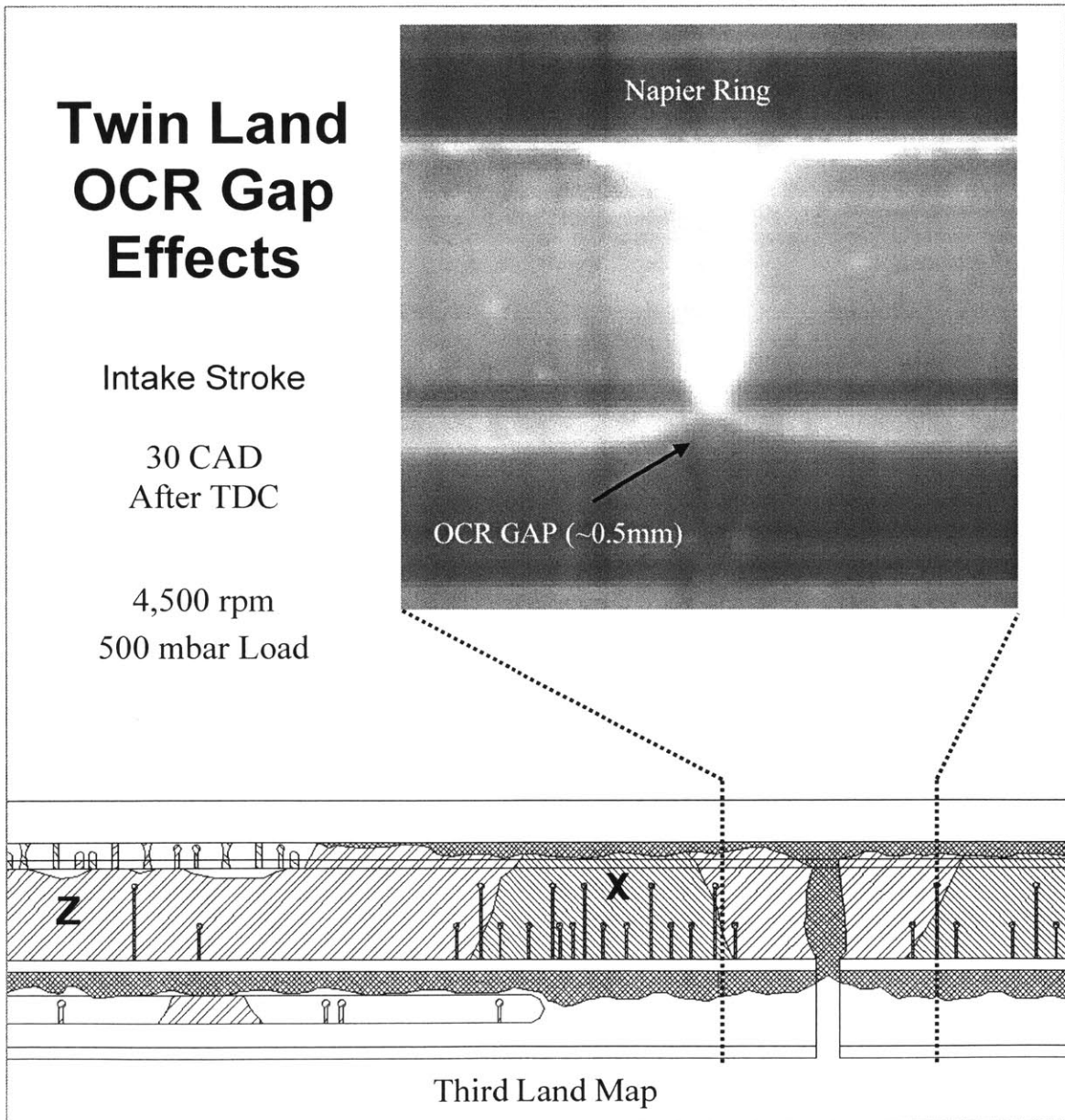


Figure 4.25 – Twin Land OCR gap phenomena and effects on general third land evolution

Individual oil maps have been made for Twin Land OCR gap region throughout the first half of the engine cycle, and are shown in Figures 4.26 and 4.27. The maps are of the same operating point as the general evolution discussion: 4,500 rpm and 500 mbar absolute intake pressure. As with the general evolution maps, only the first half of the engine cycle is discussed, as the second half should be very similar for this region of the piston ring pack. A brief description of each map follows:

0 Crank Angle Degrees (Intake Stroke, TDC) – The initial up pour has reached the Napier Hook in the gap region and begun to accumulate near the end of the exhaust stroke. Some of the accumulation has filled the Napier Hook and crossed to the liner through ‘Ring Bridging’, as described in Section 3.1. That oil is then scraped by the oil control ring and has begun a second up wave in the OCR gap region.

30 Crank Angle Degrees (Intake Stroke) – The second up wave is mostly stagnant as there is no longer a supply to feed it. Heavy amounts of up drops are leaving from the OCR top land in the gap region, probably from the remainder of oil up scraped during the very end of the exhaust stroke.

60 Crank Angle Degrees (Intake Stroke) – Similar to the general evolution, not much oil remains on the third land in the gap region. However, the massive accumulation of oil which has gathered in the Napier Hook, particularly the region lined up exactly with the gap, has created a poor scraping situation for the Napier Ring, as described in Section 3.2. There is an excess amount of oil being left on the liner in the OCR gap region after the second ring has passed; this phenomenon follows the OCR gap exactly.

90 Crank Angle Degrees (Intake Stroke) – There is a significant amount of accumulation seen in the Napier Hook. Now that inertia has shifted downward, this oil will begin to pour out of the Napier Hook and across the third land just after the midpoint of the stroke. The poor scraping phenomenon that began at the 60 CAD point continues.

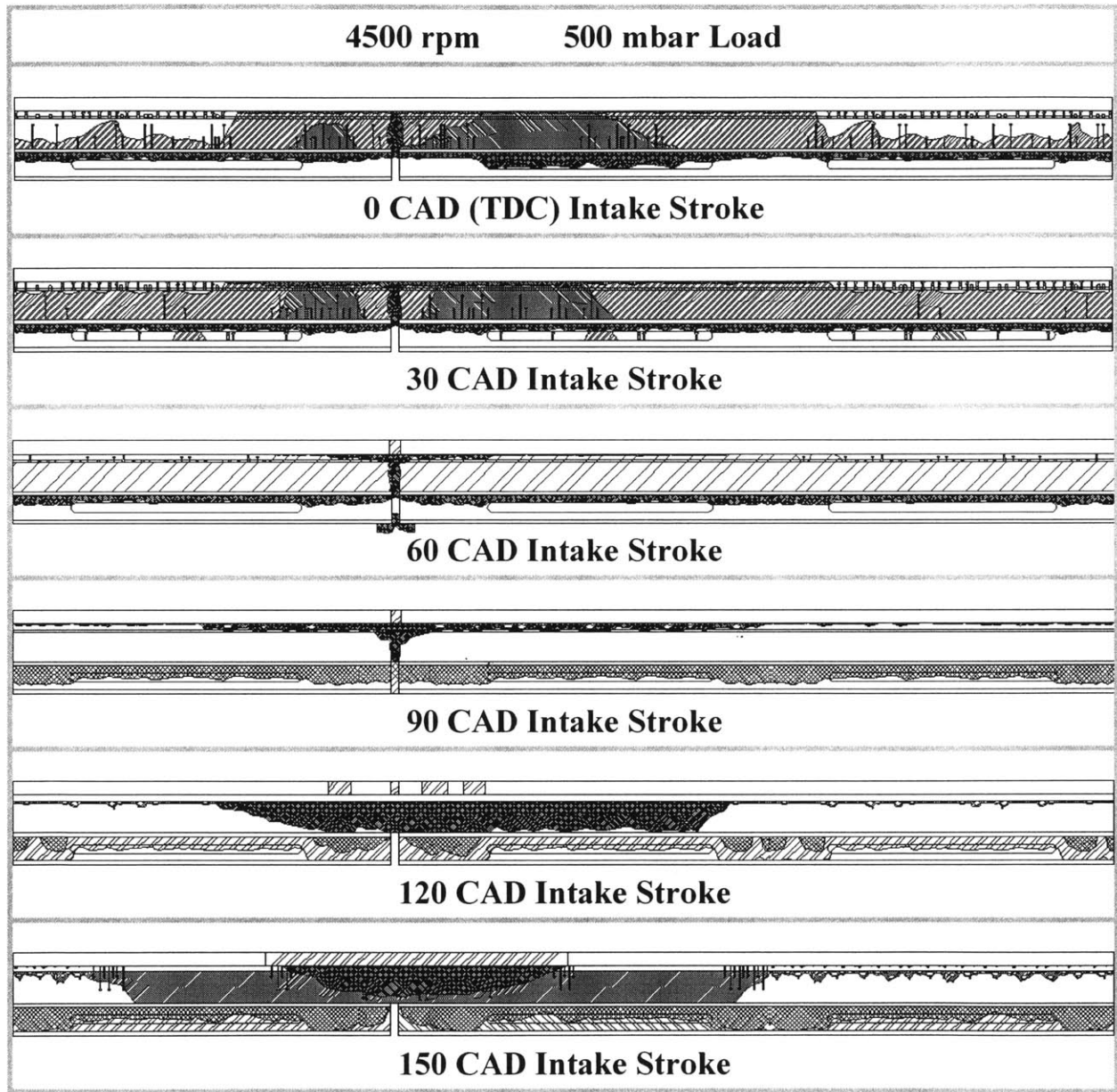


Figure 4.26 – Third land maps for the intake stroke, focusing on the Twin Land OCR gap area

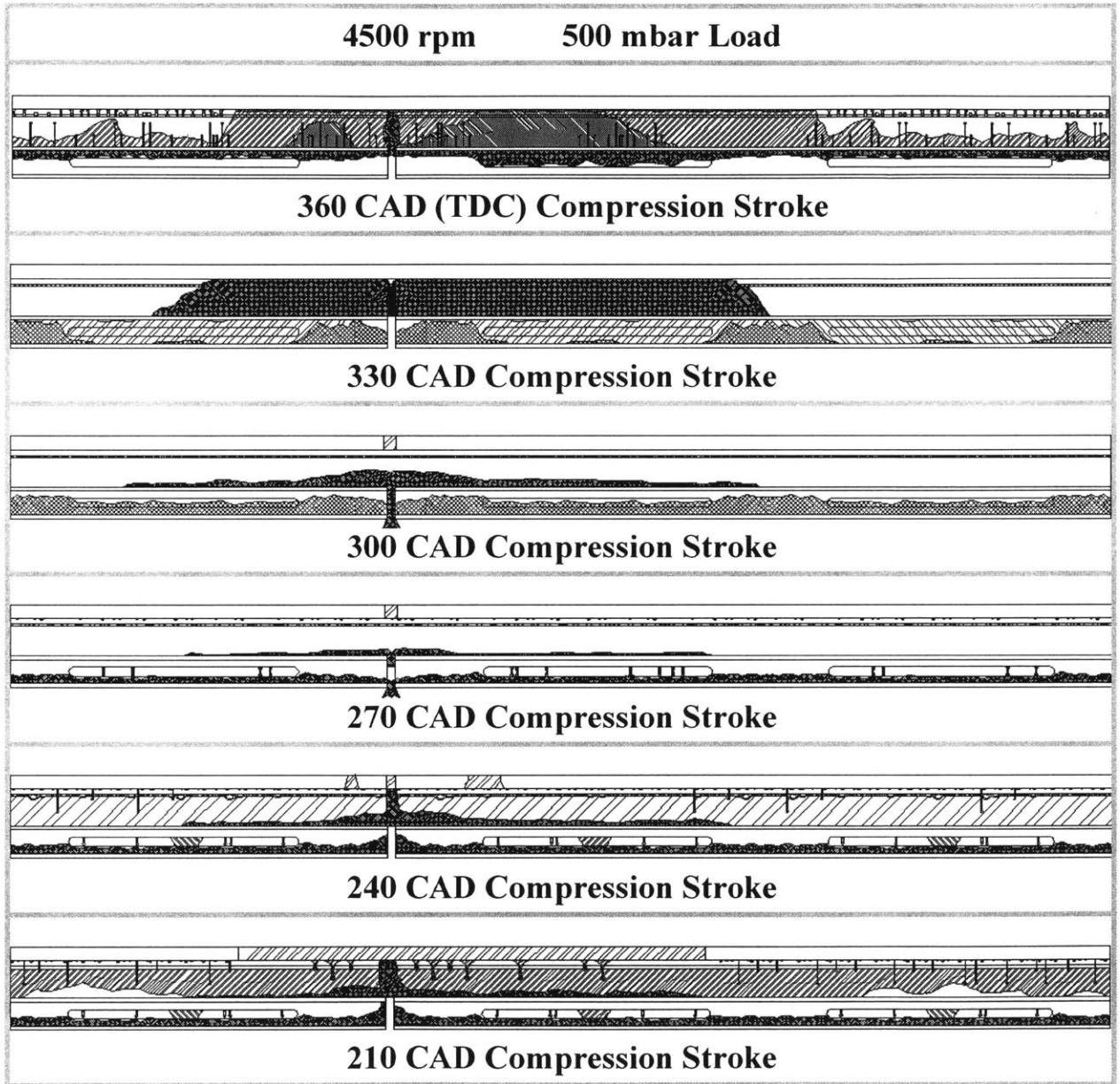


Figure 4.27 – Third land maps for the compression stroke, focusing on the Twin Land OCR gap area

120 Crank Angle Degrees (Intake Stroke) – Down pour in the OCR gap vicinity has fully traversed the third land. Some of this oil bridges the top land of the oil control ring and contacts the liner; most of this oil becomes scraped by the Napier Ring but some is seen as excess oil passing by the second ring. The massive amount of oil being scraped by the Napier Ring has spread the poor scraping phenomenon to more areas than just directly above the OCR gap.

150 Crank Angle Degrees (Intake Stroke) – The down pour in the OCR gap region expands. The area that initially crossed quickly and was being scraped by the Napier Ring now begins to form a second down wave. The poor scraping phenomenon correlates to the width of this second oil wave almost perfectly.

180 Crank Angle Degrees (Intake Stroke, BDC) – At bottom dead center, the third land was not converted to an oil map. However, by examining the 150 CAD and 210 CAD maps, it can easily be inferred what the 180 CAD map looks like. Similar to a mirror image of the TDC map, the second down wave is fairly extensive in reach. There are also a significant number of drops leaving the Napier Ring hook, most of which deposit onto the OCR. The poor scraping phenomenon continues in a wide area around the OCR gap.

210 Crank Angle Degrees (Compression Stroke) – The compression stroke has begun as the piston accelerates upward. A large amount of oil is accumulating on the top land of the oil control ring. The poor scraping phenomenon continues on the second ring; this excess oil on the liner becomes scraped by the oil control ring, only adding to the accumulation.

240 Crank Angle Degrees (Compression Stroke) – The large accumulation on the top land of the oil control ring remains. The poor scraping phenomenon past the second ring reduces as we are approaching the liner location where it began.

270 Crank Angle Degrees (Compression Stroke) – At the midpoint of the compression stroke, the inertia force is weak. The large accumulation on the top land of the oil control ring still remains, but will soon begin to pour upward across the third land. The poor scraping phenomenon reduces further to only the exact OCR gap location.

300 Crank Angle Degrees (Compression Stroke) – The large accumulation begins to pour upward across the third land. The poor scraping phenomenon remains at only the exact OCR gap location.

330 Crank Angle Degrees (Compression Stroke) – Inertia continues to grow in the upward direction, and the large accumulation which was on the top land of the OCR is now fully across the third land. This oil is filling the Napier Hook, with some ‘Ring Bridging’ and consequent scraping by the OCR taking place. The poor scraping phenomenon of the second ring has ceased.

360 Crank Angle Degrees (Compression Stroke, TDC) – A second up wave has begun in the area surrounding the OCR gap. This oil is largely supplied by the upward scraping mechanism of the OCR during the last quarter of the compression stroke.

The Twin Land oil control ring gap phenomenon behaves predictably to engine operating conditions. A faster engine speed, and thus a greater inertia force, will enhance this oil transport mechanism. Contrarily, a higher engine load will increase net blowby flow from the combustion chamber to the crankcase, and act to inhibit some of the inertia driven upward oil flow through the OCR gap. The exact magnitude of the correlation between the TLOCR gap phenomenon and engine operating conditions needs to be investigated in more detail.

The effect of the Twin Land oil control ring gap is quite significant, but it is localized and responsive to the exact gap position. Stated another way, the large oil volume, and consequent effects, associated with the region surrounding the gap will follow the ring’s circumferential movement closely. Tests were performed where the OCR was rotating

consistently at 1 rpm. The effects of the gap location are locally quite substantial to the third land oil transport processes, but the exact general evolution returns only 1 second after the gap passes. The timescale for establishing the significant oil accumulation pattern that follows the OCR gap is much less than the timescale of ring rotation. In Figure 4.28 (same as Figure 3.20) are images demonstrating this rapid timescale.

The third land transitions from the general evolution (4.28[b]), to local saturation (4.28[c]), and back to the general evolution (4.28[d]) in only 2 seconds. As stated earlier, the heavy accumulation pouring through the gap in Figure 4.28[c] saturates the second ring/groove/liner interface and has clear implications to the second land. In images 4.28[b] and 4.28[c] the quantity of oil on the second land increases substantially, establishing the Twin Land oil control ring gap as a significant transport mechanism for moving oil from the third land to the second land with near instantaneous effects. It is imperative that this transport mechanism be studied in greater detail, including the effects of speed and load, as it is clearly a key means by which oil is transported to the upper piston ring pack.

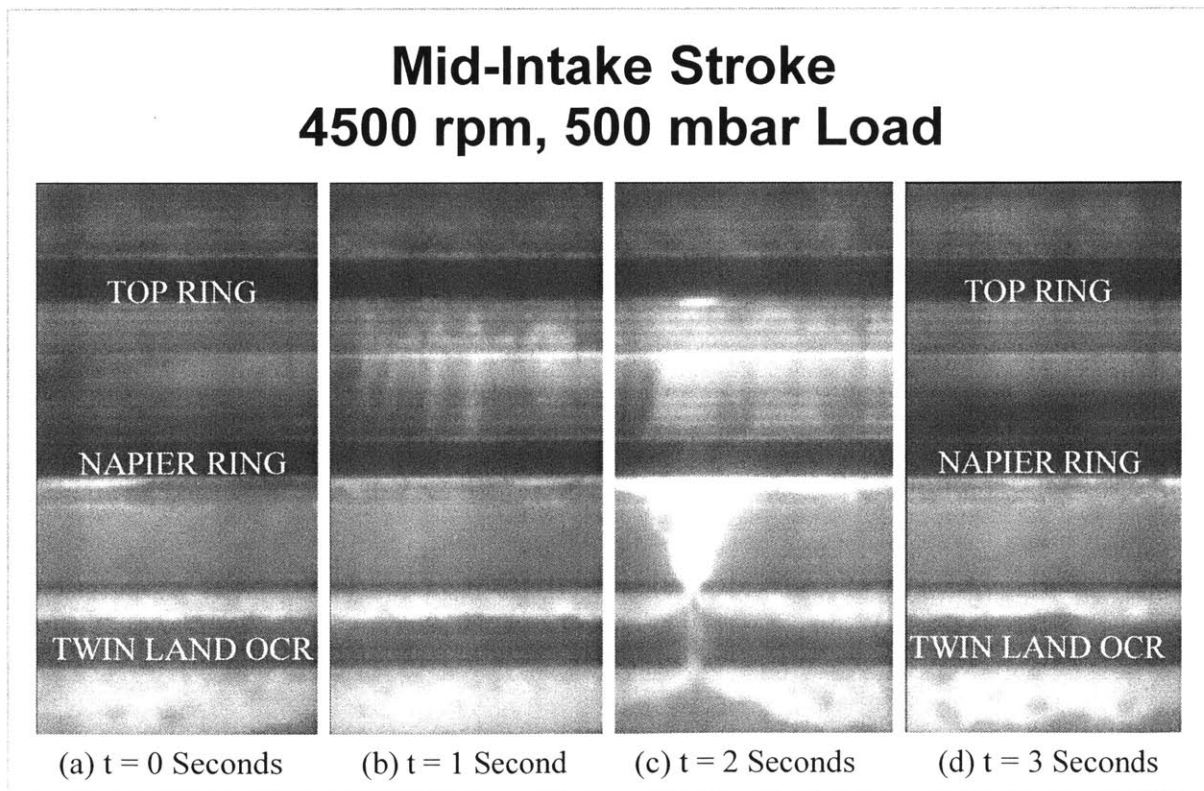


Figure 4.28 – Timescale of Twin Land OCR gap transport, and its effect on the piston ring pack

Three-Piece Oil Control Ring

A Three-Piece OCR is designed to seal both the upper and lower groove clearances through the ear angles of the expander and the two rails. The mechanics of this design was overviewed in Figure 2.24; the OCR tested in this work had a zero degree ear angle. The Three-Piece OCR, like the other oil control rings tested, follows the general evolution of the third land described above. As with the other oil control rings, however, the Three-Piece OCR does introduce gap specific phenomenon onto the third land. The gap behavior of the Three-Piece OCR lies in between the extreme natures of the U-Flex and the Twin Land OCR.

The one large ring gap of the TLOCR allowed a significant amount of liquid oil to be forced from the skirt onto the third land by inertia. The Three-Piece OCR has three separate pieces, and thus three separate gaps, all of which are offset from each other at engine installation. The three pieces rotate in unison, maintaining the exact offset gap positions; the contact force between the rails and the expander is too strong for the three pieces to rotate independently from one another. Having the gaps offset prevents a direct path for oil to flow from the skirt to the third land. Furthermore, the rail and expander design seals both the upper and lower groove clearances, restricting gas and oil flow through the groove. This geometry forces much of the gas flow through the gaps of the Three-Piece OCR. During the intake stroke, the reverse blowby through the top rail gap introduces a significant amount of liquid oil onto the third land. The chaotic nature of the oil flow through the top rail gap indicates a dominant driving force is gas flow, and not just inertia as was the case with the TLOCR. Figure 4.29 illustrates several examples of reverse blowby driven gap flow through the Three-Piece OCR top rail. The right three images were recorded at high load, over the course of a minute, with each image thirty seconds apart. Note that even during a high load situation, gap driven flow contributes significantly to upward oil transport. In image (a), the top rail gap is acting independently from the rest of the ring pack, but the second ring gap is approaching slowly from left to right. In image (b), thirty seconds later, the second ring gap and the Three-Piece OCR top rail gap are aligned and transporting a significant amount of oil to the upper regions of the piston ring pack. Image (c), thirty seconds later, shows the

Three-Piece OCR top rail gap again acting independently, as the second ring gap has rotated out of the viewing window to the right.

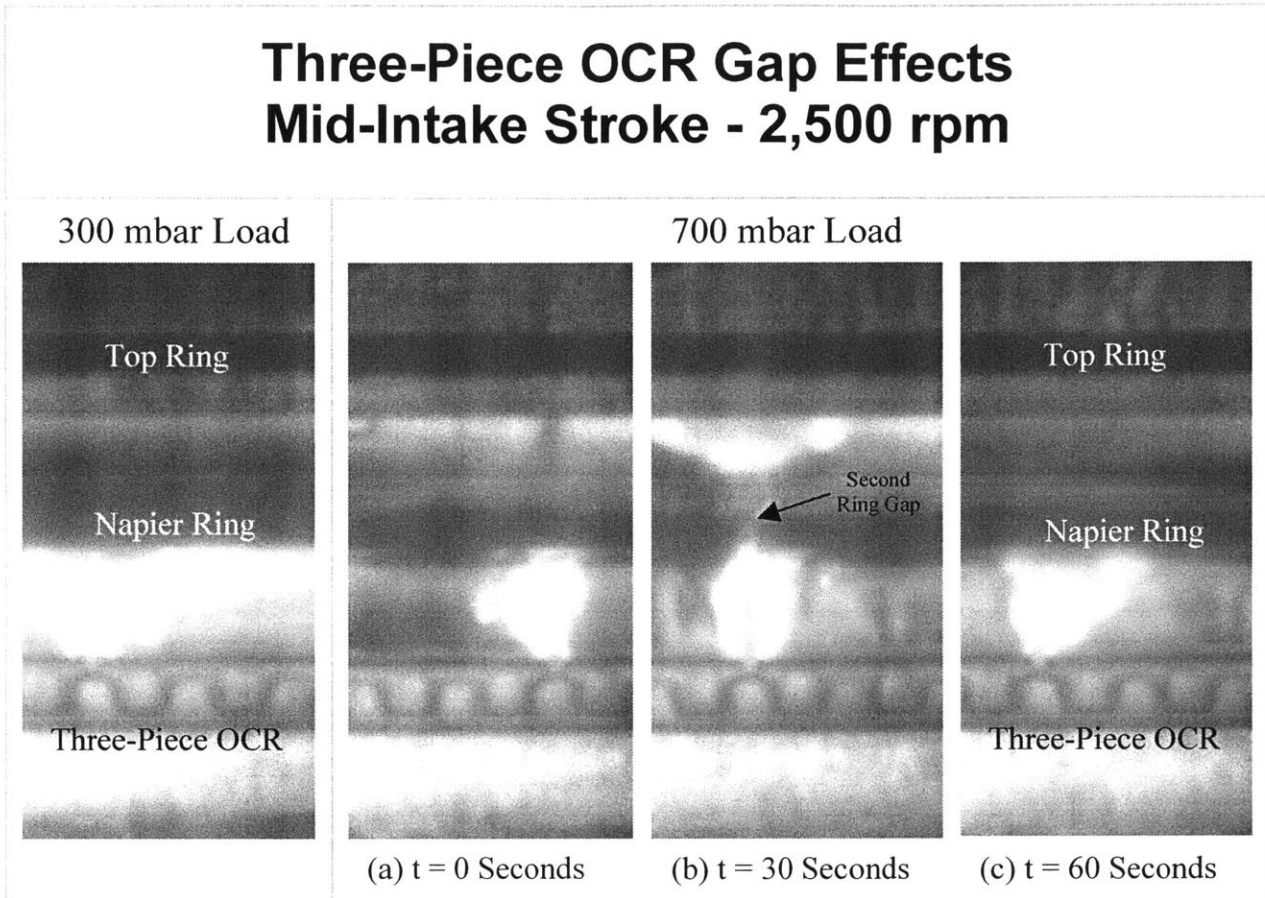


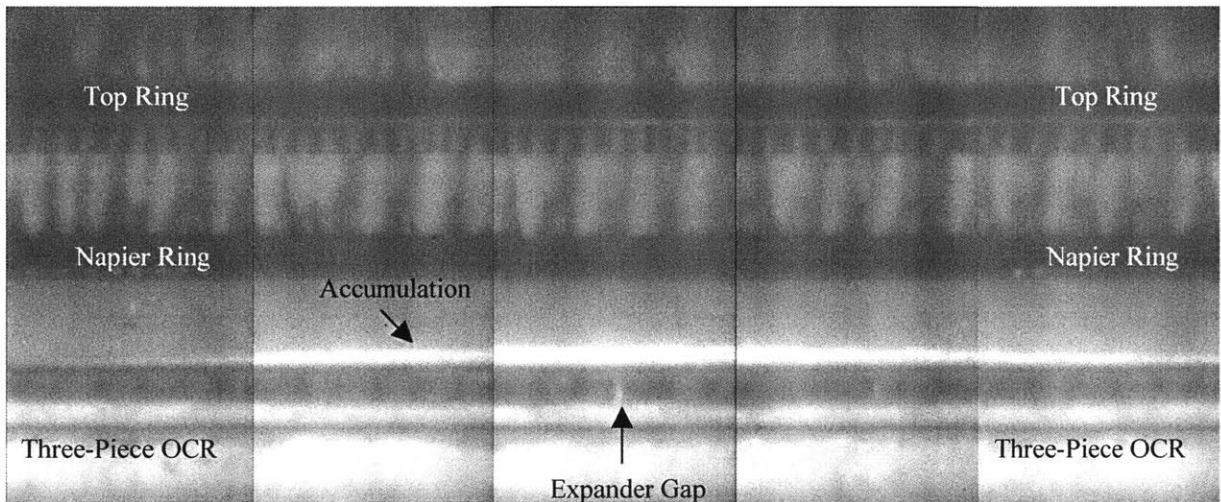
Figure 4.29 – Three-Piece oil control ring gap effects from reverse blowby

Similar to the Twin Land oil control ring, the Three-Piece OCR will introduce an oil accumulation to the third land that follows the gap movement. In the TLOCR gap discussion, a large oil accumulation was seen to follow the gap movement with a very fast timescale; the gap would introduce an accumulation to the third land, but the accumulation would disperse as fast as the ring gap rotated. The Three-Piece OCR not only introduces this same sort of accumulation around the top rail gap, but it also has a large accumulation on the third land which follows the exact motion of the expander gap as well. Figure 4.30 shows the extent of the accumulation, currently residing above the top rail, around both of these gaps in the Three-Piece OCR. All of these images came from one recording, with the still shots extracted and placed together to illustrate the scale of the accumulation, similar to the general evolution maps earlier. These oil

accumulations, and the reverse blowby gap flow, of the Three-Piece OCR are not independently as great as the Twin Land OCR gap phenomenon; however, the combination of the effects of the expander and top rail gaps may approach the same magnitude of oil transport as the effects of the single TLOCR gap. Like the other oil control rings tested, therefore, the gap related phenomenon for the Three-Piece OCR are an important element to the overall transport across the third land, but the general evolution of the third land still holds throughout.

Three-Piece OCR Gap Accumulations Mid-Compression Stroke - 4,500 rpm

Expander Gap



Top Rail Gap

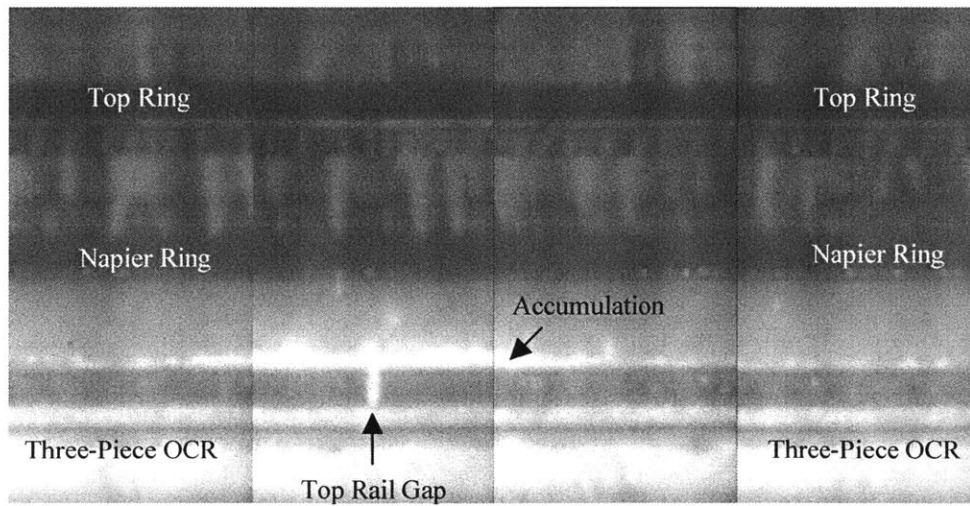


Figure 4.30 – Three-Piece oil control ring gap associated oil accumulations on the third land

Net Oil Transport to the Second Land

The intensive study conducted on the third land is focused on understanding the timing and magnitude of the oil transport processes, in attempts to reduce the net oil transport to the second land. The consistent evolution of the third land has been outlined, along with the specific phenomenon of piston ring pack designs. Therefore, we have identified the mechanisms, timing, and relative magnitude by which oil from the third land (Region One) has entered the second ring groove; some of this oil will become transported to the second land (Region Two) each cycle. The third land oil maps detail the oil waves and drops that bring oil into the second ring groove when inertia is in the upward direction. From the images in Figure 4.28, it is clear an accumulation at the second ring/groove/liner interface has direct implications for oil transport to the second land. By identifying the timing and relative magnitude of the oil transport processes through the general evolution maps and specific ring phenomenon, the foundation for oil transport to the second land has been outlined.

The effect of the various ring gap types has been shown through the U-Flex OCR ‘Gap Release’ mechanism, Three-Piece OCR gas driven gap flow, and the significant inertia driven flow through the Twin Land OCR gap. In this work we have avoided discussion of the net transport effect of the second ring gap, as we believe this to be part of Region Two and outside the control of this region of focus, the third land. Liquid oil cannot travel from the crankcase, across the third land, to the second land without following one of the paths described in this work. Removing the ring gaps from the ring pack design will be difficult, leaving the consistent inertia driven oil waves and drops the most promising aspect for control of oil transport on the third land.

Impact of Third Land Experimental Study

The impact of this work is many fold. The first impact, as discussed above, is how knowledge of the timing and relative magnitude for oil crossing the third land will allow designers to improve the third land attributes. The most obvious direction would be an attempt to limit the influence of the upward acting inertia on generating large oil waves and oil drops which cross the third land. The other main direction to augment the third

land oil transport control properties would be to enhance the effect of downward inertia on returning oil from the third land to the oil control ring groove. The second impact of this work is to assist the theoretical work and computer modeling of the oil transport processes. An accurate model of lubricating oil consumption has never been developed. The observations of the third land evolution will assist the theoretical work to establish the exact relationship between oil accumulation and engine speed and load, thereby aiding creation of a detailed model of total oil transport on the piston ring pack. And finally, the third major impact of this work is the foundation it provides. A comprehensive understanding of the third land (Region One) is necessary before attempting to fully understand the second land evolution. This third land study will form the groundwork for future comprehensive studies directed at Region Two of the piston ring pack.

4.3 Second Land (Region Two)

The second land of the piston ring pack is the source of lubrication for the top ring groove, the excess of which is believed to be consumed in the combustion chamber. Region Two is much more difficult to analyze than Region One. This work has found that the oil pattern at any crank angle is approximately known for the third land, with only the engine speed and load required knowledge. Region Two oil transport occurs over long time periods, several seconds as opposed to several crank angle degrees as was the case for Region One. The oil pattern for the third land ‘resets’ stroke after stroke; however, an oil accumulation can remain on the second land for well over 60 seconds or longer. Region Two contains less oil than Region One, which allows blowby gas dragging to become a significant oil transport mechanism, particularly in the circumferential direction, making ring rotation an important element to consider.

These reasons make Region Two difficult to analyze, for although we are aware of the driving forces, and how they would affect on oil accumulation in this Region, the amount of oil on the second land is not consistent from minute to minute. The evolution of oil transport on the second land is strongly affected by the positions of all three ring gaps,

each acting independently to influence the quantity of oil on the second land at any given moment. Therefore, the appearance of the second land will change day to day, or even test to test, as the randomness of ring rotation heavily influences the Region Two oil patterns. Attempting to make oil maps throughout the engine cycle, as was done for Region One, is therefore futile. The best approach available is to create accurate models for what happens to oil that is on the second land; the foundation for this was largely set in Chapter 3 when the general oil transport mechanisms were described. Attempts to influence the oil transport mechanisms across the second land were investigated with geometrical changes to the piston. These specific experimental studies will be relayed next.

Second Land V-Cut

Oil on the second land tends to spread out axially in both directions, driven by inertia. These puddles are also slowly driven circumferentially, as combustion blowby gases are supplied primarily from the top ring gap and flow toward the second ring gap. These basic transport mechanisms were detailed in Chapter 3. To mitigate the axial spreading of an oil accumulation on the second land, a V-Cut into the piston second land was made. The goal was to provide a reservoir or ‘Buffer Region’ for the oil to be contained during an upward inertia period; the oil would be forced into this cut, but would not be able to breach the sharp angle at the top of the V-Cut. During the ensuing downward inertia period, the oil stored in the V-Cut would easily pour down and back towards the second ring groove. This specific geometric feature was aimed primarily at reducing the negative effects of upward inertia on moving oil towards the top ring groove, while enhancing the beneficial effects of downward inertia on returning oil back to the second ring groove. The geometry of the V-Cut employed in this experimental study is shown in Figure 4.31.

The V-Cut was found to be exceptionally successful at inhibiting inertia driven transport across the second land. Oil would experimentally seen to be squeezed out of the second ring groove and onto the second land, it would then spread vertically across the second land and become contained by the V-Cut. When the accumulation in the V-Cut became

large enough, downward inertia would make the lower extremity of the puddle contact and return oil to the second ring groove. A higher engine speed would also achieve this 'return' effect, as the higher inertia force would make the puddle thinner and longer, and thus less total oil volume would be required for the oil to reach the second ring groove. The V-Cut was nearly perfect in its containment of upward moving oil, with little to no lubricant seen breaching the top of the V-Cut onto the second land portion above the cut. In fact, the portion of the second land above the V-Cut appeared to act entirely independent of the oil accumulations in and below the V-Cut. A drawing of the region of focus along with an example of the V-Cut effects is shown in Figure 4.32. Figure 4.33 details the effect engine speed has on the accumulations contained within the V-Cut; slower engine speeds allow larger wider puddles, while a greater engine speeds creates more numerous, but thinner and longer puddles on the second land. The right three images, taken over ten seconds, detail the independent movement of oil within the V-Cut as compared to above the V-Cut.

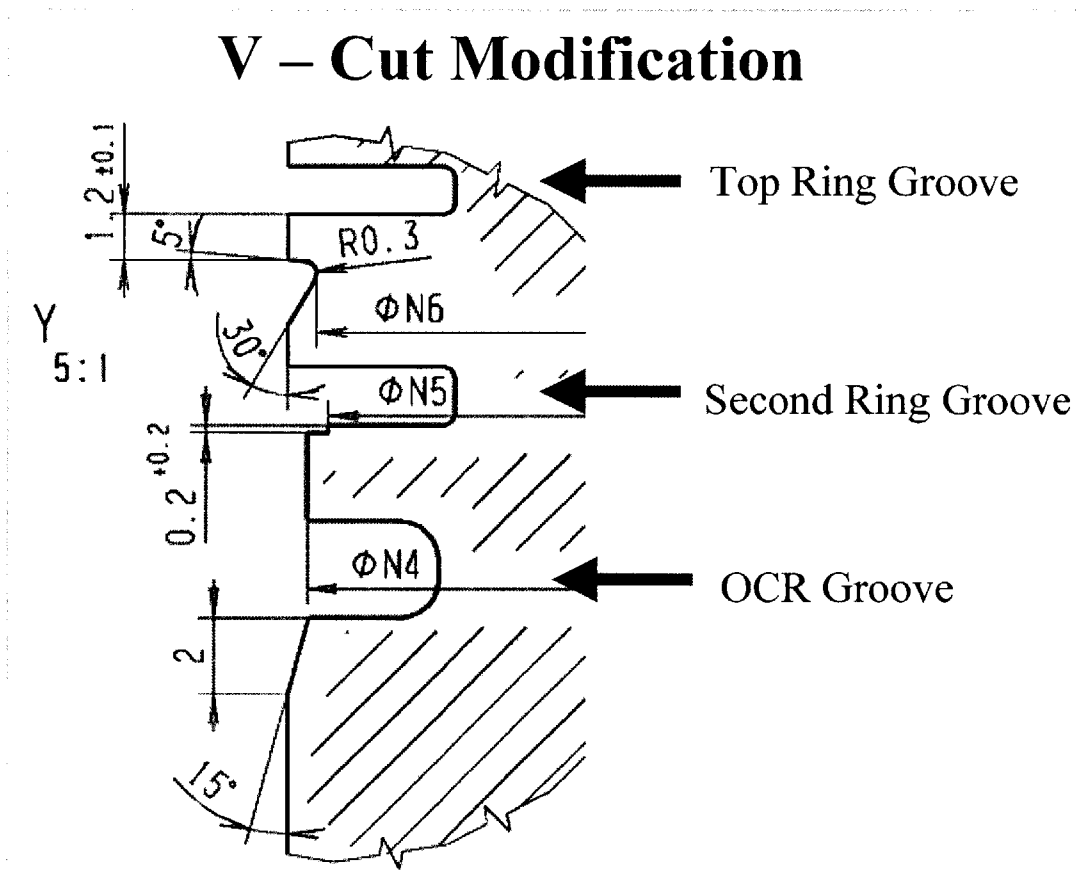


Figure 4.31 – V-Cut modification to the piston second land

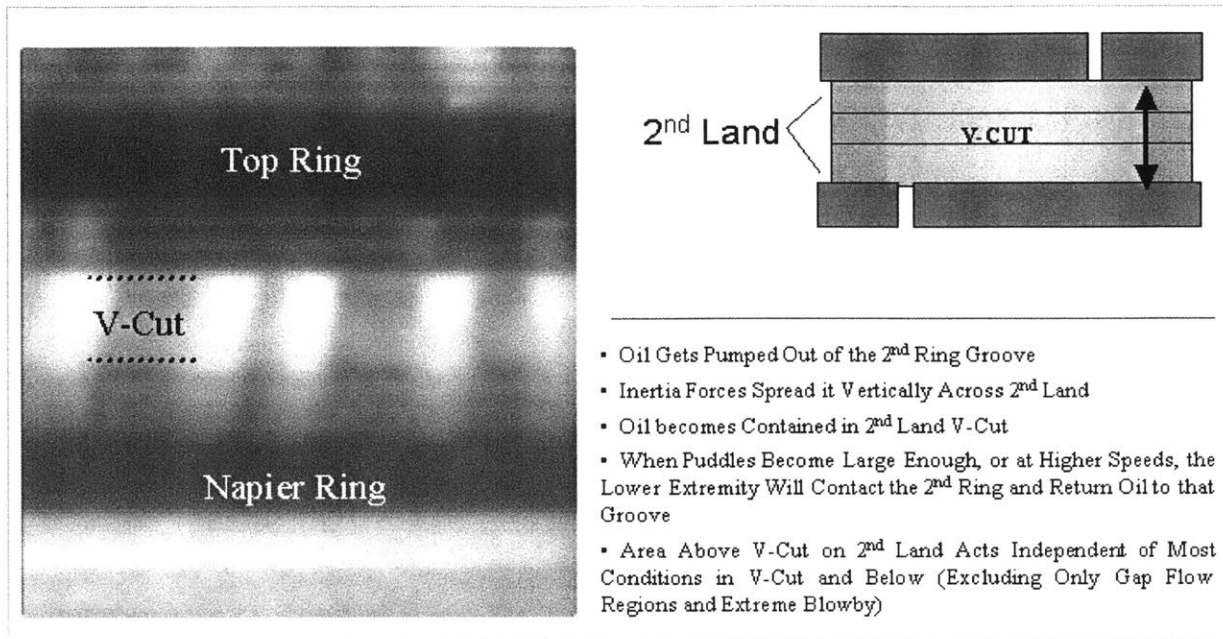


Figure 4.32 – V-Cut modification LIF image and key points

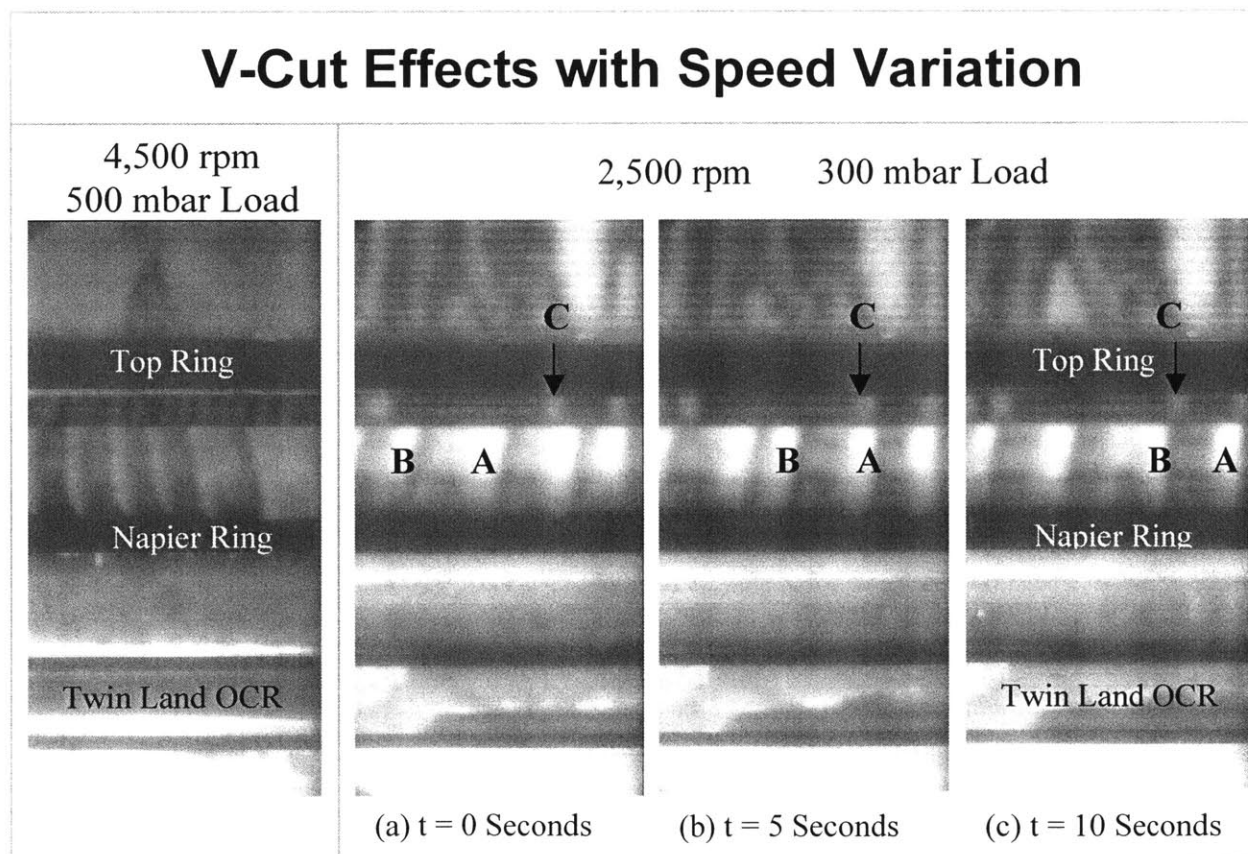


Figure 4.33 – V-Cut relationship to engine speed, a slow speed allows thicker puddles while a faster speed creates thinner and longer accumulations; the letters denote a specific oil accumulation and follow its movement over the timeline

The V-Cut appears to be a superior means to inhibit oil transport across the second land. And in fact, it is nearly perfect in controlling inertia driven transport; however, the V-Cut benefits are diminished when in the presence of the ring gaps, and sometimes the V-Cut even acts to strengthen the negative effects of ring gap driven oil transport. The ring gaps introduce two elements that act to disenfranchise the V-Cut: Quantity of oil and strength of gas flow. The amount of oil in the ring gap regions can be great enough so that not all of the oil can be contained within the V-Cut. When this occurs, some of the oil is experimentally seen to breach the V-Cut and enter the top ring groove. Also, the magnitude and direction of gas flow (axial) through the ring gaps can act to blow the oil out of the V-Cut. In fact, no oil is seen in the V-Cut when in the presence of the top ring gap. As the V-Cut generally has a significant amount of oil in it, the negative effects of ring gap driven transport may be strengthened as the V-Cut will introduce a larger supply of oil on the second land for the ring gaps to affect. Overall, the V-Cut illustrates the power a geometric feature can have on oil transport, as it will nullify the effect of inertia driven transport on most of the piston circumference. However, the net benefit of the V-Cut is strongly mitigated, or possibly reversed, by its side effect of maintaining a larger supply of oil on the second land, which strengthens the negative effects of ring gap driven transport.

Second Land Hook

An attempt to improve on the V-Cut concept made with the inclusion of a Hook onto the second land in place of the V-Cut. The Hook attempted to improve on the containment theory, by further restricting the ability of the oil to breach the cut and reach the top ring groove. The geometry of the Hook machined into the second land is shown in Figure 4.34. The general effects of the Hook on oil transport were not significantly different than the inclusion of the V-Cut. The Hook provided the same resilience towards inertia driven transport across the second land, and it had the same Achilles Heel in regards to ring gap driven transport. As they appear equally effective, the V-Cut is the optimal design because it introduces less structural concerns into the piston than the Hook does.

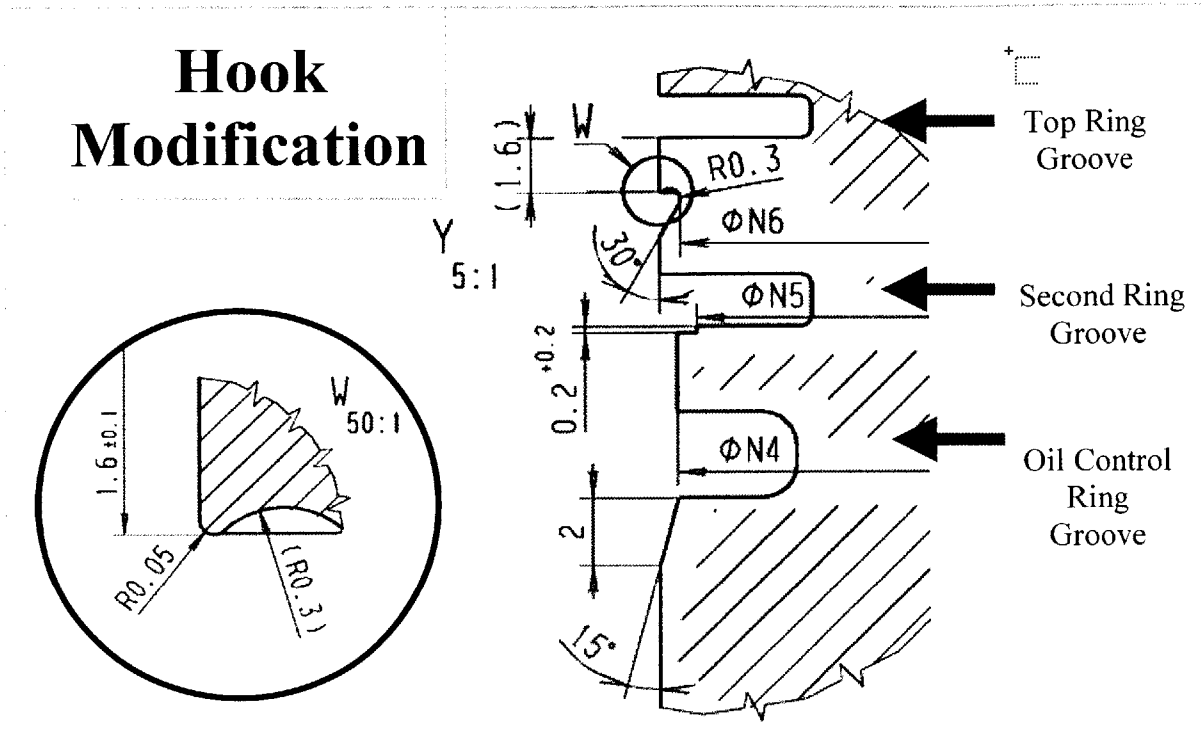


Figure 4.34 – Hook modification to the piston second land

Net Oil Transport to the Crown Land

The geometrical features inserted into the second land demonstrated the control a designer could have over inertia driven transport on the second land. Even with the V-Cut and Hook, however, a significant amount of oil still remained on the crown land at all times. This observation, along with experimental evidence that only a limited amount of oil transport was seen crossing the second land in the absence of ring gaps, leads to the conclusion that the net oil transport across the second land is determined mostly by ring gap driven transport and ring gap effects. The best enhancement to Region Two would be a feature that would mitigate the negative effects of ring gap driven transport, perhaps a modification of the ring design itself. If such a feature could be combined with a V-Cut, second land oil transport could be significantly controlled.

4.4 Crown Land (Region Three)

The crown land serves no purpose in terms of lubrication, but it is a main source of lube oil consumption. The top ring, top ring groove, and the crown land are the main locations of oil vaporization from the piston ring pack. Furthermore, liquid oil is experimentally seen to leave the piston crown during upward inertia periods, forming droplets headed towards the cylinder head. As oil consumption exists, it is believed the net transport into Region Three is always in the upward direction, with any oil on the crown land destined to be consumed eventually. The only viable way for oil to return to the second land in any significant amount is through ring gap driven transport. As the top ring rotates, downward flowing combustion gases will drag some of the oil in its direct vicinity to the land below. As the geometry of Region Three is open to the combustion chamber, no circumferential flow is established, and thus the effect of blowby combustion gases is mostly limited to the exact gap location. Figure 4.35 illustrates the main mechanisms by which Region Three directly contributes to oil consumption, and Figure 4.36 is an LIF image demonstrating the presence of oil on the crown land available for evaporation and throw-off.

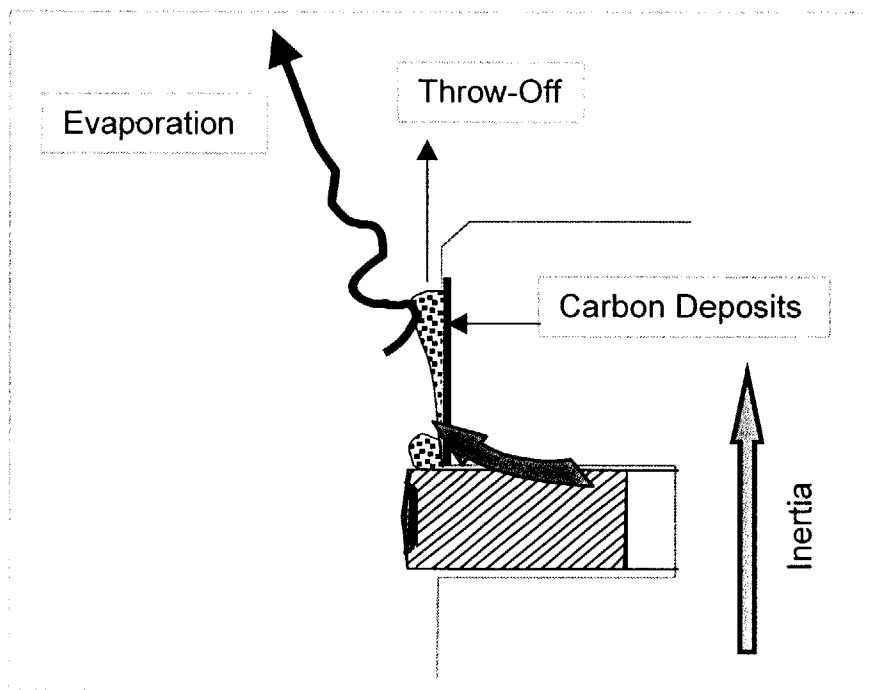


Figure 4.35 – Methods of oil consumption from the crown land

Crown Land Throw-Off

High Speed - Closed Throttle

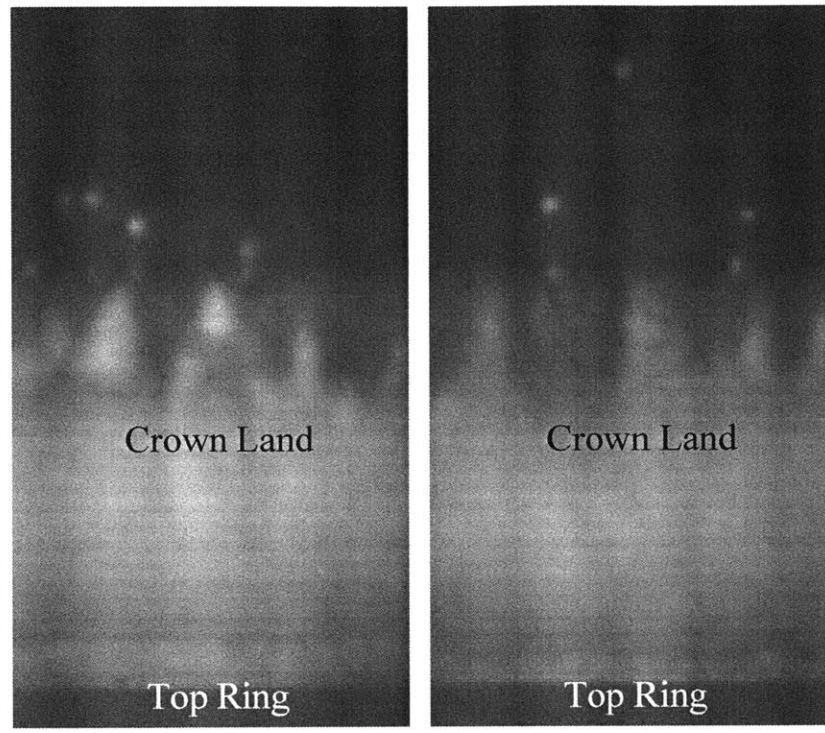


Figure 4.36 – Examples of crown land throw-off; the high speed, closed throttle operating point was chosen to amplify the quantity of oil consumed by this mechanism

Top Ring Groove

The top ring groove is the main supply of oil for Region Three, with only a moderate contribution from the top ring gap from reverse blowby, even at low loads. The squeezing action of the top ring is the source for oil accumulations on the crown land. This transport mechanism generally occurs only during the end of the exhaust stroke, as the top ring is against the lower flank of the ring groove at all other times.

Oil Evaporation

At high engine loads, the crown land can reach temperatures of up to 300°C. At this temperature, the oil can evaporate and mix with the combustion chamber gases.

Depending on the residence time of oil on these hot surfaces, the lubricant can become oxidized as it evaporates. As the lighter oil components will generally evaporate first, the heavier components will oxidize on the crown land and form carbon deposits. Crown land carbon deposits are seen on pistons with as few as twenty engine operating hours, and under normal running conditions.

CHAPTER 5: THE ROLE OF LIF TECHNOLOGY IN MARITIME ECONOMICS & EXHAUST EMISSIONS

The Marine Transportation System is vital to virtually every industry. Exhaust emissions from marine vessels utilizing this system has been the main focus of various regulating bodies in the past five years. Even though waterborne transport, when compared to trucking or rail, is more fuel efficient, cheaper, and produces less exhaust emissions per ton-mile, the amount of pollution generated is a large enough quantity to substantiate serious regulations and has begun to come under the same exhaust emission scrutiny the world has already seen in the automotive, truck, and rail industries. However, implementation and focus of emission standards is not straightforward. Great variety exists in the marine industry, from tug boats to container ships for example, requiring more detailed regulations for each segment. Additionally, regional requirements would be cumbersome to this truly international industry, thus global regulations need to evolve towards a balance between the industry and the environment.

The technology exists today for rapid improvement in exhaust emissions, but at exorbitant costs. Careful selection of emission technology to fit the industry's nature, and emission laws which keep a few paces behind technology will maintain the cost to the industry at a reasonable level while making long term improvements for the environment. LIF technology used to reduce lube oil consumption, and thus exhaust emissions, has a minimal research cost and the benefits would apply to the entire industry. The application of LIF would be across an entire engine class, as the strategy is identical for engines of similar size; additionally, the modification would be permanent, requiring no maintenance or extra work from the ship's crew. The application of LIF would be continuously reducing lube oil consumption for the lifetime of a vessel, suffering from little to no degradation in efficiency.

LIF technology aimed at reducing lube oil consumption not only affects the environment, but also the bottom line. For example, cylinder lube oil consumption is the greatest operational cost for a slow speed engine, other than fuel. If LIF technology employed on a large container ship were able to reduce cylinder lube oil consumption by a modest 10%, it would result in about \$30,000 of savings per year. Applying this research to smaller engines would reduce lube oil degradation and to a small degree costs, but most importantly great strides in improving exhaust emissions would be achieved. LIF technology has benefits for accountants and the engineers working to reduce exhaust emissions, and needs to be employed.

5.1 The Maritime Industry and the Environment

Assessing the scope and uniqueness of the maritime industry is critical to formulating an efficient analysis of maritime exhaust emission strategies. In this section, the role shipping plays in the transportation sector and environment is detailed, as well as information on the varying range in scale of the propulsion and electrical generation equipment employed by marine vessels.

Marine Transportation System

Virtually every nation heavily relies on marine transportation, and those with coastal access are directly linked to it. The flow of goods and raw materials generated would quickly bottleneck or cease if ocean and waterway access were denied. To relay the extent of the global maritime industry, the United States will be investigated in detail, though most advanced nations will have a similar network. Third world countries also rely on maritime transportation substantially, but their infrastructure will obviously be less evolved.

The U.S. Marine Transportation System encompasses a network of navigable waters, port terminals with intermodal connections, publicly and privately owned vessels, shipyards and vessel repair facilities, and a skilled labor pool operating and maintaining this infrastructure. Numerically, the Marine Transportation System consists of 25,000 miles

of navigable waterways and 3,700 marine terminals, 1,900 of which are in coastal ports and 1,800 are located on inland waterways. According to the U.S. Department of Transportation, two thirds of the consumer goods purchased by Americans move along this system [35]. Over two billion tons of cargo per year is transported upon the aforementioned 25,000 miles of navigable U.S. waterways, with comparable percentages traveling domestically and internationally. The U.S. is the world's largest trading nation, with our marine trade accounting for over 15% of the thirteen billion tons of global cargo moved by 35,000 ocean-going ships [36]. Furthermore, U.S. foreign trade is expected to more than double by the year 2020. Shipping is the preferred overseas freight transport method for strictly economic reasons as the transit time is far greater than by airplane, supported by the statistic revealing about 95% of U.S. overseas trade is by vessel. However, about 95% of the ocean-going vessels in U.S. ports are foreign flagged, creating a very international industry that is difficult to monitor and regulate effectively.

By nature, domestic shipping is easier to encompass under U.S. laws, but this side of the industry includes a wide range of applications. From the Great Lakes, to inland waterways, to coastwise transport, domestic shipping takes on many forms. From commercial fishing accommodating 110,000 vessels, to the ferry industry transporting 134 million passengers a year, to the large container ships on the west coast and chemical tankers in the gulf, all the way to the \$18 billion spent per year on wildlife watching [37,38]. Shipping is the most economical and fuel efficient means of transportation, especially when considering heavy bulk freight. The nation's highway and rail systems are not significantly expanding and will face severe constraints caused by the doubling of cargo over the next two decades. The coastal and inland waterways and the Great Lakes offer viable decongesting alternatives for cargo transportation with the added benefit of a reduction of per ton-mile fuel consumption and pollution [38].

The complexity of applying exhaust emission technology and regulations for domestic and international shipping is seen in Table 5.1, and illustrates some of the varied components of the maritime industry. The size of the vessel and engines employed can vary significantly depending on its purpose. The diversity creates difficulty for policy

makers who must achieve their goals without causing severe economic strain on the industry or creating a system where enforcement and monitoring is impractical and inefficient. The variety of engines employed also encourages the engine manufacturer to develop technologies that are applicable to all its engines under a wide array of operating conditions.

Type of Vessel	Volume of Transport	Engine Rating
Tug and Towboats	1 - 30 Barges	0.5 - 4 MW
High Speed Ferries	150 - 350 Passengers	2 - 4 MW
Roll-On/Roll-Off	200 - 600 Vehicles	15 - 25 MW
Tankers	250,000 Tons of Oil	25 - 35 MW
Container	1750 - 6000 TEU	20 - 65 MW

Table 5.1 - The diversity of marine vessels and their engine rating in megawatts [36]

The vast majority of these vessels are powered by diesel engines, in fact, 99% of the world fleet of 85,000 ships has diesel propulsion. Other industries also rely on diesels; 95% of trucks, trains, boats, and buses have diesel engines. With 16 million new diesel engines being sold each year, and the diesel industry's gross output being 85 billion dollars, the diesel engine is going to be around for a long time [39,40]. There exists a plethora of research in fuel cells and alternative power sources, but the reality is going to be diesel engines as the mainstay for quite some time. Diesel engines continually get cleaner and more efficient, making it tough for new technology to compete.

Approximately 350 U.S. ports handle the international and domestic cargo of the nation. The destination of U.S. waterborne trade by region is broken down by detailing the domestic portion, with the remaining percentage having an international destination: U.S. coastwise ~ 45% domestic, Great Lakes ~ 75% domestic, inland rivers ~ 70% domestic. The largest 50 ports handle about 80% of the waterborne trade, where as the largest 100 ports handle over 95%; the concentration of cargo creates a high density of ship transit near the major ports, necessitating a closer look at the contribution of ship exhaust emissions in these high traffic shipping lanes and ports [37]. Previously shipping

emissions were discounted, as general thinking believed the majority of exhaust output was in the middle of the ocean, but that simply is not the case. A global ship traffic density study reveals 85% of traffic is in the Northern Hemisphere and 70% is within 400 km of land [41].

It is clear shipping is an enormous industry with direct implications to virtually everyone. Keeping the Marine Transportation System well managed and regulated will keep shipping costs down and ultimately makes products more affordable. For example, for U.S. farmers to be competitive globally with countries where labor is cheap, there must be low-cost and efficient marine transportation to deliver their products overseas. This also applies to car manufacturers who must import parts or steel, and for oil companies whose tankers bring the crude oil we use for making gasoline for our automobiles; coal-fired power plants that are served by barges generate approximately 75% of the U.S. total electric power [42]. Beyond the economic aspects, it is also to everyone's benefit to keep ship emissions to a minimum, particularly near regions of high population density, but we must balance environmental impact with the economic impact of any policy. To do this, we need to examine exactly what contribution the maritime sector has on overall emissions from other sources such as automobiles, trucks, airplanes, and power plants.

Waterborne Transportation in Comparison to Other Modes

Marine transportation is well documented to be the leader when considering fuel efficiency in the movement of goods, dominating rail, airplanes, and trucking. This readily converts to cost savings for the shipper and is more pronounced when the cargo becomes denser and less valuable; the greatest advantage for airplanes and trucking is the quicker time of delivery. Waterborne transportation will consume an amazing one-tenth of the energy consumed by the U.S. trucking industry when considering fuel efficiency on a ton-mile basis. The relative energy efficiencies as well as the shipping cost per ton-mile of trucking, rail, and inland barge are shown in Table 5.2, airfreight fuel efficiency and cost comparisons are much worse than trucking.

Type of Transportation	Fuel Efficiency	Shipping Cost
Truck	59 ton-mile / gallon	\$5.35 / ton-mile
Rail	202 ton-mile / gallon	\$2.53 / ton-mile
Inland Barge	514 ton-mile / gallon	\$0.97 / ton-mile

Table 5.2 - A comparison in fuel efficiency; trucking uses almost ten times as much fuel and costs over five times more than waterborne transport [43,44]

The reason for the dramatic difference in price and fuel efficiency is in cargo capacity. The volume of cargo carried by one truck is miniscule compared to the amount carried by a train or barge. Economies of scale come into play dramatically in the transportation of goods. Large ships, which dwarf most barges, have an even better fuel efficiency and cargo capacity rating. A transport capacity comparison is made in Table 5.3. The range of scale in the table is impressive alone; however, a barge and a hopper car rarely travel as a single unit. A freight train often employs 100 hopper cars, and a barge tow might have 15 barges. A barge tow has the equivalent units of 2¼ freight trains, and an astounding 900 trucks. In addition to the volume induced fuel efficiency benefits, an Environmental Protection Agency analysis shows when comparing the three modes reveals towboats emit 35-60% fewer pollutants per ton-mile than do locomotives or trucks [38]. Fuel efficiency and pollution are not the only advantage of waterborne transportation over trucking; shifting cargo from trucks to vessels also reduces road congestion, probable accidents, and the need to dispose of worn equipment such as tires.

Type of Transportation	Cargo Capacity	Equivalent Units
1 Barge (Waterborne)	1500 Tons / 453,600 Gallons	15 Jumbo Hoppers or 60 Trucks
1 Jumbo Hopper Car (Rail)	100 Tons / 30,240 Gallons	4 Trucks
1 Large Semi (Truck)	25 Tons / 7,560 Gallons	-

Table 5.3 - A cargo capacity comparison between trucking, rail, and barge [45]

The numbers dictate waterborne transport to undoubtedly be the shipper's choice of freight movement for cost, and the world's choice for fuel efficiency and pollution

reasons. Only when delivery time is critical or special handling necessary, will trucking or air transit be the optimal choice. This data is fairly understood by those involved in the industry and in environmental pursuits. What is less understood is the actual impact shipping has on overall global emissions. Exhaust emissions from marine vessels, particularly large ships, is regulated much less than trucking or rail, but ships have much greater variety in size, engine type, and fuel burnt. Additionally, shipping is an international business, which complicates legislation and enforcement. Large ships spend a large portion of their time in the middle of the ocean with their exhaust emissions having little direct impact on the populace; however, the major coastal shipping lanes and ports are transited by vessels constantly, and thus the marine industry could contribute significantly to a region's air quality. As stated before, almost all ship traffic is in the Northern Hemisphere and 70% is within 400 km of land.

Marine vessel exhaust emissions are obviously not the only ones to affect global air quality. It is also affected by exhaust emissions from a wide range of other sources, from power plants to lawn mowers. Point sources are generally the largest emitters per unit, consisting of power plants, factories, refineries, etc... Mobile sources are the other major category, consisting of on-road and off-road vehicles. On-road vehicles consist mostly of cars and trucks, while the off-road counterpart entails construction equipment, aircraft, trains, ships, farm equipment, and recreational vehicles. The various mobile sources above have different engine types, sizes, and burn different fuels; these variations in design mean the engines will have differing fuel efficiencies and produce different exhaust emission outputs. In virtually every region across the United States, on-road mobile sources constitute the largest single source category of air pollution. The various emissions of concern currently are: Nitrogen Oxides (NO_x), Carbon Dioxide (CO₂, greenhouse gases), Carbon Monoxide (CO), Hydrocarbons (HC), Sulfur Oxides (SO_x), and Particulate Matter (PM). They all have a negative impact on the environment and human health and will be discussed in detail later.

As detailed earlier, the world relies on motor vehicles and reciprocating engines for an enormous amount of tasks. In the United States, transportation consumes two thirds of

all petroleum used, and produces one quarter of greenhouse gases, a pollutant that can only be reduced by increasing fuel efficiency. Rail and marine transportation combined contributed the least amount of pollution from the transportation sector [46]. Overall, U.S. transportation is 95% reliant on petroleum for its energy requirements; the internal combustion engine, which powers virtually every marine vessel, is going to remain the dominant source of power for a very long time. Table 5.4 shows the United States major categories of NO_x production, currently the most prominent emission of concern. The Off-Road section is then detailed further in Table 5.5.

Source of NO _x	Industrial Processes	On-Road Vehicles	Miscellaneous	Non-Road	Fuel Combustion
Contribution Percentage	3.9	29.8	1.5	19.3	45.5

Table 5.4 – NO_x source distribution; total NO_x produced in the U.S. in 1997 was 23.6 million tons [36]

Source of NO _x from Non-Road Sources	All Non-Road Other than Waterborne	River	Coastal and Great Lakes
Contribution Percentage (Total = 19.3%)	18	0.6	0.8

Table 5.5 – NO_x source distribution from Non-Road sources; waterborne production of NO_x in 1997 was 1.4% of total production from all sources [36]

The minor contribution of waterborne transit can vary from region to region, but still accounts for only 2% of the total inventory in the San Francisco Bay Area Basin which claims to be one of the most affected regions from shipping exhaust emissions [36]. Furthermore, marine vessel particulate matter emissions have been found to make up about the same percentage (1-2%) of the total U.S. PM emissions [47]. These quantities are minimal in comparison to the overall U.S. emissions scheme, and only are critical to certain local regions where they become concentrated. However, any emission reduction opportunity, however minimal the source, should be employed when available and

practical. Taking into account the rest of the world, which has far lower energy consumption per person than the U.S., shipping accounts for a substantial 14% of nitrogen emissions and 5% of sulfur emissions [48]. Though shipping is relatively clean and efficient, these world emission numbers are significant, and practical means should continue to be researched and employed to reduce these harmful exhaust emissions. The best emission characteristic of international shipping is CO₂ generation. CO₂ is a natural by-product of complete fuel combustion. Shipping contributes to only 2% of all CO₂ which comes from fossil fuels, being a natural leader in fuel economy dictates their CO₂ per ton-mile is minimal.

The overall low contribution shown above arises from waterborne transport being the clear leader in per ton-mile emissions. However, great improvements in emissions have been made in other transportation modes while the maritime sector has lagged behind. Below is a quote from the Secretary of Transportation, Norman Y. Mineta, taken from a 2002 workshop on maritime energy and clean emissions:

“Almost a half century ago, the United States determined that toxic air emissions from trucks and automobiles were a serious problem in many of the major cities around the country. In a cooperative venture with auto and truck manufacturers, air pollution reductions of 95 percent have been achieved over the last three decades, while we increased energy efficiency by 37 percent. Similar initiatives were launched in the operation of the nation’s railroads with similar positive results. Now the spotlight is on all of us in the maritime sector. Annually, ferries in the United States carry more than 134 million passengers, and ships move more than 95 percent of our overseas trade through our ports. Overall, the United States has 25,000 miles of navigable waterways. And while seagoing vessels account for only 5 percent of all transportation-related air pollution, the marine sector, relative to other modes of transportation, has not kept pace in reducing harmful air emissions.” [44]

As the Secretary of Transportation stated above, shipping produces the least amount of emissions when compared to rail or trucking. Various pollutant outputs for moving one ton of cargo 1,000 miles by utilizing trucking, rail, and tow boat are shown in Figure 5.1.

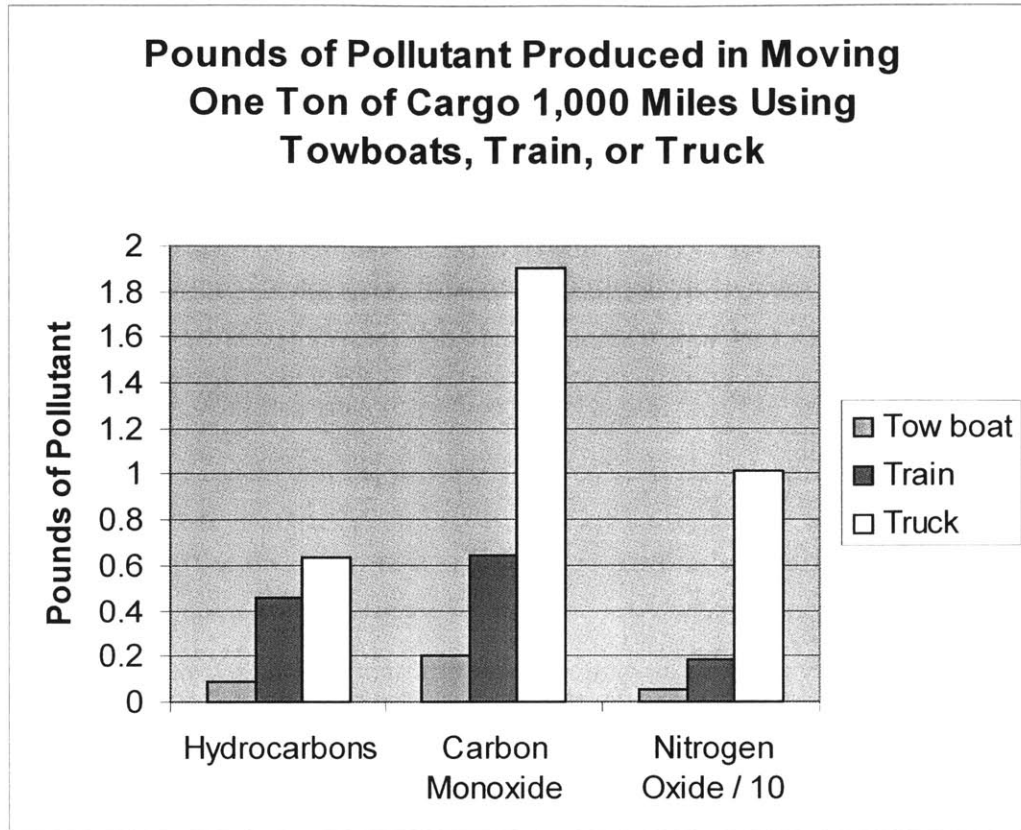


Figure 5.1 – Exhaust emissions comparison for various modes of transport: Tow boat dominates trucking by a factor of 5 in Hydrocarbons, 10 in Carbon Monoxide, and 20 in Nitrogen Oxide; note the values for Nitrogen Oxide have been multiplied by a factor of 0.1 as indicated to scale the graph [49]

Waterborne commerce has been and will continue to be the cleanest form of transportation. However, marine engines have not kept pace with other industries in regards to percentage of emission reductions over the last decades. In fact the percent contribution of pollutants from the largest of marine engines, when compared to all mobile sources, is expected to triple for NO_x and double for PM by the year 2020 [50]. The industry did get a late start from the misconception the harm was all being done in the middle of the ocean. However, marine engine manufacturers also have had difficulty applying known technologies. This stems from the wide range of applications marine vessels employ, thus limiting the number of engines produced for any one engine size far below the number of engines produced for cars, trucks, and locomotives. Therefore, the economics of creating an ultra clean engine for each marine size, as are employed in cars and locomotives of today, is prohibitive to the manufacturer. In reducing exhaust

emissions, shipping has the additional hurdle of overcoming the residual fuels (HFO, bunker oil) used in virtually all large marine vessels. This residual fuel is what remains after the higher grade fuels such as gasoline, diesel, and kerosene are produced. These dirty fuels are inexpensive and have few other applications; the level of paraffins is so high that this fuel is actually solid at room temperature, requiring heat to be pumped. Additionally, the residual fuels contain high levels of toxins such as sulfur and nitrogen, which result in higher emissions of particulate matter and sulfur oxide than cleaner fuels such as diesel oil or gasoline would emit. These are only a few factors that put large ships at a relative disadvantage for reducing emissions when compared to other modes of freight transport. The harsh sea-going environment and severe space constraints are other elements that act as barriers to reducing marine exhaust emissions.

The overall picture of the maritime contribution to exhaust emission inventories has been discussed, but the origin of emissions from within the industry must also be understood before deciding how to formulate emission reduction policies. In the United States, the largest segment of commercial marine NO_x emissions, almost half, comes from small vessels with engines approximately twice the size of a heavy diesel truck. Vessels with a medium size engine, approximately the size of a locomotive engine, and vessels with the largest class engine, which are used almost exclusively on ocean-going ships, both split the remaining percentage of NO_x [47]. Table 5.6 relates year 2000 U.S. commercial marine NO_x emission percentages to engine size and to vessel flag. The table breaks down diesel engine size the same way the Environmental Protection Agency (EPA) utilizes to separate emission regulations: Category 1 (C1) includes engines with less than 5 liters per-cylinder displacement and more than 37 kW power, Category 2 (C2) includes engines between 5 and 30 liters per-cylinder displacement, and Category 3 (C3) includes all engines greater than 30 liters per-cylinder displacement.

Engine Class	Category 1 (C1)	Category 2 (C2)	Category 3 (C3)
NO_x Contribution Percentage by Flag	44 U.S. 1 Foreign Flag	25 U.S. 2 Foreign Flag	24 U.S. 24 Foreign Flag
Total NO_x Contribution Percentage	45	27	28

Table 5.6 – 2000 commercial marine NO_x contribution by engine class and flag [47]

For obvious reasons, foreign flag vessels contribute little to no U.S. NO_x emissions in the small and medium size engine category as the majority of these engines are used on tugboats, fishing vessels, and other commercial vessels in and around U.S. ports. These engines are also often employed as electrical generators on large ships. Unlike the small foreign percentage of NO_x emission contributions from Category 1 and Category 2 engines, however, foreign flagged ships and U.S. flagged ships split the percentage of NO_x emissions from large ships. Though the total NO_x contribution is split by flag for Category 3 engines, within 25 nautical miles of port only about 6% of the NO_x is from U.S. flagged vessels. However, U.S. ships contribute near 80% of the total when in the range of 25-175 nautical miles. When vessels are emitting pollutants in the most harmful area, near ports, it is the foreign flag vessels that dominate contribution.

From Table 5.6 and the data above, it can be discerned where regulations can be implemented effectively. U.S. regulations affecting small and medium size engines are, for example, fairly easy to implement and will be more effective as compared to large engines. Regulations affecting the largest engine category are tough and costly to regulate as they will only apply when in U.S. waters and ports; additionally, the EPA is uncertain what amount of regulation of foreign ships is legal under international trade rules [50]. It is clear that regulations affecting just U.S. vessels with Category 3 engines will have a weakened impact and only act to further hinder the U.S. fleet. Before the regulations and the technology that leads them are discussed in greater detail, further insight into the differences of the marine engine classes will be revealed.

Marine Engines

The marine engine operates in one of the most difficult environments possible. Surrounded by corrosive seawater, the engine must be capable of performing when the vessel is in bad weather, sometimes rolling up to 45 degrees or more from the vertical. And unlike a car, a marine engine is the only means a vessel has to stop its motion, thus necessitating full load operation instantly upon demand. Smaller vessels must endure pounding by the ocean waves that will jolt and vibrate everything aboard, including the engines and their associated electronics. Large ships crossing the ocean have been reduced to skeleton crews, who can not perform all of the repairs and maintenance required, thus leading to a slow degradation of the engine and associated components, particularly those components not immediately required to deliver the cargo on time. The equipment neglected most often is generally safety or pollution control equipment, as it does not have immediate repercussions.

Recreational craft have traditionally employed highly polluting 2-stroke gasoline engines, to keep the motor size as small and inexpensive as possible. Manufacturers have recently introduced many 4-stroke varieties to improve the combustion process; however, these engines lack the exhaust after treatment devices found on cars because of limited space. Therefore, an LIF application to these engines would be ideal as it would reduce harmful exhaust emissions and would require no additional space.

Larger pleasure craft, fishing vessels, small commercial vessels, and tug boats employ primarily 4-stroke diesel engines for propulsion and electrical generation. These engines range from a size similar to truck engines up to locomotive engines and fit into both Category 1 and Category 2 of the EPA's regulations. A high proportion of vessels operating on inland waterways are equipped with propulsion engines of this size. These engines have a trunk piston design, similar to an automotive engine; however, the availability of oil in the cylinder is more prevalent as these engines, unlike automotive engines, are required to operate at a wide range of angles and pitches. The additional presence of oil makes LIF technology to control oil transport even more applicable. The LIF strategy and techniques utilized on the marine engines of these sizes would be quite

similar to those in the automotive counterpart as the speeds and loads experienced are of the same magnitude. The largest class of vessel employs these engines only for electrical generation.

For the largest of vessels, those employing Category 3 engines as main propulsion, the sheer size dictates a different engine strategy. Unlike the Category 1 and 2 engines above, there are relatively few of these engines produced each year, with the main applications in marine propulsion and stationary power generation. The Category 3 grouping is further split into medium and slow speed engines; these two groups are compared in Table 5.7. The medium speed propulsion engine, employed on approximately 40% of all Category 3 vessels, is 4-stroke and similar in design to the Category 2 engines [50]. However, the larger parts and slower speeds dictate different controlling forces for lubricating oil transport, thus a modified LIF strategy would need to be employed as the differences from the scale of automotive engines are just too great.

Engine Type	Fuel Type	Size (Liters/Cyl)	Rated Speed (rpm)	Stroke/Bore Ratio	Number of Cylinders	Power Range (Total kW)
Slow Speed 2-Stroke	Residual	57-2006	54-250	2.38-4.17	4-14	1,100-103,000
Medium Speed 4-Stroke	Residual, Distillate	30-290	327-750	1.15-1.71	5-20	1,000-18,100

Table 5.7 – General characteristics of Category 3 marine diesel engines [50]

The other 60% of Category 3 vessels utilize the 2-stroke slow speed engine [50]. Because of the incredible size of these engines, which are substantially larger than the medium speed variant, the trunk piston design cannot be employed. A crosshead design is used, where the piston and cylinder are separated from the crankcase by a stuffing box. Therefore little to no crankcase oil is consumed, and the lifetime of the crankcase oil is often 25 years or more. However, the piston still needs lubrication and thus high grade

cylinder lube oil is intentionally inserted and is expected to be burnt. This oil is quite expensive, and thus the LIF strategy here is to make the smallest amount of oil do the most good. For this engine, lube oil consumption is not of primary concern for environmental reasons, but rather for economic reasons to the ship operator as cylinder lube oil is the greatest operational cost besides fuel. These slow speed engines are designed for maximum durability and fuel efficiency, to maintain the lowest operating costs possible [50].

Further detail must be given on these slow speed engines, as they are quite unique in the engine world. Unlike the medium speed engine that uses reduction gears or an electric drive propulsion system, the slow speed engine is typically directly coupled to the propeller shaft and operates around 100 rpm. The pistons, rings, liners, and cylinder lube oil operate in the most extreme of conditions, where individual cylinders produce up to 5500 kW, maximum cylinder pressures peak around 150 bar, and a standard piston speed is 8.5 m/s. Additionally, these engines use the dirty residual fuels mentioned earlier and are expected to operate for 12,000 hours (approximately 2 years of ship service) between overhauls with a liner diameter wear of only 0.1mm/1000 hours, all while using as little cylinder lubricant as possible. To further illustrate the lubrication requirements, imagine a Sulzer RTA84T cylinder (3.15 meter stroke) lubricated with less than a gram of cylinder lube oil per revolution spread over a running surface of 8.3 m³ [51].

The cylinder lube oil is inserted into the liner through a number of lubricating orifices (quills), which include non-return valves. The oil is inserted when the piston rings pass the quills on the upward stroke. Traditionally the flow was speed dependent, where a set amount of oil was fed to the cylinder each engine revolution. This method has cylinder lube oil consumption rates from 0.8-1.2 g/kWh. In a constant effort to reduce the high costs of cylinder lube oil consumption, the manufacturers created an electronic means to have computer controlled lube oil injection. The computer can be set to increase dosage during load transients or adjust the flow rate and timing depending on running characteristics such as fuel quality, which is very important when utilizing high sulfur fuels. With computer controlled injection, cylinder lube oil consumption rates are 0.7-1.1

g/kWh [52]. This small reduction, 0.1 g/kWh, is still quite substantial, with manufacturers claiming the computerized injection can save up to \$340,000 per year in lube oil consumption and reduced wear [53].

As stated earlier, these engines have few practical applications, and thus very few of them are produced each year; there exist only a few companies world wide who manufacturer such engines. In this fairly concentrated market, just four companies produce nearly 75% of medium speed engines and 100% of slow speed engines. These four companies (MAN B&W Diesel, Wartsila/New Sulzer, Caterpillar/MaK, and Mitsubishi) dominate an industry that produced approximately 500 medium speed engines and 750 slow speed engines in 1998 [50]. The relatively low number of engines produced by a handful of companies prevents a large amount of money being spent on research and pollution reduction techniques. Unlike automotive engines, which are mass-produced, ship engines are often heavily tailored for the individual ship class to which they are installed. Additionally, they are often required to have the ability to operate on several types of fuels and fuel qualities. These variables make developing and employing emission reduction equipment difficult and costly. A common way to reduce pollution in cars, which is also being researched for marine engines, is to install an exhaust after treatment device to 'clean' the exhaust emissions. While quite effective in set environments, the range of marine fuels and ships makes these devices very expensive to develop and employ. Developing LIF technology for each major marine engine size, however, would benefit the industry as a whole while providing a fixed, maintenance free way to reduce lube oil consumption and the associated pollutants. Before further detail is provided on exhaust treatment options, the regulations guiding them and the various pollutants in question will be addressed.

Pollutants

Diesel engines are the most efficient use of fossil fuels for mobile sources. They have a high power density, and their reliability is impressive. Many believe other power sources such as fuel cells will replace the internal combustion engine, but with approximately one billion engines in service throughout the world, it won't be for a long time. Additionally,

technology is continually creating a cleaner and more efficient diesel engine, making it harder and harder to find an adequate replacement through renewable sources. As an example of a modern diesel engine pollutant output, the flow through a slow speed diesel engine is shown in Figure 5.2 and includes the exhaust gas constituents.

Slow speed, two stroke diesel engines operate with an excess air ratio of more than 3 to 1. The majority of the air is available for combustion, with the remaining percentage utilized as scavenge air. It is this excess air that makes the free N_2 and O_2 the major constituents of the air intake and exhaust emissions. The carbon dioxide and water vapor portion of the exhaust gas are the natural products of hydrocarbon combustion. Carbon dioxide is not toxic, but has been given recent attention from concern of the 'greenhouse effect'. High fuel efficiency engines, which the marine field dominates all others, are the only viable means to limit carbon dioxide production.

Nitrogen Oxides (NO_x) are formed during the combustion of the fuel, with the combustion temperature and oxygen availability as the driving factors. The high temperatures allow the normally inactive nitrogen to react with oxygen to form oxides of nitrogen. To illustrate the importance of temperature, it can be approximated that every $100^\circ C$ rise in combustion temperature increases the NO_x production by a factor of 3. This presents a dilemma, however, as marine engine manufacturers increase the fuel efficiency of their engines there is a resulting increase in the peak combustion temperature. A compromise must be made between fuel efficiency and NO_x production by limiting the peak combustion temperatures through modified injection timing or the addition of water into the combustion process. Extensive research is being done to develop a practical and affordable after treatment device to clean nitrogen oxides from marine exhaust. NO_x in the atmosphere contributes to the formation of smog in the presence of heat and sunlight, causing many respiratory problems in urban areas. In addition, some of the NO_x is washed out of the air and acts to increase the acidity of the soil, thus harming vegetation. NO_x control is advocated by environmentalists and legislators and is the current number one emission control issue [54].

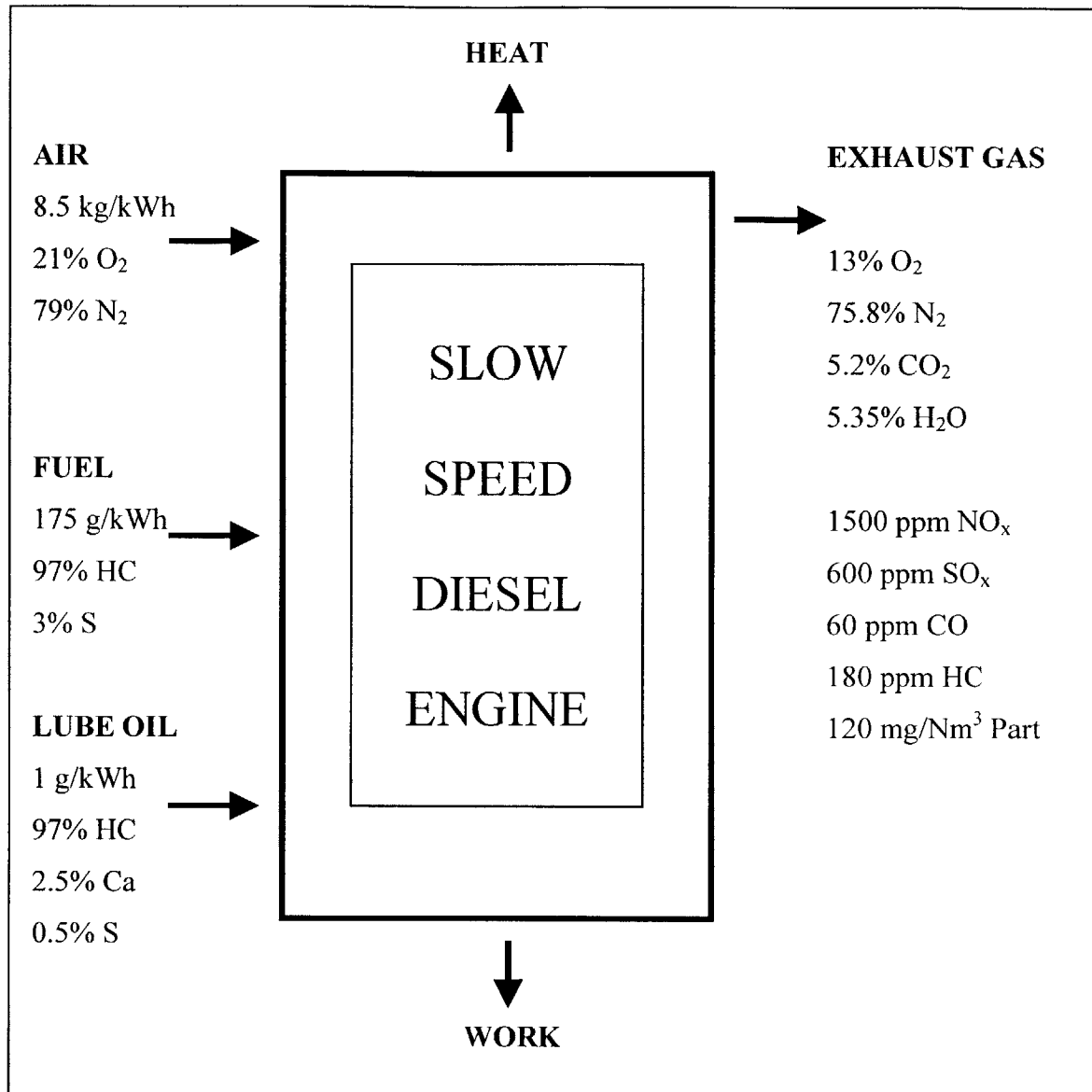


Figure 5.2 – Flow diagram for a slow speed diesel engine commonly employed on ocean-going ships [54]

Sulfur Oxides (SO_x) are a product of combustion originating solely from the type of fuel burnt. As fuel oil is organic in nature, it contains various amounts of sulfur. The main way to reduce this pollutant is to buy fuel with low sulfur content, but the price of such fuels is higher. SO_x can also be cleaned from the exhaust gases through the use of a scrubber, but the resulting sulphuric acid creates a disposal problem difficult in the marine environment. SO_x in the atmosphere will be washed out and contribute to acid rain, similar to NO_x. Sulphur oxides are the major source of acid rain, having detrimental effects on plant life, respiration, and buildings [55].

Carbon monoxide (CO) is a toxic gas formed from incomplete combustion. Formation of carbon monoxide is heavily influenced by the uniformity of the air/fuel mixture and the amount of excess air. Diesel engines produce much less CO than gasoline engines as diesels operate with an excess air ratio above one.

Hydrocarbons (HC) will sometimes escape the combustion process and leave the engine unburned, and others will sometimes be formed in the exhaust stream. The fuel and lube oil are both sources of hydrocarbons in the exhaust gases. Hydrocarbons are classified as volatile organic compounds (VOC); these compounds combine with NO_x to form smog.

Particulate matter (PM) is the next greatest pollutant of concern for diesel engines after NO_x . Particulate emissions in the exhaust gas originate from various sources: Agglomeration of very small particles of partly burned fuel, partly burned lube oil, ash content of fuel and lube oil, sulphates, and sulphate-bound water [54]. In medium and high speed engines, the lube oil is 15-20% additives, which can add to the particulate problem when lube oil is burnt or partially burnt. One of the lube oil contributions is calcium compounds, as calcium is the main carrier of alkalinity in lube oil to neutralize sulphuric acid. Particulate matter can be characterized as discrete particles that exist in the condensed, liquid or solid, phase spanning several orders of magnitude in size [50]. The particles emitted from a diesel engine are generally small, with most being under 1 μm when heavy fuel oil is used [54]. The small size allows the particulates to be readily transported by air currents and have a low settling velocity. Therefore, detrimental effects may be encountered in regions away from the vicinity of the exhaust gas plume [55]. Particulates are considered carcinogenic and can cause respiratory problems and are receiving more and more attention. The mechanisms by which particles harm the human body are not well understood, but there is general agreement that the cardio-respiratory system is the most affected [50]. Secondary effects of particulate matter are associated with impairment of visibility over urban areas and even some entire regions. Particulates are also harmful to the ship, as they may deposit in the exhaust gas boiler, thereby increasing back pressure and representing a boiler fire hazard. Quantification of particulate emissions is difficult on account of their diverse nature and sources. A variety

of terminology and sampling methods have been devised, but different techniques yield quite different results. Wartsila/New Sulzer, an extensive marine engine manufacturer, stated in a 1998 publication, “Independent of the existing confusion, it has to be stated that reduction of the particulate emissions of diesel engines may represent the greatest challenge for the future development of diesel engines” [55]. Utilizing LIF technology to control lube oil transport would create a fixed way to reduce particulate emissions from marine diesel engines, by lowering the contribution from lube oil consumption.

To illustrate the scope of marine engine pollutants with time and geography, emission inventories from Category 3 engines in the U.S. will be overviewed. Within a radius of 25 nautical miles of ports in 1996, Category 3 engines contributed on average, 100 tons of NO_x and 10 tons of PM. In the concentric donut ranging from the 25 mile radius to a radius of 175 miles, the same amount, approximately 100 tons of NO_x and 10 tons of PM were contributed. Clearly the pollution is greatest where it is the most damaging, near the areas of population. Without implementation of stricter regulations, the yearly contribution of these pollutants will double by the year 2020, and triple by the year 2030. And even if further regulations are enacted, the ships being built today will still be active in 2030, heavily delaying the effects of any regulations by the lifespan of vessels. [50]

5.2 Regulations

Maritime exhaust emission has been the focus of many regulatory bodies in the past few years as pollution improvement in this segment has lagged far behind other industries such as trucking and power generation. The two main hurdles for implementing regulations are the truly international aspect of the industry and the great variety of fuels, engines, and ships that traverse the oceans. Implementation must be paced with technology and be easily monitored so as to be effective without hindering the industry. The next few sections detail the main regulations in effect, or soon to be in effect. It is important to understand the regulatory expectations for shipping exhaust emissions, because regulations drive pollution technology just as much as technology dictates the pace of regulations.

Three main bodies have legislation restricting marine vessel emissions: MARPOL Annex VI, EU Directive 1999/32, and the EPA U.S. Clean Air Act. These regulations vary in which pollutants are monitored and how much of each is permitted in the exhaust stream, thereby making compliance more complicated as a ship may be required to follow one or more depending on its area of operation. The EPA regulations are intended to reduce emissions of NO_x, total hydrocarbons, carbon monoxide, and particulate matter; whereas, MARPOL rules are more focused on NO_x and SO_x emissions. The EU Directive largely involves SO_x production by setting maximum sulfur limits in the fuel oil. The specific demands of each regulating body will now be discussed in more detail.

EU Directive 1999/32

The EU Directive has strict regulations on SO_x emissions. Sulfur is a major component in the HFO burned by most large vessels, mainly because it is a low-grade fuel. Throughout the EU, all regular passenger vessels will be required in 2007 to use fuel containing less than 1.5% sulfur. Similarly, all ships operating in the North Sea and Baltic Sea will also be required to comply with this limit, as these are environmentally sensitive regions. Currently, all ships in EU ports must use fuel containing less than 0.2% sulfur, with that limit likely to be reduced to 0.1% by 2008 [56]. The time span is provided because the ability of the refineries to produce the required amounts of these compliant fuels must be increased. Presently, the world average sulfur content for residual fuels is about 3.0%, peaking at up to 7.0%. U.S. non-road distillate for construction vehicles and such ranges from 0.2% to 0.3%, with a U.S. on-road trucking requirement set at 0.015% for 2007 [57]. This sulfur discrepancy is one factor that puts shipping at a relative disadvantage when trying to clean up exhaust emissions, as they are operating with a fuel containing 200 times the sulfur content.

EPA U.S. Clean Air Act

Recent adoptions to the U.S. Clean Air Act of 1990 have involved marine vessels. Many of the regulations are similar to the ones in MARPOL Annex VI, but the EPA has accelerated the timeline of implementation. The EPA rules are divided into three categories, as described previously: Category 1 includes engines with less than 5 liters

per-cylinder displacement and more than 37 kW power, Category 2 includes engines between 5 and 30 liters per-cylinder displacement, and Category 3 includes all engines greater than 30 liters per-cylinder displacement. The first set of standards to apply to these engines is labeled Tier 1, and was adopted in 1999.

Tier 1 standards apply to marine diesel engines manufactured January 1st, 2004 or later if they will be installed on vessels flagged or registered in the United States which operate between two U.S. ports or spend 25% their time within 200 nautical miles of the United States. These regulations are also applicable to older land or marine engines if they are installed on a new vessel. The Tier 1 standards focus on NO_x emissions, and are identical to the MARPOL Annex VI limits. Originally these standards were only a voluntary compliance regulation until the more stringent Tier 2 standards were to come into effect in 2007, but since engine manufacturers are already producing engines that are certified under the international MARPOL standards, the Tier 1 standards are now mandatory for all three categories of engines. In Figure 5.3 is a graph of the allowable NO_x production based on engine speed as per the Tier 1 regulations.

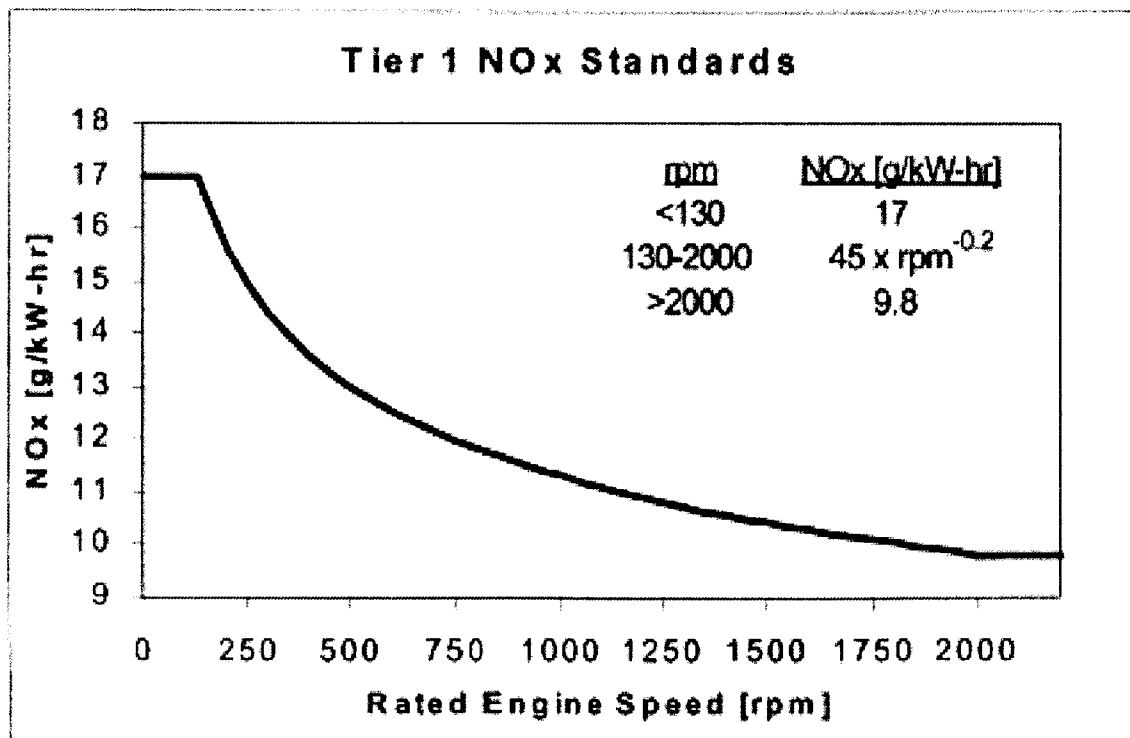


Figure 5.3 – EPA Tier 1 NO_x standards; they are identical to the MARPOL Annex VI requirements.

The Tier 1 standards will continue to apply to all three categories of engines until 2007 when Category 1 and Category 2 will come under the more stringent Tier 2 regulations. Tier 2 standards reduce the amount of NO_x permitted and also include limits for particulate matter, carbon monoxide, and hydrocarbon emissions. Implementation of LIF technology would assist these Category 1 and 2 engines in meeting the HC and PM regulations without requiring expensive and bulky after treatment devices. Category 3 engines will remain under Tier 1 regulations indefinitely, as the EPA researches the best feasible course of action for these large and more international engines [58]. Below is a segment of a 2003 announcement from the EPA about their course of action for Category 3 engines:

“The final rule commits us to adopt technology-forcing Tier 2 standards for Category 3 marine diesel engines by April 2007. We will consider the availability of advanced technologies such as those used in other diesel engine applications as well as water emulsification and selective catalytic reduction. Engine manufacturers are already developing ways to apply these technologies to marine diesel engines. While there is a certain amount of information available about these advanced technologies now, there are several outstanding technical issues concerning their widespread commercial use, including the impacts of fuel sulfur on emissions, emissions at low engine loads, and particulate matter emissions. Adopting the standards at a later date will allow us to obtain important information on the use of these advanced technologies that we expect to become available over the next few years. This will allow us to pursue further negotiations in the international arena to achieve more stringent global emissions standards for marine diesel engines.

We will also consider whether we have the discretion under the Clean Air Act to apply any second tier of standards to engines on foreign vessels that enter U.S. ports. Most ocean-going vessels that come to the U.S. are flagged in other countries and are subject to the international standards [of MARPOL]. The U.S. will be participating in discussions under the International Maritime Organization to advocate a new set of more stringent emission standards for marine diesel engines that would apply to engines on both U.S. and foreign vessels. These discussions are expected to begin in the next few years. The schedule for our future rulemaking will allow us to take into account progress in the international arena toward more stringent emission standards for marine diesel engines.” [58]

The EPA is aware of the difficulty monitoring and enforcing emission laws on Category 3 engines, where the majority of vessels are foreign flagged. To avoid putting U.S. flagged ships at a severe disadvantage, the EPA is hoping to increase the emissions reductions called for through the international standards on these large engines. This would also vastly reduce the costs associated with Coast Guard monitoring of rules applicable only in the U.S. for foreign flag vessels. The U.S. Maritime Administration

(MARAD) is a strong proponent for international environmental standards, as their annual report to congress for 2001 suggests:

“Because of the international nature of maritime affairs, much of the focus on standards is in the international arena. Facing some of the most stringent requirements in the world, the domestic industry welcomes and actively fosters this approach. Such an approach will help to ‘level the playing field’, thereby improving U.S. industry’s international competitiveness.” [42]

The EPA knows, however, the stricter Tier 2 rules for Category 1 and Category 2 engines will be enforceable and effective. The emissions standards will also be quite achievable by the 2007 timeline. Without hampering the industry with exorbitant emissions reduction costs, the EPA is lowering pollutant output at a reasonable pace for all involved. In the future, a Tier 3 for Category 1 and Category 2 engines will be adopted; the EPA is waiting to see the evolution, effect, and cost of current and future emission reduction technologies before setting these standards.

Compliance with the Tier structure will mirror the provisions of MARPOL Annex VI until the Tier 2 standards come into effect. The MARPOL regulations stipulate the engine manufacturer will test emissions compliance on the test bed and re-tests may be required after overhauls; as long as the ship engine operates according to the manufacturer and only uses parts exactly as specified by the engine drawings, the engine will always be considered in compliance. The EPA, however, desires to ensure the engine is producing only emissions claimed by the manufacturer during actual in-use conditions. This involves the manufacturer demonstrating the emission controls will be durable for the full useful life of the engine, based on the scheduled rebuild time; for example, the useful life specified for some Category 3 engines is three years, at which time the engine is generally rebuilt for the first time. These procedures involve possible monthly on-ship testing and monitoring. The procedures are not currently required, allowing manufacturers time to incorporate these changes in their testing and certification procedures [58].

MARPOL Annex VI

MARPOL Annex VI was set forth in 1997, and applies to engines installed on vessels constructed after January 1st, 2000. However, Annex VI is not yet in effect, which is why the EPA and the EU created their own regulations to increase the timeline of implementation. The MARPOL Annex VI limits will go into international force twelve months after 15 countries representing at least 50% of the gross tonnage of the world's merchant shipping fleet have ratified the Annex. Though not yet in effect, it may be enforceable back to engines newly installed or converted after January 1st, 2000. The International Maritime Organization (IMO), which in September of 1997 adopted the new protocol to MARPOL (International Convention for the Prevention of Pollution from Ships) has recently commented on the ratification process. "To date it is not clear why more States have not ratified MARPOL Annex VI. However, following the indications made at Marine Environmental Protection Committee 48 [of IMO] in October 2002, by several countries close to completing the ratification process, the Annex should enter force early to mid 2004 [59]." The goal of MARPOL is to reduce pollution from all aspects of marine vessel operation. To achieve this goal, the Treaty and its previous Annexes also contain requirements to control the accidental and deliberate discharge of substances such as oil, chemicals, and garbage.

MARPOL Annex VI specifies that any diesel engine over 130 kW that is installed on a vessel constructed, or one that undergoes a major conversion, after January 1st, 2000 must comply with Annex VI NO_x limits. These NO_x requirements are intended to apply for all vessels in a country's fleet; however, a country has the option of setting alternative NO_x control measures for engines on vessels that are not operated internationally [59]. Annex VI also set standards on shipboard incineration, general fuel oil quality, volatile organic compounds (VOC's), and sulfur oxides (SO_x) through limiting the sulfur content of fuel. The Annex VI NO_x limits are identical to those for Tier 1 engines specified by the EPA. Additionally, the Annex limits maximum fuel sulfur content to 4.5%, with specific SO_x Emission Control Areas such as the Baltic and North Seas where the maximum sulfur content is 1.5%. There also exist some minor requirements regarding

fuel oil quality and shipboard incineration, such as allowing incineration of sewage sludge and sludge oil only when outside of port areas [57].

As stated earlier, compliance is mainly done when the engine is on the test bed before installation into the vessel. Annex VI survey requirements apply to vessels larger than 400 gross tons. A ‘Pre-Certification Survey’ is performed while the engine is on the test bed, where actual NO_x output is measured for running conditions expected on the vessel. Next comes the ‘Initial Certification Survey’; this survey comes after the engine is installed onboard the ship, but before the ship is placed into service. ‘Periodic and Intermediate Surveys’ occur about every five years and are designed to confirm nothing has been done to the ship’s equipment which would take it out of compliance. A ‘Modification Survey’ exists for cases where a major conversion was performed. In most surveys other than the ‘Pre-Certification’ and ‘Modification’, the inspecting body will come aboard and simply ensure the engine is utilizing only manufacturer specified parts and operating settings, the actual NO_x levels will not be measured. This is especially critical as most NO_x reduction techniques reduce fuel efficiency, and thus altering engine settings could be done to save fuel.

Regulation Overview

The international nature of shipping and the marine equipment supply infrastructure lends itself to harmonious regulations. Wartsila/New Sulzer stated the following comment about regulations in an emission technology publication: “A proliferation of national or regional regulations based on different standards would be highly disruptive and costly to the marine industry and would create needless barriers to international trade [55].” Regulations affecting strictly national craft, such as Category 1 and 2 engines, will be highly effective and manageable. This is in large part due to the greater number of engines produced, and their similarity in scale to truck engines that makes applying known technologies easier. These engine manufacturers will need to continue to find new ways to reduce exhaust emissions as the regulations become more stringent and focus on different pollutants. LIF technology could assist these engines as they prepare for the next regulatory Tier. Large marine engine manufacturers have also been successful at applying known emission reduction technologies to their engines with high

effectiveness; however, the costs in maintenance and size of these devices have greatly restricted their implementation. Permanent means to reduce exhaust emissions, which requires little to no maintenance, would be the ideal solution for these Category 3 engines. LIF technology would fit this ideal, with the added benefit of reducing the high costs associated with lube oil consumption. The next section will review some current research endeavors to reduce marine exhaust emissions as per regulatory bodies, and prove the practicality and simplicity benefits of LIF technology.

5.3 Exhaust Emission Reduction Techniques

A great proportion of today's engine research dollars are being spent on pollution reduction. The legal atmosphere and general concern for the health of the Earth has forced the world onto a never ending quest to continually improve our power generation means. Factories and power plants, extensive point sources of pollution, were the first to face scrutiny as the residents continually witnessed the effects. Next, car and truck engines were improved as congested urban areas became filled with smog. The marine industry is relatively new to the spotlight, and is unique in its fuel variability, low production number, and space constraints. These challenges are proving difficult for engineers to develop practical and efficient means to reduce marine exhaust emissions. Most of the techniques currently under consideration are bulky, expensive, and require substantial amounts of maintenance. It is hard to imagine a ship owner who wants to sacrifice cargo space for a costly exhaust treatment device. And even assuming they are required by law and placed on ships, such delicate, maintenance intensive technology does not bode well with the overworked marine engineer. The few marine engineers aboard the vessel are tasked with operating the ship and maintaining all equipment, which leaves little time to fiddle with a complicated emission reduction device thus resulting in greatly reduced effectiveness of the device. Technology such as LIF, which is built into the engine by design of the piston ring pack, would continually act to reduce lube oil consumption to the benefit of the environment and cost savings, and would require no additional work for the engine operator. A modest initial investment by the marine

engine manufacturer into LIF, for each engine scale, would act to benefit every engine produced.

Primary and Secondary Measures

To reduce exhaust emissions from engines, both primary and secondary means may be employed. Primary measures focus on decreasing the production of the pollutant during the combustion process, whereas secondary measures, or after treatment techniques, work to reduce the level of pollutant from the exhaust stream itself. Marine engine variability and size constraints make complex and bulky after treatment techniques very unattractive. For these reasons, Wartsila/New Sulzer states in an emission technology publication, “Primary reduction techniques are the first choice to reduce the formation of pollutants on board ships [55]”. However, primary countermeasures to reduce exhaust emissions may be inadequate for reaching levels required by legislation. It is then necessary to apply treatment with secondary measures to the exhaust gases after they have left the engine cylinders. The devices which are leading the research for each pollutant are: Oxidizing catalysts for hydrocarbons and carbon monoxide and reducing catalysts for NO_x, thermal reactors for hydrocarbons and carbon monoxide, and traps or filters for particulate matter.

Unlike spark ignition automobile engines that operate stoichiometrically, diesel engines always operate lean as their load is controlled only by the amount of fuel injected. Diesel exhaust, therefore, contains a large percentage of oxygen and is a relatively low temperature, approximately 350°C, from the dilution by unused gases. The high oxygen content and low temperatures make employing the very effective three-way catalyst, similar to a catalytic converter found in virtually every automobile, not possible. For this reason and the general nature of marine engines, relatively undeveloped emission reduction technologies must be sought and honed exclusively for the marine industry. Currently, engine manufacturers have developed extremely effective after treatment devices, but they have yet to find a way to simplify them, to incorporate the industry’s range of fuels, and to reduce the high costs.

The main problem with maintenance intensive and complex exhaust treatment devices can easily be seen by examining current ship operations. The oily water separator is a required piece of machinery onboard large vessels, as waste water pumped to sea must contain less than 15 ppm of oil. The oily water separator's main task is to clean the ship's bilge water, by removing the oil content to a sludge tank. These machines rarely operate as intended, and are a source of constant problems for the marine engineers aboard. Generally over tasked, the marine engineer's priority is to maintain and operate the propulsion engine and other vital equipment. If two jobs need to be performed, the one that is required to get the ship to port on time will be completed, and the other, maintenance on the oily water separator for example, has to wait. Marine engineers are responsible for a plethora of equipment, and often one has to spend day upon day working to get the finicky oily water separator functioning properly. If exhaust after-treatment devices are installed on vessels before they are highly refined, they will become like the oily water separator. By never quite operating as intended, and with the devices begging to be neglected, as they are not the main priority of the engineer, it will lead to a greatly reduced effectiveness. Some of the reduction techniques currently being researched and tested will be discussed next; revealing the complexity and scope of these devices will further bolster the simplistic benefits of LIF as a primary reduction method.

NO_x Reduction Techniques

Nitrogen Oxides (NO_x) is currently the most prominent pollutant of concern for marine diesel engines. NO_x is formed during the combustion of the fuel, with the combustion temperature and oxygen availability as the driving factors. The high temperatures allow the normally inactive nitrogen to react with oxygen to form oxides of nitrogen. The initial strategy for reduction of NO_x, therefore, was to limit peak temperatures within the cylinder. This is an effective strategy, however, decreasing peak temperatures adversely effects fuel efficiency and particulate emissions. A balance among the parameters is found, but other techniques needed to be found to further lower NO_x. Another means to lower peak temperatures without engine tuning was sought out. A method of direct water injection, timed to enter the cylinder near peak temperatures, limits the temperature rise of combustion without adversely affecting cylinder pressures. This technique has been

shown to reduce NO_x emissions by up to 50%, but requires advanced injection equipment and a pure water supply. Direct water injection costs the ship owner approximately \$200,000 for installation and operation, discounted at 7% [50]. However, additional shipboard complication and maintenance of the injection and water generation system, coupled with the slight decrease in fuel efficiency and knowledge that this is still a relatively untested technology, have still prevented its implementation. Similar to direct water injection is another method of using water to cool the peak temperatures, water emulsified into the fuel oil. By injecting this water fuel mixture, reductions of NO_x of up to 70% are gained. Many problems with maintaining the proper mixture have been encountered, as well as damage to the resized injection equipment from the poor lubricating properties of the water-fuel mixture. Additionally, the lower peak temperatures would create an environment that reduces PM oxidation, thereby increasing particulate matter in the exhaust stream. The extent of such an increase is not well known, however, as the technology has not been extensively tested [50].

The most prominent of all NO_x reduction techniques being researched is selective catalytic reduction (SCR). Theoretical work on SCR dates back to the 1960's, with the first commercial application in the 1970's. Legislation in the 1980's made all parties involved in the diesel engine industry begin to further investigate SCR. In SCR systems, a reducing agent, most likely urea, is injected into the exhaust stream. The urea breaks down and reacts with the exhaust gases to reduce some NO_x into NO_2 and water. The urea is generated from an ammonia supply that must be stored in a tank on the vessel, creating additional health risks for the crew. An SCR unit is the most effective technology on the horizon for reducing NO_x in the exhaust stream. Improvement in NO_x production of up to 90% has been found, however, SCR systems available today only exist for a very narrow range of exhaust temperatures, about 320-480°C. The effectiveness of the system is greatly reduced by lower temperatures, which is of great concern to large vessels with slow speed engines as they have low exhaust temperatures. When a vessel is maneuvering into port, it is generally operating at low load, further reducing exhaust temperatures in the populated port region where it is desired for NO_x production to be least. In fact, an engine can reasonably operate at only 25% load while

maneuvering, because of the cubic relationship between power and ship speed; at these low loads the SCR unit would create no NO_x reduction at all [50].

Another hurdle with SCR technology is the size of the units. Traditionally they have required a significant amount of space on a vessel, thereby taking up room available for cargo, and in some cases the SCR unit was as large as the engine itself. Research is progressing to minimize the space required by combining the SCR with the muffler into a 'compact SCR' unit, which may improve acceptance of this technology. However, maintenance intensive technology coupled with an insulated muffler in the exhaust stack will have to be well designed to avoid complicated access procedures. Additionally, operating on fuel with a sulfur level above 1% greatly reduces the effectiveness of the system as sulfur becomes trapped in the active catalysts. Most large vessels operate on approximately 3% sulfur fuel, which would require extensive maintenance to continually deal with the sulfur poisoning of the SCR system, not to mention increased sulfuric acid condensation. If the system were combined with the muffler, as in the compact system described above, the engine would have to be shut down for extensive periods of time to perform the maintenance required. A vessel operating with fuel containing a very minimal amount of sulfur, well below the average fuel sulfur level, would still require 6 hours of maintenance each port call for the SCR unit, with the number increasing greatly as the quality of fuel diminishes [50].

Clearly the numerous restrictions and technical challenges make SCR technology appropriate for a limited range of applications. It may be feasible and required for ferries or passenger vessels with long down periods and areas of operation in populated areas. However, it will be a long time before the technology fits well into the operation of a large cargo vessel. It must be stressed again that this is the most prominent reduction technique on the horizon for NO_x, and its effective implementation seems to be a long way off. If the technical aspects aren't enough of a hindrance, the bottom line will be. Discounted at 7% the total cost of an SCR system, including maintenance and operation, is approximately \$2,000,000 per vessel equipped with a slow speed engine, though great variance exists [50]. Approximately \$600,000 and \$100,000 are the average costs for

maintenance and urea respectively over the lifetime of the vessel, again discounted at 7% [50]. An additional \$2,000,000 for a pollution control unit, half of which requires capital outlay or immediate financing, is a large chunk of a 40 million dollar tanker. Thinking of it a different way, purchasing the after treatment device, for only one pollutant, is 1/40 the entire cost of the vessel and it takes up a good portion of cargo volume. Additionally, these expensive numbers assume the SCR works exactly as the manufacturer intended, without sulfur related problems.

Reduction Techniques for Other Pollutants

As Nitrogen Oxides are the most prominent emission of concern they receive the most attention and reduction efforts, however, research is being conducted for reduction of the other main pollutants as well. Most of the promising techniques are as complicated and large as the SCR described in NO_x section above, preventing their implementation anytime soon.

For reduction of Sulfur Oxides (SO_x), a desulphurization plant would work quite effectively, but the size and associated costs prevents their employment. The system works by washing the sulfur out of the exhaust gases with an alkaline solution such as lime milk or sodium carbonate, and creating gypsum. This creates a serious disposal problem as the gypsum will be contaminated with particulates and heavy metals, and not many governments will allow cheap disposal in their ports. It is generally understood that the only practical way to reduce sulfur emissions from a marine diesel engine is to burn fuel with less sulfur content. As stated earlier, Category 3 vessels operate on fuel with sulfur content on average of approximately 3%, as compared to highway trucks that by 2007 will have to operate on fuel with only 0.015% sulfur content. If vessels were required to operate on low sulfur fuel whenever operating within 175 nautical miles of the U.S. coast, the costs would be quite substantial. At a 7% discount rate, operation on 1.5% sulfur fuel would cost each large vessel about \$200,000; operation on 0.3% sulfur fuel would cost over \$300,000 [50]. These regulations would be extremely difficult to monitor, and by international trade regulations may only be applicable to U.S. flagged vessels, thereby greatly reducing their effectiveness. However, if a Category 3 vessel

were forced to switch from average heavy fuel to 1.5% sulfur fuel, the SO_x emitted would decline by 40%; if the vessel switched to 0.3% sulfur fuel, the SO_x produced would be 90% less, as all of the SO_x in the emissions stems directly from the fuel [50]. Though not attractive to the bottom line or easy to implement, operating with low sulfur fuel reduces the SO_x output and improves particulate matter emissions.

Reducing the sulfur content of the fuel oil utilized to 1.5%, reduces particulate emissions by approximately 20%; reducing the sulfur percentage to 0.3% reduces the PM emissions by an astounding 60% [50]. Clearly the majority of particulate matter comes from utilizing heavy fuel. Lube oil consumption is a significant contributor to PM emissions, but is almost negligible when heavy fuel is in operation. However, with continued demand for emission regulations, ships will be forced to utilize cleaner fuel. When cleaner distillate fuel is in operation, which is almost always the case for medium and high speed engines, lube oil consumption becomes a large contributor to particulates by percentage. Forcing ships to use cleaner fuel, a point not so far into the future, will allow marine engine manufacturers a door to further reduce particulate matter by lowering a now significant contributor, lube oil consumption, with technology such as LIF. Reducing particulate matter with an after treatment device is an option, but relatively undeveloped. Particles can range in size over several orders of magnitude, making it virtually impossible to remove them all by centrifugal forces, as in a cyclone. Particle traps are an option for small engines, but have problems when being expanded to service large engines including poisoning by sulfur from the fuel and calcium from burnt lube oil. Electrostatic precipitators, where the particles are ionized thereby making them stick to electrodes to be washed out later, requires extensive amount of space which is not available on ships. A combination of a cyclone and electrostatic precipitator is showing promise, but is a long way off. As with most pollutants, the best way to reduce particulates is to avoid their formation. Some are formed by trade offs from NO_x reduction techniques that lower peak temperatures; however, cleaner fuels and reducing lube oil consumption greatly reduce their formation. The costs of the aforementioned particulate matter after treatment devices are not well known, as they are not very progressed into the implementation phase of research.

Reduction Technique Costs

The total cost of employing any reduction technique is difficult to know, but generally stretches far beyond the simple acquisition price. The many exhaust after treatment devices described above had additional costs measured in space and complexity. Space is money on a vessel as everything comes down to transporting cargo. Most of the techniques currently being researched would add a great amount of monitoring and work for the marine engineer, were they to be installed on the vessel. The source of resistance for stronger emission regulations is clear, the research is progressing too slowly, and efficient means for reduction are far off.

Rather than continuing to look for bulky and complicated secondary means to clean the exhaust emissions, marine engine manufacturers would be better off spending their dollars on preventing the pollutants from forming by researching primary measures. Perhaps all the primary measures are exhausted in certain circumstances, but not for most. Reduction of lube oil consumption benefits the ship operator and the environment, as it is a primary means of reducing particulate matter and hydrocarbon emissions. To employ LIF technology to control oil transport, the marine engine manufacturer would have a significant initial cost in testing various new ring and piston designs for each engine scale; however, the research would be valid for virtually every engine in a similar size range for decades. The cost for applying LIF technology to a marine engine can only be estimated, but from comparing automotive LIF research expenses with research expenses for other marine exhaust emission technologies, it appears \$1,000,000 would be a high end estimate for each engine scale [50]. This cost per engine scale is paltry in comparison to the high cost per ship of some other reduction techniques being researched. Additionally, the entire benefit would be reaped without any complexity, operational, or maintenance costs for the lifetime of the vessel. The initial research cost, and a very minor cost for alteration of the piston or ring design, would be the only required investment to improve lube oil consumption. The exhaust emission improvement would not be as great when compared to SCR for example, but the expense per ship plus maintenance and complexity would be far less. The next section further

details the role of lube oil in marine engines, and how applying LIF would aid every facet of the marine engine industry.

5.4 Lubricating Oil

Lubricating oil has been referred to as the ‘life blood’ of engines. Without lube oil coursing through engine passages and between moving parts, the engine would quickly seize with catastrophic results. The focus of this research is to understand and control the transport of oil on the piston ring pack. A minimum amount of oil is required between moving parts; however, the problem more commonly lies in how to reduce the overabundance of oil. Having an excess amount of oil in the piston cylinder promotes lubrication degradation and lube oil consumption in the combustion chamber. As discussed previously, lube oil consumption is a significant contributor to pollutants in the exhaust stream. As diesel engines have optimized fuel efficiency to a great extent, lube oil consumption has become a larger and larger portion of hydrocarbon emissions [55]. Additionally, the extensive additives within the lubrication to improve its performance contribute significantly to particulate matter emissions when the lube oil is consumed in the combustion chamber. Aside from air pollution concerns, lube oil combustion chamber exposure also amounts to added costs for the engine operator for replacement of dirty or burnt lube oil. Laser Induced Fluorescence technology studies the movement of oil along the piston and the ring-liner interface. Applying this technology to the various scales of marine engines would allow engineers a relatively inexpensive way to develop means to better control the transport of lubrication on the piston ring pack, thereby reducing emission output and lubrication costs.

Medium and High Speed Marine Engines

Medium and high speed marine engines, discussed in detail in Section 5.1, are the work horses of the industry. Outfitted on tugboats, pleasure craft, or as large generators, these engines must be able to handle both fast load transients and constant operation, sometimes for days on end. These engines must be capable of operating on rough seas, and thus at several angles depending to the motion of the vessel. To maintain proper

lubrication at all times, an oversupply is generally provided to ensure all surfaces are coated, even at extreme angles. This oversupply, however, adversely affects lube oil consumption and degradation. Lube oil consumption leads to an increase in harmful exhaust emissions, particularly hydrocarbons and particulate matter, and added cost of oil replacement. For these classes of engines, which generally operate on cleaner fuels, the generation of pollutants is the main driving factor for reducing lube oil consumption. The cost of oil replacement, while not negligible, does not warrant the research alone. LIF technology could be used to understand oil transport for these engine scales, thus finding means to reduce consumption and lower pollutant output.

Understanding the oil transport mechanisms will also reduce general oil degradation. Some of the lubricating oil that nears the combustion chamber becomes scraped back down to the crankcase, or finds another means of returning to the oil supply. When the oil is near the combustion process, however, it becomes contaminated with some of the harmful combustion elements, such as sulfur, heavy metals, or soot. For example, the relatively small amount of oil that is present in the compression ring grooves translates to a significant exposure time to sulfur acids and other harmful compounds [60]. Oil that is significantly contaminated will have diminished effectiveness at lubricating the cylinder walls. Lube oil is not only used in the cylinder, however, it is needed in other components such as the governor, turbocharger, and starting mechanism. It is therefore in the best interest of the engine designer to control lube oil transport to not only prevent consumption, but also to limit exposure to combustion products. Keeping the oil free of combustion products improves its reliability and the reliability of the additional equipment that uses it.

Slow Speed Marine Engines

Slow speed marine engine designers are constantly striving to reduce oil consumption as well. The driving factor in these engines is not solely to reduce exhaust emissions; instead, the primary motivation is money. The crosshead design of these large engines, discussed in detail in Section 5.1, requires the addition of cylinder lube oil to lubricate the cylinder walls. This high-grade oil is a very expensive item for a vessel operator; in fact

it is the greatest operational cost for the engine after fuel oil. Therefore, minimizing the amount of cylinder oil consumed is a high priority for the bottom line. Employing LIF technology would allow a smaller amount of cylinder lube oil to become more effective, thereby reducing the quantity required. This would translate directly into substantial daily savings in operational costs for the vessel. A financial analysis of the potential benefits of a reduction in cylinder lube oil consumption follows below.

The operational costs for an engine, other than fuel, depend largely on engine settings. For instance, the costs associated with cylinder liner wear and piston reconstruction are directly correlated to the amount of cylinder lube oil injected. The engine manufacturer will specify a recommended range for cylinder lube oil insertion. In Figures 5.4 and 5.5, the operational costs associated with the low and high recommended dosages for a six cylinder, slow speed VLCC super tanker are shown. The operational costs for a twelve cylinder, slow speed container ship are shown in Figures 5.6 and 5.7. Clearly in every situation, cylinder lube oil is the greatest cost in maintaining the operational status of the engine. When the operator chooses a lower cylinder lube oil dosage, the engine will operate equally, however, the parts will encounter more wear. The greater wear translates to greater costs when the engine is rebuilt, as is shown in the added costs for liner wear, rings, crown reconstruction, and the additional labor required. Notice in the cases of both vessels it is better financially to operate with a lower dosage, and pay more for parts and labor; operating at the low level dosage saves approximately \$10,000 per cylinder per year, even with the added cost for parts and labor [61].

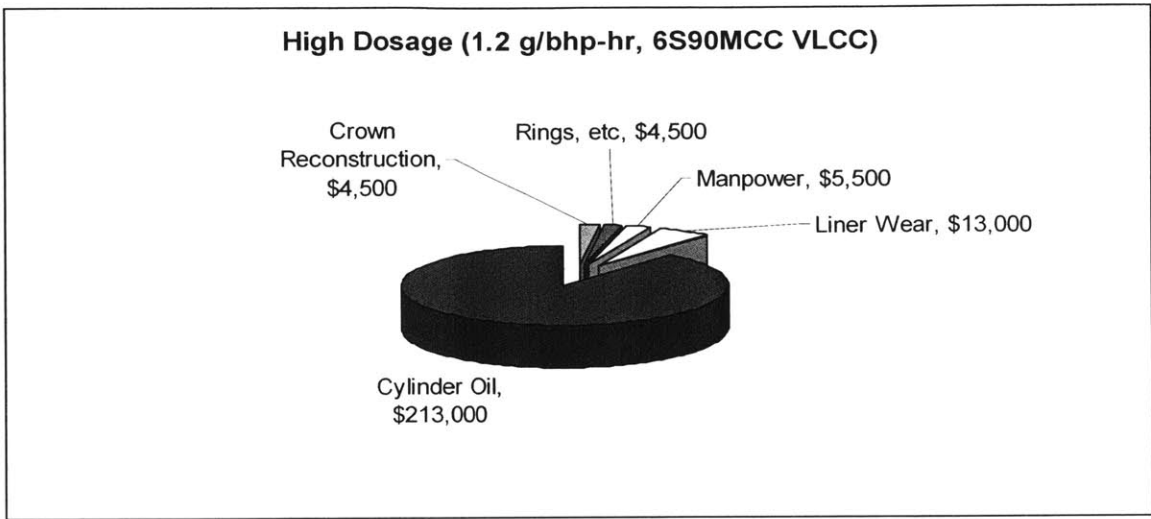


Figure 5.4 – Annual Operating Costs for MAN B&W 6 Cylinder Engine on an Oil Tanker with a High Cylinder Lube Oil Dosage, Total Cost is \$240,000 per year [61]

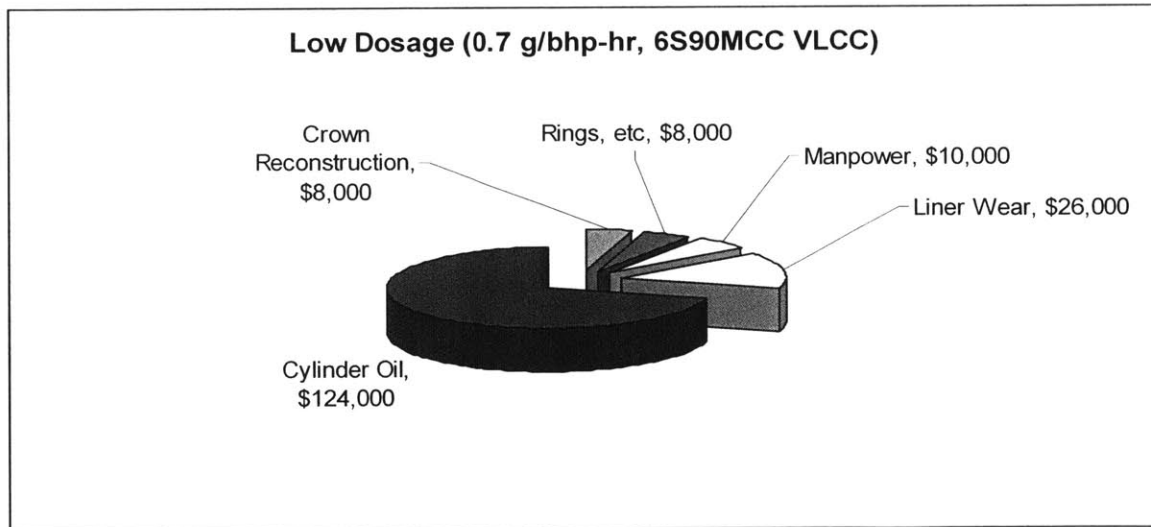


Figure 5.5 – Annual Operating Costs for MAN B&W 6 Cylinder Engine on an Oil Tanker with a Low Cylinder Lube Oil Dosage, Total Cost is \$176,000 per year [61]

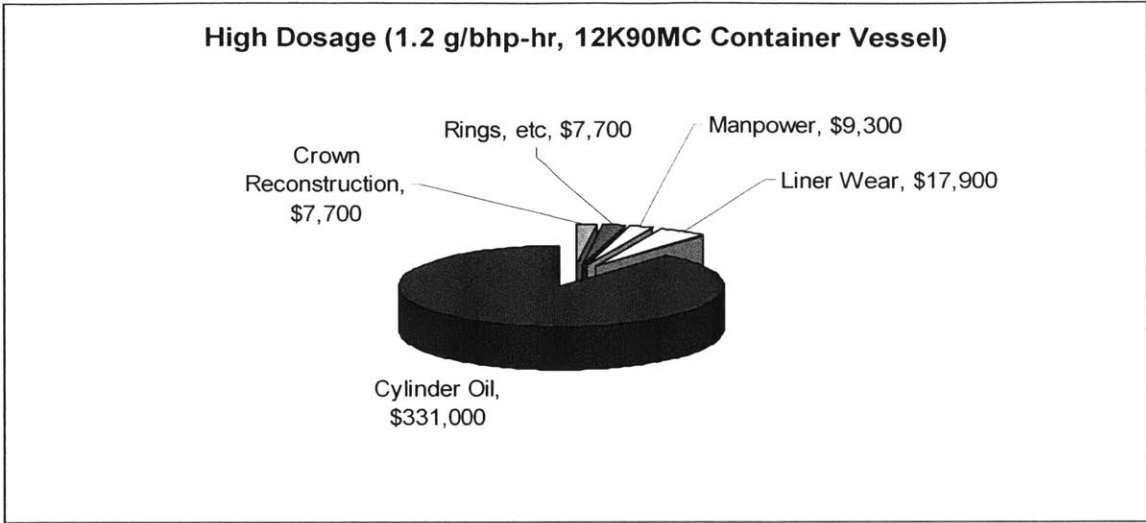


Figure 5.6 – Annual Operating Costs for MAN B&W 12 Cylinder Engine on a Container Ship with a High Cylinder Lube Oil Dosage, Total Cost is \$373,000 per year [61]

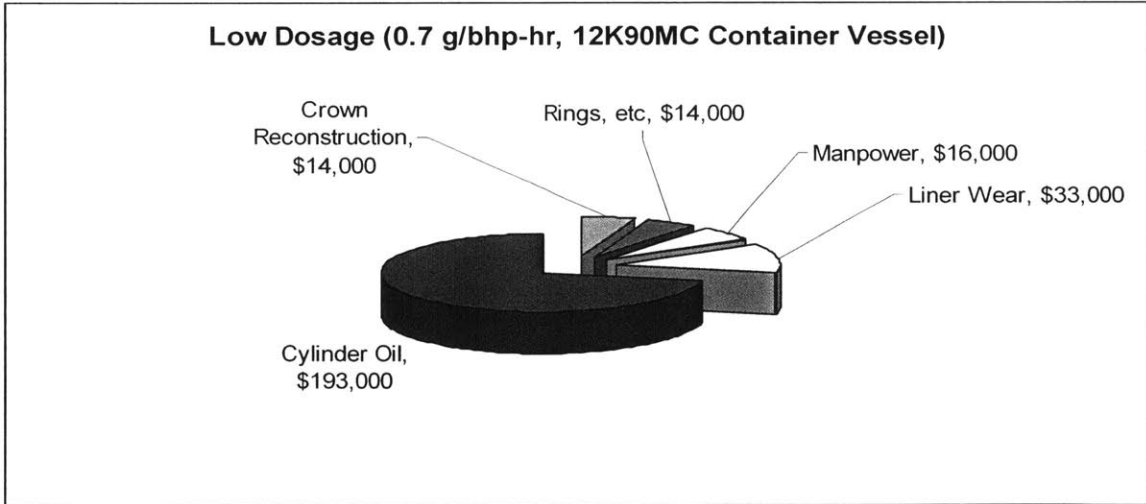


Figure 5.7 – Annual Operating Costs for MAN B&W 12 Cylinder Engine on a Container Ship with a Low Cylinder Lube Oil Dosage, Total Cost is \$269,000 per year [61]

Reducing cylinder lube oil consumption is one of the greatest demands the engine manufacturers receive from their clients. Clearly, any research leading to a reduction in oil consumption would save the operator a great deal of operating costs. Application of LIF technology would allow better means to control oil transport and thus reduce cylinder lube oil consumption. Even if LIF technology becomes only marginally beneficial, creating a 5% oil consumption reduction, this would save the engine operator from \$1,000 to \$1,750 per cylinder, per year; for a twelve cylinder, slow speed container ship the operator would save about \$15,000 a year in costs. This estimate assumes LIF technology creates only an incremental improvement in lube oil consumption, the savings would be more substantial if LIF technology could improve cylinder lube oil effectiveness by a more realistic estimate of 10%, or even an optimistic estimate of 20%. The annual savings in these cases average \$30,000 and \$60,000 respectively [61].

Anti-Polishing Ring

In response to vessel operators' demands to reduce costs, engine manufacturers developed the anti-polishing ring around 1990 to drastically reduce cylinder lube oil consumption. The anti-polishing ring (APR) maintains the condition of the cylinder liner by limiting carbon deposit build up on the crown of the piston. If the build up were to continue unchecked, the deposits would eventually contact the liner wall and act to scrape oil up from lower regions into the upper combustion chamber. Introduction of the APR, which is now standard on virtually all marine engines, has cut lube oil consumption by an amazing 50% [62]. The internal diameter of the APR is slightly less than the cylinder bore, and is inserted into the liner, just above top dead center for the top compression ring. The APR, therefore, scrapes off any build up on the crown land every up stroke of the piston, keeping the deposits small enough to prevent contact with the liner in the lower regions. Removing the deposits also prevents metal to metal contact which could occur if the deposits were to entirely wipe off the lubricating oil film from an area of the cylinder liner. The APR has the additional benefit of significantly reducing cylinder liner wear.

The anti-polishing ring is an example of a primary means to reduce exhaust emissions, with the added benefit of a decrease in operational costs, especially for slow speed engines as their cylinder lube oil is quite expensive. The APR very inexpensive, and is a permanent fixture in the engine, working effectively for the entire lifetime of the vessel. This is in contrast to some of the secondary measures, such as the SCR described in Section 5.3, which had many drawbacks. The SCR is quite effective, but has substantial installation, complexity, and maintenance costs. Additionally the delicate technology of SCR may create decreasing effectiveness over time. The simplicity and success of the APR is outstanding, and should be a model for future research exploits. LIF technology would provide benefits very similar to the APR. Once researched, LIF would provide permanent means of controlling oil transport and reducing lube oil consumption, with no additional work for the marine engineer. The next section details how LIF could be employed on marine engines.

Application of LIF to Marine Engines

Current research at the Sloan Automotive Laboratory of MIT is applying LIF technology to improve automobile engine lubrication transport. We have learned what drives oil along the piston ring pack, and into the combustion chamber. Techniques to control oil motion were analyzed by testing various ring designs and geometrical variations of the piston lands. This exact process could be reproduced on marine engines to improve their lube oil transport qualities and reduce oil consumption.

As noted in the technical portions of this paper, inertia and blowby are the main forces directing oil flow. Thus variations in engine size, pressures, and speed will alter the transport qualities. I recommend the marine industry test each engine scale, in regards to bore size, starting from an automobile engine size (100mm) and researching each 100mm increment up to the largest engine bore size (1,000mm). Once the LIF research has been done on a 500mm bore engine for example, the information learned can easily be applied to all other engines having a similar bore size. In other words, this research has to be done on only 10 engines, and the rewards are almost indefinite and across every engine to be produced. Only if the shape of the piston ring pack were to be altered significantly, to

improve some other aspect of the engine for example, would the LIF tests need to be redone to verify the impact of the change.

For medium and high speed engines, the driving factors of lube oil transport are going to be very near those of an automobile engine. The relatively high speed of operation for these engines makes inertia a key component in oil transport. The most effective means of controlling inertia flow is to add a geometrical shape to the piston ring pack to ‘catch’ the oil as it flows upward, and release the oil when inertia shifts back downward. Harnessing blowby through ring gap shape and ring motion is also valuable to controlling oil transport. The recent advancements in lube oil consumption, namely the anti-polishing ring discussed above, have made LIF technology important for preventing degradation. The anti-polishing ring has cut lube oil consumption in half, thus topping-up takes place less often and the original oil is in service for longer periods in these trunk piston engines. Longer service creates greater wear on the oil additives and more degradation through contamination from combustion products [60]. Because the anti-polishing ring has extended oil residence time within the engine, employing LIF technology to control oil transport and avoid combustion products would maximize the oil’s utility by preventing degradation. Applying LIF technology to medium and high speed engines would reduce operating costs to some degree, but more importantly the improvements would greatly reduce particulate matter and hydrocarbon emissions.

The significant driving factor for lube oil transport in slow speed engines is going to be quite different than for an automobile engine. The relatively slow speed and large scale of operation for these engines will make blowby the key component in oil transport. The very high combustion pressure, coupled with the slow engine speed, creates substantial gas flow that has ample time to affect oil patterns. The most effective means of harnessing blowby is to optimize ring gap shape and ring motion, both axially and circumferentially. The final design should use the blowby gasses to keep oil away from the combustion chamber, while maintaining sufficient lubrication at all times. Applying LIF technology to these slow speed engines will not create large improvements in emission output, mostly because the majority of pollutants originate from the heavy fuel

generally used in these engines, and thus the lube oil consumed contributes a smaller percentage to the exhaust. Reducing lube oil consumption, however, will greatly reduce the operating costs incurred by the vessel operator, as cylinder lube oil is the greatest cost of operation, other than fuel.

5.5 LIF Implications to the Maritime Industry

The Marine Transportation System is vital to virtually every industry, and will only continue to grow. Though cleaner per ton-mile than any other means of transportation, the maritime industry is near worst in improvement. Exhaust emissions from marine vessels has been the main focus of various regulating bodies in the past five years, and continues to grow. Various means to reduce pollutants are being researched extensively, though most appear too complicated and expensive to be practical. LIF technology has the ability to improve exhaust emissions for certain pollutants on all scales of engines. The technology is inexpensively researched and employed, and is perhaps the simplest of technologies being investigated. The design is a permanent fixture on the piston or rings, and requires no maintenance or input from the marine engineer. Great variety exists in the marine industry, from tug boats to container ships for example, requiring different LIF solutions for each engine scale. However, once an effective LIF strategy has been found for an engine scale, every engine of similar size and power can employ the same strategy in the production engine. The application of LIF would be continuously reducing exhaust emissions for the lifetime of a vessel, suffering from little to no degradation in efficiency. LIF technology to reduce lube oil consumption not only affects the environment, however, but can also result in substantial cost savings. Cylinder lube oil consumption is the greatest operational cost for a slow speed engine, other than fuel. Employing LIF technology could reduce cylinder lube oil consumption by 10%, resulting in \$30,000 of savings per year. If LIF technology proved more effective, by reducing lube oil consumption for a large container vessel by 20%, the savings would near \$60,000 annually. LIF technology has far reaching benefits for accountants and the engineers working to reduce exhaust emissions, and needs to start being utilized by the maritime industry.

CHAPTER 6: CONCLUSIONS

Understanding the complex oil transport mechanisms is critical to matters involving lubricating oil consumption and engine friction. Enough lubricating oil must be provided to the upper ring pack region to prevent dry running and limit friction and wear, but any excess oil will hasten oil degradation or become consumed. This oil consumption leads to harmful hydrocarbon and soot emissions as well as poisoning of the exhaust after-treatment equipment.

Lubricating oil travels through distinct regions along the piston ring pack before being consumed in the combustion chamber. The oil distribution and driving forces vary considerably throughout the regions of the piston ring pack. This 2D LIF work focuses on a single cylinder spark ignition engine, investigating the oil transport mechanisms across these regions, and in particular the evolution of the third land throughout an entire engine cycle. The impact of speed and load were experimentally observed with the LIF generated real time high-resolution images, as were changes in piston and ring design.

Specific piston designs, particularly those including a second land V-Cut or Hook, were experimentally studied. These geometric features were found to greatly inhibit inertia driven flow across the second land; however, their effectiveness heavily wanes in the presence of ring gaps where the oil quantity and gas flow are too great to be contained by the tested features. Experimental evidence suggests ring gap driven transport to be the main mechanism by which oil becomes transported across the second land.

A significant percentage of the liquid oil which becomes consumed in the combustion chamber will cross the third land at some point; understanding the third land evolution, therefore, is necessary for understanding lube oil consumption. The third land is consistent and predictable, as can be seen in the repeatable transport features seen in every LIF image. A compilation of detailed third land oil maps has been generated for an engine cycle, in intervals of 30 crank angle degrees. These maps relay the mechanisms

by which the majority of oil employs to cross the third land. The general evolution for this region is driven primarily by inertia, an absolute constant for a steady operating condition. A faster engine speed will induce the transport mechanisms earlier in the cycle. Conversely, a lower speed will delay their occurrence. Engine load will not significantly alter the general third land evolution, but it will adjust the timing and magnitude of the individual processes. A greater engine load will delay the start of the transport mechanisms and reduce their magnitude, while a low engine load acts contrarily.

Specific ring types will induce their own phenomenon on top of the general third land evolution. The 'Buffer Region' of the Napier Hook and third land chamfer contrast to the simplicity of the Negative Twist scraper ring in the location of temporary oil storage. Similarly, the gap effects of the U-Flex oil control ring differ greatly from the Twin Land oil control ring or Three Piece OCR. The Twin Land OCR gap induces substantial oil transport at one location on the piston circumference; in opposition, the U-Flex gaps release a small quantity of oil at about 50 evenly spaced locations around the circumference of the third land. The Three Piece oil control ring has significant accumulations around both the expander gap and the top rail gap, whose combined volumes are similar to the amount of oil accumulation associated with the Twin Land OCR gap.

Comprehensive knowledge of the consistent third land oil transport evolution will allow directed control features to be developed. These features will act to reduce net transport to the upper piston ring pack, or enhance downward transport of oil back to the crankcase. Discovery of the consistency and balance in the third land pattern and ring induced features will set the framework for oil consumption modeling and further transport studies.

The ability to control, or influence, oil transport on the piston ring pack will have an impact on all engine classes, including engines in the maritime community. This experiment study is directly comparable to small marine engines, and can be used to help

reduce maritime exhaust emissions related to lubrication consumption; additionally, this approach would be much more rugged and cost effective than other current technological improvements being investigated. Were a similar 2D LIF experiment to be performed on large slow speed diesel engines, the annual savings per vessel, assuming only a 10% reduction in lube oil consumption was achieved, could amount to \$30,000 as cylinder lube oil is one of the most expensive operating costs for large slow speed diesel engines.

REFERENCES

- [1] - Burnett, P.J., 1992, "Relationship Between Oil Consumption, Deposit Formation and Piston Ring Motion for Single-Cylinder Diesel Engines", SAE paper 920089.
- [2] - Munro, R., 1990, "Emissions Impossible – The Piston and Ring Support System", SAE paper 900590.
- [3] - Mayer, W.J., Lechman, D. C., and Hilden, D. L., 1980, "The Contribution of Engine Oil to Diesel Particulate Emissions", SAE 800256.
- [4] - Schneider, E. W., Sell, J. A., Siekkinen, J., W., 1998, "The Contribution of Lubricating Oil to Exhaust Deposits and Exhaust Particulates from Gasoline Engines – A Radiotracer Method", SAE paper 982580.
- [5] - Drury, C., and Withehouse, S., 1994, "The Effect of Lubricant Phosphorus Level on Exhaust Emissions in a Field Trial of Gasoline Engine Vehicles", SAE Paper 940233.
- [6] - Ueda, F., Sugiyama, S., Arimura, K., Hamagushi, K., Akiama, K., "Engine Oil Additive Effects on Deactivation of Monolithic Three-Way Catalysts and Oxygen Sensors", SAE Paper 940746.
- [7] - Nakada, M., 1993, "Piston and Piston Ring Tribology and Fuel Economy", Proceedings of International Tribology Conference, Yokohama, 1993.
- [8] - Heywood, J. B., 1988, *Internal Combustion Engines Fundamentals*, McGraw-Hill.
- [9] - Sasaki, M. et al., 1997, "The Effect of EGR on Diesel Engine Oil and its Countermeasures", SAE Paper 971695.
- [10] - Tamai, G., 1995, "Experimental Study of Engine oil Film Thickness Dependence on Liner Location, Oil Properties, and Operating Conditions", M.S. Thesis, Department of Mechanical Engineering, MIT, September 1995.
- [11] - Noordzij, L. B., 1996, "Measurement and Analysis of Piston Inter-Ring Pressures and Oil Film Thickness and their Effects on Engine Oil Consumption", M.S. Thesis, Department of Mechanical Engineering, MIT, June 1996.
- [12] - Tian, T., 1997, "Modeling the Performance of the Piston Ring-Pack in Internal Combustion Engines", Ph.D. Thesis, Department of Mechanical Engineering, MIT, June 1997.
- [13] - Thirouard, B., 2001, "Characterization and modeling of the fundamental aspects of oil transport in the piston ring pack of internal combustion engines", Ph.D. Thesis, Department of Mechanical Engineering, MIT, June 2001.
- [14] - Hoult, D. P., Takigushi, M., 1991, "Calibration of Laser Fluorescence Technique Compared with Quantum Theory", STLE Tribology Transactions, Volume 34 (1991), 3, pp 440-444.
- [15] - Shaw, B. T., Hoult, D. P., Wong, V. W., 1992, "Development of Engine Lubricant Film Thickness Diagnostics Using Fiber Optics and Laser Fluorescence", SAE 920651.
- [16] - Casey, S., 1998, "Analysis of Lubricant Film Thickness and Distribution Along the Piston/Liner Interface in a Reciprocating Engine", Department of Mechanical Engineering, MIT.

- [17] - Casey, S.M., Tamai, G., and Wong, V.W., 1998, "Effects of Engine Operating Conditions on Oil Film Thickness and Distribution along the Piston/Ring/Liner Interface in a Reciprocating Engine," presented at the ASME Fall Technical Conference, Clymer, NY, ICE-Vol. 31-2, Sept. 27-30, 1998.
- [18] - Takigushi, M., Nakayama, K., Furuhashi, S., Yoshida, H., 1998, "Variation of Piston Ring Oil Film Thickness in an Internal Combustion Engine", SAE Paper 980563.
- [19] - Nakayama, K., Seki, T., Takiguchi, M., Someya, T., Furuhashi, S., 1983, "The Effect of Oil Ring Geometry on Oil Film Thickness in the Circumferential Direction of the Cylinder", SAE Paper 830068.
- [20] - Froelund, K., Schramm, J., Noordzij, B., Tian, T., and Wong, V., 1997, "An Investigation of the Cylinder Wall Oil Film Development During Warm-Up of an SI-Engine Using Laser Induced Fluorescence," SAE paper 971699.
- [21] - Inagaki, H., Saito, A., Murakami, M., and Konomi, T., 1995 "Development of Two Dimensional Oil Film Thickness Distribution Measuring System," SAE Paper 952346.
- [22] - Thirouard, B., Tian, T., 2003, "Oil Transport in the Piston Ring Pack (Part I): Identification and Characterization of the Main Oil Transport Mechanisms", SAE Paper 2003-01-1952.
- [23] - Thirouard, B., Tian, T., 2003, "Oil Transport in the Piston Ring Pack (Part II): Zone Analysis and Macro Oil Transport Model", SAE Paper 2003-01-1953.
- [24] - Tian, T., Noordzij, B. L., Wong, V. W., Heywood, J. B., 1996, "Modeling Piston-Ring Dynamics, Blow-by, and Ring-Twist Effects", ICE-Vol. 27-2, October 1996 ASME Fall Technical Conference, Volume 2, pp 67-80, Fairborn, Ohio.
- [25] - Tian, T., Wong, V. W., 2000, "Modeling the Lubrication, Dynamics, and Effect of Piston Tilt of Twin-Land Oil Control Rings in Internal Combustion Engines", Transactions of ASME, Journal of Engineering for Gas Turbines and Power, January 2000, Vol. 122, pp 119.
- [26] - Tian, T., Wong, W. V., Heywood, J. B., 1998, "Modeling the Dynamics and Lubrication of a Three Piece Oil Control Ring in Internal Combustion Engines", SAE Paper 982657.
- [27] - Haugland, R. P., 1999, "Handbook of Fluorescent Probes and Research Chemical", Seventh Edition, Molecular Probes.
- [28] - Malhe, "Mini Piston Manual", Issue 1995, Mahle GmbH, D-70369 Stuttgart.
- [29] - Hidrovo, C. H., Hart, D. P., 2000, "Dual Emission Laser Induced Fluorescence Technique (DELIF) for Oil Film Thickness and Temperature Measurement", Proceeding of ASME FEDSM'00, ASME 2000 Fluids Engineering Division Summer Meeting June 2000.
- [30] - Saito, K., Igashira, T., Nakada, M., 1989, "Analysis of Oil Consumption by Observing Oil Behavior Around the Piston Ring Using a Glass Cylinder Engine", SAE Paper 892107.
- [31] - Carrié, O., Maerky, C., "U-Flex as an Oil Control Ring for New Generation Engines", Motortechnische Z., 1999, 60, pp 570-575.
- [32] - Kataoka, I., Ishii, M., Nakayama, A., 2000, "Entrainment and deposition rates of droplets in annular two-phase flow", International Journal of Heat and mass Transfer, Vol. 43, pp 1573-1589.

- [33] - Tian, T., Wong, V. W., Heywood, J. B., 1996, "A Piston Ring-Pack Film-Thickness and Friction Model for Multigrade Oil and Rough Surfaces", SAE Paper 962032.
- [34] - Tian, T., Rabute, R., Wong, V. W., Heywood, J. B., 1997, "Effects of Piston-Ring Dynamics on Ring/Groove Wear and Oil Consumption in a Diesel Engine.
- [35] - "UD Professor to Highlight Marine Transportation at May 24 Lecture in Lewes". University of Delaware, College of Marine Studies. May 11th, 2001.
<http://www.ocean.udel.edu/newscenter/CorbettLewes.html>
- [36] - Sources and Transport of Air Pollution from Ships: Current Understanding, Implications, and Trends. Dr. James J. Corbett and Dr. Paul Fischbeck.
<http://www.epa.gov/region09/air/marinevessel/pdfs/fischbeck.pdf>
- [37] - "U.S. Marine Transportation Policy". Jeremy M. Firestone, University of Delaware, College of Marine Studies. <http://www.mast.udel.edu/670/Slides-week12.ppt>
- [38] - Challenges and Opportunities for the U.S. Marine Transportation System. Marine Transportation System Advisory Council. June 28, 2001.
<http://www.mtsnac.org/mtsnactest2/images/whiterev.pdf>
- [39] - Scope of Marine Diesel Applications. Diesel Technology Forum. Applications and Economics. September, 2003. <http://www.dieselforum.org/background/marineapplications.html>
- [40] - Environmental Considerations in Commercial Marine Industry. Conference on Marine Vessels and Air Quality. American Bureau of Shipping. February 1, 2001.
<http://www.epa.gov/region09/air/marinevessel/pdfs/tanwar.pdf>
- [41] - "Global Ship Traffic Density". IMO Study on Greenhouse Gas Emissions from Ships, MEPC 45(8), 2000. <http://www.epa.gov/region09/air/marinevessel/pdfs/fischbeck.pdf>
- [43] - "Transportation Mode Comparison – Energy – Environment – Efficiency". Environmental Advantages of Barge Transportation, USDOT – Maritime Administration.
www.mvr.usace.army.mil/navdata/tr-comp.htm
- [42] - MARAD 2001, Maritime Administration's Annual Report to Congress. U.S. Department of Transportation. Maritime Administration.
- [44] - "Remarks for the Honorable Norman Y. Mineta, Secretary of Transportation, Maritime Energy and Clean Emissions Workshop, Washington, D.C., January 29, 2002".
www.dot.gov/affairs/012902sp.htm
- [45] - "Transport Comparison Chart". Iowa Department of Transportation. September, 2003.
www.mvr.usace.army.mil/navdata/tr-comp.htm
- [46] - Intercity Freight and Passenger Rail: Air Quality. Federal Railroad Administration, U.S. Department of Transportation. August, 2003.
www.fra.dot.gov/policy/RailProjectPlanningandFinancingGuide_5c.htm
- [47] - Commercial Marine Emission Inventory. Jean Marie Revelt, Environmental Protection Agency. Conference on Marine Vessels and Air Quality. February 1st, 2001.
<http://www.epa.gov/region09/air/marinevessel/pdfs/reveltinventory.pdf>
- [48] - Ship Emissions Assessment (SEA). James J. Corbett, Paul S. Fischbeck, and Spyros Pandis.
<http://hdgc.cpp.cmu.edu/projects/abstracts/ship-emissions.html>

- [49] - "Pollutants Produced in Moving One Ton of Cargo 1,000 Miles". Environmental Protection Agency, Emission Control Lab. September, 2003.
www.mvr.usace.army.mil/navdata/tr-comp.htm
- [50] - Control of Emissions from Compression-Ignition Marine Diesel Engines At or Above 30 Liters per Cylinder. Draft Regulatory Support Document. U.S. Environmental Protection Agency. April 2002.
- [51] - TriboPack for Sulzer RTA Engines. Kaspar Aeberli. Marine News. No. 3 – 1999.
- [52] - Engine Selection Guide, MC Programme. Electronic Project Guides, Version 11. September 2002. MAN B&W.
- [53] - Tests Confirm Cylinder Lubrication Savings. MAN B&W Press Release. September 24th, 2002.
- [54] - Emission Control – Two-Stroke Low-Speed Diesel Engines. MAN B&W. August, 2002.
- [55] - Exhaust Emissions Reduction Technology for Sulzer Marine Diesel Engines: General Aspects. Rudolf Holtbecker and Markus Geist. Sulzer, RTA Series. Wartsila NSD. July 1998.
- [56] - Meeting the Regulatory Requirements on Air Emissions. Dragos Rauta, Intertanko. Chemical Carriers Association. League City, Texas. November 22nd, 2002.
www.intertanko.com/pubupload/Speech-Power-CCA-Annual-Meeting--.PPT
- [57] - Federal Regulations and International Treaties. Jean Marie Revelt, Environmental Protection Agency. Conference on Marine Vessels and Air Quality. February 1st, 2001.
<http://www.epa.gov/region09/air/marinevessel/pdfs/reveltregs.pdf>
- [58] - Emission Standards Adopted for New Marine Diesel Engines. Environmental Protection Agency, Regulatory Announcement. Office of Transportation and Air Quality. January 2003. EPA420-F-03-001. <http://www.epa.gov/otaq/regs/nonroad/marine/ci/f03001.pdf>
- [59] - An Overview of Marine Environmental Initiatives at the IMO. Michael Julian, Chairman Marine Environmental Protection Committee, International Maritime Organization. An Address to the Institute of Marine Engineering, Science and Technology. London, November 14th, 2002. <http://www.imarest.org/events/IMOMEPC/IMOenvironint.pdf>
- [60] - New Demands on Lubricating Oil Quality. Global Care News. Service News from Wartsila NSD Corporation. Number 1, 1999.
- [61] - MAN B&W Service Experience, MC Engines, U.S. Owners, March-April 2003.
- [62] - Wartsila Environmental Report 2000. Mauri Palvi and Mikael Niskala. May 29th, 2001.
- [63] – Dowson, D., and Taylor, C. M., 1979, "Cavitation in Bearings," Ann. Rev. Fluid Mech. 1979, pp. 35-66.

5568-51